University of Glasgow

The Regulatory Role of the Transcription Factor PdhR in modulation of Bacterial Virulence

Kabo Ronald Wale

BSc, MSc

A thesis submitted in fulfilment of the requirements for the award of Doctor of Philosophy

School of Infection and Immunity

College of Medical, Veterinary and Life Sciences

University of Glasgow

February 2024

Declaration

I hereby declare that this thesis is the result of my own work and has been composed for the degree of PhD at the University of Glasgow. This work has not been submitted for any other degree at this or any other institution. All work presented was performed by myself unless otherwise stated. All sources of information and contributions to the work have been specifically acknowledged in the text.

Kabo Ronald Wale

(Candidate)

February 2024

Date

Abstract

An emerging theme in infection biology is the link between metabolic capacity and the ability to colonise specific niches. We previously showed that the transcriptional regulator PdhR was highly downregulated by the pathogen *Citrobacter rodentium* during colonisation of the murine GI tract. This colonisation is dependent on the type 3 secretion system (T3SS) which is encoded on a pathogenicity island, named the locus of enterocyte effacement (LEE). The T3SS regulation centres on sequential expression of the LEE in response to multitude of signals and cues that are encountered in the intestinal environment of the host. This prompted us to propose that PdhR, could be important in regulation of both metabolism and, directly or indirectly, virulence of *C. rodentium*. Moreover, given that *Citrobacter* shares a similar LEE island to *E. coli* O157, we asked if PdhR controls virulence in both these pathogens. Deletion of p*dhR* led to a significant decrease in transcript levels of LEE-encoded genes and proteins as elucidated by quantitative reverse transcription PCR and transcriptomic analysis. Cell infection assays demonstrated that loss of *pdhR* attenuates pathogen colonisation and attachment. We also demonstrated that PdhR directly binds to the *ler* regulatory region possibly to activate *ler* transcription, and consequently LEE-gene expression. Through transcriptomics we showed that LEE regulation is very complex, and several carbon metabolism pathways maybe wired into global LEE gene regulation in EHEC. Impairing the metabolism of these substrates through deletion of the TF PdhR results in various virulence defects in EHEC and underlies pathogenic outcome of an infection.

Furthermore, it was revealed that PdhR is essential not only for early host colonisation but also required for further persistence of enteric pathogens during host infection. In addition, the *pdhR* mutant strain showed a lower degree of dysbiosis in the microbial community with no significance at the peak of infection. Thus, this work highlights that PdhR, a transcriptional regulator that is known to regulate central metabolism underpins the intimate relationship between virulence and metabolic flux in EHEC. Potentially understanding this complex relationship could lead to better dietary interventions to reduce EHEC mediated disease.

Acknowledgements

I want to thank Professor Andrew Roe, and Dr. James Connolly, who served as my PhD advisors, for their invaluable insight, counsel, and support. Professor Roe, you've always been a fantastic boss. For your thoughtfulness and steadfast support over the past four years, I owe you a debt of gratitude. I appreciate all the lessons you have taught me; they will be with me always.

Dr Nicky O'Boyle, your encouragement when I first started my PhD and lacked specific molecular skills was crucial. Your expertise and ideas made it simpler to move on with this project and finish it. For all meaningful comments, encouragement, and understanding over the years we interacted, Dr Rebecca McHugh, Dr. Ester Serrano, and Dr. David Mark, I am eternally thankful. Saying "thank you" is inadequate to adequately convey my gratitude to you guys.

I want to express my gratitude to the Roe group (Dr Jennifer Hallam, Dr Natash Turner, and Patricia Rimbi Sophia Sandali) who have offered assistance and guidance along the route. Thank you for always being wonderful teammates who are extremely nice and supportive.

The final acknowledgement goes to, my parents, my wife Tshegofatso Wale and my kids Sarona Wale and Oreneile Wale for their patience, support, and love; my studies have been in their honour.

Table of contents

List of figures

List of tables

Chapter 1: Introduction

1.1 Enteropathogens

Health care systems are seriously threatened by enteric illnesses, which are also becoming an increasingly significant public health problem. Enteric diseases are often regarded as a group disease that are associated with the ingestion of food and/or water contaminated with microorganisms (Bahrani-Mougeot et al., 2009). The etiological agents of enteric disease include bacteria, viruses, and parasites (de Nisco et al., 2018).

Infections caused by enteric pathogens have a high mortality and morbidity burden, as well as significant social and economic costs. In 2019, there were 6.60 billion incident cases and 98.8 million prevalent cases of enteric infections, resulting in 1.75 million deaths, and 96.8 million disability-adjusted life years (Gizaw et al., 2023). This data shows an increase from 351,000 related deaths caused by 22 types of foodborne illness reported by the World Health Organization (WHO) in 2015. The greatest burden is excessively high in the global south (Africa and Southeast Asia) (Petri et al., 2008). Sadly, 40% of the illnesses occurs in children under the age of 5 (Caballero-Flores et al., 2019).

In spite of the fact that enteric diseases are characterized by overwhelmingly short-term gastrointestinal side effects, post disease complications may follow. For instance, enterohemorrhagic *Escherichia coli* (EHEC) infections can result in renal dysfunction, whereas yersiniosis can lead to chronic arthritis (Reiter's disorder)(Bahrani-Mougeot et al., 2009). *Campylobacter* disease may cause the neuroparalytic Guillain–Barre´ disorder and typhoid fever can turn into a life-long repetitive ailment (Bahrani-Mougeot et al., 2009). In addition, enteric diseases range from acute or chronic diarrhoea to life-threatening sepsis with gastrointestinal tract infections being the most common diseases caused by these pathogens (Kim et al., 2017). Enteropathogenic bacteria represent a unique group of pathogens that can establish infections in the small or large intestine despite many challenges encountered in the gut (Fig.1-1). These challenges include pathogen-specific immune responses and gastrointestinal complications such as reduced intragastric pH (Chen et al., 2020), the presence of bile in the small intestine and reduced iron availability (Chatterjee et al., 2019), and an established commensal microbiota consisting of billions of

bacteria from hundreds of different species, which produce several antimicrobial metabolites and toxins (Kim et al., 2017). Pathogenic *E. coli* pathotypes, Enteropathogenic *Escherichia coli* (EPEC) and Enterotoxigenic *Escherichia coli* (ETEC) infect and colonise the small intestine (Fig. 1-1 A), while (EHEC) colonises the colon (Fig. 1-1B) by encoding virulence factors, typically fimbriae and enterotoxins (Rojas-Lopez et al., 2018). This allows the pathogen to outcompete commensal bacteria. Typhoidal strains of *Salmonella enterica* serovar Typhimurium (*Salmonella* Typhimurium) causes systemic sickness by spreading to the liver, spleen, and lymph nodes (Wanyin Deng et al., 2012). On the other hand, nontyphoidal strains induce self-limiting, localized infection by invading macrophages and epithelial cells lining the small intestine (Kumar et al., 2019). Like EHEC, the spiral-shaped, Gram-negative bacteria *Campylobacter jejuni* causes bloody diarrhoea. *C. jejuni* invades and colonises the distal ileum as well as the colonic epithelium (Fig.1-1 B). Distinct from other Gram-negative bacteria, *C. jejuni* lacks a type-III secretion system (T3SS) that is necessary for the direct insertion of effector proteins into the host cell (Sistrunk et al., 2016). Alternatively, it uses invasion associated effector molecules (homologous to T3SS system) secreted through the flagella (Sistrunk et al., 2016).

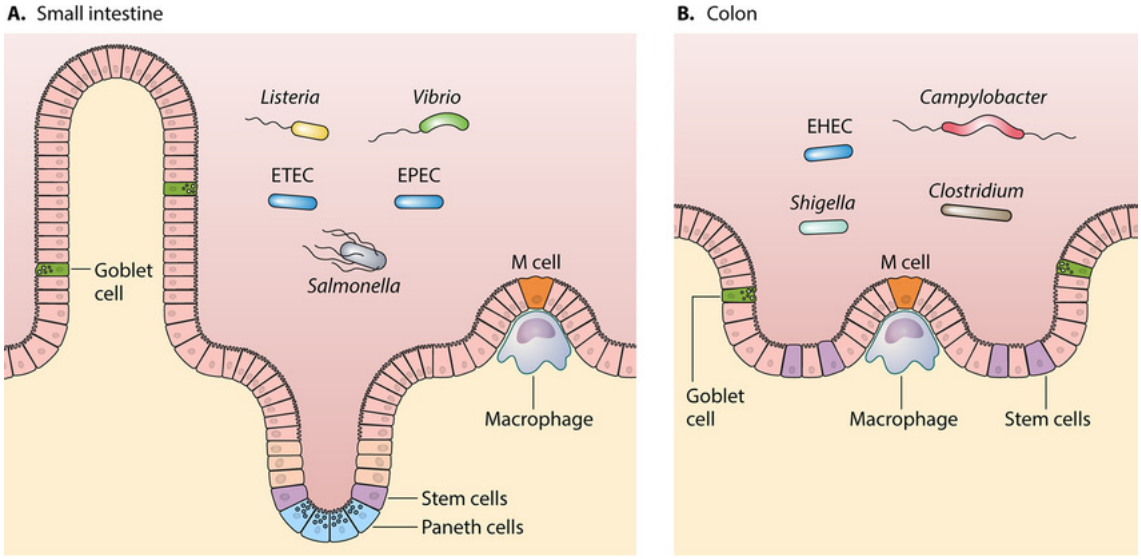

Fig. 1-1. Different niches of enteropathogens within the gastrointestinal tract. Enteropathogens have been shown to infect the small intestine (A) or the large intestine (B). The mechanism of infection involves adhesion or invasion of epithelial cells lining the gastrointestinal tract. *Listeria, Vibrio, Salmonella*, and some pathogenic *E. coli* strains (EPEC and ETEC) infect the small intestine, and *Campylobacter*, EHEC, *Shigella*, and *Clostridium* infect the colon (Sistrunk et al., 2016).

Rotavirus and diarrheagenic *Escherichia coli* (DEC) have been reported as the main causative agents of diarrhoea in developing countries (World Health Organization, 2017). DEC comprises of *E. coli* pathotypes including, Shiga toxin-producing *E. coli* (STEC) enteroinvasive *E. coli* (EIEC), as well as ETEC (W. Deng et al., 2001). After ingestion of a contaminated food, STEC penetration through the mucus layer and the intestinal barrier are facilitated by a toxin delivery system termed the Locus of Enterocyte Effacement (LEE) (Turner et al., 2018), which is key in the survival and persistence of enteric pathogens. The LEE encodes the type III secretion system (T3SS) which is very essential for pathogenesis in many Gram-negative bacteria (Deng et al., 2004).

Current antibiotic therapies cannot effectively treat most gastrointestinal infections, predominantly those that are caused by STEC and its subgroup EHEC, because they either cause severe gut microbiome dysbiosis or may increase the risk of haemolytic–uremic syndrome (HUS) (Karpman & Ståhl, 2014). Pathogenesis of STEC and its subgroups have been equitably well characterized, nonetheless, new therapies are required for control of disease progression, because of complications in the treatment of STEC infections (Hwang et al., 2021).

1.2 Enterohemorrhagic *E. coli* a subset of STEC

1.2.1 Clinical manifestation

EHEC is a subgroup of Shiga toxin (Stx)-STEC also known as “verocytotoxin-producing *E. coli*. EHEC infectious dose is very low, only 100 cells are required to cause disease (Jubelin et al., 2018). Unless *E. coli* O157:H7 infection is asymptomatic, the sickness begins with severe stomach cramps and non-bloody diarrhoea after an incubation period of 3 to 4 days (Wong et al., 2011). After two or three days, the watery diarrhoea in the majority of patients turns bloody. Fever may be completely absent, but vomiting may occur. The diarrhoea usually lasts 1 to 8 days and the infection clearance appears to be age dependent (Karpman & Ståhl, 2014). Compared to older children and adults, children under the age of five continue to carry the organism after infection clearance (Karpman & Ståhl, 2014). *E. coli* O157:H7 infection-related symptoms often resolve within a week and majority of patients thereafter make a full recovery with no significant aftereffects. However, one week following

haemorrhagic colitis, 5-10% individuals may acquire HUS and 3-12% percent of HUS-patients die (Rahal et al., 2012). HUS, is a condition that might be fatal and can make the infection worse (Rahal et al., 2012). Low platelet counts and microangiopathic haemolytic anaemia, (which is anaemia caused by damaged blood arteries that results in the destruction of red blood cells) and acute kidney failure are two symptoms of HUS (Cramer, 2014). Severe complications of HUS are characterized by acute renal failure, microangiopathy, thrombocytopenia, and haemolytic anaemia (Crepin et al., 2016). In other cases, neurological symptoms such as aphasia, tremors, and coma may occur (Karpman & Ståhl, 2014).

About 5% of people who survive the acute phase of HUS experience severe renal failure or persistent brain impairment (Rahal et al., 2012). Supplemented oral rehydration seems the best management for *E. coli* O157:H7 infections , while antibiotics is prohibited as they may cause bacterial lysis that leads to increased Stx release (Rahal et al., 2012).

1.2.2 Shiga toxin production

Shiga toxin is an AB5 protein that contains an enzymatically active A subunit and five B subunits that are responsible for binding to globotriaosylceramide-3 (Gb3), a cellular receptor present in several organs, including the kidney, brain, liver, and pancreas (Etcheverría & Padola, 2013). The expression of Stx is mainly induced by activation of the bacterial SOS response by DNA damaging agents, in particular antibiotics. *E. coli* pathotypes can produce Stx type 1 (Stx1), type 2 (Stx2), or both, encoded by the *stx1* and *stx2* genes, respectively, carried by lysogenic phages (Ballem et al., 2020). Stx1 subtypes include Stx1a, Stx1c and Stx1d, whereas Stx2 comprises seven subtypes (Stx2a, Stx2b, Stx2c, Stx2d, Stx2e, Stx2f, Stx2g) these are well documented (Detzner et al., 2022). In addition, new Stx2 subtypes (Stx2h and Stx2k) have been recently reported (Ballem et al., 2020). EDL933 subtype strains carrying *stx2* are more virulent and more likely to be associated with HUS than strains carrying only *stx1* or both (Etcheverría & Padola, 2013). In particular, Stx2a, alone and in combination with other Stx subtypes, had the highest rates of HUS, hospitalisation and bloody diarrhoea within the EU (Koutsoumanis et al., 2020). In addition, O157:H7 serotype Stx2a was reported to be an emerging highly

pathogenic strain of Stx producing *E. coli* in England and Wales (Byrne et al., 2018). Using whole genome sequencing the group investigated the evolutionary context of the serotype. From their analysis the emerging strain revealed that it evolved from STEC O157:H7 Stx-negative ancestor approximately 10 years ago after acquiring a bacteriophage encoding Stx2a (Byrne et al., 2018).

Ruminants are the main reservoir of EHEC and humans are usually infected through consumption of contaminated water or food (Ballem et al., 2020). Complications in EHEC cases can reach heights of 8%, with most cases occurring in children under 5 years of age, with a mortality rate of 1-2% (Huerta-Uribe et al., 2016). Scotland had the highest rate of human infection by EHEC (4.4/100,000) in the UK in 1998-2008 (Herbert et al., 2014). Indeed, a 2017 study by Henry et al. found that EHEC was detected on 23% of Scottish farms. Further, all but one of the farms were found to be contaminated with EHEC that produced Shiga toxin, which is associated with severe disease in humans including kidney (Lewis et al., 2015) and even brain damage (Karpman & Ståhl, 2014). 8161 human cases of STEC were confirmed in Europe in 2018. In fact, STEC ranks third after *Campylobacter* and *Salmonella* spp. among the most relevant foodborne pathogens within the European Union (Ballem et al., 2020).

1.2.3 STEC serotypes

More than 400 EHEC serotypes have been recorded and many epidemiological studies have shown that five serotypes are more frequently involved in outbreaks than others in many countries (Segura et al., 2021). In the EU, five major human STEC serogroups were identified as serotypes O157:H7, O26:H11, O103:H2, O91:H21, and O145:H28 from 2012 to 2017 (Table 1- 1) (Koutsoumanis et al., 2020). Additionally, serogroups O157:H7 and O26:H11 were most commonly associated with severe STEC infections (HUS, hospitalization, or BD) (Koutsoumanis et al., 2020). Similar serotypes except for the O91:H21 serotype were found to be circulating in France (Bibbal et al., 2015). In the United States, the major STEC serogroups associated with human disease are O157:H7, O26:H11, O145:H28, O145:H28, O103:H2, and O145:H28 (CDC, 2018).

Table 1-1 STEC serogroup distribution for human cases associated with HUS, BD or hospitalisation(TESSY data, 2012-2017) (Koutsoumanis et al., 2020).

Serogroup	Number of HUS cases	%	Serogroup	Number of hospitalised cases	%	Serogroup	Number of BD cases	%
157	634	38.4	**157**	2,753	60.4	**157**	4,245	71.6
26	403	24.4	**26**	705	15.5	**26**	582	9.8
111	85	5.1	**145**	137	3.0	**103**	162	2.7
80	74	4.5	**103**	107	2.4	**145**	159	2.7
145	68	4.1	**111**	97	2.1	**91**	64	1.1
55	48	2.9	**146**	51	1.1	**146**	51	0.9
121	44	2.7	**91**	33	0.7	**111**	49	0.8
103	42	2.5	**55**	32	0.7	**128**	32	0.5
91	17	1.0	**5**	26	0.6	**5**	28	0.5
104	6	0.4	**174**	21	0.5	**55**	27	0.5
Other	232	14.0	**Other**	598	13.1	**Other**	532	9.0
Total	1,653	100.0	**Total**	4,560	100.0	**Total**	5,931	100.0

The most common EHEC strain serotype O157:H7 (discovered in the United States in 1982) and O145:H28 are known to be associated with the eae-γ1 subtype. The STEC serotype O26:H11, O103:H2, and O111:H8 have eae-β1, eae-ε, and eae-θ subtypes, respectively (Bibbal et al., 2015). When isolated from the food chain, these "top five" STEC have been shown to be major cause of severe complications among *E. coli* pathotypes (Coldewey et al., 2007). Apart from serotype O157:H7, Stx-producing strains O104:H4 have also been reported, which were the causative of a large-outbreak in northern Germany in 2011 (Cramer, 2014). Further, the outbreak affected sixteen other countries, causing HUS and deaths (Cramer, 2014).

1.2.4 EHEC pathogenesis and associated virulence factors

The main virulence factor associated with EHEC pathogenicity is the production of Stx (Chong et al., 2007). Besides production of Stx, EHEC expresses intimin, encoded by the protein *eae* gene, involved in binding to the enterocytes. There are 17 types of intimin, these include, α1, α2, β1, ξR/β2B, δ/κ/β2O, γ1, θ/γ2, ε1, νR/ε2, ζ, η, ι1, μR/ι2, λ, μB, νB, and ξB, while the γ and β are more prevalent *eae* variants, while ε was found to be present at a lower degree from isolates obtained from cattle and food (Etcheverría & Padola, 2013). Intimin is key for colonisation, in particular it is required for bacterial adhesion to epithelial cells inducing a characteristic histopathological lesion defined as "attaching and effacing" (A/E) (Fig.1-2A and Fig.1-2B).

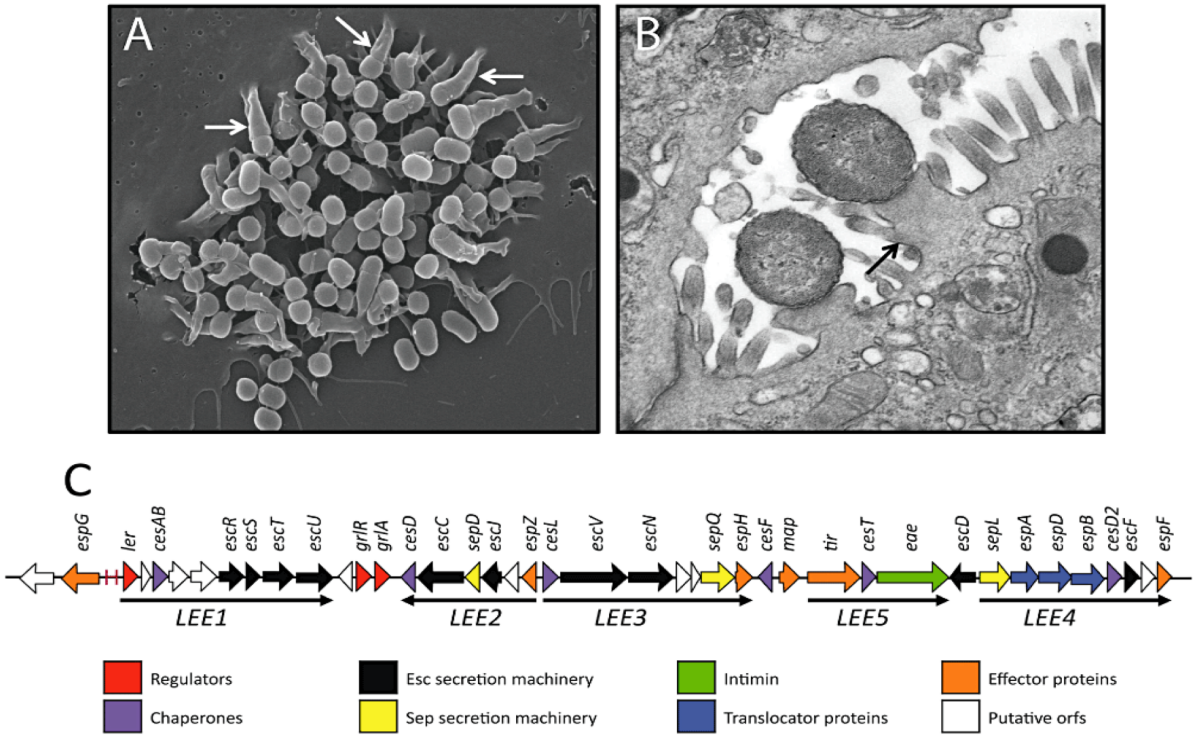

Fig. 1-2. Attaching and effacing phenotype typical of EHEC in host colonisation. (A). Pedestal formation attaching and effacing (A/E) pathogens strains. (B) intestinal A/E lesions shown by transmission electron micrograph. (C) Diagram illustrating organization of the operon, LEE1-LEE5 (Wong et al., 2011).

The A/E pathology is determined by a pathogenicity island (PAI) termed as the locus of enterocyte effacement (LEE) (Deng et al., 2001). This PAI island has been well characterized and studies have shown that it comprises 41 genes, largely across five polycistronic operons, LEE 1 to LEE 5 (Deng et al., 2004). The first open reading frame, LEE1, encodes for the LEE master regulator (Ler), which blocks H-NS, a DNA binding protein that suppresses transcription of LEE from having its inhibitory impact (Connolly et al., 2016). Activation *ler* stimulates the transcription of LEE2-5 and map, the gene product of which is known to target host cell mitochondria (Arbeloa et al., 2009). *ler* is highly regulated and under the control of several global regulators, including QseA, FIS, HIS, H-NS (Sharp and Sperandio, 2007; Bustamante et al., 2011). In addition, the LEE also encodes GrlA which also activates *ler* and GrlR a repressor which interacts with GrlA to prevent its activity on LEE activation. Other global regulators such as RpoS, ClpXP and DegP have also been reported to regulate LEE expression at post-transcriptional level (Gaytán et al., 2016). The LEE operon encodes a type III secretion system (T3SS) and an outer membrane adhesin intimin and its translocated receptor Tir, and several secreted proteins

(Shames et al., 2010). Tir binding to intimin triggers the recruitment of the effector, EspFu, which its binding is facilitated by host proteins IRTKS and IRSp53. The complex between EspFu and either IRTKS and IRSp53, triggers EspFu bind to the neural Wiskott-Aldrich syndrome protein (N-WASP) and in turn activates the host Arp2/3 complex, leading to actin polymerization pedestal formation (Ho et al., 2013). Furthermore, the T3SS injects several other EHEC proteins encoded by LEE known as *E. coli* secreted proteins (Esp), including EspA, EspB, and EspD which function as structural proteins of the T3SS molecular syringe and facilitate the delivery of other effector proteins into the host cell. As many as 41 effector proteins are secreted by certain EHEC serotypes and about 30 are secreted by *C. rodentium* (Deng et al., 2012).

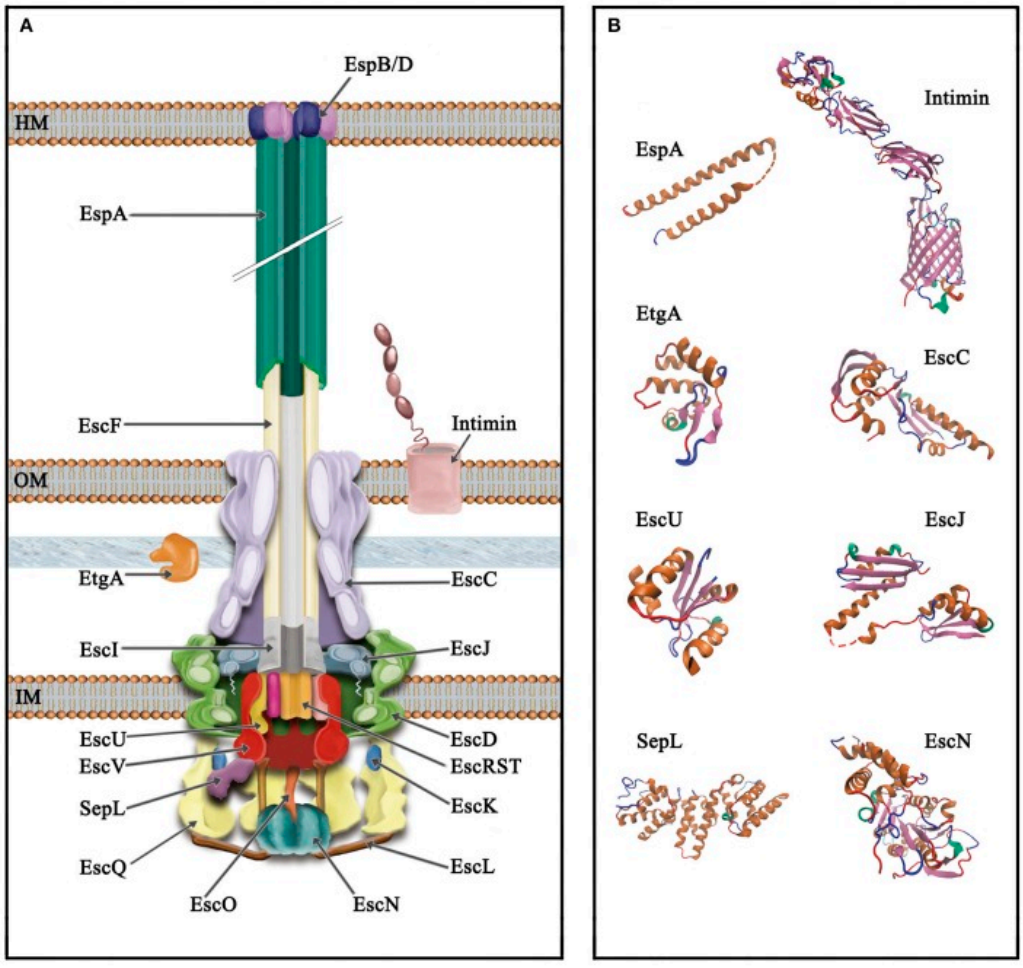

Fig. 1-3. Schematic representation of EHEC T3SS injectosome. (A) The basal body that spans the bacterial membrame (IM), outer membrame (OM) harboring the adhesin intimin, Host membrane (HM). The colors of the proteins correspond to the various parts of the T3SS. EspA which interacts with the host membrane is marked in green. (B) Protein structures showing common T3SS associated proteins.Adapted from (Gaytán et al., 2016)

The roles of effector proteins range from reorganization of host cell actin, effacement of the microvilli around A/E lesions and disruption of tight junctions to immune response modulation and inhibition of apoptosis (Connolly et al., 2018). Specifically, the LEE-encoded effectors including Map, EspG, EspF, EspH, SepZ and mitochondrial-associated proteins, all influence host cell signalling (Garmendia et al., 2004). The protein translocation is facilitated by the proteins, EspA, EspB, and EspD which plays a role in forming the hollow T3SS filament, and form channels into the host membrane. In addition, to the delivery of LEE encoded effectors the T3SS also allows the translocation of non-LEE-encoded effectors, such as NleA, NleB, NleC, NleD, NleE, NleF, and NleG. This non-LEE-encoded effectors have been shown to influence EHEC pathogenesis and host colonization which also plays a role in EHEC persistence (Nguyen & Sperandio, 2012).

The T3SS directly translocate effector proteins from the bacterial cytoplasm into the host cytosol. Because of its important role in virulence, transcription of LEE-associated genes is highly regulated by many transcriptional regulators and specific environmental cues, such as quorum-sensing signalling, ammonium, temperature, pH, iron, calcium, bicarbonate, etc (Woodward et al., 2019). For a well-coordinated T3SS gene expression, EHEC has evolved several specific signalling mechanisms to respond to cues or signals from both the environment and host and integrate the recognition of these signals into the regulatory control of the pathogen through the LEE and non-LEE encoded effector proteins (Mellies & Lorenzen, 2014). The T3SS is of great importance, as the protein secretion system is crucial in the pathogenicity of the family of A/E pathogens. An indispensable trait about the T3SS is that it does not rely on a tissue-receptor molecule to mediate attachment, but rather its regulation centres on sequential expression of the T3SS in response to the multitude of signals and cues that are encountered in the environment (Connolly et al., 2018). Despite the fact several studies on EHEC virulence have been conducted, much of them are based on *in vitro* systems which do not give a true reflection of what really transpires during host infection. For example, cell culture techniques are of inadequate use in modelling the interaction of EHEC and the human immune system with an intact microbiota (Law et al., 2013). Despite being a great *in vitro* model for studying EHEC infections, polarized intestinal

in vitro organ culture (IVOC) systems are not easily accessible to most laboratories as regular tissue culture cell lines. Furthermore, compared to entire animal models, cultivated organ parts have a shorter lifespan and *in vitro* systems cannot metabolize drug candidates, making them impractical for drug action investigations (Law et al., 2013). Host constituents are likely to be key factors in affecting the dynamics of an infection of a given pathogen (Connolly et al., 2018), and hence *in vivo* model systems remain significant in deciphering host pathogen infection and ultimately can lead to a better control method in this era of increased antimicrobial resistance.

1.2.5 pO157 in EHEC virulence

EHEC O157:H7 also harbours a highly conserved nonconjugative F-like plasmid called pO157, with a molecular weight ranging from 92 kb to 104 kb. Other EHEC virulence-related markers include the plasmid-encoded enterohemolysin and the auto-aggregating adhesin (Saa), which is considered to play a role adhesion in strains lacking *eae* (McWilliams & Torres, 2014). However, the exact role of pO157 in disease development is still not well defined, and published studies have reported conflicting results.

1.2.6 Classification of STEC

Emerging STEC pathogens are usually classified according to virulence factors, infection strategy, interaction with host immune system, and tissue tropism (Rojas-Lopez et al., 2018). Together with serotypes epidemiological tracking, standards have been put in place to help with surveillance of STECs, in particular, ISO 13136:2012 standard which describes a real-time PCR-based approach to detect five major STECs, with the aim of monitoring these STECs along the food chain (Ballem et al., 2020).

When *E. coli* O157 are shed in animal faeces, they can survive in the underlying soil and grass for extended periods ranging from several weeks to many months. This provides an important transmission route for pathogens within herds, farms, the fresh food chain, water courses, and the wider environment. It can pose a risk when contaminated land or water is used for recreational purposes. This is limited data on the survival characteristics of other EHEC serogroups in the environment. EHEC outbreaks have been traced to direct handling or petting of animals, particularly petting zoos frequented by young children.

There have also been more reports linking contaminated water to human EHEC infections (Duffy, 2014). Not surprising, identical EHEC O157 isolates were found in sheep faeces, and from patients after a scouting event conducted in Scotland on a muddy sheep-grazed field (Doyle et al., 2006). Additionally, attendees at a music festival were found to have isolates of EHEC O157 that matched a herd of cattle localised in the same area (Ferens & Hovde, 2011).

1.3 Models for EHEC infections

The gastrointestinal pathogen EHEC remains a major global health problem. While other *E. coli* pathotypes causes diarrhoea in children in mostly third world countries, EHEC is mainly found in developed countries and in extreme cases it can lead to haemorrhagic colitis and HUS (See 1.2.1). Several animal models have been used to study EHEC *in vivo*. EHEC has been shown to infect rabbits, chickens and gnotobiotic piglets (Coburn et al., 2007). Studies have since confirmed the characteristic A/E phenotype in epithelial cells and in tissue culture cells infected with EHEC (Deborah Chen and Frankel, 2005).

1.3.1 Cell line as EHEC infection models

Cell lines are used extensively to study human pathogens as they simplify very complex processes *in vivo*. Intestinal epithelial cell (IEC) lines have been shown to be an excellent tool to study A/E pathogen host-cell dynamics, however these systems do not answer fundamental questions such as, host immune interactions, host microbiome interactions and other important physiological conditions that influence host microbiome-pathogen interactions (Law et al., 2013).

1.3.2 *Caenorhabditis elegans* as an infection model

A study by Mellies et al. (2006) demonstrated that EPEC can both infect and kill *Caenorhabditis elegans* via a "slow killing" mechanism which result from accumulation of bacteria in the nematode intestine, as well as forming colonies which resemble those generated by EPEC during infection of epithelial cells. The study further showed that deletion of *ler* reduced the ability of EPEC to colonize the nematode gut. There are several drawbacks allied with the use of *C. elegans* as an *in vivo* system to study *E. coli* pathotypes attachment and colonization mechanisms. Firstly, the model cannot survive at optimal temperature required for expression T3SS genes in A/E pathogens; secondly it

is not quite easy to administrate the correct required bacterial dose; thirdly, *C. elegans* does not give a true representative of immunological responses as compared to mammalian models such as mice and rabbits. Human infection models should display the same pathomechanisms and tissue specificity as in humans, such as, endothelial dysfunction, the hyperinflammatory state and variability regarding susceptibility to infectious diseases (Loewa et al., 2023).

1.3.3 *C. rodentium* as model for EHEC infections

Mouse models have demonstrated to offer many benefits, including low relative maintenance costs and the ease of manipulating host genetics (G. Singh et al., 2020). Studies have demonstrated that murine infection with the *C. rodentium*, do give a true representative of the inflammatory response seen in EHEC infections. Similar to human specific EHEC strains, *C. rodentium* promotes formation of A/E lesions and intestinal pathology during host colonisation (Kumar et al., 2020). Among *in vivo* model studies, the murine bacterial pathogen has proven to be a better alternative given the difficulty of infecting laboratory mice with EHEC (Borenshtein, McBee and Schauer, 2008). Further, EHEC does not efficiently colonize the murine gastrointestinal tract in the presence of an intact microbiome (Borenshtein, McBee and Schauer, 2008). *C. rodentium* is a is a Gram-negative bacterium that colonizes the distal colon of murine and causing transmissible murine colonic crypt hyperplasia, resulting in colitis and epithelial cell hyperproliferation in mice (Caballero-Flores et al., 2020). In fact, like EHEC, *C. rodentium* relies on attaching and effacing (A/E) to colonize the host gastrointestinal tract and share a similar infection strategy (Mallick et al., 2012). These A/E lesions are characterized by close pathogen adherence to epithelial cells, effacement of the brush border microvilli and resulting in pedestal-like structures beneath the attached bacteria (Petty et al., 2010). Both pathogens rely on the LEE PAI to form A/E lesions. As already outlined the LEE encodes a T3SS and several effector proteins translocated to the host during bacterial-host interaction.

One of the impediments in understanding initial colonization and disease progression is the limited data on molecular interaction between the human host and A/E pathogens (Griesenauer et al., 2019). In a previous study by Wiles et al. (2005) they observed that *C. rodentium* becomes hyper-virulent after

passage through the gut of murine as compared to LB broth grown strains during *in vivo* mice infections. In the same study, it was observed that *C. rodentium* ICC 180 which was the host passaged strain, rapidly colonized the colon without initially attaching to the caecal patch of infected mice. In contrast, overnight LB grown *C. rodentium* attached to the caecal patch en route to the colon, which is the preferred niche for *C. rodentium* colonization. Undoubtedly the transcriptome and proteome of passaged and LB grown strains are expressed differently as accorded by the fact that the passaged *C. rodentium* ICC 180 is required in low doses to cause an infection and the difference in intermediate and final attachment sites in the gut of infected mice. A more in-depth study on the transcriptome, proteome, and metabolic flux during infection of *C. rodentium* and EHEC pathogens is required in order to gain a comprehensive understanding of how both pathogens behave during host infection. Since *C. rodentium* shares an infection strategy and virulence genes with EHEC (Crepin et al., 2016), a better understanding of EHEC pathogenesis can be derived from the transcriptomic analysis of *C. rodentium* during *in vivo* infection. In addition, the data can aid in the development of novel drugs and vaccines.

1.4 Host pathogen interaction

1.4.1 Gut metabolites and signals: in regulation of EHEC and *C. rodentium* virulence

Upon host infection bacterial pathogens must constantly monitor the gastrointestinal tract environment and ultimately find a suitable niche to colonize before they could express a plethora of mechanisms to invade the host. Colonization does not rely solely on virulent traits the pathogen portrays but also on the ability of the pathogen to timely express T3SS in response to signals and cues encountered in the gastrointestinal tract of the host (Connolly et al., 2018). Furthermore, expression of T3SS does not rely on tissue-receptor molecules to mediate attachments (Connolly et al., 2018).

Host diet plays a substantial part in regulation of virulence factors such as expression of the T3SS. A reduced fat diet, supplementation with vitamins, selenium iron and fibre were found to protect mice against *C. rodentium* induced colitis (Smith et al., 2011; Ryz et al., 2015; Desai et al., 2016). EHEC has adopted to metabolise alternative nutrients as opposed to limiting nutrients to avoid competition with host microbiota hence increased chances of colon

colonization. In the case of EHEC and *C. rodentium* LEE is expressed in recognition of two environments within the host gut, thus glycolytic and gluconeogenic environments. The mammalian intestinal lumen has high fucose concentration which is cleaved by fucosidases produced by *Bacteroides thetaiotaomicron* from host glycans and not a suitable niche for EHEC strains (Mullineaux-Sanders et al., 2019). EHEC senses fucose via the FusKR two-component system (TCS), FusK is the histidine sensor kinase while FusR is the response regulator (Cameron and Sperandio, 2015). FusKR signalling repress *ler* transcription and ultimately inhibits expression of LEE (Weigel and Demuth, 2016). *B. thetaiotaomicron* has been linked to contributing to virulence of EHEC as it cleaves fucose abundant in the intestine thereby activating the FusKR system leading to T3SS expression (Mullineaux-Sanders et al., 2019).

D-serine has also been found to suppress LEE expression by reducing ler expression in EHEC when 1 mM D serine was added to MEM-HEPES and interestingly, the reduction on host cell colonization by EHEC cells was significantly reduced by 62% (Connolly et al., 2015). A more detailed mechanistic study by the same group Connolly et al. (2016) interpreted the role of YhaO, a D-serine transporter and YhaJ, a LysR transcriptional regulator in EHEC virulence. They showed that since D-serine is detrimental to EHEC strains and EHEC sense D-serine in the environment through YhaO which is regulated by YhaJ, this in turn repress LEE expression up until the right niche without the presence of high concentration of D-serine is detected.

EHEC and *C. rodentium* senses galacturonate in the colon, thereby activating virulence gene expression via the ExuR transcription factor (Fig. 1-4A) (Jimenez et al., 2020). Indeed, mice infected with Δ*exuR* have a better survival rate compared to WT *C. rodentium*, as evidenced by the absence of histopathological damage and reduced *C. rodentium* faecal shedding (Jimenez et al., 2020). Notably, the incapability of commensal *E. coli* to metabolise galacturonate greatly reduces competition with enteric pathogens allowing them to establish a critical nutrient niche within the colon.

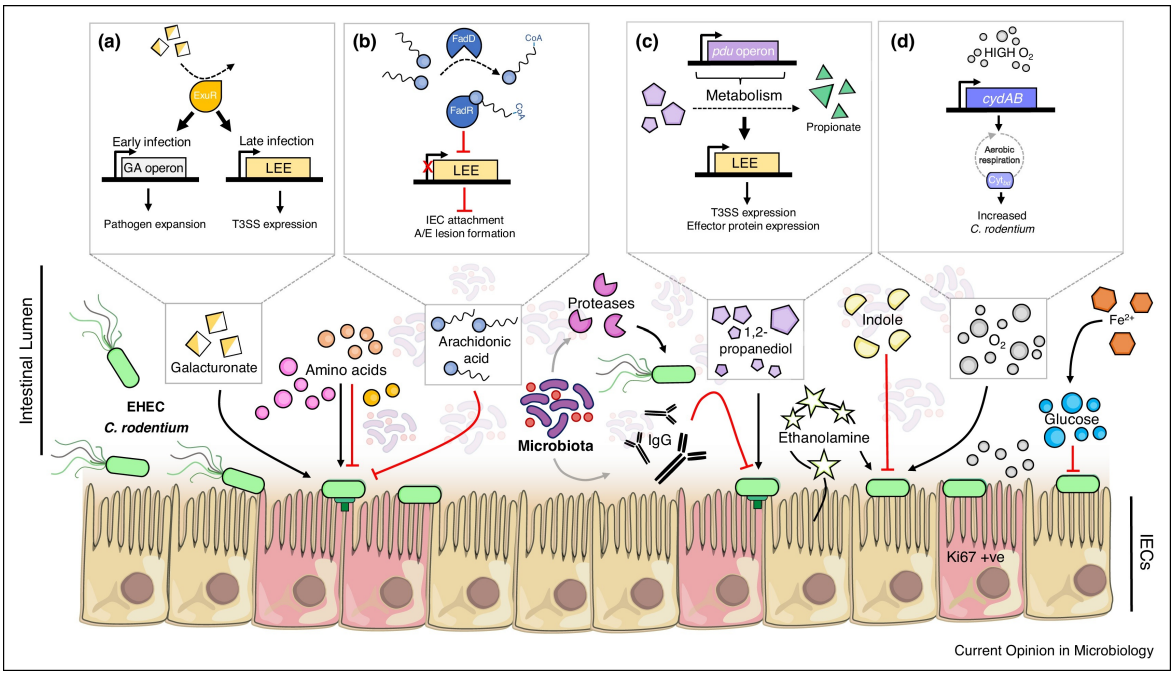

Fig. 1-4. Overview of transcriptional and metabolic regulation of EHEC and *C. rodentium* pathogenesis in the small intestine. (a) ExuR induces the expression of genes for galacturonate metabolism, leading to increased pathogen via LEE and T3SS expression. **(b)** FadR repression greatly reduce LEE expression. **(c)** Propionate is used as a metabolic signal to enhance LEE expression via its breakdown from 1,2-propanediol. **(d)** Colonic crypt hyperplasia by *C. rodentium* causes an increase in mucosal oxygen concentrations. This enhance *C. rodentium* expansion and to outcompete the native microbiota. Red lines represent those metabolites that repress virulence expression, whilst black lines represent any metabolites that promote virulence expression (Wale et al., 2021).

A recent study has also inked metabolic transcription factors CutR which is a cysteine-responsive transcription factor and FadR which maintains balance of expression of long chain fatty acids, to contribute to regulation of virulence in EHEC (Pifer et al., 2018). In the absence of arachidonic acid, the TF FadR binds to the LEE promoter region and induce LEE expression (Ellermann et al., 2021). However, when arachidonic acid is present, it binds to FadR in its acyl-CoA form, as a result the affinity for DNA is decreased and LEE expression is suppressed (Ellermann et al., 2021). The study demonstrated that FadR is a repressor of the LEE and CutR acts as an activator of LEE expression (Fig. 1-4B). An interesting study by Connolly et al. (2018), linked the presence of microbiota-derived 1,2 propanediol as a signal to modulate virulence in *C. rodentium* via its breakdown into propionate (Fig. 1-4C). In addition, the study compared RNA-seq profiles between the caecum and rectum of mice infected with *C. rodentium* to try and find any site-specific transcriptional signatures between the two different environments. A number of differentially regulated

genes expressed in this study during infection were found to be site specific. The expression levels of the LEE genes were relatively consistent between the caecum and rectum, except for less significantly downregulated LEE genes in the rectum. This may be correlated with the hypervirulent state of *C. rodentium* after shedding (Connolly et al., 2018). Further work on this study may shed light on the significant role of each differentially expressed gene in virulence in *C. rodentium* and related pathogens, particularly EHEC. *C. rodentium* and EHEC Bacteriophages studies are one avenue which are widely explored and play a crucial rule in both *C. rodentium* and EHEC virulence. Hernandez-Doria and Sperandio, (2018) reported that EHEC T3SS is activated by the transcription factor Cro during the lysogeny cycle of EHEC phages.

Though Ler is regarded as the master regulator of LEE. *E. coli* pathotypes possess several mechanisms that have been shown to be responsible for regulation of LEE during host infection, and this demonstrates how *E. coli* pathotypes might have a competitive advantage in sensing and responding to environmental cues and ultimately leading to colonization of preferred niches within the host.

1.4.2 Host immune response to EHEC infections

Different microorganisms can infect people differently, and if they do, the results can range from asymptomatic colonization to death (Petri et al., 2008). Individuals differ in their vulnerability to infection with enteric pathogens for a variety of reasons, including their genetic make-up and their capacity to build effective immune responses in the gut.

Innate immune system activation is one of the host's initial lines of defence against EHEC infections. To initiate a protective antimicrobial immune response, pattern recognition receptors are employed to identify pathogen-associated molecular patterns (PAMPs) generated by microbes (Ho et al., 2013). PAMPs are particular pathogen-associated molecules that are identified by innate immune system cell receptors like TLRs, which are transmembrane receptors. TLR stimulation leads in the release of cytokines and chemokines from cells through a downstream cellular signal. Intracellular adaptor proteins are attracted by TLRs. All TLRs share the adaptor protein MyD88, except for TLR3. When LPS binds to the MD2-TLR4 receptor complex, either MyD88-

dependent or MyD88-independent pathways are used to start a signal cascade (Toledo et al., 2008). The significance of TLR4, TRIF, and MyD88 for the pathogenesis of EHEC infection was shown in wild-type and knockout mice infected with *E. coli* O157:H7 (both Stx2-producing and non-producing) (Home et al., 2014). Mice infected with Stx2-producing strain exhibited symptoms, whereas MyD88-deficient mice had the most severe symptoms and pathology (Toledo et al., 2008).

In vitro investigations have shown that T84 intestine cells treated with EHEC produce interleukin-8 (IL-8), resulting in increased inflammatory influx (Thorpe et al., 2001). IL-8 and other CXC chemokines can also be secreted in the gut in the presence Stx. Mitogen-activated protein (MAP) kinase pathways were elevated when Stx was present, and this resulted in increased IL-8 expression (Thorpe et al., 1999). Further, intestinal epithelial cells express Jun N-terminal protein kinase, stress-activated protein kinase, and p38 triggered by the presence of EHEC (Home et al., 2014).

C. rodentium is a natural mouse enteric pathogen that produces acute colitis and serves as a reliable model for the attaching and effacing (A/E) human pathogens EPEC and EHEC. Early stages of *C. rodentium* infection result in the production of the proinflammatory cytokines IL-22 and IL-17, and IL-22-deficient mice develop a leaky gut, which results in systemic bacterial spread and death (Mullineaux-Sanders et al., 2022) (Fig.1-5). During the later stages of infection, Th1/17 cells produce interferon gamma (IFN-γ), IL-21, IL-22, and IL-17, with IFN-γ knockout (KO) mice exhibiting poor clearance and increased colonic pathology in comparison to wild-type (WT) (Mullineaux-Sanders et al., 2022).

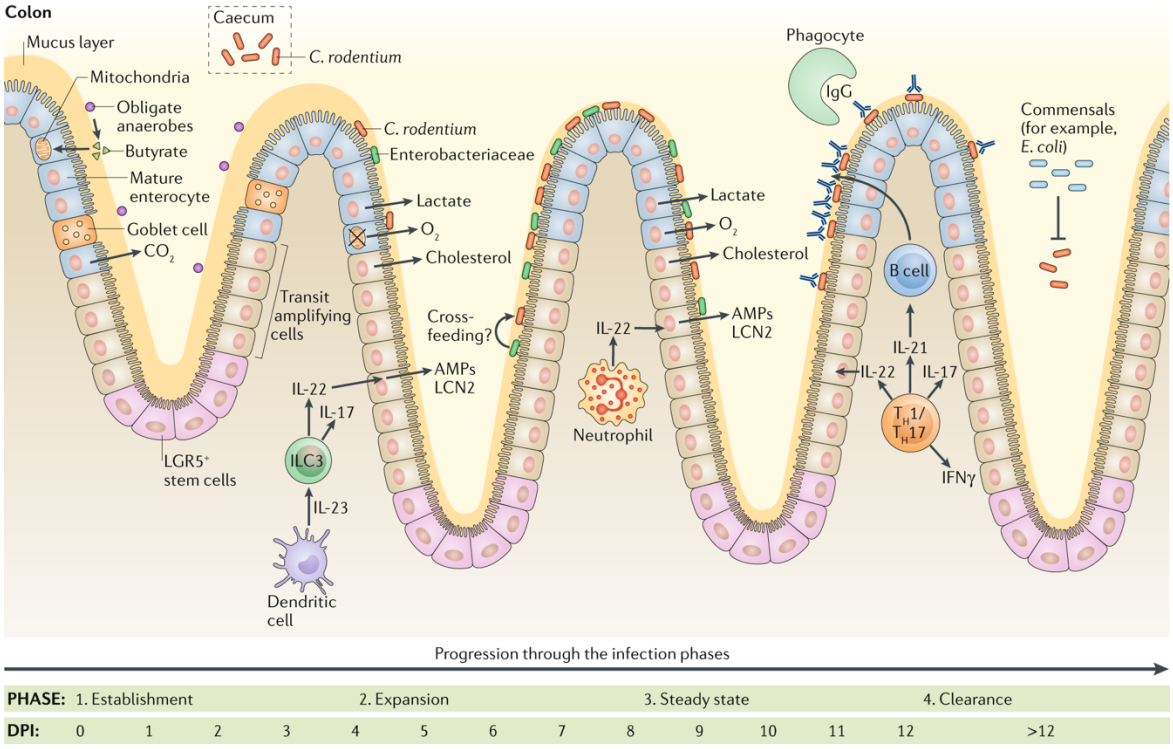

Fig. 1-5. Stages of a mild illness model's *Citrobacter rodentium* infection. The pathogen is present in the caecum during the establishment phase,3 days after i nfection (DPI). From 4 DPI *C. rodentium* colonizes the colonic mucosa and grows throughout the expansion phase.The proinflammatory cytokines IL-22 and IL-17 are released at the early stages of infection. During 8-12 DPI, *C. rodentium* keeps colonizing the mucosa of the colon and reaches a plateau in shedding at around 10^9 CFU per gram of feces. Immunoglobulin G (IgG) opsonizes mucosal-associated *C. rodentium* during the clearance phase (12 DPI). Adapted from (Mullineaux-Sanders et al., 2019).

According to Pickert et al.(2009), the main roles of IL-22 are to encourage mucosal epithelial cell survival and proliferation as well as to initiate the production of antimicrobial peptides like regenerating islet-derived protein 3 gamma (RegIIIγ). Exogenous RegIIIγ has also been shown in other studies to partially prevent the mortality of IL-22 defective mice (Zheng et al., 2008) In murine macrophages, Stx was found to activate tumour necrosis factor (TNF-α) and IL-6 (Karpman & Ståhl, 2014). EHEC long-polar fimbriae were also shown to activate host proinflammatory response in T84 cells (Home et al., 2014). While the host has several mechanisms in place to control EHEC infection, many pathogens including EHEC can subvert host responses to increase their own expansion and survival. For instance, EHEC can suppress both intestinal epithelial cytokine and inhibit gamma interferon-mediated epithelial cell activation, thus these mitigate strategies can promote bacterial colonization (Home et al., 2014).

1.4.3 Metabolic responses triggered during EHEC/*C. rodentium* infection

Pathogens can impact the programming of host metabolic pathways to better adapt to changes encountered in the gut in addition to regulating their own virulence factors in response to the host environment (Kitamoto et al., 2020). In addition to acting as a physical barrier, IEC also identify pathogens through pattern recognition receptors (Peterson & Artis, 2014) and trigger immunological responses, such as LDHA, MCT4, ALPKP1, and NLRP3 in C3H/HeN IEC (Carson et al., 2020). To combat this, *C. rodentium* alters IEC metabolism in order to escape host innate immune responses and multiply inside the colon (Hopkins et al., 2019). This is demonstrated by the considerable downregulation of several important host metabolic processes, such as the tricarboxylic acid (TCA) cycle, oxidative phosphorylation, gluconeogenesis, and lipid metabolism, during colonic inflammation in the host (Berger et al., 2017). *In vivo* proteomic and lipidomic investigations during the *C. rodentium* infection revealed a considerable decrease in carbohydrates, plasma membrane, and mitochondrial lipid (Berger et al., 2017). Additionally, in *C. rodentium* infected IEC, levels of crucial mitochondrial transporters such the 2-oxoglutarate carrier (Ogcp), citrate transporter Sfxn5, and pyruvate transporter Mpc1 are decreased (Berger et al., 2017). These transporters feed the TCA cycle. As a result of disrupting the host's mitochondrial activity, *C. rodentium* promotes the generation of glycine aminotransferase and creatine while blocking potentially harmful nitric oxide (Berger et al., 2017, McAdam et al., 2012).

A pathogen-driven change to the host's aerobic respiration allows *C. rodentium* to outcompete strict anaerobes and become abundant in the colon (Lopez et al., 2016) (Fig.1-4D). This is evidenced by the fact that deletion of *C. rodentium* cytochrome bd oxidase (*cydAB*), which is required for aerobic respiration, decreased *C. rodentium* numbers in colon contents during infection. Fatty acids, glycerol, pyruvate, lactate, and C4-dicarboxylates may be used during host infection since Enterobacteriaceae can catabolize C2-, C3-, C4-, and C5-carbon substrates (Eisenreich et al., 2015). Key metabolic processes, including amino acid biosynthesis, monosaccharide catabolism, metal ion homoeostasis, nutrient transport, and respiration, are elevated during *C. rodentium* infection (Connolly et al., 2018). Following carbohydrate deficit, *C. rodentium* relies on gluconeogenic substrate acquisition and substrate metabolism through TCA

cycle, both of which are necessary for fitness within the gut biogeography (Fernández-Veledo & Vendrell, 2019). A decrease in obligatory anaerobes, which are involved in the breakdown of dietary fibre and eventually reduce the availability of monosaccharides, is a sign of intestinal inflammation. In such an environment *C. rodentium* to reprogram its metabolic pathways to use other nutrition sources, including amino acids and outcompetes commensal bacteria (Kitamoto et al., 2020).

1.4.4 Quorum sensing during Host-pathogen interaction

Bacteria use quorum sensing (QS) for cell-to-cell communication which enables coordination of group behaviour as a response to environmental changes. In *E. Coli* O157:H7, QS systems have been identified as key regulatory mechanisms that govern the expression of several cellular activities, including motility, adhesion to epithelial cells, and flagellation (Barrasso et al., 2020). The transcriptional factor LuxR identifies and binds to certain QS signalling molecules known as autoinducers in some Gram-negative bacterial species, including *E. coli* (Coulthrust et al., 2007).

Many proteobacteria encode the histidine kinase QseC, which has been extensively studied elsewhere (Barrasso et al., 2020). Qsec is a QS receptor, which plays a role in detecting the neurotransmitters epinephrine (Epi) and norepinephrine (NE) produced by the host as well as auto-inducers derived by bacteria (Fig. 1-6). Because *C. rodentium* carries the same LEE island as that of EHEC it was used to study the *in vivo* involvement of QseC sensing of Epi/NE in host colonization (Moreira et al., 2016). Mice lacking dopamine ß-hydroxylase (Dbh−/−), do not generate Epi/NE, and were not colonized by *C. rodentium* (Moreira et al., 2016). Similarly, the ability of *qseC* mutants to colonize the mouse gut was greatly reduced, emphasizing the significance of signal detection in host colonization (Moreira et al., 2016). Collectively these data demonstrated that QseC serves as an essential connection between host-derived signals (Epi and NE) and self-produced bacterial AI molecules (AI-3).

Recent studies have linked attenuation of disease in murine infected with *C. rodentium* with elevated 2-arachidonoyl glycerol (2-AG), which offered protection by activation of the pro-virulence receptor QseC (Ellermann et al., 2020). The findings support other studies showing 2-AG and anandamide host

endocannabinoids are involved in regulating gut physiology and several immune system components (Chiurchiù, 2016).

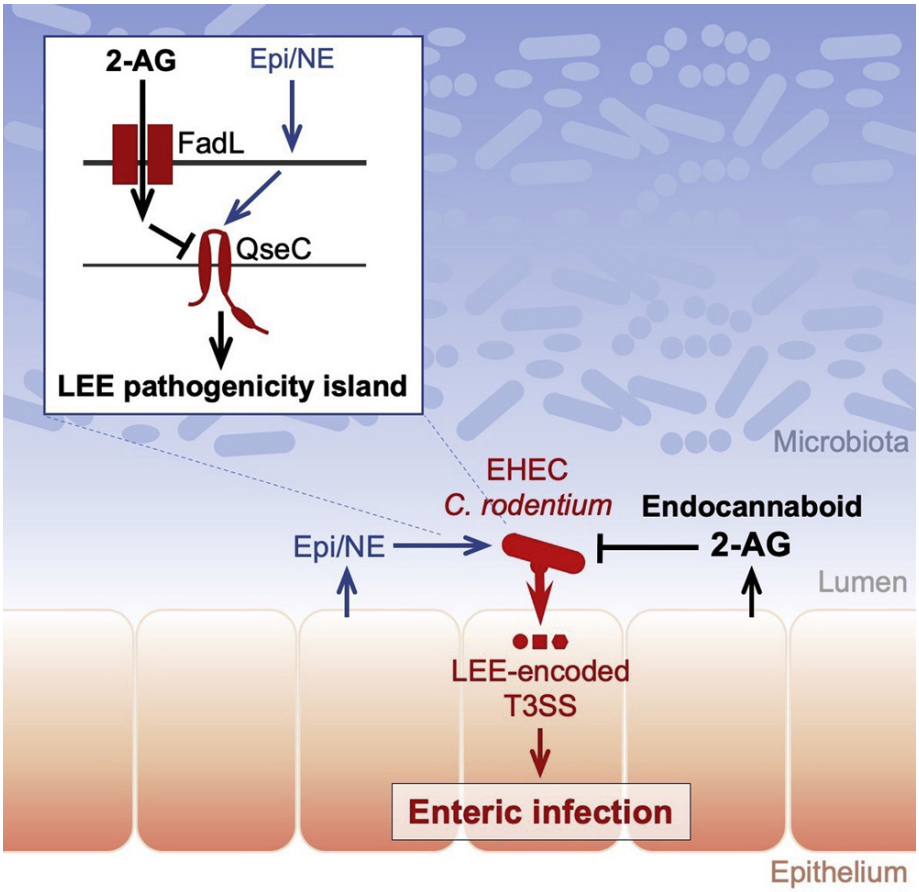

Fig. 1-6. QseC is a histidine kinase encoded by many proteobacteria. As a QS receptor, it plays a fundamental role in detecting both bacteria-derived auto-inducers and host-generated neurotransmitters, epinephrine and norepinephrine. Adapted from (Weigel & Demuth, 2016)

The microbiota produces indole, which is derived from tryptophan. *C. rodentium* was used to study the *in vivo* function of CpxA, a histidine kinase sensor, in host colonization (Kumar & Sperandio, 2019). It was discovered that *C. rodentium* senses indole through CpxA, which inhibits LEE expression. A correlation between indole concentrations *in vivo* and disease was also made possible by experiments utilizing mutants of *C. rodentium* and Bt with defective of indole synthesis (Kumar & Sperandio, 2019). As a result, indole's repressive effects are reversed in *C. rodentium* mutants missing TnaA (which synthesizes Indole from Tryptophan) and CpxA (Kumar & Sperandio, 2019). Taken together,

these investigations demonstrate the importance of inter-kingdom signalling during host colonization.

1.4.5 Dysbiosis during EHEC infection

The gut microbiota is dominated by the groups Firmicutes, Bacteroidetes, Actinobacteria, and Proteobacteria (Alam et al., 2020). Increase in abundance of *E. coli* during peak of infection causes dysbiosis due to several changes within the gut environment. Dysbiosis refers to an imbalance in the composition of the gut microbiota, changes in their metabolic processes, or changes in their distribution (Schierova et al., 2021). IBD, allergies, diabetes, obesity, and multiple sclerosis are some few of the conditions that may be accompanied by dysbiosis (Fomby & Cherlin, 2011). Some studies have associated dysbiosis with STEC infection and may increase the risk of several gut bacterial infections (Guevarra et al., 2023). A previous report showed that faeces of patients with STEC O26:H11 infection had lower levels of *Bifidobacteriales* and *Clostridiales* in their stools than did healthy individuals. *Bifidobacteriales* have been shown to have a protective effect in mice infected with EHEC O157:H7, via Nuclear factor kappa B (NF-κB) and suppressor of cytokine (SOCS) signalling pathways that help in controlling bacterial infections (Gigliucci et al., 2018). *Clostridium* spp. have been shown to regulate the intestinal inflammatory response brought on by lipopolysaccharides (LPS), indicating that they help prevent EHEC infection (Takahashi et al., 2004).

C. rodentium infections are associated with expansion of undifferentiated epithelial cells, thereby changing the expression profiles of host cells to favour oxidative phosphorylation and raise oxygen levels at the mucosal surface (Carson et al., 2020). This often results in a decline in the abundance Bacteroidetes and Firmicutes and a substantial increase in Enterobacteriaceae (Mullineaux-Sanders et al., 2017). In other studies, the increase in *Akkermansia* spp. abundance is linked with increase in levels of *C. rodentium* during peak of infection. *Akkermansia muciniphila* is a mucin degrading bacterium linked with anti-inflammatory immunological markers healthy subjects (Mengyu Zheng et al., 2023).

1.5 Transcription factors and virulence regulation

1.5.1 Transcription factors

Many biological processes, including DNA recombination, transcription, replication, and repair depend on interaction between DNA and proteins complexes (Menezes-Garcia et al., 2020). In addition, this aid pathogens to timely respond to ever the changing environment to guarantee their survival. One of the main mechanisms of regulation of gene expression is specific binding of transcription factors (TFs) to DNA (O'Boyle et al., 2020). TFs have been widely reported to regulate the expression and repression of several genes involved in transport and metabolism of different carbon sources, cell division, biofilm formation and as well as control virulence in pathogenic bacteria (Gao et al., 2021). Gene expression is the process by which DNA is transcribed into functional gene products such as proteins by RNA polymerase (J. Kim & Copley, 2007). Transcriptional regulation can occur at any stage of transcription which includes, (1) initiation, (2) elongation, and (3) termination (Denzer et al., 2020). While up to 10% of genes in genomes of bacteria encode transcription factors, their structure, function, and DNA-binding specificity are usually unknown (Fitzgerald et al., 2023; Suvorova et al., 2015).

1.5.2 PdhR a subfamily of GntR family of Transcription factors

GntR family of transcriptional regulators, forms one the largest group of prokaryotic TFs with members found in Archaea, the Bacteria, and the Eukarya. (Ogasawara et al., 2007). The members of this family are characterized by two functional domains made of a conserved N-terminal HTH (helix-turn-helix) DNA-binding domain but differ in the a C-terminal effector-binding and oligomerization (E-O) domain (Suvorova et al., 2015). The C-terminal does not bind to DNA but can change conformation of the DNA-binding domain by interacting with a specific effector, or a small organic molecule thereby altering the HTH motif, resulting in transcriptional regulation (Suvorova et al., 2015). Variations in the secondary structure of the E-O domain is used to categorize the GntR family and to date the family is grouped into seven subfamilies, that is, FadR, YtrA , MocR, , AraR, DevA, HutC, and PlmA (Rigali et al., 2002; Meiying Zheng et al., 2009).

The majority of known GNTR-family TFs belong to the FADR subfamily which is made up of 150-170 amino acids in length (Suvorova et al., 2015). The FADR subfamily of transcription factors undergo conformational changes that impact DNA binding after binding effectors, such as small chemical ligands such as carboxylic acids and regulates various metabolic pathways including, glycolate (GlcC), galactonate (DgoR), pyruvate (PdhR), lactate (LldR), or gluconate (GntR) (Suvorova et al., 2015). Of interest is the TF PdhR, that controls the regulation of genes involved in central metabolism through the repression the *pdh* operon (*pdhR-aceE-aceF-lpdA*) encoding pyruvate dehydrogenase complex (PDHc) and derepressed by the presence of pyruvate (Ogasawara *et al.*, 2007) (Fig.1-7). Although PdhR TFs plays a critical role in controlling carbon influx its role in bacterial virulence remains elusive. The catabolite repressor/activator protein Cra, which is involved in both metabolism and virulence in pathogenic organisms, has been comprehensively researched (Curtis et al., 2014; Njoroge et al., 2012). Cra also known as FruR, is a member of the LacI family that regulates the expression of its target genes by taking advantage of variations in sugar concentrations (Njoroge et al., 2012). Studies have showed that Cra regulates a large number of genes involved in gluconeogenic pathway, TCA cycle, glyoxylate shunt, and Entner-Doudoroff (ED) pathway and regulates glycolytic flux via sensing the concentration level of fructose-1,6-bisphosphate (Curtis et al., 2014; Sarkar et al., 2008; Yimga et al., 2006). Taken together we hypothesised that PdhR might have a similar role in enteric pathogen virulence.

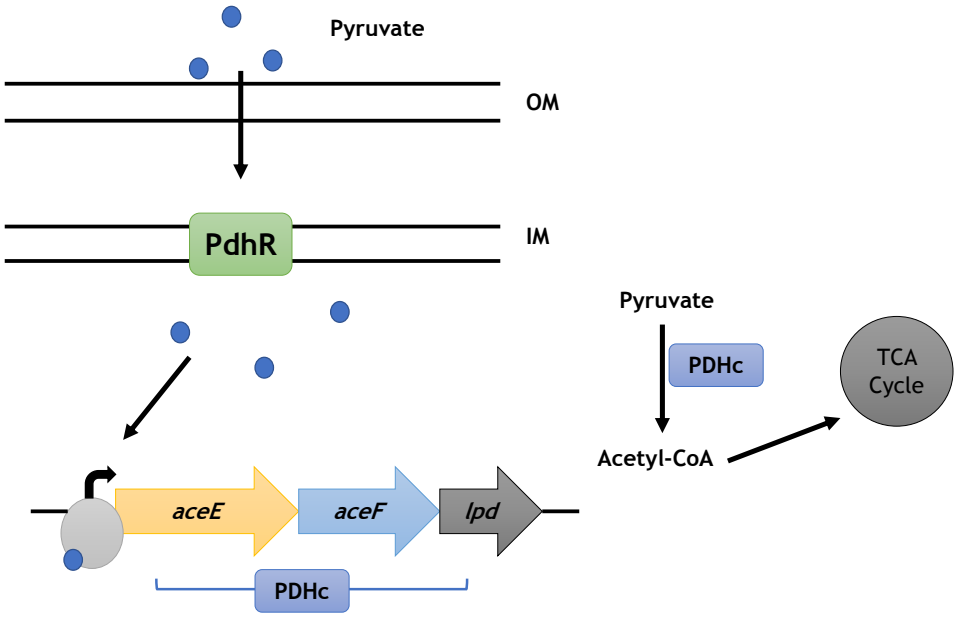

Fig. 1-7. Pyruvate dehydrogenase complex. The transcriptional regulator PdhR represenses the PDHc complex in the absence of pyruvate. When pyruvate is present, it interacts with PdhR which then derepresses the PDHc complex causing an increase in expression of the PDHc. PDHc breaks down pyruvate into Acetyl-CoA, which subsequently enters the TCA cycle.

1.5.3 Role of PdhR in Bacteria

Pyruvate dehydrogenase complex (PDHc) links the glycolysis and the tricarboxylic acid cycle (TCA) via the oxidative decarboxylation of pyruvate to acetyl-coenzyme A (CoA) (Fig. 1-7). The PDHc across the 3 domains of life is compresses of three catalytic enzymes, namely, pyruvate dehydrogenase, dihydrolipoamide acetyltransferase, and dihydrolipoamide dehydrogenase (Göhler et al., 2011). Undoubtedly, the PDHc plays an important role in bacterial physiology, and hence it is tightly regulated. Many studies have implicated PdhR in regulating *ndh* encoding NDH-2 and the *cyo* operon (*cyoABCDE*) encoding Cyt bo3 involved in the respiratory chain (Göhler et al., 2011). This is not surprising considering that the PDHc reaction yields NADH, which must be re-oxidized by respiration. PdhR is now recognized as a global regulator controlling more than 20 genes largely involved in aerobic glucose metabolism in *E. coli* (Anzai et al., 2020).

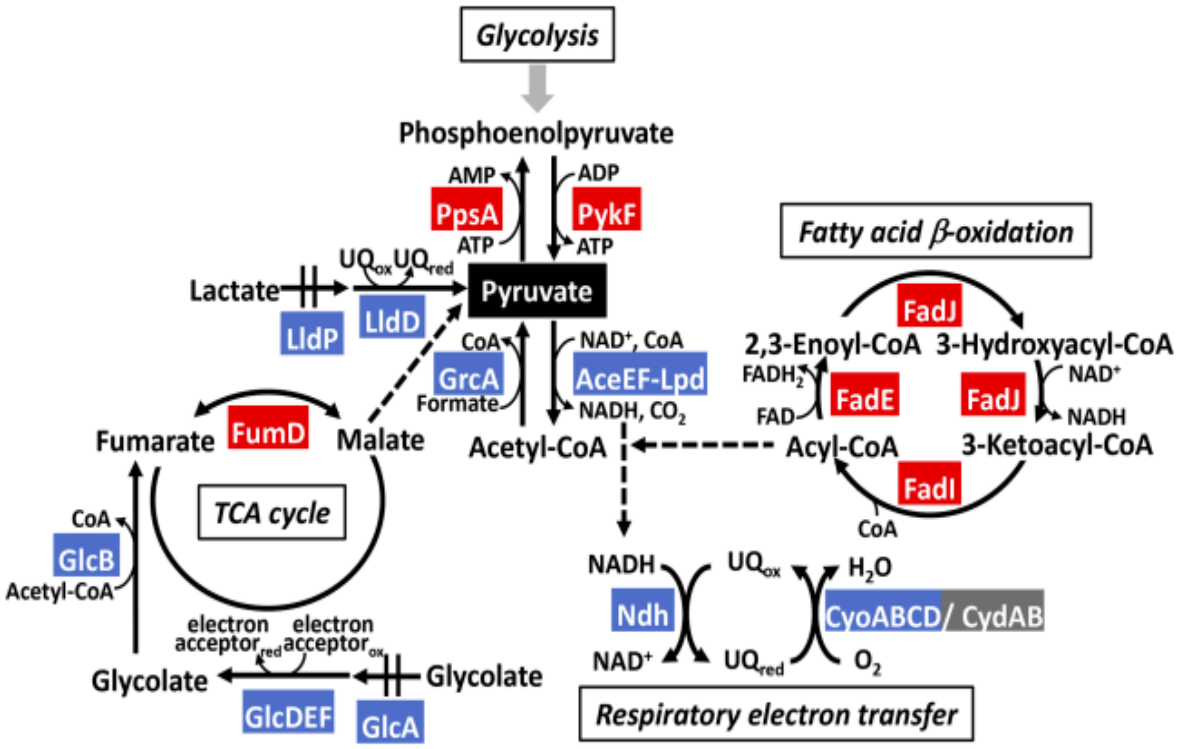

Fig. 1-8. PdhR regulon. PdhR regulates genes involved in carbon catabolism from pyruvate dehydrogenase complex to respiratory electron transport and TCA cycle. Genes repressed by PdhR are shown in blue while the genes activated by PdhR are shown in red. The figure was adapted from (Anzai et al., 2020).

Thus, it was speculated that a *pdhR* knockout may enhance central metabolism by increasing the activities of PDHc, NDH-2, and Cyt bo3 during aerobic growth of *E. coli* on glucose. Indeed, in *E. coli* K12 metabolism in the *pdhR* mutant reduced acetate secretion was observed while there was an increase TCA cycle flux compared WT strain. The phenotype is fundamental in an industrial setup as the *pdhR* mutant strain can be used to reduce acetate accumulation, which is an undesirable metabolite in bioprocessing due to its toxicity (Maeda et al., 2017). Moreover, it provides a better alternative in the efficiency of fermentative production systems using *E. coli*. Interestingly, PdhR has recently been linked to flagellar regulation via RpoF which its regulation is under the control of PdhR, suggesting that flagella regulation is controlled by the level of pyruvate concentration (Anzai et al., 2020).

1.6 Aims of project

Previous work by Connolly et al. 2018, identified several transcription factors which were regulated by the pathogen *C. rodentium* during colonisation of the murine gastrointestinal tract, and of particular interest was PdhR encoded by

the *pdhR* gene. Pyruvate dehydrogenase catalyses the formation of acetyl-CoA from pyruvate which subsequently enters the citric acid cycle which is critical for bacterial survival. *C. rodentium* colonisation is dependent on T3SS encoded by the LEE. The T3SS regulation centres on sequential expression of the LEE in response to multitude of signals and cues that are encountered in the intestinal environment of the host. This prompted us to propose that this regulator, could be important in regulation of both metabolism and, directly or indirectly in virulence of *C. rodentium*. Moreover, given that *Citrobacter* shares a similar LEE island to *E. coli* O157, the following aims were developed to probe the role of this transcriptional regulator in EHEC virulence:

1. To elucidate the physiological role of the PdhR in O157:H7.
2. To investigate the regulation of O157:H7 LEE by PdhR.
3. To establish whether PdhR is required for enteric pathogen colonisation.

Chapter 2 describes the materials and methods used in this study. Chapter 3 discusses the potential role of PdhR in O157:H7 virulence. Chapter 4 discusses the regulation and validation of PdhR on O157:H7 LEE-depended virulence. Finally, Chapter 5 provides insights into the importance of PdhR in host colonisation.

Chapter 2: Material and Methods

2.1 Chemicals and growth media

2.1.1 Chemicals and reagents

All chemicals used in this study were purchased from Invitrogen, Sigma Aldrich, Merck, and Thermo Fisher Scientific unless otherwise stated. PCR primers, 1 kb Plus DNA ladder, and SeeBlue Plus 2 protein standards were all purchased from Invitrogen. Chemiluminescent Western Blot Substrates, including, Pierce ECL, and Pierce ECL Plus were all purchased from Thermo Fisher Scientific. Restriction enzymes were purchased from New England Biolabs. Antibodies: Anti-6X His tag, and anti-mouse HRP conjugates were purchased from Sigma-Aldrich.

2.1.2 Growth media and Buffers

All growth media and buffers were prepared using nuclease-free water (NucH2O), distilled deionized water (ddH_2O) and autoclaved or filter sterilized (0.2 µM). To prepare solid media, 15 g/L agar to the liquid medium before autoclaving sterilization. All growth media and buffers were prepared to 1 litre unless otherwise stated. Then the pH was adjusted, and the medium was adjusted with ddH2O to 1 litre before sterilization. MEM-HEPES and DMEM tissue culture media were purchased from Sigma-Aldrich and stored at 4℃.

Table 2-1 LB recipe;pH 7.5

Ingredient	Quantity
Tryptone	10 g
Yeast extract	5 g
NaCl	10 g

Table 2-2 SOC Media (1L; pH 7.0)

Ingredient	Quantity
Tryptone	20 g
Yeast extract	5 g
NaCl	0.5 g
1M KCl	10 mL
1M $MgSO_4$	2 mL

* SOC components were added to 950 mL of ddH_2O, pH adjusted, and then topped up to 1 L and autoclaved. Then 5 ml of sterile $MgCl_2$ (2M) and 20 ml of glucose (1M) were added to the medium before use.

Table 2-3 M9 minimal media recipe; pH 7.5

Ingredient	Quantity
M9 Salts (5X)	40 mL
1M $MgSO_4$	200 µL
1M $CaCl_2$	10 µL
Glucose (20%)	5 ml

M9 media was made to a final volume of 200 mL with ddH_2O.

Table 2-4 Phosphate buffered saline Tween (PBST)

Ingredient	Quantity
10X phosphate buffered Saline	100 mL
Tween-20	0.4 mL

Table 2-5 Tris-acetate-EDTA (TAE)

Ingredient	Quantity
Tris	242 g
Acetic acid (glacial)	57.1 mL
0.5M EDTA (pH 8.0)	100 mL

Table 2-6 Tris buffered saline (TBS)

Ingredient	Quantity
Tris-HCl (pH 7.5)	20 mM
NaCl	150 mM

Table 2-7 Tris- EDTA (TE) buffer

Ingredient	Quantity
Tris-HCl (pH 7.5)	10 mM
EDTA	1 mM

Table 2-8 Tris- Western blot stripping buffer

Ingredient	Quantity
Glycine	3.75 g
SDS	0.25 g
Tween-20	2.5 mL

Table 2-9 Coomassie blue

Ingredient	Quantity
Methanol	500 mL
Coomassie blue	2 g
Acetic Acid	100 mL
ddH_20	400 mL

Table 2-10 Coomassie blue de-stain

Ingredient	Quantity
Methanol	100 mL
Acetic Acid	100 mL
ddH_20	800 mL

Table 2-11 4X sample buffer (100 mL)

Ingredient	Quantity
Tris-HCl (pH 6.8)	8.52 g
Bromophenol blue	0.43 g
Glycerol	42.6 mL
ß-mercaptoethanol	4.97 mL

Table 2-12 4% PFA (500 mL)

Ingredient	Quantity
Paraformaldehyde (PFA)	20 g
10X PBS	50 mL
1M NaOH	5 mL
ddH_20	445 mL

*PFA was dissolved in PBS and 250 mL ddH2O with gradual heating. Temperature was monitored to not exceed 50℃. After the PFA had completely dissolved, NaOH was added, and the volume was made up to 500 ml with ddH_2O. Then it was filter sterilized (0.2 µM) after it the liquid cooled down, and aliquoted into sterile 50 ml centrifuge tubes and finally stored at-20 ℃.

Table 2-13 His-tag buffer (Buffer A)

Ingredient	Quantity
Tris	50 mM
NaCl	0.5 M
Glycerol	5 %

Table 2-14 His-tag elution buffer (Buffer B)

Ingredient	Quantity
Tris	50 mM
NaCl	0.5 M
Imidazole	5 mM
Glycerol	5 %

2.1.3 Growth media supplements

Antibiotics were prepared in either ethanol or ddH_2O, according to manufactures recommendations (Table 2-15). For antibiotics prepared in water, they were filter sterilised (0.2 µM) before use. Stocks were made by aliquoting prepared solutions in 1mL Eppendorf tubes and stored at -20℃.

Table 2-15 Antibiotic stock concentrations

Antibiotic	**Stock (mg/mL)**	**Solvent**	**Final concentration (µg/mL)**
Chloramphenicol	25	Ethanol	25
Ampicillin	100	ddH_2O	100
Kanamycin	10	ddH_2O	50
Hygromycin	100	ddH_2O	100
Nalidixic acid	30	ddH_2O	30

2.2 Strains and plasmids used in these studies

For the purpose of this project, bacterial strains and most plasmids were sourced from Roe laboratory inventory culture collection, while some plasmids were purchased from commercially available deposits.

Table 2-16 List of bacterial strains used in these studies

Strain	Characteristics	Source
EHEC TUV93-0	Wild type *E. coli* 0157:H7(Stx negative)	Roe lab inventory
Δ*yfeC*	TUV93-0 *ΔyfeC* knockout (Cmr^R)	This study
Δ*pdhR*	TUV93-0 Δ*pdhR* knockout (Cmr^R)	This study
Δ*bssS*	TUV93-0 Δ*bssS* knockout (Cmr^R)	This study
Δ*rcnR*	TUV93-0 Δ*rcnR* knockout (Cmr^R)	This study
ICC168	Wild type *C. rodentium*	Roe lab inventory
ICC169	Wild type *C. rodentium* (Nalidixic acid resistant)	Roe lab inventory
C. rodentium Δ*yfeC*	ICC169 *yfeC* knockout	This study
C. rodentium Δ*pdhR*	ICC169 *pdhR* knockout	This study
C. rodentium Δ*rcnR*	ICC169 *rcnR* knockout	This study
C. rodentium Δ*bssS*	ICC169 *bssS* knockout	This study
BL21 (DE3)	Commercial *E. coli* expression strain	Invitrogen
DH5α	Commercial *E. coli* storage strain	Invitrogen

Table 2-17 Plasmids used in these studies

Strain	Characteristics	Source
pET-21a(+)	Plasmid for overexpression of N-terminal His tagged proteins (Kan^R)	Roe lab inventory
pET-21a(+)_*pdhR*	His-tag overexpression plasmid with CE10 derived *pdhR* inserted between NdeI and XhoI (Kan^R)	This study
pKD3	Template plasmid for Lambda Red mutagenesis (Kan^R)	Datsenko and Wanner., 2000.
pKD4	Template plasmid for Lambda Red mutagenesis (Kan^R)	Datsenko and Wanner., 2000.
pKD46	Template plasmid for Lambda Red mutagenesis (Kan^R)	Datsenko and Wanner., 2000.
pSIM18	Temperature inducible Red recombinase system; 42°C inducible; Hygromycin resistant	Chan et al. 2007
pAJR70	pACYC184 containing single *BamhI*/*KpnI* cloning site in-frame with eGFP (Cmr^R)	Roe lab inventory
prpsM: GFP	pAJR70 containing rpsM promoter fused to gfp+ (Cml^R)	Roe lab inventory
p*LEE1*: GFP	TUV93-0 LEE1 promoter region cloned in-frame into pAJR70 (Cml^R)	This study
p*LEE1*P1: GFP	TUV93-0 distal LEE1 promoter region (Promoter 1) cloned in-frame into pAJR70 (Cml^R)	This study

p*LEE1*P2: GFP	TUV93-0 proximal LEE1 promoter region (Promoter 2) cloned in-frame into pAJR70 (Cml^R)	This study
Cr*LEE1*: GFP	*C. rodentium* LEE1 promoter region cloned in-frame into pAJR70 (Cml^R)	This study
p*pdhR*	pACYC184-*pdhR* complementation construct	This study
p*yfeC*	pACYC184-*yfeC* complementation construct	This study
p*rcnR*	pACYC184-*rcnR* complementation construct	This study
p*bssS*	pACYC184-*bssS* complementation construct	This study

2.3 Phenotypic characterisation techniques

2.3.1 Bacterial growth curves and calculation colony forming units (CFU)

Bacteria were inoculated using single colonies and grown overnight (16 h) in 5 mL of Luria-Bertani broth (LB) at 37°C and 200 rpm (New Brunswick Scientific controlled environment incubator shaker). The next day, the culture was then diluted at a concentration of 1/100 in fresh pre-warmed (37°C) media containing necessary antibiotics or supplements until the desired OD_{600} was reached. To obtain a growth curve, triplicate measurements of OD_{600} were recorded every hour for 8 hours.

CFU/mL from liquids and CFU/g from solids were determined from an aliquot of the bacterial suspension and serially diluted in PBS. For each sample, 20 µL of each dilution was spotted onto a solid LB agar plate, and the plate was dried and incubated overnight at 28°C. Then the CFU was calculated by counting the individual colonies within each spot and multiplying by the appropriate dilution factor. Serial dilutions were performed in triplicate, and CFU was determined as the average number of colonies at a given dilution.

2.3.2 Bacterial motility assay

The motility assay was carried as previously described by Wolfe and Berg (1989). Fifty µL of overnight bacterial culture was inoculated into 5 mL pre-warmed (37˚C) MEM-HEPES media with no supplements and grown to an OD of 0.6 (OD_{600}) at 37˚C, 220 rpm. Five µL of this culture was transferred to the centre of 0.25% Tryptone agar plate and incubated for 8 hours at 30˚C and all test samples were tested in triplicates. The diameter of the bacterial swarm was measured and recorded.

2.3.3 Biofilm assay

The assay for biofilm formation was carried out using a method reported elsewhere (Koseoglu et al., 2006). Polyvinyl chloride 96-well microtiter plates (BD Science, USA) were used as the abiotic surfaces for biofilm formation. Briefly, 1.3 µL of overnight bacterial cultures were inoculated into 130 µL of media with appropriate supplements and antibiotics were required. The cultures were then incubated at 37˚C without agitation for 24 hours. Following incubation, the microtiter plates were rinsed thoroughly with PBS and the cells were stained with 0.1% w/v crystal violet (CV) for 15 minutes at room temperature. After staining at room temperature, the CV was removed, and the wells were rinsed three times with PBS. Resuspend the remaining stain using 130 µL 30% acetic acid for 15 mins. The absorbance of the solubilized dye was measured at 550 nm.

2.3.4 BIOLOG phenotype microarrays

The BIOLOG phenotype microarray (PM) test on EHEC WT and Δ*pdhR* strains was conducted with PM carbon sources following the manufacturer's instruction. The PM plates (Biolog Inc., Hayward, CA, USA) used consisted of 96-well plates containing different sources of carbon (PM1 and PM2). Bacterial cultures were grown overnight at 37˚C on Biolog universal growth (BUG) + B agar plate. Single colonies were picked from the agar surface and suspended in inoculating fluid (IF) containing the indicator dye tetrazolium violet. The IF-0 media was used for plates PM1 and PM2 to resuspend carbon sources. All PM plates were inoculated with cell culture suspensions at 100 µL/well and incubated in an OmniLog incubator (Biolog Inc.) at 37˚C for 30 hours. Three independent PM tests were performed on EHEC WT and Δ*pdhR* by varying the carbon source for

the plates PM1 and PM2. The PM data was analysed using the opm R package (Waligora et al., 2014), and the bacterial cell growth in each well was classified into negative, weak and positive growths.

2.3.5 Storage of bacterial strains

For each bacterial strain, a single colony was selected from the LB plate and grown overnight (16 h) at 37°C and 200 rpm (New Brunswick Scientific controlled environment incubator shaker). 0.5 ml of this culture was placed in a sterile tube and 1 ml of sterile glycerol (40%) and peptone (2%) was added. Stocks were labelled accordingly then frozen at -80°C.

2.4 Molecular biology

2.4.1 Polymerase chain reaction (PCR) and primers

Primers used in this study were designed using Primer3web. Primers were designed to a length of approximately 20 bp in length (unless otherwise stated) and a melting temperature (Tm) of 50 to 72°C. Primers involved in cloning and Lambda Red mutagenesis were designed with relevant base flanks. All primers were ordered from Life Technologies and provided as lyophilized samples at a concentration of 100 µM. A 10 µM working stock as a standard was prepared for use in PCR reactions.

GoTaq Green Master Mix (Promega) or Q5 High-Fidelity 2X Master Mix (NEB) were used for application. A single colony of bacteria was mixed with 50 µl of NucH_2O or purified DNA template were used as a template for the PCR reaction. PCR Mix was then loaded on Eppendorf Mastercycler Nexus gradient thermocyclers.

Table 2-18 Oligonucleotides used in this study

Primer name	Description	Sequence (5' -3')
Lambda Red mutagenesis		
pdhR-Red-F	Forward for pdhR lambda red mutagenesis in TUV93-0	GAAATTGGTAAGACCAATTGACTTCGGCAAGTGGC TTAAGACAGGAACTCGTGTAGGCTGGAGCTGCTTC
pdhR-Red-R	Reverse for pdhR lambda red mutagenesis in TUV93-0	TATGCGCTTGATTTACAACATCTTCTGGATAATTTT TACCAGAAAAATCACATATGAATATCCTCCTTAG
pdhR-184-F	Check forward for pdhR lambda red mutagenesis in TUV93-0	TGAAGTCAGCCCCATACGATTCAAGAATAATGGTA TGCGGCA
pdhR-184-R	Check reverse for pdhR lambda red mutagenesis in TUV93-0	CAATCCATGCCAACCCGTTCGGGAAACGTTCTGAC ATGGG
bssS-Red-F	Forward for bssS lambda red mutagenesis in TUV93-0	GCATTGAACCTCGAATAACGTTGTCTAGTAACACG AATTAG GGGGCCATGGTGTAGGCTGGAGCTGCTTC
bssS-Red-R	Reverse for bssS lambda red mutagenesis in TUV93-0	AATGGTAAAGGCACCGGTGAGGTGCCTTTTGGGT GGATGG TCATGTCATGCATATGAATATCCTCCTTAG
bssS -184-F	Check forward for bssS lambda red mutagenesis in TUV93-0	TGAAGTCAGCCCCATACGATTTATCGGTTATTGGC GCGAC
bssS -184-R	Check reverse for bssS lambda red mutagenesis in TUV93-0	CAATCCATGCCAACCCGTTCCGTCGGTCATAAGCA CGTTT
yfeC-Red-F	Forward for yfeC lambda red mutagenesis in TUV93-0	GTGCTATAAAATGAACTACTAATAGACCCACATACA TTCAGGGAATTGTTGTGTAGGCTGGAGCTGCTTC
yfeC -Red-R	Reverse for yfeC lambda red mutagenesis in TUV93-0	CATTCAGCCAGTTCTTCGGTGGTCATTTTATTGCG TAATCTTTTCATACCCATATGAATATCCTCCTTAG
yfeC 184-F	Check forward for yfeC lambda red mutagenesis in TUV93-0	TGAAGTCAGCCCCATACGATCCCGTCACGTAAAGC TTGTC
yfeC -184-R	Check reverse for yfeC lambda red mutagenesis in TUV93-0	CAATCCATGCCAACCCGTTCCAAACTTGCGTATCGA CCAGA
rcnR-Red-F	Forward for rcnR lambda red mutagenesis in TUV93-0	TAGATTAATAGTGCTATGATTTTTCATGTTCTTGTT AACCAGGTGTTGCCGTGTAGGCTGGAGCTGCTTC
rcnR -Red-R	Reverse for rcnR lambda red mutagenesis in TUV93-0	GTCACTTGTCCCTCTATTTATTGCCTCAACTACGGC CATATTAGGCACTTCTAAGGAGGATATTCATATG
rcnR -184-F	Check forward for rcnR lambda red mutagenesis in TUV93-0	TGAAGTCAGCCCCATACGATCGCCTGTTTAATGGT GCCTT
rcnR -184-R	Check reverse for rcnR lambda red mutagenesis in TUV93-0	CAATCCATGCCAACCCGTTCTGACGGTAGAAATCC AGAGC
pdhR-C-Red-F	Forward for pdhR lambda red mutagenesis in ICC169	TAATTGGTAAGACCAATTGACTCCGGGCAAATGGC TTAAGACAGGACATCGTGTAGGCTGGAGCTGCTTC
pdhR-C-Red-R	Reverse for pdhR lambda red mutagenesis in ICC169	TTTTGCGCTTTATTAACAACATCTTCTGGTAAACGT ACTGCCAGAAAAAACATATGAATATCCTCCTTAG
pdhR-C-184-F	Check forward for pdhR lambda red mutagenesis in ICC169	TGAAGTCAGCCCCATACGATCAGTGGAATGCACCT GGTTT
pdhR-C-184-R	Check reverse for pdhR lambda red mutagenesis in ICC169	CAATCCATGCCAACCCGTTCTGTCCCATTAAACTTT CGTCGG
bssS- C-Red-F	Forward for bssS lambda red mutagenesis in ICC169	GCATTGAACCTCGAATAACGTTGTCTAGTAACACG AATTAGGGGGCCATGGTGTAGGCTGGAGCTGCTC
bssS- C-Red-R	Reverse for bssS lambda red mutagenesis in ICC169	AATGGTAAAGGCACCGGTGAGGTGCCTTTTGGGT GGATGGTCATGTCATGCATATGAATATCCTCCTTG

bssS - C-184-F	Check forward for bssS lambda red mutagenesis in ICC169	TGAAGTCAGCCCCATACGATTTATCGGTTATTGGC GCGAC
bssS - C-184-R	Check reverse for bssS lambda red mutagenesis in ICC169	CAATCCATGCCAACCCGTTCCGTCGGTCATAAGCA CGTTT
yfeC- C-Red-F	Forward for yfeC lambda red mutagenesis in ICC169	GTGCTATAAAATGAACTACTAATAGACCCACATACA TTCAGGGAATTGTTGTGTAGGCTGGAGCTGCTTC
yfeC - C-Red-R	Reverse for yfeC lambda red mutagenesis in ICC169	CATTCAGCCAGTTCTTCGGTGGTCATTTTATTGCG TAATCTTTTCATACCCATATGAATATCCTCCTTAG
yfeC -C-184-F	Check forward for yfeC lambda red mutagenesis in ICC169	TGAAGTCAGCCCCATACGATCCCGTCACGTAAAGC TTGTC
yfeC - C-184-R	Check reverse for yfeC lambda red mutagenesis in ICC169	CAATCCATGCCAACCCGTTCCAAACTTGCGTATCGA CCAGA
rcnR- C-Red-F	Forward for rcnR lambda red mutagenesis in ICC169	TAGATTAATAGTGCTATGATTTTTCATGTTCTTGTT AACCAGGTGTTGCCGTGTAGGCTGGAGCTGCTTC
rcnR - C-Red-R	Reverse for rcnR lambda red mutagenesis in ICC169	GTCACTTGTCCCTCTATTTATTGCCTCAACTACGGC CATATTAGGCACTTCTAAGGAGGATATTCATATG
rcnR - C-184-F	Check forward for rcnR lambda red mutagenesis in ICC169	TGAAGTCAGCCCCATACGATCGCCTGTTTAATGGT GCCTT
rcnR - C-184-R	Check reverse for rcnR lambda red mutagenesis in ICC169	CAATCCATGCCAACCCGTTCTGACGGTAGAAATCC AGAGC
Gibson assembly and cloning		
pAJR70_fwd	Forward for pACYC-184 linearisation	ACGATGCGTCCGGCGTAGAGGATCC
pAJR70_rev	Forward for pACYC-184 linearisation	GCCCTTGCTCACCATGGTACC
pdhR_fwd	Forward for pdhR for gibson assembly	ACGATGCGTCCGGCGTAGAGGATCCAACCCCTCTC AATATGCAG
pdhR_rev	Reverse for pdhR for gibson assembly	GCCCTTGCTCACCATGGTACCCCAGTTGCTGCTCA ATCAC
pdhR_fwd_Check	Check forward for pdhR for gibson assembly	ATCGGTGATGTCGGCGATAT
pdhR_rev_Check	Check reverse for pdhR for gibson assembly	TCCAGCTCGACCAGGATG
pAJR71_partial_fwd	Forward for pAJR71 linearisation	CGCTAATAGCTTAAAATATTAAAGC
pAJR71_partial_rev	Forward for pAJR71 linearisation	CTCATGAGCGCTTGTTTC
LEE1_P1_fwd	Forward amplification of LEE1 promoter 1 from pAJR71	CCGAAACAAGCGCTCATGAGCTGTGGCGCCGGTGA TGC
LEE1_P1_rev	Reverse amplification of LEE1 promoter 1 from pAJR71	AATATTTTAAGCTATTAGCGAAATCATCTCGTTAAC AAAC GACTTTAATAATTGCATTTCCATTTAG
LEE1_P2_fwd	Forward amplification of LEE1 promoter 2 from pAJR71	CCGAAACAAGCGCTCATGAGTAATGTATTTTACACA TTAG AAAAAAGAG
LEE1_P2_rev	Reverse amplification of LEE1 promoter 2 from pAJR71	CTCATGAGCGCTTGTTTC
LEE1_P_Check-fwd	Check forward for LEE1 for gibson assembly	AAGGAATGGTGCATGCAAGG
LEE1_P_Check_rev	Check reverse for LEE1 for gibson assembly	GAACTTCAGGGTCAGCTTGC
pdhR_NedI-F	Forward pdhR cloning into pET21	GATATACATATGGCCTACAGCAAAATCCG
pdhR_XhoI-R	Reverse pdhR cloning into pET21	GTGGTGCTCGAGATTCTTTCGTTGCTCCAGACG

Site directed Mutagenesis		
Mutation_Sub1-Frwd	Forward for substitution 1 mutations gibson assembly	TGATTAATTGCCAACTCTTCCTGATAAGGTCG
Mutation_Sub1_Rev	Reverse for substitution 1 mutations gibson assembly	AATGATATAAATTATGTGAGATAAC
Mutation_Sub2_Frwd	Forward for substitution 2 mutations gibson assembly	AGCAAGGTCGCTAATAGCTTAAAATATTAAAG
Mutation_Sub2_Rev	Reverse for substitution 2 mutations gibson assembly	GAAGAGGACCAACAATTAATCAAATG
Mutation_Sub3_Frwd	Forward for substitution 3 mutations gibson assembly	CCTTCAGCAAGGTCGCTAATAGCTTAAAATATTAAAG
Mutation_Sub3_Rev	Reverse for substitution 3 mutations gibson assembly	AAGTTGGTGATTAATCAAATGATATAAATTATGTGAGATAAC
Mutation_Sub4_Frwd	Forward for substitution 4 mutations gibson assembly	CTTCCTCTGATAAGGTCGCTAATAG
Mutation_Sub4_Rev	Reverse for substitution 4 mutations gibson assembly	TTGGTGATTAATCAAATGATATAAATTATGTGAG
Mutation_Del1_Frwd	Forward for deletion 1 mutations gibson assembly	CCTTCCTGATAAGGTCGC
Mutation_Del1_Rev	Reverse for deletion 1 mutations gibson assembly	CAATTAATCAAATGATATAAATTATGTGAG
Mutation_Del2_Frwd	Forward for deletion 2 mutations gibson assembly	GATAAGGTCGCTAATAGC
Mutation_Del2_Rev	Reverse for deletion 2 mutations gibson assembly	AAGGACCAACAATTAATCAAATG
Mutation_Del3_Frwd	Forward for deletion 3 mutations gibson assembly	AAGGTCGCTAATAGCTTAAAATATTAAAG
Mutation_Del3_Rev	Reverse for deletion 3 mutations gibson assembly	ATTAATCAAATGATATAAATTATGTGAGATAAC
TUV93-0 RT-qPCR Primers		
Ler_qPCR_F	Forward for *ler* gene expression using RT-qPCR	CGAGAGCAGGAAGTTCAAAGTG
ler_qPCR_R	Reverse for *ler* gene expression using RT-qPCR	ACACCTTTCGATGAGTTCCG
escC_qPCR_F	Forward for *escC* gene expression using RT-qPCR	CTGAAGACAATGGCAAGTAATGG
escC_qPCR_R	Reverse for *escC* gene expression using RT-qPCR	ACTGCATTAAGACGTGGATCAG
escV_qPCR_F	Forward for *escV* gene expression using RT-qPCR	GAGTGCAAAAGGAAAGCCAG
escV_qPCR_R	Reverse for *escV* gene expression using RT-qPCR	ATGATACCAGCAATAGCGTCC
tir_qPCR_F	Forward for *tir* gene expression using RT-qPCR	GAGGGAGTCAAATAGCGGTG
tir_qPCR_R	Reverse for *tir* gene expression using RT-qPCR	ATCTGAACGAAGGCTGGAAG
eae_qPCR_F	Forward for *eae* gene expression using RT-qPCR	TGGGATGTTCAACGGTAAGTC
eae_qPCR_R	Reverse for *eae* gene expression using RT-qPCR	TTTAACCTCAGCCCCATCAC

espA_qPCR_F	Forward for *espA* gene expression using RT-qPCR	AGCTATTTGAGGAACTCGGTG
espA_qPCR_R	Reverse for *espA* gene expression using RT-qPCR	CATCTTTTGTGCCGTGGTTG
espB_qPCR_F	Forward for *espB* gene expression using RT-qPCR	GGTCAAGGCTACGGAAAGTG
espB_qPCR_R	Reverse for *espB* gene expression using RT-qPCR	TCTTCAGCAAAGTCAGAGGC
espZ_qPCR_F	Forward for *espZ* gene expression using RT-qPCR	GGAAGCAGCAAATTTAAGCCC
espZ_qPCR_R	Reverse for *espZ* gene expression using RT-qPCR	CACCCCTGTCTTCTCATCCA
ndH_qPCR_F	Forward for *ndH* gene expression using RT-qPCR	AAATTGTGATTGTCGGCGGC
ndH_qPCR_R	Reverse for *ndH* gene expression using RT-qPCR	AGGTGGCTGTGGTTACGATC
gapA_qPCR_F	Forward for housekeeping control (*gapA*) used in RT-qPCR	TTTCCGTGCTGCTCAGAAAC
gapA_qPCR_R	Reverse for housekeeping control (*gapA*) used in RT-qPCR	GGCCGTGAGTGGAGTCATAT
ICC169 LEE genes RT-qPCR primers		
ler qPCR F	Forward for *ler* gene expression using RT-qPCR	GAGCAGGAGATTCAAACTGT
ler qPCR R	Reverse for *ler* gene expression using RT-qPCR	TACCCCAGTTCTTGTAAGGT
grlA qPCRF	Forward for *grlA* gene expression using RT-qPCR	GTAAATTGCAGGAGAAATGG
grlA qPCRR	Reverse for *grlA* gene expression using RT-qPCR	AATAAATGACGCTCTCCTCA
espD qPCR F	Forward for *espD* gene expression using RT-qPCR	GCTACGGCTATTTCAGGTAT
espD qPCR R	Reverse for *espD* gene expression using RT-qPCR	GATGGGGCAAAAGATTTAAC
eae qPCR F	Forward for *eae* gene expression using RT-qPCR	TTATTCATGGTTTTTGCACC
eae qPCR R	Reverse for *eae* gene expression using RT-qPCR	AAAACAATCCTAAACCAGCA
mpc qPCR F	Forward for *mpC* gene expression using RT-qPCR	TTTTATTGAGGTAATTGGTGG
mpc qPCR R	Reverse for *mpC* gene expression using RT-qPCR	AGGGCACTGAAGAAAGAAA
espZ qPCR F	Forward for *espZ* gene expression using RT-qPCR	CTGCAATAAATGGAAATGGT
espZqPCRR	Reverse for *espZ* gene expression using RT-qPCR	AAAACTCTGACATTGCGACT
espI qPCR F	Forward for *espL* gene expression using RT-qPCR	TGAACATTCAACCGAACATA
espI qPCR R	Reverse for *espL* gene expression using RT-qPCR	GCTAGAGACAGGCACTTGTT

espS qPCR F	Forward for *espS* gene expression using RT-qPCR	TAGGTATTCTTGGCAAAAGG
espS qPCR R	Reverse for *espS* gene expression using RT-qPCR	TCCTACGGATTTTTCACCTA
espO qPCRF	Forward for *espO* gene expression using RT-qPCR	GGCCTGTAATTGATAAACCA
espO qPCRR	Reverse for *espO* gene expression using RT-qPCR	TGGTCCTTCTGTTTA TGACC
espM3 qPCR F	Forward for *espM3* gene expression using RT-qPCR	GTTGTAAAATGCTCAATGGG
espM3 qPCR R	Reverse for *espM3* gene expression using RT-qPCR	TTTAGTACTCTGCCGGGTTA
EMSA primers		
EMSA rpoS 1 F	Forward for EMSA for validation of *pdhR* binding at *rpoS* fragment 1 promoter region	CGGAACAGCGCTTCGATATT
EMSA rpoS 1 R	Reverse for EMSA for validation of *pdhR* binding at *rpoS* fragment 1 promoter region	GGTTTGCTGGGGTACGAAG
EMSA rpoS 2 F	Forward for EMSA for validation of *pdhR* binding at *rpoS* fragment 2 promoter region	AGGTAATGCGCTCGTTAAGAC
EMSA rpoS 2 R	Reverse for EMSA for validation of *pdhR* binding at *rpoS* fragment 2 promoter region	TCACATCGTAAAGGAGCTGAAC
EMSA rpoS 3 F	Forward for EMSA for validation of *pdhR* binding at *rpoS* fragment 3 promoter region	TCTGACTCATAAGGTGGCTCC
EMSA rpoS 3 R	Reverse for EMSA for validation of *pdhR* binding at *rpoS* fragment 3 promoter region	CCAGTTCAACACGCTTGCAT
EMSA_ler_P1_FWD	Forward for EMSA for validation of *pdhR* binding at *ler* fragment 1 promoter region	CTGTAACTCGAATTAAGTAGAG
EMSA_ler_P1_REV	Forward for EMSA for validation of *pdhR* binding at *ler* fragment 1 promoter region	AAATCATCTCGTTAACAAACGACTTTAATAATTGCA TTTCCATTTAG
EMSA_LEE1_P2_FWD	Forward for EMSA for validation of *pdhR* binding at *ler* fragment 2 promoter region	CTAAATGGAAATGCAATTATTAAAGTCGTTTGTTAA CGAGATGATT
EMSA_ler_P2_REV	Forward for EMSA for validation of *pdhR* binding at *ler* fragment 2 promoter region	GTATGGACTTGTTGTATGTGAATT
EMSA_ler_4_FWD	Forward for EMSA for validation of *pdhR* binding at *ler* fragment 4 promoter region	CTGTAACTCGAATTAAGTAGAG
EMSA_ler_4_REV	Forward for EMSA for validation of *pdhR* binding at *ler* fragment 4 promoter region	GTATGGACTTGTTGTATGTGAATT

EMSA_eae_FWD	Forward for EMSA for validation of *pdhR* binding at *eae* promoter region	TCTGTGCTATGAGGCTGGAG
EMSA_eae_REV	Reverse for EMSA for validation of *pdhR* binding at *eae* promoter region	TGTTTATTGTCGCTTGAACTGAT
EMSA_Firm_FWD	Forward for EMSA for validation of *pdhR* binding at *Firm* promoter region	GCCGTCCGCTTCTTTGATTT
EMSA_Firm_REV	Reverse for EMSA for validation of *pdhR* binding at *Firm* promoter region	TGACAACATGCTGCCAGACA
EMSA_FliZ_FWD	Forward for EMSA for validation of *pdhR* binding at *fliZ* promoter region	TGCCGTAAATTGCTCGATCG
EMSA_Fliz_REV	Reverse for EMSA for validation of *pdhR* binding at *fliZ* promoter region	TTCCGTTTGCCAGCCATTTT
EMSA_Amp_FWD	Forward for EMSA for validation of *pdhR* binding at *Ampicillin* gene promoter region	CGCGGAACCCCTATTTGTTT
EMSA_Amp_REV	Reverse for EMSA for validation of *pdhR* binding at *Ampicillin* gene promoter region	AAGGGAATAAGGGCGACACG
EMSA_sepZ_FWD	Forward for EMSA for validation of *pdhR* binding at *sepZ* promoter region	AGGTCGCCAGCGGCATTACTGC
EMSA_sepZ_REV	Reverse for EMSA for validation of *pdhR* binding at *sepZ* promoter region	AATAGTTGCCTATGGGATAATT
EMSA_grlA_FWD	Forward for EMSA for validation of *pdhR* binding at *grlA* promoter region	GGTTCCGATAGAAAGTCCTGGA
EMSA_grlA_REV	Reverse for EMSA for validation of *pdhR* binding at *grlA* promoter region	TAACTCTCCTTTTTCCGC
EMSA_PdhR_FWD	Forward for EMSA for validation of *pdhR* binding at *pdhR* promoter region	TGTGCACAGTTTCATGATTTCA
EMSA_PdhR_REV	Reverse for EMSA for validation of *pdhR* binding at *pdhR* promoter region	GCTGCTCAATCACATCGGAG
Balb/c mice Inflammation and imuunity RT-qPCR primers		
Reg3ß_qPCR _F	Forward for *Reg3ß* gene expression using RT-qPCR	TGGTGAAGAGAACAGGAAACAG
Reg3ß_qPCR _R	Reverse for *Reg3ß* gene expression using RT-qPCR	GGCAGTAGATGGGTTCCTC
Reg3γ_qPCR _F	Forward for *Reg3γ* gene expression using RT-qPCR	TTACATCAACTGGGAGACGAATC
Reg3γ_qPCR _R	Reverse for *Reg3γ* gene expression using RT-qPCR	GGCCTTGAATTTGCAGACATAG
Dmbt1_qPCR _F	Forward for *Dmbt1* gene expression using RT-qPCR	TGGAGGCTATGAGGACTATCTG
Dmbt1_qPCR _R	Reverse for *Dmbt1* gene expression using RT-qPCR	TGGTTTGGTCAGTTGGGTAG
Ido1_qPCR _F	Forward for *Ido1* gene expression using RT-qPCR	CAATCAAAGCAATCCCCACTG
Ido1_qPCR _R	Reverse for *Ido1* gene expression using RT-qPCR	AAAACGTGTCTGGGTCCAC
CXCL_qPCR_F-1	Forward for *CXCL* gene expression using RT-qPCR	AACCGAAGTCATAGCCACAC

CXCL-_qPCR_R1	Reverse for *CXCL* gene expression using RT-qPCR	CAGACGGTGCCATCAGAG
Ifn-γ__qPCR F	Forward for *Ifn-γ* gene expression using RT-qPCR	ATGCATTCATGAGTATTGCCAAG
Ifn-γ__qPCR R	Reverse for *Ifn-γ* gene expression using RT-qPCR	ACTCCTTTTCCGCTTCCTG
IL-22__qPCR F	Forward for *IL-22* gene expression using RT-qPCR	AGCTTGAGGTGTCCAACTTC
IL-22__qPCR R	Reverse for *IL-22* gene expression using RT-qPCR	GGTAGCACTGATCTTTAGCACTG
Gapdh__qPCR F	Forward for housekeeping control (*Gapdh*) used in RT-qPCR	TCAACAGCAACTCCCACTCTTCCA
Gapdh__qPCR R	Reverse for housekeeping control (*Gapdh*) used in RT-qPCR	ACCCTGTTGCTGTAGCCGTATTCA
Ftl1__qPCR F	Forward for *Ftl1* gene expression using RT-qPCR	CTCTGGGCGAGTATCTCTTTG
Ftl1__qPCR R	Reverse for *Ftl1* gene expression using RT-qPCR	AGTGGCTTGAGAGGTTCATTC
Mt2__qPCR F	Forward for *Mt2* gene expression using RT-qPCR	GCTCCTAGAACTCTTCAAACCG
Mt2__qPCR R	Reverse for *Mt2* gene expression using RT-qPCR	CAGGAAGTACATTTGCATTGTTTG
Aim2__qPCR F	Forward for *Aim2* gene expression using RT-qPCR	TTGTGAATGGGCTGTTTAAAGTC
Aim2__qPCR R	Reverse for *Aim2* gene expression using RT-qPCR	CCTTCCTCGCACTTTGTTTTG
Wfdc2__qPCR F	Forward for *Wfdc2* gene expression using RT-qPCR	GCTGGCCTCCTACTAGGGTT
Wfdc2__qPCR R	Reverse for *Wfdc2* gene expression using RT-qPCR	AACACACAGTCCGTAATTGGT
Tmem173__qPCR F	Forward for *Tmem173* gene expression using RT-qPCR	AGCGGAAGTCTCTGCAGTCT
Tmem173__qPCR R	Reverse for *Tmem173* gene expression using RT-qPCR	GGAGCCCTGGTAAGATCAAC
Zbp1__qPCR F	Forward for *Zbp1*gene expression using RT-qPCR	TGTTGACTTGAGCACAGGAG
Zbp1__qPCR R	Reverse for *Zbp1* gene expression using RT-qPCR	TTCAGGCGGTAAAGGACTTG

Table 2-19 Volumes used for a PCR reaction

Component	Volume
GoTaq Green Master Mix 2X	12.5 µl
Forward primer (10 µM)	2.5 µl
Reverse primer (10 µM)	2.5 µl
Template DNA	1µl
NucH_2O to	25 µl

Table 2-20 Thermocycler conditions for PCR

Step	Temperature (°C)	Time (min) Cycles	Cycles
Initial denaturation	95	3.00	1
Denaturation	95	0.30	35
Annealing	55-72	0.30	
Extension	72	1.00	
Final extension	72	5.00	1

*Allowed approximately 1 minute for every 1kb of DNA to be amplified depending on the PCR product.

2.4.2 Agarose gel electrophoresis

Agarose gel electrophoresis was used to confirm and separate PCR products. A standard 0.8% agarose gel was prepared by adding agarose powder to TAE buffer to the required volume. The solution was boiled to completely dissolve and GelRed Nucleic acid gel stain (Cambridge Bioscience) was added at a ratio of 1:10 per volume of buffer. The mixture was then left to set in a gel casting tray at room temperature. Once the gel was set, it was placed in electrophoresis tanks which were then filled with TAE buffer to the recommended level. Electrophoresis was performed at 100 volts for 1 hour. The DNA was visualised using a UV transilluminator.

2.4.3 PCR template and plasmid purification

DNA was purified using 50-100 µl of the PCR product and the QIAQuick PCR purification kit (QIAGEN) was used as per the manufacturer's instructions. The purified DNA was then eluted with 30 µl- 50 µl of NucH2O, and the final concentrations was measured using a NanoDrop DS-11+ Spectrophotometer (DeNovix).

Ten mL of overnight cultures containing the plasmid of interest was centrifuged at maximum speed (13,000 g) for 5 minutes and the resulting pellet collected. The QIAprep Spin Miniprep kit (QIAGEN) was then used as per the manufacturer's instructions to purify the plasmid DNA. The plasmid DNA was then eluted with 50 µL of NucH2O and the final concentrations was measured using a NanoDrop DS-11+ Spectrophotometer (DeNovix).

2.4.4 Restriction enzyme digest and DNA ligations

For restriction enzyme digestion, 1 µg of purified DNA sample was incubated with 1 µL of each Fast-digest enzyme (NEB) and 2 µL of each buffer, brought to a total volume of 20 µL with NucH_2O. These were incubated for 1 h at 37°C unless otherwise stated. Digestion was performed on a 0.8 % agarose-TAE gel, and samples were purified using the QIAquick gel extraction kit (QIAGEN) as stated above. Digested DNA was ligated into linear plasmids at a 2:1 ratio. One µL of T4 ligase (NEB) and 2 µL of T4 buffer (NEB) were added to the reaction with NucH_2O to a total volume of 10 µL. These were incubated for 2 hours at room temperature. Five µL of sample was used for transformation, added to 50 µL of competent cells and transformed by heat shock method. After transformations the culture was plated onto relevant antibiotic plates for selective screening, and positive colonies were confirmed by both PCR and DNA sequencing (Eurofins).

2.4.5 Plasmid vector transformations

A single colony or a 1:100 dilution from an overnight culture was inoculated into a culture flask with 5 mL LB media and incubated until it reached a final OD of 0.3-0.5 (OD_{600}). The culture was then centrifuged at 10,000 g for 5 minutes at 4ºC to make cells competent (2.4.6). The supernatant was discarded, and pellet was washed with 1 mL ice cold ddH_2O then centrifuged at 10,000 g for 5 minutes at 4ºC. The washing process was repeated three times.

After the last wash, the pellet was retained and resuspended in 50 µL ddH_2O. The 50 µL cells were then mixed with 100ng of plasmid DNA and dispensed into a pre-chilled electroporation cuvette. Electroporation was performed either by heat shock (2.4.7) or by using an electroporator (Eppendorf Eporator) at 2,500 volts (2.4.8), then either 450 µL SOC or LB media was instantly added to cuvette. The transformed cells were then transferred to 1.5 mL Eppendorf tubes and incubated with shaking at 37°C for 2 hours (New Brunswick Scientific controlled environment shaker) for recovery. 100 µL of the recovered cells were spread on LB plate with appropriate antibiotic and incubated overnight at 37°C.

2.4.6 Preparation of competent cells

A single colony or 1:100 dilution was inoculated in 5 ml of LB and grown to an OD_{600} of 0.4 at 37°C, with shaking at 200 RPM (New Brunswick Scientific controlled environment incubator shaker). The cells were then collected by centrifugation at 3,750 g for 5 minutes at 4°C. The supernatant was discarded, and the cells were washed and centrifuged at 15,000 RPM, the washing step was repeated three times in 1 ml of ice cold ddH_2O. Cells were then collected by suspending them in 50 µl of ice cold ddH_2O and used in subsequent transformations.

2.4.7 Heat shock transformation

Fifty µl of competent cells (2.4.6) was mixed with 1-5 µl of plasmid DNA and incubated on ice for 30 minutes. The samples were then heat shocked at 42°C for 30 seconds on heat block and placed back on ice for 10 minutes. 950 µl of pre-warmed SOC or LB media was added to each reaction and incubated for 2 hours at 37°C to recover positively transformed cells. 100 µL of the recovered cells were spread on LB plate with appropriate antibiotic and incubated overnight at 37°C.

2.4.8 Electrocompetent cell transformation

For electroporation, 50 µl of competent cells (2.4.6) was mixed with 1-5 µl of plasmid DNA and samples were added to a pre-chilled electroporation cuvette and shocked at 2,500 volts in an electroporator (Eppendorf). 450 µl of pre-warmed SOC was added to each reaction and incubated for 2 hours at 37°C. 100 µL of the recovered cells were spread on LB plate with appropriate antibiotic and incubated overnight at 37°C.

2.4.9 Lambda red genetic recombination

Isogenic mutants were generated using Lambda Red recombineering (Datsenko and Wanner, 2000). Briefly, the FRT-chloramphenicol cassette was amplified from the pKD3 plasmid using primers containing 50 bp 5'-end flanking regions bearing homology to the 50 bp regions immediately upstream and downstream of the gene to be deleted. One µg of the resultant PCR product was transformed into competent WT cells carrying pKD46 plasmid initially cultured in SOB media (100 µg/ml ampicillin; 30°C) containing 10 mM arabinose grown to an OD_{600} of 0.4 (New Brunswick Scientific controlled environment shaker). Cultures were centrifuged at 3,750 g for 5 minutes and the supernatant was removed, then, the cells were washed and resuspended three times with ice-cold ddH_2O. Then 50 µL cells were then mixed with 100ng PCR product and dispensed into a pre-chilled electroporation cuvette. Electroporation was performed using an electroporator (Eppendorf Eporator) at 2,500 volts, then either 450 µL SOC or LB media was instantly added to cuvette. Recovery was carried out at 37°C on LB (chloramphenicol 25 µg/ml) to eliminate the pKD46 plasmid and select for successful recombinants. Positive mutants were identified by colony PCR and purified on LB agar at 37°C.

2.4.10 Phenol-chloroform extraction and ethanol precipitation

DNA samples to be concentrated were brought to a total volume of 400 µL with NucH_2O and then mixed with an equal volume of phenol:chloroform:isoamyl alcohol 25:24:1 (PCIA, Sigma Aldrich). The samples were then centrifuged at room temperature at 13 000 g for 5 minutes, then the upper layer solution was removed and placed in a new 1.5mL microcentrifuge tube. Then 400 µL of Chloroform:isoamyl alcohol (24:1) (CIA, Sigma Aldrich) was added to the upper layer in the clean 1.5mL microcentrifuge tube, and the tube was vortexed briefly and then centrifuged for an additional 1 min at maximum speed. After centrifugation, the upper layer was removed and placed in a new Eppendorf tube containing 1 µL glycoblue coprecipitate (ThermoFisher Scientific), 40 µL sodium acetate, and 800 µL 100% ethanol. Samples were vortexed gently and stored at −80°C for 1 hour. After incubation samples were centrifuged at 13 000 g for 20 min at 4 °C. The supernatant was carefully removed to avoid disturbing the pellet. Subsequently, after adding 1 mL of 70% ethanol, the samples were centrifuged for an additional 5 min at 13 000 g. After centrifugation, the

supernatant was carefully removed, and the pellet was air-dried. Finally, the pellet was resuspended in 100 µL of $NucH_2O$, and the concentration was measured using a NanoDrop DS-11 spectrophotometer (DeNovix).

2.4.11 Gibson assembly

NEBuilder assembly tool (NEB) was used to design primers for Gibson assembly cloning. Sequences were amplified by PCR with the relevant overhangs and pACYC184 was linearised. Gibson assemblies were carried out using a Gibson Assembly Cloning Kit (NEB) to the manufacturer's instructions. The following reaction was set up on ice; 0.5 pmols of vector:insert at a ratio of 1:1, 10 µl of NEBuilder HiFi DNA Assembly Master Mix, and $NucH_2O$ to a total volume of 20 µl. Samples were incubated in a thermocycler at 50°C for 15 minutes. 2 µl of the sample was transformed into competent cells (DH5α) using the heat shock method (2.4.7). DNA from selected colonies was amplified and sent out for sequencing to ensure for correct insertion.

2.4.12 Construction of GFP reporters and assay promoter activity

Gene reporter expression analysis was performed using WT TUV 93-0 for EHEC strains and WT ICC169 for *C. rodentium* strains transformed with GFP promoter transcriptional fusion constructs previously constructed by Roe et al. (2003). Bacterial strains transformed with pAJR71 (LEE1 promoter) were grown overnight in LB (chloramphenicol 20 µg/ml). 50 µL of bacterial overnight culture was then inoculated into 5 mL pre-warmed MEM-HEPES (EHEC) and DMEM (*C. rodentium*) and grown to an OD of 0.8 (OD_{600}) at 37°C with 200 rpm speed. To measure GFP expression, 200 µL of the test sample was transferred to a black flat bottom 96 well microtiter plate and analysed using a FLUOstar Optima Fluorescence plate reader (BMG, Labtech, UK). Background fluorescence was measured using WT respective strains containing pAJR70 (promoter less strain) which was used as a negative control. Experiments were performed in triplicate.

2.4.13 Site-Directed Mutagenesis

Substitutions and deletion site directed mutagenesis was carried out using the Q5® Site-Directed Mutagenesis Kit (NEB) according to the manufacturer's recommendations. Briefly, primers were designed, and annealing temperature was calculated using the NEBaseChanger™ (NEB online primer design tool).

Substitutions are designed by including the desired nucleotide change in the centre of the forward primer, including at least 10 complementary nucleotides on the 3´side of the mutation(s). The reverse primer is designed so that the 5´ ends of the two primers anneal back-to- back. While deletions are designed by engineering standard, non-mutagenic forward and reverse primers that flank the region to be deleted. Then the assembly mix was prepared as shown in Table 2-21. The assembly mix was then ran using a standard PCR machine (Eppendorf Mastercycler Nexus gradient thermocyclers) with outlined conditions (Table 2-22).

Table 2-21 **Q5® Site-Directed Mutagenesis Kit assemble reagents**

Component	**volume**	**Final concentration**
Q5 Hot Start High-Fidelity 2X Master Mix	12.5 µL 1X	1X
10 µM Forward Primer	1.25 µL	0.5 µM
10 µM Reverse Primer	1.25 µL	0.5 µM
Template DNA (1–25 ng/µL)	1 µL	1-25 ng
Nuclease-free water	9.0 µL	Nuclease-free water 9.0 µL

Table 2-22 Q5 Hot Start High-Fidelity thermocycling conditions

Condition	**Temperature (°C)**	**Time (mins)**
Initial Denaturation	98	0.30
25 cycles	98	0.10
	50-72	0.30
	72	0.30
Final Extension	72	2
Hold	4-10	

One µL of the amplified PCR product was then incubated for 5 mins with 1 µL 10X KLD enzyme mix (containing a kinase, a ligase and DpnI), 5 µL 2X KLD reaction buffer and NucH_2O. These enzymes allow for rapid ligation of the PCR

product and removal of the template DNA. Then 5 µL KLD mix was added to NEB 5-alpha competent *E. coli* cells placed on ice for 30 mins. The samples were then heat shocked at 42°C for 30 seconds on heat block and placed back on ice for 10 minutes. 950 µl of pre-warmed SOC or LB media was added to each reaction and incubated for 2 hours at 37°C to recover positively transformed cells. 100 µL of the recovered cells were spread on LB plate with appropriate antibiotic and incubated overnight at 37°C.

2.5 Genomic and transcriptomic analysis

2.5.1 Genomic DNA extraction

For genomic DNA was isolated from faecal samples using DNeasy PowerSoil Pro Kit (QIAGEN, USA) in strict accordance with the manufacturer's recommendations. 3 to 5 faeces of mice were collected in 1.5 ml Eppendorf tubes and weight accordingly and processed immediately. Samples were collected every second day till day 24 PI. Bacterial cultures were centrifuged at 10,000 x g for 5 min at RT. DNA was extracted from the pelleted cells after the supernatant was discarded. DNA concentration was measured using a NanoDrop DS41 11 spectrophotometer (DeNovix), and samples were stored at -80°C till awaiting microbiome sequencing.

2.5.2 RNA Extraction and Purification

RNA was extracted from three biological replicates using the PureLink RNA Mini Kit (Thermo Fisher Scientific) according to the manufacturer's instructions. Cultures were grown in MEM-HEPES supplemented with 0.2% succinate at 37°C at a speed of 200 rpm to OD0.8 (OD_{600}). Cells were harvested by centrifugation and resuspended in RNA Protect Bacteria Reagent (Qiagen). After for 10 mins incubation at room temperature, cells were centrifuged at maximum speed for an additional 10 min and the supernatant was discarded. The pellet was resuspended in 100 µL of TE buffer containing lysozyme (10 mg/ml), then 0.5 µL of 10% SDS solution was added before the pellet was resuspended by vortexing. The samples were incubated for 5 min at room temperature, then 350 µL of lysis buffer containing 1% B-mercaptoethanol was added to each tube and the samples were mixed by vortexing. 250 µL of 100% ethanol was added to the samples and then they were vortexed to remove any visible precipitate. Samples were transferred to spin columns and RNA extraction was performed

using the PureLink RNA Mini Kit (Thermofisher Scientific) according to the manufacturer's instructions. RNA was eluted in a final volume of 100 µL of NucH_2O, and TurboDNase treatment (ThermoFisher Scientific) was used to remove contaminating DNA from the samples. To each sample, 4 µL of TURBO DNase and 10 µL of 10X TURBO DNase buffer were added, and the samples were then centrifuged at maximum speed for 15 seconds, followed by incubation at 37° C for 1 hour. During the incubation period, samples were vortexed and centrifuged at 30 mins intervals. RNA samples were then subjected to phenol-chloroform extraction and ethanol precipitation (see 2.4.7) before final resuspension in 100 µL NucH2O. RNA concentration was measured using a NanoDrop DS41 11 spectrophotometer (DeNovix), and samples were normalized with 100 µL of NucH2O to a final concentration of 10 ng/µL. RNA samples were stored at -80 °C till further analysis.

2.5.3 Transcriptome profiling by RNA-Seq

RNA samples were extracted as describe above (2.5.1). RNA quality was assessed by Agilent Bioanalyser 2100 with 100ng/ µL accept as a threshold for individual samples. Ribosomal depletion was carried out using MICROBExpress (ThermoFisher Scientific) according to the manufacturer's instructions. Library preparation and sequencing was carried out at the University of Glasgow Polyomics facility. Sequencing libraries were prepared with the TrueSeq Stranded mRNA Library Prep kit (Illumina) according to manufacturer's recommendations. Sequencing was carried out on the Illumina NextSeq 500 platform with at least 10 million 100 bp single end reads being obtained. FastQC (Babraham Bioinformatics) was used to assess the quality of raw reads (minimum Phred threshold of 20). All experiments were normalized by reads assigned per kilobase of target per million mapped reads. Raw data from RNA-Seq experiments were processed using CLC Genomics Workbench 20 and mapped to the EDL933 genome and plasmid (NCBI accession number: NC_002655). This was done using EdgeR, which was developed for the analysis of replicate count-based expression data, was used to compute differential gene expression (Robinson et al., 2009). Corrected *p*-value threshold [false discovery rate (FDR)] was 0.05 and absolute fold change ≥ 1.5. ≤ -1.5 was considered significant. Normalized RNA-seq data transcript quality assessment was analysed using principal component analysis (PCA) plots to visualize

relationships between samples. Pairwise comparison between EHEC WT and Δ*pdhR* strains was conducted to identify any changes in gene expression caused by the deletion of the transcription factor PdhR.

2.5.4 Quantitative real time PCR (RT-qPCR)

Ten nanograms of total RNA free from DNA, extracted as described earlier (2.5.1), was used as a template to prepare 10 µL cDNA using LunaScript®RT SuperMix (New England Biolabs) according to manufacturer's instructions. Two µL of 5X LunaScript RT SuperMix was mixed with 7 µL of NucH_2O and 1 µL of RNA template to make a final volume of 10 µL. The samples were run on the Eppendorf Mastercyler Nexus gradient, using the following conditions (Table 2-23).

Table 2-23 LunaScript®RT SuperMix cDNA synthesis thermocycling conditions

Condition	Temperature (°C)	Time (mins)
Annealing	25	2
cDNA synthesis	55	10
Heat inactivation	95	1

Luna® Universal qPCR Master Mix (New England Biolabs) was used for RT-qPCR according to the manufacturer's instructions. Biological cDNA samples were analysed in triplicate by performing duplicate technical reactions of 20 µL using a 1 µL volume of cDNA as template. RT-qPCR was performed on a CFX-Connect real-time PCR detection system (BIO-RAD). The following conditions were used: initial denaturation at 95˚C for 1 min. Denaturation 95˚C, 15 seconds. Extension at 60°C for 30 seconds, 39 cycles. Prior to RT-qPCR, the primer efficiency of each primer pair was evaluated using the thermocycling conditions described above. A series of concentration standards were prepared using template cDNA (100, 4, 0.8, and 0.16 ng/µL), and only primers with efficiencies between 90 and 110% were selected for use in the experiments. Analysis was performed using CFXConnect software (BIO-RAD), and *gapA* housekeeping gene was used as a control and for calculating gene expression relative to tested samples using the $2^{-\Delta\Delta ct}$ method.

2.5.5 Mice faecal microbiome processing

Genomic DNA was isolated from faecal samples using DNeasy PowerSoil Pro Kit (QIAGEN, USA) in strict accordance with the manufacturer's instructions. Concentration and purity of extracted DNA was confirmed by NanoDrop DS-11+ Spectrophotometer (DeNovix). Samples were sent out for sequencing to Novagen Europe. Briefly, PCR amplification of targeted bacterial 16S rRNA gene V3-V4 regions [Primers F (50-ACTCCTACGGGAGGCAGCA-30) and R (50-GGACTACHVGGGTWTCTAAT-30) was performed by using specific primers connecting with barcodes. The PCR products with proper size were selected by 2% agarose gel electrophoresis. Same amount of PCR products from each sample was pooled, end-repaired, A-tailed and further ligated with Illumina adapters. Libraries were sequenced on a paired-end Illumina platform to generate 250bp paired-end raw reads. The library was checked with Qubit and real-time PCR for quantification and bioanalyser for size distribution detection. Quantified libraries were pooled and sequenced on Illumina Sequencing PE250, according to effective library concentration and 30 K tags of raw data per sample being the average number of reads required.

2.6 Protein Work

2.6.1 Secreted T3SS associated proteins assay

Secreted protein assay from EHEC and ICC169 strains was carried out using the method previously described (Tree et al., 2011). Overnight cultures were inoculated at a ratio of 1:100 into 50 mL of MEM-HEPES for EHEC and Dulbecco's Minimal Eagles Medium (DMEM) (Thermofisher) for ICC169 and grown at 37°C, with shaking (200 RPM) (New Brunswick Scientific controlled environment shaker) until an OD_{600} nm of ~0.8 was reached. The supernatant was then collected by centrifuge at 3,750 g for 10 minutes, and pellet discarded stored at -20°C. The collected supernatant was then filtered through a 0.2 µM filter (Fisher) into fresh 50 mL centrifuge tubes before ice cold Trichloroacetic acid (TCA) was added to a final concentration of 10% (v/v); 5 mL TCA to 45 mL supernatant. One µL of lysozyme (2 mg/mL) was added to each sample, as a co-precipitant for maximum protein recovery, then samples were briefly vortexed and stored at 4°C overnight. After overnight precipitation, secreted proteins were collected by centrifuging the samples at 4°C for 30 min, 6000 g. The supernatant was carefully removed to not disturb the protein pellet, and

the tubes were inverted and allowed to air dry for 15 minutes. The pellet was then resuspended in 25 µL of 1X protein sample buffer and transferred to a fresh 1.5 mL Eppendorf tube. Samples were then boiled at 97 ºC for 10 min and analysed by SDS-PAGE as described below (2.6.2).

2.6.2 Sodium dodecyl sulphate-polyacrylamide gel electrophoresis (SDS-PAGE)

SDS-PAGE was performed by using commercially prepared NuPage 4–12% Bis-Tris protein gels (Invitrogen). Stored proteins were thawed and then boiled at 97ºC for 5 mins, while fresh proteins were mixed with 1X sample buffer and denatured by heating the samples at 95˚C for 10 minutes. Protein samples were loaded onto a polyacrylamide gel and placed in NuPage MES (Invitrogen) running buffer, SeeBlue Plus2 protein standard (Invitrogen) was ran alongside the protein samples. The samples were then separated by applying a voltage of 160 volts for 30 minutes. For further analyses were transferred to a 0.45 µM (ThermoFisher) nitrocellulose membrane by standard electroblotting. Electrophoresis was performed in NuPage transfer buffer (Invitrogen) at a constant voltage of 30 volts for 1 hour. Alternatively, gels were stained with Coomassie blue for 1 h and de-stained for 3 hours or overnight in ddH_20. De-stained SDS-PAGE gels were then visualized using a transilluminator (BIO-RAD ChemiDoc MP Imaging System).

2.6.3 Western blot

For Western blot analysis, proteins transferred from SDS-PAGE gel to a 0.45 µM nitrocellulose membrane (ThermoFisher) were used. Electroblotting was performed in NuPage transfer buffer (Invitrogen) at 30 volts for 1 hour as described above (2.6.2). 5% milk prepared with PBST was used to block nitrocellulose membrane for 1 h. The primary antibody [with Anti-6X His tag (1/5000)] (Sigma) was prepared to the required concentration with 5% BSA in PBST and added to the membrane and incubated for 1 hour at RT with shaking. The membrane was washed three times with 50 ml phosphate-buffered saline with Tween (PBST) for 10 min each. The membrane was then incubated for 1 hour with a secondary antibody (HRP-conjugated secondary antibodies) (Sigma). at in 1% milk in PBST and washed three times with PBST. Finally, the membranes were developed using Pierce ECL Plus Substrate for 5 mins and imaged using the and imaged using ChemiDoc imaging system (BioRad).

2.6.4 Recombinant PdhR overexpression and purification

PdhR was cloned into pET21a (+) to express recombinant 6XHis-PdhR protein. The vector was then transformed into BL21 DE3 cells. A single colony from EHEC stock culture plate was used to grow an overnight culture at 37°C with shaking (200 rpm). A 1:100 dilution of the overnight culture was inoculated into 2 L of fresh LB and cultured until an OD_{600} of 0.5 was reached. Then 0.5 mM IPTG was then added, and the cultures were allowed to grow overnight at 30°C to express the PdhR protein. Bacterial cells were collected by 20 minutes centrifugation at a speed of 5000 rpm and the supernatant was discarded. The cell pellet was resuspended in protein buffer (50 mM Tris, 0.5 M NaCl, and 5% glycerol) containing lysozyme, EDTA-free protease inhibitor mix, and DNase (Promega). Cells were lysed by sonication on ice, with 1 second on and 1 second off for 6 minutes and following centrifugation for 50 minutes at 4°C at 18,000 rpm. Following centrifugation, the 6XHis-PdhR protein was collected in the soluble fraction. The supernatant was removed and filtered through a 0.22 µM filter and applied to a Ni2+-chelating column (HisTrap High Performance, GE Healthcare) equilibrated with protein buffer A containing 5 mM imidazole. 6XHisPdhR was then eluted with a linear gradient from 10 to 300 mM imidazole added to buffer A. Fractions containing 6XHis-PdhR were pooled and dialyzed against buffer A and stored at −20°C in buffer A and long-term storage samples were stored at −80°C.

2.6.5 PdhR binding motifs within the LEE

The consensus recognition sequence for PdhR consists of a 17 bp long palindromic sequence made of AATTGGTnnnACCAATT (Quail et al., 1994; Quail & Guest, 1995). Prediction of the binding sites of PdhR on the LEE operon was done by MEME-Suite software (version 5.1.0) with default parameters (match p-value=0.001) which enriched a set of sequences for individual matches to the PdhR binding motif.

2.6.6 Electrophoretic mobility shift assay (EMSA)

Electrophoretic Mobility Shift Assay (EMSA) purified recombinant PdhR protein was used in this experiment. The gel retardation assays were performed as previously described (P. K. Singh et al., 2020). Different fragments of the promoter regions predicted to be binding sites were amplified by PCR using genomic DNA of EHEC as a template. The resulting PCR fragments were purified,

and equal concentrations of 150 nM were incubated on ice in binding buffer [250mM Tris-HCl pH8, 0.5mM EDTA, 25mM MgCl, 25mM MgCl, 5mM DTT, 25% glycerol] without and with increasing amounts of purified PdhR-His and 0.5 µg/ml of polydIdC in a total volume of 16 µL. After careful mixing, samples were incubated for 20 min at 30◦C, placed back on ice for 10 min, and then loaded onto 2% agarose gel in 0.5X TBE. Electrophoresis was carried out in 0.5X TBE at 50 V at 4◦C for 4 hours. Finally, the gel was stained with gel red, de-stained in 0.5X TBE and exposed on the transilluminator (BIO-RAD Chemidoc).

2.7 *In vitro* and *in vivo* infection models

2.7.1 Cell adhesion assay

Cultures of ICC169, Δ*pdhR* and Δ*pdhR*:pACYC;pdhR were grown in MEM-DMEM supplemented with either 0.2% succinate from overnight cultures to reach an OD_{600} of 0.4 (37 °C with 5% CO_2) before back diluting to 0.1 with DMEM-HEPES. Human epithelial cervix adenocarcinoma (HeLa) cells were seeded (10^4 cells per well in 24-well plates) on wells with sterile coverslips in MEM-HEPES with 10% fetal calf serum. One hour prior to infection cells were washed three times with PBS and fresh DMEM was added with any supplementary antibiotics or additions described below. A volume of 100 µL (4 x10^4 cells/well) of bacterial culture was added per well was used for infection. The plates were centrifuged at 300 × g for 3 min and incubated at 37 °C with 5% CO_2 for 2.45 hrs. After incubation, the cells were next washed five times with PBS and fixed with 4% paraformaldehyde and incubated for 15 min. Next, cells were permeabilized with 0.1% triton x-100 for 10 min before washing and staining for 1 hour with phalloidin-Alexafluor 488. Coverslips were washed before mounting and analysing using a Zeiss Axioimager M1 and Zen Pro software. A/E lesions could be identified by condensation of host actin around the site of bacterial attachment. Host cell-associated bacteria were quantitated using the event counter tool in Zen and the total percentage of infected cells was also determined. Data were analysed by imaging 10 random fields of view from at least three coverslips.

2.7.2 Infection of BALB/c mice with *C. rodentium*

Specific pathogen free (SPF) female BALB/c mice 6 weeks of age were used. WT ICC169 and Δ*pdhR* were grown in DMEM to an OD_{600} of ~0.7 before being

centrifuged and resuspended at 100× concentration in PBS. Groups of six BALB/c mice were then inoculated by oral gavage with 200 µL of PBS bacterial suspension (3×10^9 CFU). Mice were checked daily for survival and weighed. For analysis of CFU counts, stool samples were recovered aseptically and homogenized in PBS before serial dilution. The number of viable CFU per gram of stool was determined by plating onto LB agar with the appropriate antibiotic selection. Tissues were collected for analysis of inflammation at 20 days post infection which was the last day of the experiment.

2.7.3 Total RNA extraction from mice tissue

After mice were culled different colon parts (upper, lower and caecum) were used to extract total RNA tissue. Tissue RNA was extracted using RNeasy Mini Kit as per the manufacturer's instructions. Briefly, frozen tissues were thawed on ice, media from tissues was removed and the excess was blotted on blue roll before transferring it to a fresh RNase-free Eppendorf. 750uL Qiazol and one homogenisation ball was added to each new Eppendorf with tissue and lysed on a tissue lyser at 25 Hz (250 frequency) x 2 minutes. Then 150uL of chloroform was added to samples and vortexed for 10 seconds, following incubate at RT for 5 minutes. After incubation samples were centrifuged for 15-30 minutes, at 4ºC, with a speed of 12,000 x g. The upper Transfer clear phase was collected and transferred to a fresh RNase-free Eppendorf and 1.5 x (approximately) volume of 100% EtOH was. The mixture was then briefly vortexed for 15 seconds for each tube. 700uL of the solution was transferred to RNeasy column and centrifuged at 8,000 x g for 1 minute, at RT and the flow throw discarded. 350uL RW1 buffer was added, and columns were centrifuged at 8,000 x g for 30 seconds, at RT and the flow through discarded. Columns were then washed with 500uL RPE buffer and span at 8,000 x g for 30 seconds, at RT and the flow through discarded. The process was repeated three times. Finally, the RNA was collected with 30uL NucH_2O and RNA concentration was measured with a NanoDrop DS-11+ Spectrophotometer (DeNovix).

2.8 Bioinformatics and statistical analysis

2.8.1 Faecal microbiome bioinformatics analysis

In order to analyse the diversity, richness and uniformity of the communities in the sample, alpha diversity was calculated from 7 indices in QIIME2, including

Observed_otus, Chao1, Shannon, Simpson, Dominance, Good's coverage and Pielou_e. Three indices were selected to identify community richness: Observed_otus - the number of observed species; Chao- the Chao1 estimator; Dominance - the Dominance index; Two indices were used to identify community diversity: Shannon - the Shannon index; Simpson - the Simpson index; One indice was used to calculate sequencing depth: Coverage - the Good's coverage; One indice was used to calculate species evenness: Pielou_e - Pielou's evenness index.

In order to evaluate the complexity of the community composition and compare the differences between samples(groups), beta diversity was calculated based on weighted and unweighted unifrac distances in QIIME2. Cluster analysis was performed with principal component analysis (PCA), which was applied to reduce the dimension of the original variables using the ade4 package and ggplot2 package in R software (Version 3.5.3). Principal Coordinate Analysis (PCoA) was performed to obtain principal coordinates and visualize differences of samples in complex multi-dimensional data. A matrix of weighted or unweighted unifrac distances among samples obtained previously was transformed into a new set of orthogonal axes, where the maximum variation factor was demonstrated by the first principal coordinate, and the second maximum variation factor was demonstrated by the second principal coordinate, and so on. The three-dimensional PCoA results were displayed using QIIME2 package, while the two-dimensional PCoA results were displayed using ade4 package and ggplot2package in R software (Version 2.15.3).

To study the significance of the differences in community structure between groups, the adonis and anosim functions in the QIIME2 software were used to do analysis. To find out the significantly different species at each taxonomic level (Phylum, Class, Order, Family, Genus, Species), the R software (Version 3.5.3) was used to doMetaStat and T-test analysis. The LEfSe software (Version 1.0) was used to do LEfSe analysis (LDA score threshold: 4) so as to find out the biomarkers. Further, to study the functions of the communities in the samples and find out the different functions of the communities in the different groups, the PICRUSt2 software (Version 2.1.2-b) was used for function annotation analysis.

2.8.2 Statistical analysis

Statistical analysis was performed using GraphPad Prism (Version 8) unless otherwise stated. For comparison between 2 samples, an unpaired Student t-test was used. RT-qPCR was carried out using CFX-Connect BIORAD software, according to the $2^{-\Delta\Delta ct}$ method. RNA-seq was computed using CLC Genomics Workbench (CLC BIO, version 20.

Chapter 3: Screening of transcriptional factors for their ability to regulate type three secretion system in EHEC

3.1 Introduction

An emerging theme in infection biology is the link between metabolic capacity and the ability of Enterohaemorrhagic *Escherichia coli* O157:H7 (EHEC) and related pathogens to colonise specific niches (Carlson-Banning & Sperandio, 2016a). This colonisation is dependent on the type 3 secretion system (T3SS) which is encoded on a PAI, named the locus of enterocyte effacement (LEE) (Gaytán et al., 2016). The T3SS regulation centres on sequential expression of the LEE in response to multitude of signals and cues that are encountered in the intestinal environment of the host (Connolly et al., 2018). The ability to sense different stimuli can be used by EHEC to gain a competitive advantage by appropriate regulation of different virulence factors. Transcriptional regulators tightly control the expression of virulence genes in response to these environmental signals by acting as either activators or repressors upon binding to specific promoters (O'Boyle et al., 2020). Thus, appropriate expression of infection relevant genes increases the overall virulence of EHEC (Mellies & Lorenzen, 2014).

Previous work by Connolly et al. 2018, identified several transcription factors which were regulated by the pathogen *C. rodentium* during colonisation of the murine gastrointestinal tract, but of notable interest were BssS, YfeC, RcnR and PdhR (Table 3-1). These regulators have been reported to have a potential role in regulation of bacterial virulence (Anzai et al., 2020; Domka et al., 2006; Ibáñez de Aldecoa et al., 2017). *pdhR*, *yfeC*, *rcnR* and *bssS* genes encodes pyruvate dehydrogenase transcriptional regulator (PdhR), extracellular DNA (eDNA) binding regulator, metal binding family protein specific to Ni/Co (RcnR) and the biofilm regulator protein (BssS), respectively. The pyruvate dehydrogenase catalyses the formation of acetyl-CoA from pyruvate which subsequently enters the citric acid cycle which is critical for bacterial survival (Fig.3-2). The pyruvate dehydrogenase complex (PDHc) is composed of the following ezymes, pyruvate dehydrogenase, dehydrolipamide acyltranferase and dihydrolipoamide dehydrogenase encoded by *aceE*, *aceF*, and *lpdA* genes which form a single operon together with PdhR gene (a self-regulator of this operon) in the order *pdhR-aceE-aceF-lpdA* (Ogasawara et al., 2007). Pyruvate-sensing PdhR, a GntR family of transcription regulators represses PDH complex and depresses it in the presence of pyruvate.

Table 3-1 *C. rodentium in vivo* differentially expressed transcriptional regulator genes (Connolly et al., 2018).

C. rodentium	Fold Change	Regulation	EHEC Orthologue	Role
bssS	3	Up	*bssS*	Biofilm regulator
rcnR	7	Up	*rcnR*	eDNA release regulator
pdhR	-3	Down	*pdhR*	pyruvate sensing
yfeC	5	Up	*yfeC*	metal binding family to Ni/Co

Escherichia coli RcnR is a metal-responsive DNA-binding protein which represses transcription of *rcnA* encoding the Ni(II) and Co(II) exporter proteins RcnAB (Higgins, 2019). Transition metals are crucial trace nutrients for microorganisms which are regulated through a number of metal-sensor proteins that sense the bioavailability of particular metals in the cell in order to regulate the expression of genes encoding proteins that contribute to metal balance (Baksh & Zamble, 2020).

Deletion of genes encoding proteins that regulate metal homeostasis can lead to detrimental conditions in the bacterial cell as they can be either high concentration or less importation of a specific essential metal in the bacterial cell (Baksh & Zamble, 2020). Bacteria employ cell signalling communication within large groups of cells to coordinate different processes, such as antibiotic production, swarming motility and the formation of biofilms(Ibáñez de Aldecoa et al., 2017).

Extracellular DNA (eDNA) is a major component of the polymeric matrix of biofilms of bacterial pathogens (Karygianni et al., 2020). eDNA is usually produced in response to an increase in the cell density of the population. Deletion of *yfeC* gene has been shown to increase eDNA of *E. coli* K12 strains grown in liquid culture (Y. Gao et al., 2021), thus can increase several processes associated with cell density, for example biofilm formation and bacterial motility. Biofilm formation aid in bacterial colonisation of the host and provides resistance to host immune system. Exploring genes involved in biofilm formation is of great importance as it can help in better understanding *E. coli* virulence and ultimately give insights on how to prevent and treat *E. coli* infections. *bssS* gene encodes BssS protein which is characterized as a biofilm

regulator in *E. coli* K-12 strains and reported to be a putative global regulator of several genes involved regulation of the uptake and export of signalling pathways (Domka et al., 2006).

Developing drugs inhibiting the virulence of pathogenic bacteria can act as alternative to traditional antibiotics. The first step in establishing this as a feasible and efficient tool, is to understand how to control genes which encode virulence factors in pathogenic bacteria. One major setback in understanding initial colonization and disease progression is the lack of data or information about molecular interaction between the human host and pathogens (Griesenauer et al., 2019). Since *C. rodentium* shares an infection strategy and virulence genes with EHEC (Crepin et al., 2016). This prompted us to propose that these transcription factors, could be important in regulation of both metabolism and, directly or indirectly, virulence of *C. rodentium*. Moreover, given that *Citrobacter* shares a similar LEE island to EHEC, we hypothesized that the transcription factors may control virulence in EHEC and *C. rodentium*. This chapter aims to address these questions by characterizing the role of BssS, YfeC, RcnR and PdhR in EHEC virulence. LEE reporters, motility and biofilm assays were used as an initial screen for transcriptional response of isogenic Δ*pdhR*, Δ*yfeC*, Δ*rcnR* and Δ*bssS* strains in comparison to wild type EHEC. TUV93-0, a Stx-negative derivative of EDL933 strain was used to generate the mutants used in this study, from here on the TUV93-0 strain shall be referred to as EHEC for ease of reference.

3.2 Results

3.2.1 Role of transcriptional regulators in modulation of virulence in EHEC.

3.2.2 Deletion of transcriptional regulator genes

To study the overall function of this regulators, mutant strains of EHEC were generated for (Δ*bssR*, Δ*yfeC*, Δ*yrcnR* and Δ*pdhR*) (Fig.3-1) using the Lambda Red Recombination previously described (Datsenko & Wanner, 2000).The FRT-chloramphenicol cassette was amplified from a pKD3 plasmid using primers with 50 bp overhangs up- and downstream regions of the gene of interest. One µg of the resultant PCR product was transformed into EHEC competent cells transformed with pSIM18 plasmid. Successful recombinants were selected on LB plates supplemented with 25 µg/ml chloramphenicol. The generated mutants were then tested for growth/motility defects and their role in EHEC virulence.

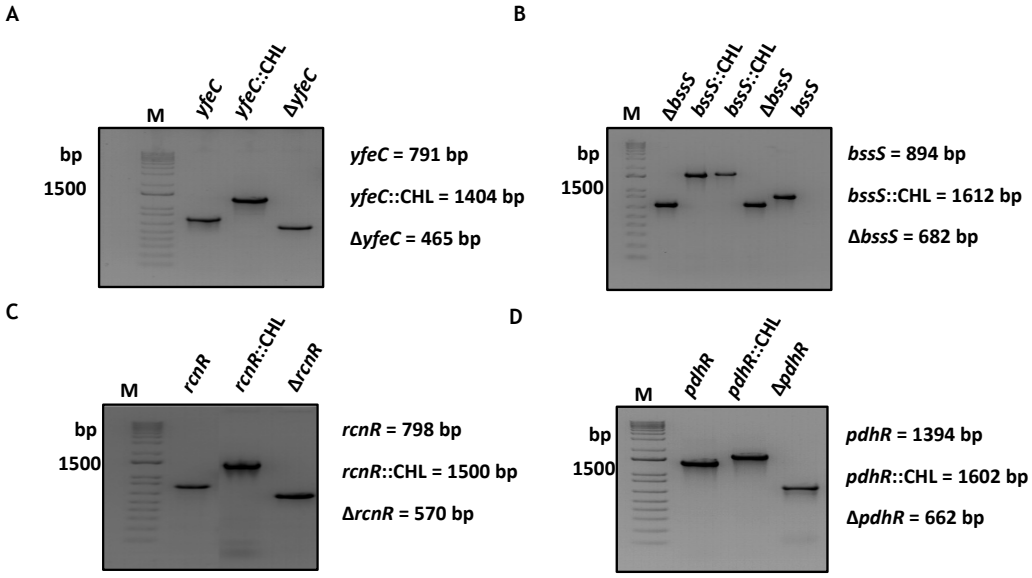

Fig. 3-1. Generation of TUV93-0 mutants by Lambda Red. Confirmation of EHEC mutants (A) *yfeC*, (B) *bssS* (C) *rcnR* and (D) *pdhR* mutants was done by colony PCR. Genomic DNA from the TUV93-0 and mutants was used to amplify the Chloramphenicol resistant cassette after Lambda Red mutagenesis using primers specific to regions of interest. Corresponding band sizes are indicated.

3.2.3 Growth analysis of generated mutants

The mutants were cultured in minimal media (M9 and MEM-HEPES tissue culture media) at 37°C and compared to the growth of EHEC Wild Type (WT) under similar conditions to evaluate if deletion of the transcriptional regulators had any growth defects. Deletion of the regulators had no significant growth defects when grown in M9 and MEM-HEPES tissue culture media (Fig.3-2, A, B and C), except for the Δ*pdhR* strain which had a lag in growth as compared to the WT strain (Fig.3-2D), but with no statistical significance. However, the slight growth defect phenotype was completely restored when *pdhR* was complemented back to the Δ*pdhR* strain and grown again in M9 and MEM-HEPES media (Fig.3-2D). These data suggests that PdhR regulates growth in nutrient limiting conditions.

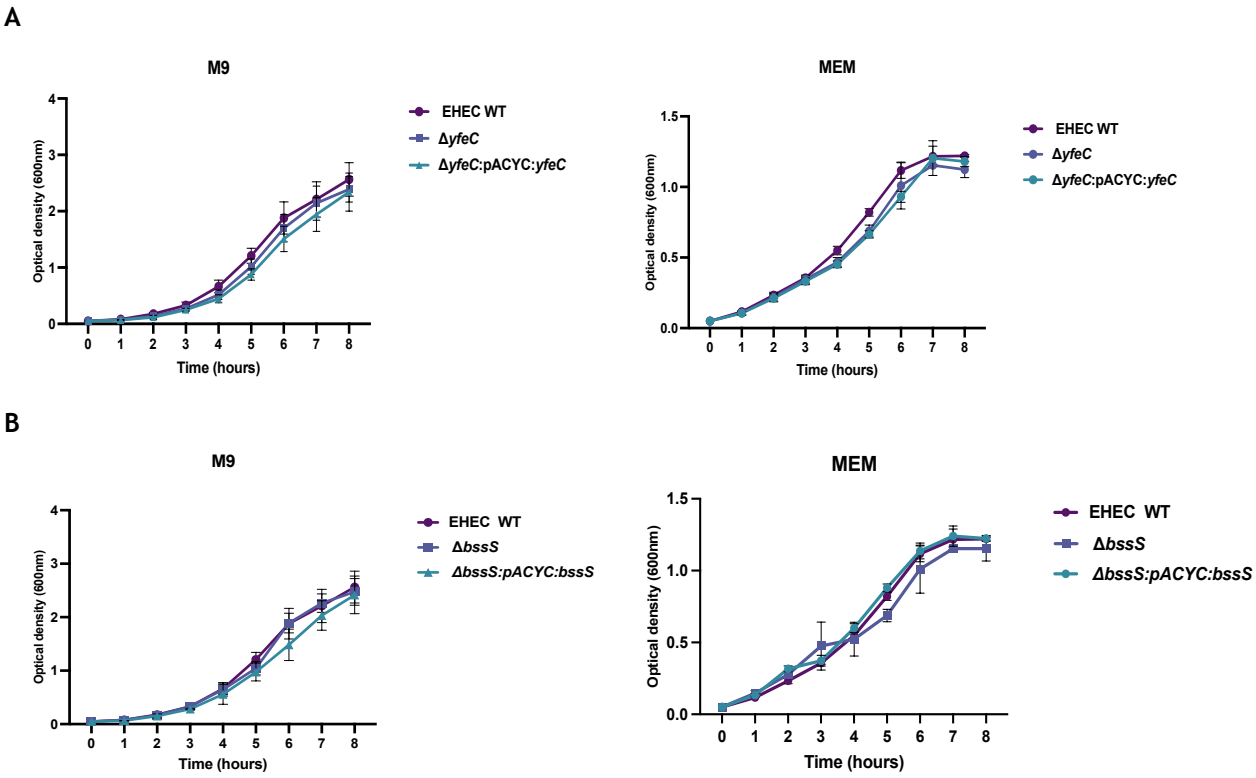

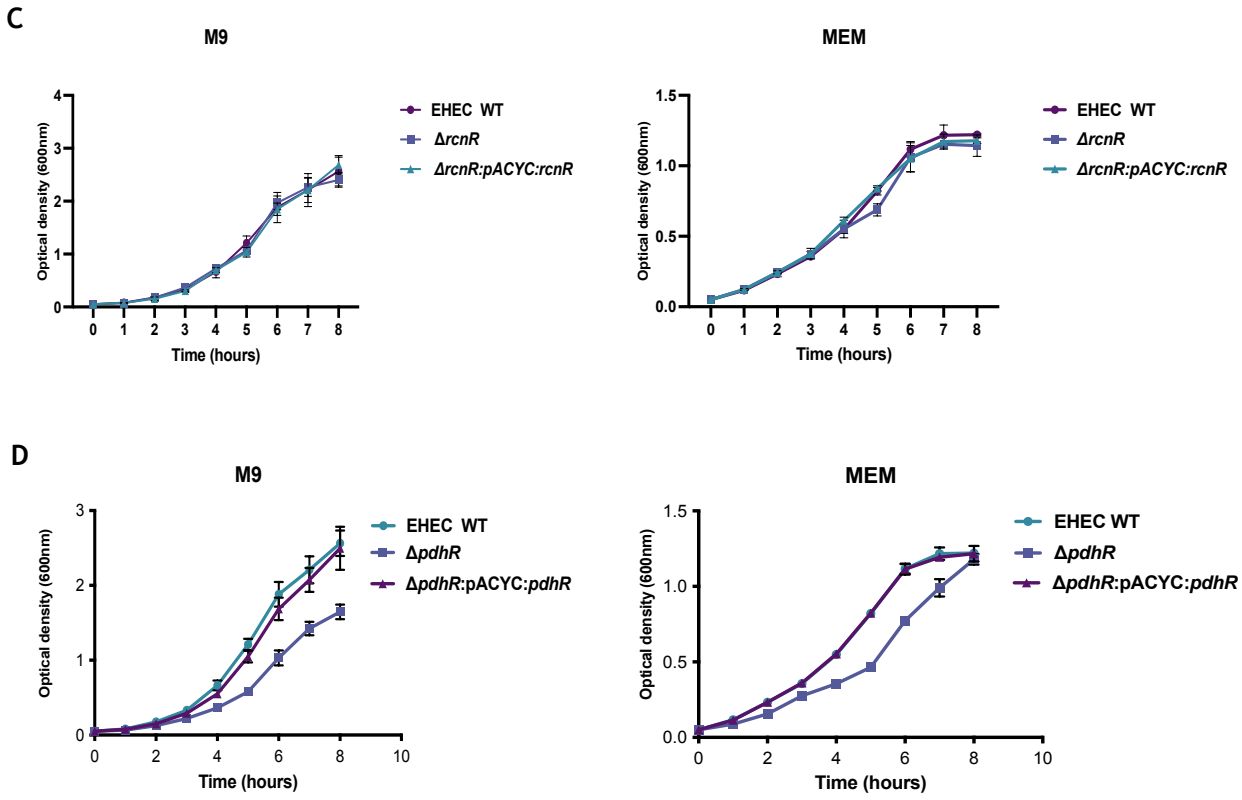

Fig. 3-2. Growth profiles of WT and mutants. Growth curves of each mutant compared to the wild type grown in M9 and MEM-HEPES media, measured as OD_{600} overtime. Growth curves shown represent mean values of triplicate experiments with error bars indicating standard error of the mean (SEM).

3.2.4 Phenome analysis of EHEC and Δ*pdhR* mutant

Qualitative assessment of Figure 3-3D revealed that, deletion of the PdhR regulator resulted in a lag on the growth of EHEC in MEM-HEPES media, though not statistically significant. No growth retardation was observed when growing Δ*pdhR* strain on rich media such as LB (Table S1 and S. Fig.1-3). The next step was to test the role of the regulators on LEE expression. To proceed, the growth defect observed on the Δ*pdhR* strain sought to be corrected. This enabled to test the regulatory function of PdhR irrespective of niche advantage or disadvantage in EHEC. These data implied that the lag defect could be overcome with sufficient nutritional support.

Based on this observation, Phenotype MicroArray (PM) assay (also referred to as Phenome analysis) was used to assess carbon source utilization profiles of the WT and Δ*pdhR* strain, to select a suitable carbon source supplement to eliminate the minor growth defect. PM1 plates comprising of 95 carbon sources were used to monitor phenotypic reactions at 37ºC for 24 hours. The WT and the mutant strain did not have much variation in the growth patterns on

individual carbon sources. Among the 95 carbon sources, the WT grew on 64 sources while the *pdhR* mutant grew on 62 (S Fig.1-1 and S Fig.1-2). The WT and the Δ*pdhR* strain showed no significant difference in growth on most carbon sources, including succinic acid, D-glucuronic acid, D-Fructose-6-Phosphate, trehalose, sucrose, thymidine, and D-glucose-6-phosphate (Fig.3-3 A, B, C and S Fig.1-1).

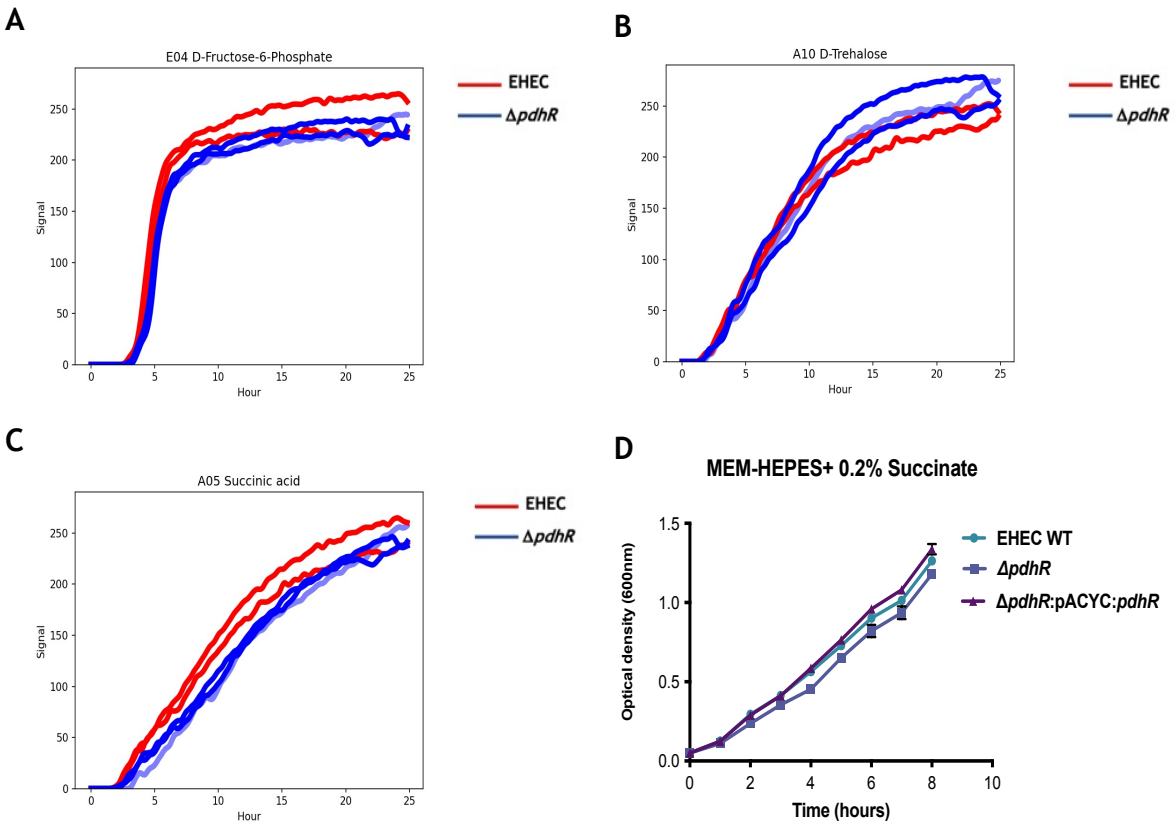

Fig. 3-3. Growth profiles of WT and mutants. (A) BIOLOG phenotype microarray results of WT strain vs. Δ*pdhR* strain on plate PM1 showing less variation among carbon sources. (B) Growth curves of the EHEC, Δ*pdhR* and PdhR complement strain in MEM supplemented with 0.2% succinate at 37 °C. Data represent mean values of triplicate experiments with error bars indicating standard error of the mean (SEM).

The difference in carbon source utilization of WT and Δ*pdhR* are summarized in (S Fig.1-1). No growth of *pdhR* mutant strain was observed when galactitol (formerly dulcitol) was used as the sole carbon source (Fig.3-4A). Galactitol is one of the four naturally occurring hexitols and a few strains of *E. coli* isolates have been reported to ferment galactitol as an energy source (Lengeler, 1977). Compared to the WT there was a lag in growth of the *pdhR* mutant in 8 carbon sources such as, L-malic acid, acetic acid, propionic and L-threonine (Fig.3-4A and S Fig.1-1). Remarkably, the mutant outgrew the WT in 6 carbon sources,

including, N-acetyl-D-glucosamine, L-fucose, D-fructose and Mannose (Fig. 3-4B and S Fig.1-1). The data suggest that PdhR might be a regulator for genes associated with the carbon sources where growth variation was observed.

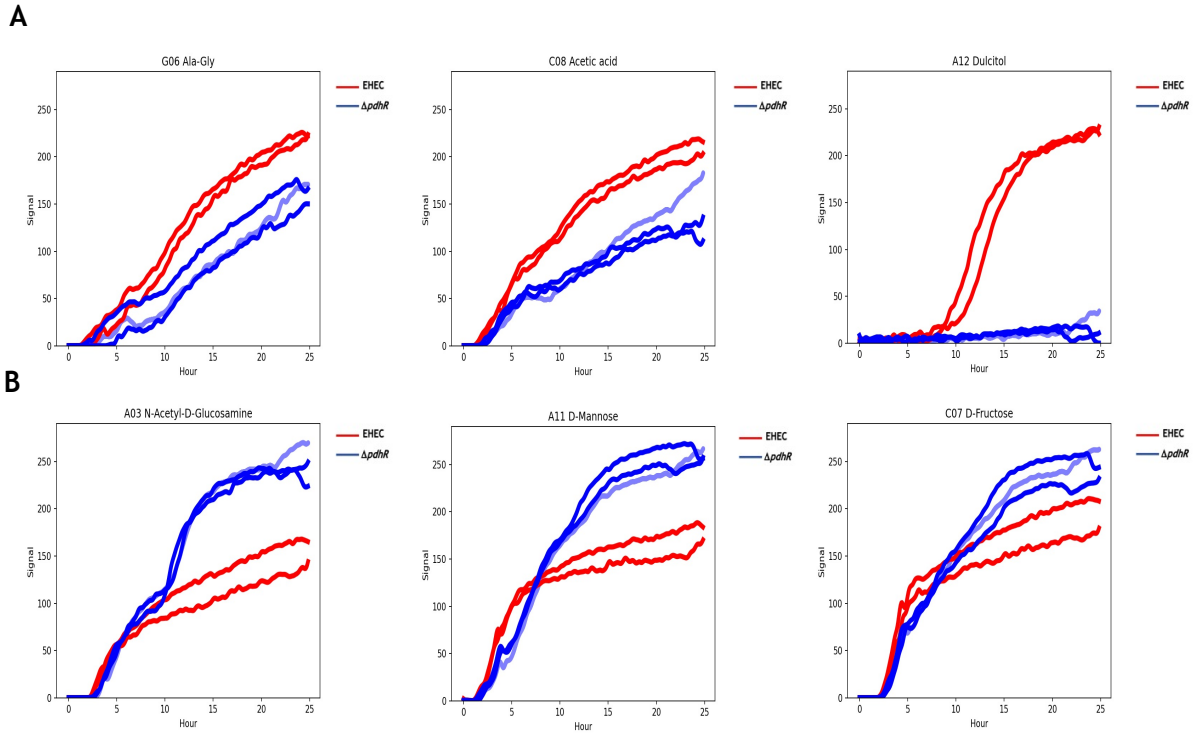

Fig. 3-4. BIOLOG phenotype microarray profiles of WT strain (Red) vs. Δ*pdhR* strain (Blue). (A) PM1 plates showing lag growth by the *pdhR* mutant and (B) PM1 plates showing lag growth by the WT on selected carbon sources. The reaction was monitored for 24 hours at 37ºC.

PdhR is the negative regulator of pyruvate dehydrogenase complex (PDC). PDC links the glycolysis and tricarboxylic acid cycle (TCA) through the oxidative decarboxylation of pyruvate to acetyl-coenzyme A (Lazzarino et al., 2019) and its loss limits aerobic growth (Maeda et al., 2017). Supplementing growth media with succinate, a metabolic intermediate of the TCA cycle after deletion of the *pdhR* gene was shown to restore *E. coli* K12 parent growth phenotype (Anzai et al., 2020). The same observation was found in the phenome data and the simulated experimental growths with addition of 0.2% succinate to MEM-HEPES media (Fig.3-3C and Fig.3-3D). In addition, there was no statistical difference in the generation time of EHEC and the *pdhR* knockout grown in MEM-HEPES supplemented with 0.2% succinate (Table S1 and S. Fig 1-3). Hence, going forth 0.2% succinate was added as a supplement to any growth media for experimental designs involving the WT and the *pdhR* mutant strain.

3.2.5 Analysis of biofilm and cell motility

To study the effect of these regulators on biofilm formation, 96 well flat-bottom plates were used to quantify biomass in M9 media and M9 with succinate for the *pdhR* mutant strain. Biofilm biomass was quantified using the crystal violet assay. To date there is limited data on the role of these regulators, e.g the role of PdhR in biofilm formation in EHEC. Contrary to previous reports (Domka et al., 2006), our data indicates that *bssS* and *rcnR* deletions had no effect on biofilm formation (Fig.3-5A). The most drastic changes were observed on the *yfeC* mutant strain which showed a significant increase in biofilm formation under similar conditions with other test strains ($p < 0.0001$). Δ*pdhR* strain developed the lowest biomass activity after 24 hrs of growth ($p \leq 0.05$), implying that deleting *pdhR* results in decreased biofilm formation.

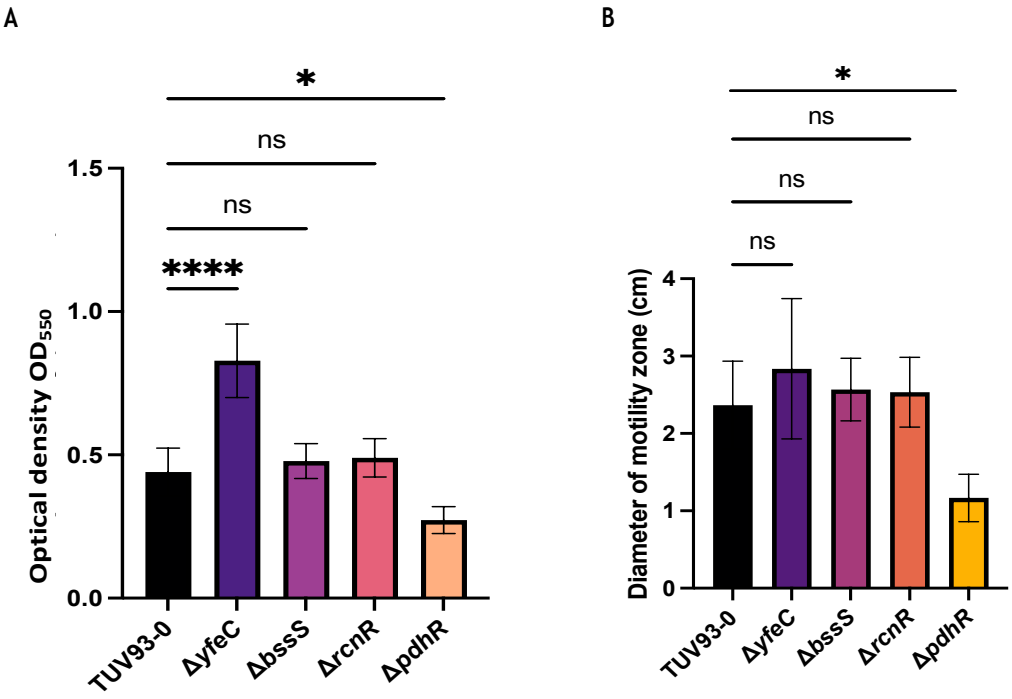

Fig. 3-5. Effect on motility and biofilm formation. (**A**) Biofilm assay, following growth to an OD of 0.6 (OD_{550}), biofilm biomass was quantified using crystal violet assay. (**B**) The motility assay was carried as previously described by Wolfe and Berg (1989). Five µL of this culture was transferred to the centre of 0.25% Tryptone agar plate and incubated for 8 hours at 30°C. Each bar represents the mean data obtained from three technical repeats of independent biological triplicates. Data was analysed by one-way ANOVA with Dunnett's test. * denotes $p \leq 0.05$; **** $p \leq 0.0001$; ns (no significance) $p > 0.05$.

Deletion of these regulators had no significant difference in cell motility when compared to the WT, except for PdhR which showed a significant decrease (Fig.3-5B). Though *yfeC* deletion affected biofilm formation, this phenotype was not directly linked with cell motility, since increase in biofilm formation but not cell motility was observed (Fig.3-5A and Fig.3-5B). The findings implied that *yfeC* and *pdhR* genes may be important for EHEC biofilm formation and motility, therefore may play a role in EHEC virulence.

3.2.6 Role of the transcriptional regulators on *LEE1* activity

The T3SS is a key virulence factor and expression is shown to be affected by many regulators (Connolly & Roe, 2016). Several transcriptional regulators have been extensively characterized and shown to regulate the five LEE operons. EHEC LEE1 operon promoter region is located upstream from the *ler* gene. To measure the activity of the *LEE1*, a *LEE1*: GFP reporter construct was used, carrying both LEE1 promoters, P1 and P2 upstream the ATG start of the *ler* (Roe et al., 2003).

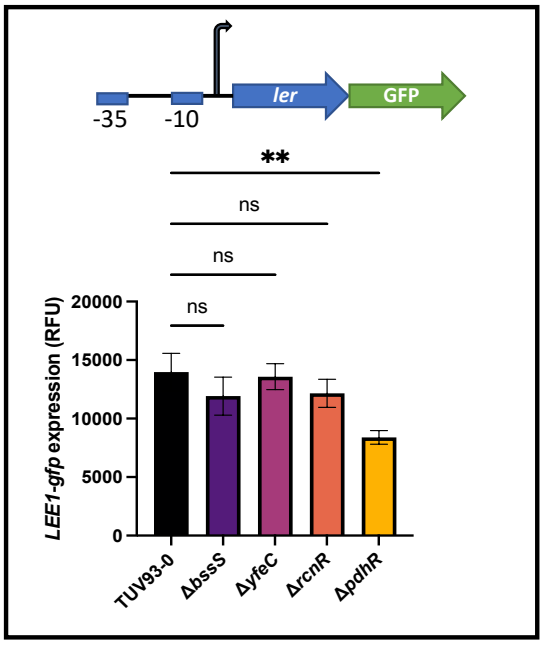

Fig. 3-6. Effects of regulators on LEE1 activity. The expression of LEE1 promoter activity was measured at exponential phase and plotted against OD_{600}. Each bar represents the mean of data obtained from three technical repeats of independent biological triplicates. Data was analysed by one-way ANOVA with Dunnett's test. ** denotes $p \leq 0.01$; ns (no significance) $p > 0.05$.

Activity was measured after growing cells in MEM-HEPES and MEM-HEPES supplemented with 0.2% succinate for the *pdhR* knockout strain to an optical

density of 600nm of ~0.8 at 37°C.There was no significant difference in the growth of mutants and WT strain. This enabled to study the expression of *LEE1* irrespective of growth advantage. The LEE1 reporter showed no difference in activity for the Δ*yfeC*, Δ*bssS* and Δ*rcnR* strains at exponential phase, indicating that these regulators are not essential in EHEC LEE dependent virulence (Fig.3-7). Only the Δ*pdhR* strain showed a significant reduction in *LEE1* activity ($p < 0.001$), suggesting that this regulator is required for virulence and may directly, or indirectly regulate *LEE1* expression. The *pdhR* mutant strain exhibited a significant decrease in virulence in relation to the parent strain. Therefore, it was chosen for further investigation.

3.2.7 Discussion

Transcriptional regulators provide a potential source of new targets to combat specific pathogens. Through the generation and screening of EHEC mutants, two mutants with potential virulence regulation were identified. This first mutant had a deletion of the *pdhR* gene, which encodes pyruvate dehydrogenase complex regulator (PdhR). The regulator represses the *pdh* operon (*pdhR-aceE-aceF-lpdA*) encoding PDHc (Maeda et al., 2017). PDHc serves as an important link between glycolysis and tricarboxylic acid (TCA) cycle by catalysing the conversion of pyruvate to acetyl coenzyme A (acetyl-CoA) (Lazzarino et al., 2019). In addition, it is reported to regulate the respiratory electron transport chain as well as fatty acid metabolism (Anzai et al., 2020). The complex structure differs among Gram-positive and Gram-negative bacteria, with the Gram-positive bacteria structure more related to eukaryotic genomes (Schutte et al., 2015).

Deletion of the regulator resulted in a growth defect when the Δ*pdhR* strain was grown in MEME-HEPES and M9 media supplemented with different substrates used as sole carbon source. This correlates with data reported in *E. coli* K12, where loss of the same regulator caused a growth defect when grown in minimal media, interestingly no growth phenotype was observed when the strain was grown in Luria-Bertani (LB) medium (Göhler et al., 2011). Indeed, all PDHc encoding genes are essential in *E. coli* when glucose is the sole carbon source and are not required when the organism is grown in complex LB medium (Schutte et al., 2015). The 4-fold upregulation of PHDc resulted in an increased

transcription of NADH dehydrogenase in the deletion of *pdhR* (Anand et al., 2021). The loss of the PdhR regulator in *E. coli* K12 resulted in about 20% growth impairment and, however optimal growth was restored by 300 generations of adaptive laboratory evolution (ALE) of the Δ*pdhR* strain (Anand et al., 2021). In a different study, significant growth restoration was achieved by supplementing M9 media with 0.2% succinate (Anzai et al., 2020). The conversion of succinate to fumarate carried out by succinate dehydrogenase is a key step in the TCA cycle (McNeil et al., 2012). Supplementing selected minimal growth media with succinate rewired the TCA cycle and oxidative stress response pathways and allowed efficient growth in Δ*pdhR* strain in this study.

During infection, EHEC requires nitrogen and carbon sources to proliferate, colonize the host at cellular level and evade host immune response to evoke disease. Nonetheless, it faces major challenges in the intestine from commensal microbiota for competition for available substrate in the host environment. Like many other enteropathogens EHEC has evolved specific metabolic mechanisms to overcome these limitations in the host gut, which includes utilization of 1,2-propanediol, L-serine, ethanolamine, and galacturonate (Connolly et al., 2018; Jimenez et al., 2020; Kitamoto et al., 2020; Rowley et al., 2020). Besides serving as important energy source, these metabolites are important cues to regulate expression of virulence genes. Hence, studying metabolic profile of EHEC and the PdhR regulator was of interest.

The Δ*pdhR* strain did not grow on galactitol when it was as a sole carbon source. Galactitol has been shown to be transported and phosphorylated through a phosphoenolpyruvate (PEP)-dependent phosphotransferase system (II^{Gat}) (Nobelmann & Lengeler, 1996). During Galactitol uptake, galactitol 1-phosphate (Gat1P) is converted into D-tagatose 6-phosphate (Tag6P) by genes *gatC,A,D* (*gat* operon). The genes *pfkA* or *pfkB* control the kinases phosphofructokinase I and phosphofructokinase II, respectively, which catalyse the phosphorylation of this intermediate to D-tagatose 1,6-bisphosphate (Nobelmann & Lengeler, 1996). Loss of a functioning phosphofructokinase system has been shown to prevent the growth of *E. coli* K12 on galactitol (Lengeler, 1977). Furthermore, the *gat* gene cluster has been reported to be

pertinent for *Salmonella enterica* colonisation in livestock, as deletion of this gene cluster resulted in attenuated colonisation (Serovar, 2017). PdhR acts as positive regulator for the *pykF* and *ppsA* genes which encodes pyruvate kinase (PykF) and phosphoenolpyruvate (PpsA), respectively (Anzai et al., 2020). PykF converts PEP to pyruvate while PpsA converts pyruvate back to PEP. Taken together, it is possible that PdhR has a similar effect on the two kinases (*pfkA* and *pfkB*) and its deletion may also inhibit galactitol metabolism in EHEC.

Interestingly, compared to *pdhR* mutant, the WT strain did not efficiently metabolise mannose, D-fructose, and N-Acetyl-D-Glucosamine (NAG) tested on PM plates (Fig.3-4B and S Fig.1-1). There is evidence that EHEC can utilise mucin-derived sugars such as (mannose and NAG) as sole energy sources, in addition use them as signalling metabolites for virulence expression (Garimano et al., 2022). Furthermore, EHEC can utilise lactulose as well as benefit directly or indirectly from galactose and fructose made available by degradation of lactulose in the gut by different microbiota (Wotzka et al., 2018). The efficient gain in function of the *pdhR* mutant in metabolising NAG, D-fructose, and mannose carbon sources demonstrates that the regulator may be interlinked with pathways and/or as a negative regulator of genes involved in metabolism of these mucin-derived sugars.

EHEC causes serious infections that are strongly associated with its planktonic and biofilm lifestyles. Biofilm formation aid in bacterial colonisation of the host and provides resistance to host immune system (Kim et al., 2016). Exploring genes involved in biofilm formation is of great importance as it can help in better understanding EHEC virulence and ultimately give insights on how to prevent and treat EHEC infections. Genes which induce *E. coli* biofilms were previously described by Domka et al. (2006). In their study, they found out that BssS regulate *E. coli* K-12 biofilm formation by influencing cell signalling. Other genes which may participate in biofilm formation remains unknown in *E. coli* isolates particularly in *EHEC strains*. A regulator that appears to be involved in control of biofilm formation (YfeC) has been identified from previous work (Connolly et al., 2018). An increase in biofilm formation was observed in the *yfeC* mutant strain. These data compare with those from previously reported experiments indicating that deleting *yfeC* gene in *E. coli* K12 increased eDNA

from planktonic cultures and was found to be a negative transcriptional regulator of genes encoding proteins related to eDNA and biofilm formation (Ibáñez de Aldecoa et al., 2017). The biofilm polymeric matrix constitutes mainly of eDNA, extracellular polysaccharides, lipids, proteins and nucleic acids (Flemming and Wingender, 2010). Deletion of *yfeC* led to an increase in biofilm formation as result of unregulated eDNA expression in EHEC. However, the gain in LEE-dependent virulence was reduced which is the most important virulence factor in EHEC pathogenesis.

It was demonstrated that deletion of *pdhR* from EHEC results in a significant decrease in biofilm formation. This suggest that PdhR, which controls central metabolic fluxes in *E.coli* (Giannakopoulou et al., 2018), may also regulate biofilm mediated virulence in EHEC. Apart from controlling metabolic fluxes, PdhR was also found to be involved in cell division (Giannakopoulou et al., 2018), hence the suggestion that it might have a central importance in EHEC biofilm function and formation. The minor sigma factor of RpoF, FliA, regulates a number of genes related to motility and flagellar production (Mellies et al., 2007). In a study by Anzai et al. (2020), they revealed that pyruvate sensing PdhR regulates the synthesis of flagellar components under RpoF regulation. The expression level of flagellar genes increased in the absence of PdhR, suggesting a novel paradigm in which the level of pyruvate controls flagella regulation in *E. coli* K12 (Anzai et al., 2020). This was further confirmed by motility assay in which the *pdhR* knock out strain showed an increase in swimming compared to the wild type strain (Anzai et al., 2020). However, the same phenotype was not observed in EHEC strain, as we found a decrease in motility assays in the absence of PdhR suggesting a strain specific role of PdhR. Taken together, YfeC and PdhR maybe key for EHEC biofilm formation thereby providing a new and totally unexplored target that could be inhibited to reduce EHEC colonization.

To confirm whether the identified transcriptional regulators affect the expression of the LEE in EHEC, a *LEE1*:GFP reporter assay was used. *LEE1* expression was significantly reduced ($p \leq 0.05$) as shown in the *pdhR* knock strain, while disruption of other regulators resulted in no significant difference in *LEE1* expression. The results suggest that *pdhR* plays an important role in

either directly or indirectly coordinating *LEE1* expression in EHEC. Previous studies have shown that the master regulator Ler encoded by LEE1 operon activates LEE2 to LEE5 operons (Mellies et al., 2006). In addition, Ler controlled EHEC virulence is coordinated by many TFs which bind on the open reading frame (ORF) of the promoter region of the Ler in response to different environmental signals (O'Boyle et al., 2020). Thus, it is likely that in EHEC, PdhR represent an alternative route to activate LEE gene expression in response to myriad environmental signals.

3.3 Conclusion

This chapter highlights that, PdhR a transcriptional regulator that is known to control central metabolic fluxes in microorganisms can provide a new and totally unexplored target that could be inhibited to reduce LEE expression and biofilm formation in EHEC. The work also highlights how horizontally acquired virulence factors are "wired" into central metabolism by conserved regulators, such as PdhR. Because of the important phenotype observed on the *pdhR* knock strain in EHEC virulence, it was therefore decided to proceed with PdhR for further evaluation on its role on EHEC virulence.

Chapter 4: Molecular mechanisms underpinning PdhR, a GntR/FadR family regulator affecting the type three secretion system

4.1 Introduction

To respond to the ever-changing milieu, EHEC strains have evolved efficient regulatory strategies to guarantee their survival and proliferation in a given environment. This is achieved by integration of global transcriptional regulators and regulatory pathways that tightly control gene expression. One way of regulating transcription is through TFs, possibly the most used mechanism by bacteria (O'Boyle et al., 2020). TFs have been widely reported to regulate the expression and repression of several genes involved in the transport and metabolism of sugars, cell division, biofilm formation and virulence in response to cellular signal shifts (Gao et al., 2021).

ler is the first gene of the *LEE1* operon and is a master regulator of the *LEE1* operon and consequently the rest of the LEE operons (Turner et al., 2018). The expression of *ler* is controlled by several global regulators, including QseA, FIS, HIS, H-NS (Bustamante et al., 2011; Sharp & Sperandio, 2007). In addition, the LEE also encodes GrlA which acts as an activator and GrlR a repressor which binds GrlA to prevent its activity on LEE transcription (Bustamante et al., 2011). In EHEC, *LEE1* promoter region is located upstream the *ler* gene and has two promoters, the distal P1 promoter and the proximal P2 promoter, located 163 and 32 base pairs respectively, respective to the *ler* translation start site (Fig.4-2 A) (Sharp & Sperandio, 2007).

From the previous chapter the screened transcriptional regulator PdhR was shown to potentially affect LEE activity and biofilm formation. PdhR is a member of GntR family of transcriptional regulators, which forms one the largest group of prokaryotic transcription factors (Ogasawara et al., 2007). The family include two functional domains made of a conserved N-terminal HTH (helix-turn-helix) DNA-binding domain but differ in the C-terminal effector-binding and oligomerization domain (Suvorova et al., 2015). The C-terminal does not bind to DNA but can change conformation of the DNA-binding domain thereby altering the HTH motif, consequently playing a role in gene regulation (Suvorova et al., 2015). FadR, Hutc, MocR and YtrA form the main four group of GntR family classified using the un-conserved C-terminal domain, while AraR and PlmA make the two minor subfamilies (Rigali et al., 2002; Meiying Zheng et al., 2009). FadR which is the largest of the main four comprises ~40% of the GntR

family of TFs (Arya et al., 2021). This family of TFs has been well characterised in several bacteria, and it has been shown to regulate oxidised substrates or at the crosslink of metabolic pathways such as, pyruvate (PdhR), galactonate (DgoR), galacturonate (ExuR) and glucuronate (XxuR) (Suvorova et al., 2015). This sugar acids are mostly reported in bacterial virulence. PdhR/GntR family include approximately 16-23 targets identified in Gram-negative bacteria (Anzai et al., 2020). In *E. coli* K12, PdhR controls the expression of genes involved in central metabolism through the repression the *pdh* operon (*pdhR-aceE-aceF-lpdA*) encoding PDHc and is derepressed by the presence of pyruvate (Ogasawara *et al.*, 2007). In addition, it is involved in regulation of the respiratory electron transport chain as well as fatty acid metabolism (Maeda et al., 2017). Recently it has been shown that RpoF which regulates flagellar formation is under the control of PdhR, suggesting that flagella regulation is controlled by the level of pyruvate (Anzai et al., 2020).

Several studies have described the role of PdhR not only in bacterial physiology (Anand et al., 2021; Maeda et al., 2017; Ogasawara et al., 2007) but have also demonstrated its function in bacterial virulence through flagella regulation (Anzai et al., 2020). However, there is limited information on its role in EHEC virulence and no report in the association of PdhR in EHEC metabolism and virulence particularly through direct or indirect regulation of *LEE1* encoding *ler*.

Here, a comprehensive detail of the role of the TF PdhR in carbon signalling to regulate EHEC virulence is reported. The functional relevance of PdhR in *ler* transcription through binding to the promoter region of *ler* was studied by EMSA. To identify relevant bases essential for PdhR binding to the *ler* promoter region, a site directed-based mutagenesis screening was performed. Finally, an insight on the involvement of PdhR in overall global gene transcription in EHEC was elucidated by quantitative reverse transcription PCR and transcriptomic analysis.

4.2 Results

4.2.1 Effect of carbon substrates utilization on PdhR *LEE1* expression

Upon host infection EHEC constantly monitors the gastrointestinal environment not only to adapt to accessible nutrients present in the gut, but rather also to utilise these signals to control colonization mechanisms (Fomby & Cherlin, 2011). One such metabolite is succinate, which acts as a signal for the expression of the LEE-encoded proteins in EHEC via the TF Cra (Curtis et al., 2014). Related studies on the TF Cra and pyruvate, have shown that Cra increases secretion of EspB and overall T3SS transcription in EHEC via sensing pyruvate (Carlson-Banning & Sperandio, 2016b).

To explore the role of PdhR in metabolite signalling to activate LEE virulence gene expression in EHEC, the *LEE1*:*gfp* reporter which carries a *LEE1* regulatory coding sequence from position -388 to +6 (404 bp) in respect to the ATG start site of the *ler* gene was used (Roe et al., 2003). The reporter plasmid was transformed into EHEC WT and Δ*pdhR* strains. The strains were grown in MEM-HEPES alone and under increased LEE inducing conditions (MEM-HEPES supplemented with either 8.5 mM succinate or 1mM pyruvate). These concentrations have been previously shown to induce LEE expression in EHEC (Carlson-Banning & Sperandio, 2016b). Addition of succinate resulted in an increased expression of *LEE1* activity in both the EHEC WT and Δ*pdhR* strain (Fig 4-1A). Supplementing the growth media with pyruvate also increased *LEE1* activity in EHEC WT, while the *pdhR* knockout strain remained unresponsive to pyruvate (Fig 4-1B). In the previous section addition of succinate corrected the growth defect observed in the *pdhR* mutant. The data here shows that PdhR works in a succinate independent manner in activating LEE expression. Further, the addition of succinate made more relevance to test the regulatory function of PdhR irrespective of niche advantage in EHEC. Taken together, the data implies that the TF PdhR activates EHEC virulence gene expression when pyruvate is present while succinate does not act as an environmental cue for PdhR-dependent LEE expression.

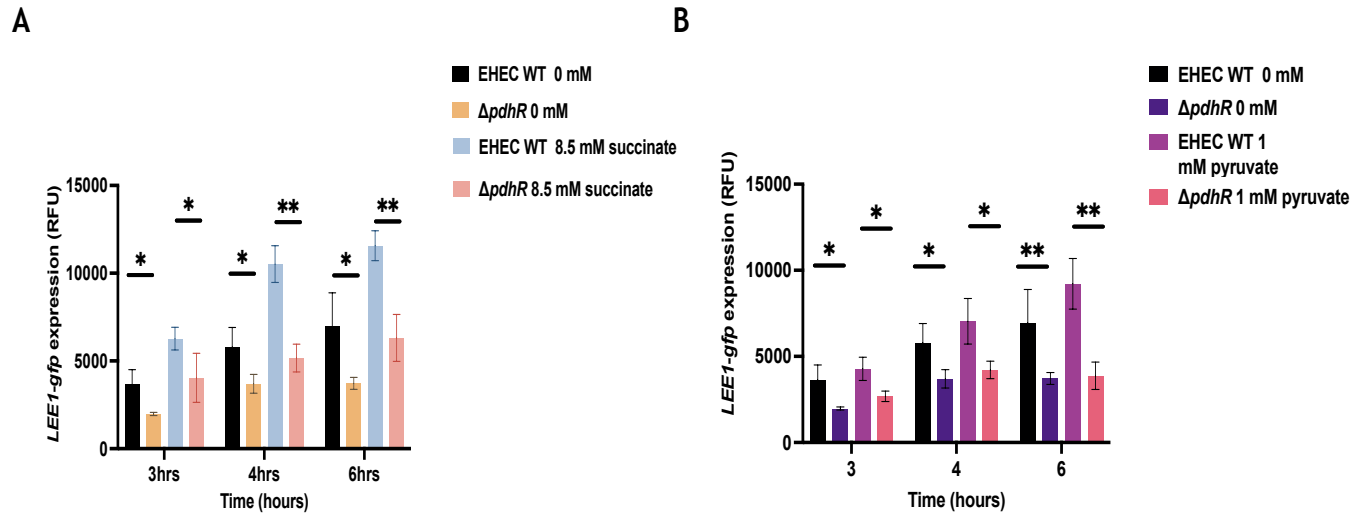

Fig. 4-1. *LEE1* expression is responsive to environmental succinate and pyruvate. EHEC and *pdhR* were transformed with a plasmid containing a GFP-*LEE1* promoter fusion (p*LEE1*:GFP). Activity of the *LEE1* promoter was measured during growth in relative fluorescence units (RFU) using EHEC WT and *pdhR* in MEM-HEPES alone and MEM-HEPES supplemented with **(A)** Growth of EHEC and Δ*pdhR* in 8.5 mM Succinate **(B)** Growth of EHEC and Δ*pdhR* 1mM pyruvate. Data was calculated from three biological replicates and was analysed by one-way ANOVA with Dunnett's test. * denotes p≤0.05; ** p≤0.01.

4.2.2 Regulation of *LEE1* by PdhR at promoter 1 and promoter 2 region

EHEC genome contains a PAI known as the LEE, encoding the T3SS (Zambelloni et al., 2017). The LEE is composed of five polycistronic operons, *LEE1* to *LEE5*. The first operon, *LEE1*, encodes *ler* which is a master transcriptional activator of all the LEE operons and has two promoters P1 and P2 (Sharp & Sperandio, 2007). The *ler*-dependent virulence expression is influenced by many global and specific regulators outside the LEE (O'Boyle et al., 2020). To investigate the role of PdhR on *LEE1* promoter activity, the *LEE1*:*gfp* reporter described earlier was used (Roe et al., 2003). Fig 4-2A illustrates two nest deletions of the fragment. The P1 reporter carries the base sequence from position -138 to -388 and P2 promoter +6 to -138. The fragments were fused to *gfp* and cloned to pACYC184 plasmid. The resulting plasmids containing *LEE1* P1:*gfp* and *LEE1* P2:*gfp* were transformed into EHEC WT and Δ*pdhR*. Measurements of *gfp* expression show the effects of the deletions on the activity of the *LEE1* promoters (Fig 4-2B). There is an increase in expression in both EHEC WT and Δ*pdhR* transformed with P1 reporter though lower expression was still observed in the *pdhR* mutant. Both strains transformed with the P2 reporter had significantly low expression. Thus, it can be concluded that P1 is the major promoter

of the *LEE1* operon in conditions used as previously reported (Sharp & Sperandio, 2007).

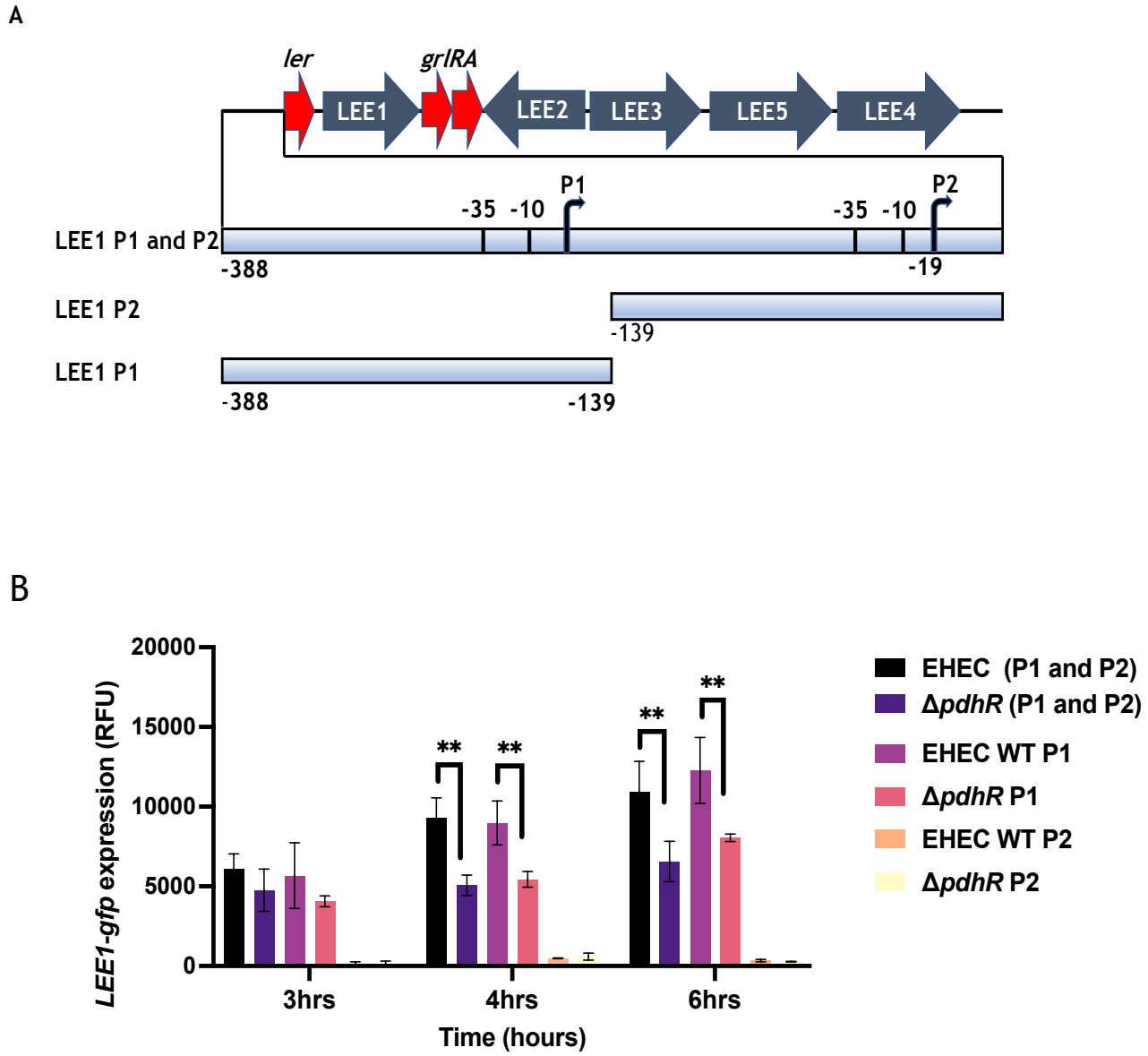

Fig. 4-2. LEE regulon and activity. (A) Schematic representation of the *LEE1* operone regulatory region nested deletions. The coordinates refers to the number of base pairs upstream the functional ATG start codon of the *ler* gene. EHEC promoter 1 (P1) and promoter 2 (P2) together with the -10 and -35 elements are indicated. **(B)** Fluorescence activity of EHEC and Δ*pdhR* transformed with plasmids containing the whole *ler* promoter region (*LEE1* P1 and P2), promoter 1 (*LEE1* P1) and promoter 2 (*LEE1* P2), were fused to GFP. Activity of the nested deleted derivatives of *LEE1* promoter region was measured at an OD_{600} of 0.7 in relative fluorescence units (RFU) during growth in MEM-HEPES supplemented with 0.2% succinate acid. Data was calculated from three biological replicates and was analysed by one-way ANOVA with Dunnett's test. ** denotes $p \leq 0.01$.

4.2.3 PdhR binding motifs within the LEE

The consensus recognition sequence for PdhR consists of a 17 bp long palindromic sequence made of AATTGGTnnnACCAATT (Quail et al., 1994; Quail & Guest, 1995). In recent studies, PdhR was shown to have a higher affinity to DNA sequences with a palindromic trinucleotide sequence GGTnnnACC which is required for tight binding of PdhR (Anzai et al., 2020). Most TFs binding within intragenic sites have been shown to have little to no effect on the transcriptional level in bacteria (Fitzgerald et al., 2023; Martin & Zabet, 2020). Hence, we focused on transcription factor binding sites (TFBSs) in the intergenic regions of the LEE operons and other genes associated with virulence in EHEC. Prediction of the binding sites of PdhR on the LEE operon was done by MEME-Suite software (version 5.1.0; using software default parameters) which enriched a set of sequences for individual matches to the PdhR binding motif.

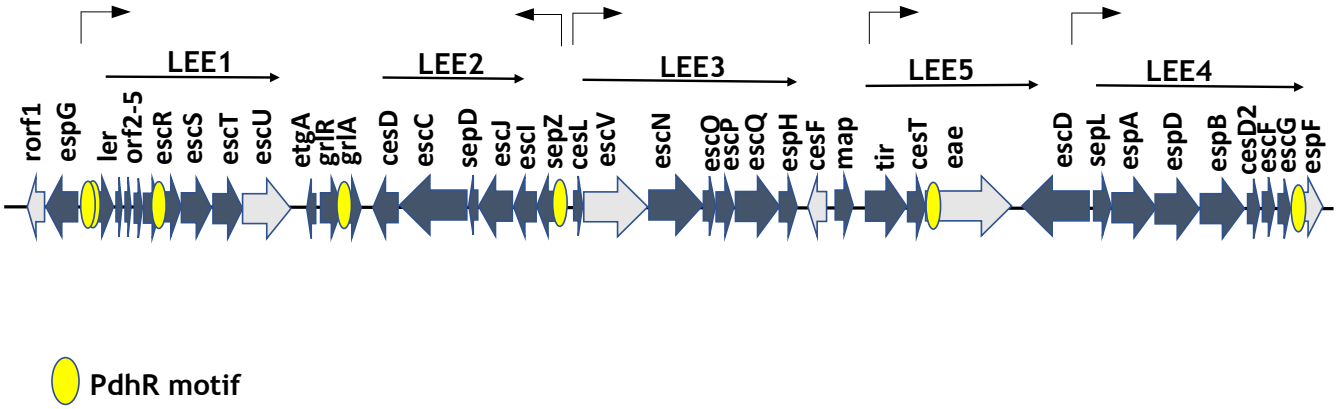

Fig. 4-3. Illustration of predicted PdhR binding motif within the LEE. Predicted binding motifs were generated using the PdhR consensus motif, AATTGGTnnnACCAATT, as reported by (Anzai et al., 2020) using MEME-Suite. The motif occurrences of PdhR binding sites within the LEE were screened according to a *p*-value less than 0.01.

Although TFs can be predicted to bind to many sites within a given genome, they would only bind to a few of them (Martin & Zabet, 2020). Thus, we then associated unique PdhR binding sites which bind only to the promoter regions within the LEE operons and other genes associated with virulence (Table 4-1). Figure 4-3 shows an illustration of predicted binding sites across the LEE operons and 20 of these sites are summarised in Table 4-1.

Table 4-1 Predicted PdhR binding Motifs sequences within the LEE, RpoS gene and PDHc

Motif ID	Gene Name	Start	End	p-value	q-value	Consensus sequence (PdhR box: AATTGGTnnnACCAATT)	Binding sites relative to -10 and -35 hexamers	Conservation
1	*Ler*_1	2111	2127	0.000673	0.622	GTTTGTAATGAACAATT	+2(-10); -14(-35)	9/14
2	*Ler*_2	2737	2753	0.000673	0.622	AATGGATATGGGCAATA	-54(-10); -76(-35)	10/14
3	*Eae*	24141	24157	0.000673	0.622	ATTTGGTATTACATAAT	+85(-10); +70(-35)	10/14
4	*grlA*	8905	8921	0.000849	0.622	TATGGATAGAACAAATT	-20(-10); +1(-35)	10/14
5	*Ler*_3	2562	2578	0.00154	0.698	GATAGGTGCGACAAAGA	-770(-10); -791(-35)	9/14
6	*Ler*_4	3278	3294	0.00154	0.698	AATAGATGTGTCCTAAT	-1029(-10); 1051(-35)	9/14
7	*rpoS*	99	115	3e-05	0.0676	AACTGGCTTATCCAGTT	+27(-10); +52(-35)	10/14
8	*pdhR*	31	47	1.07e-10	1.77e-07	AATTGGTAAGACCAATT	+39(-10); +16(-35)	14/14

The table shows a summary of sequences of occurring PdhR motifs within the LEE. The consensus sequence of PdhR was evaluated using the whole LEE operon and 500 bp of sequence from EHEC *rpoS* gene and the *pdhR* which included promoter regions. 20 targets were generated using the MEME-suite program with a cut off value of p-value less than 0.01. The table was also filtered using the 9-bp-long PdhR-box sequence which was reported to be needed for tight binding of PdhR (Anzai et al., 2020).

4.2.4 Cloning and overexpression of PdhR

PdhR coding sequence was PCR purified using *E. coli* EDL933 genome as a template and cloned into pET21a (+) vector between *Nde*I (5') and *Xho*I (3') restriction sites with the 6xhistag at the N-terminal of PdhR. The plasmid construct was then cloned into *E. coli* BL21 (DE3) and selected for growth on ampicillin plates. Colony PCR was used to confirm positive colonies by amplifying for the presence pET21a (+)-PdhR and the PCR templates was sent out for sequencing. The BL21 (DE3) construct produces a Lac repressor which binds to the Lac operator and prevents the promoter from transcribing the T7 RNA polymerase. However, in the presence of IPTG, which is an analog of lactose this repressor drops off and the T7 RNA polymerase is expressed. The T7 RNA polymerase then recognize the T7 promoter on the pET21a (+) vector and anything downstream would be transcribed and translated, in this case PdhR, our protein of interest. A small-scale experiment was then set up to find the most favorable conditions for overexpressing PdhR and it was found out that 24 hours of induction with 1mM IPTG at an $O.D_{600}$ of 1 and incubation at either 18^{o}C or 37^{o}C was optimal for PdhR overexpression (Fig. 4-4 A).

Subsequently cells were cultured in 2-litre batches of LB at 37^{o}C and incubated for 30^{o}C with shaking at 200 rpm. Cells were then induced with 1 mM of IPTG once they reached an OD_{600} of 1. The cell pellets were then harvested by centrifuge. The supernatant after cell lysis was used to analyse for PdhR overexpression by SDS-PAGE (Fig 4-4 B) and western blotting using anti-His antibody, which revealed bands at ~30 kDa and ~60 kDa, which confirms two oligometric states of PdhR (Fig. 4-4C). PdhR protein was purified by high-performance immobilized metal affinity chromatography procedure with the use of nickel (Cytiva HisTrap) columns used for His-tag recombinant protein purification. GntR family of transcriptional regulators ordinarily form dimers and binds to two-fold symmetric DNA operator sequences in such a way that each monomer recognizes a half site (Feng & Cronan, 2014).

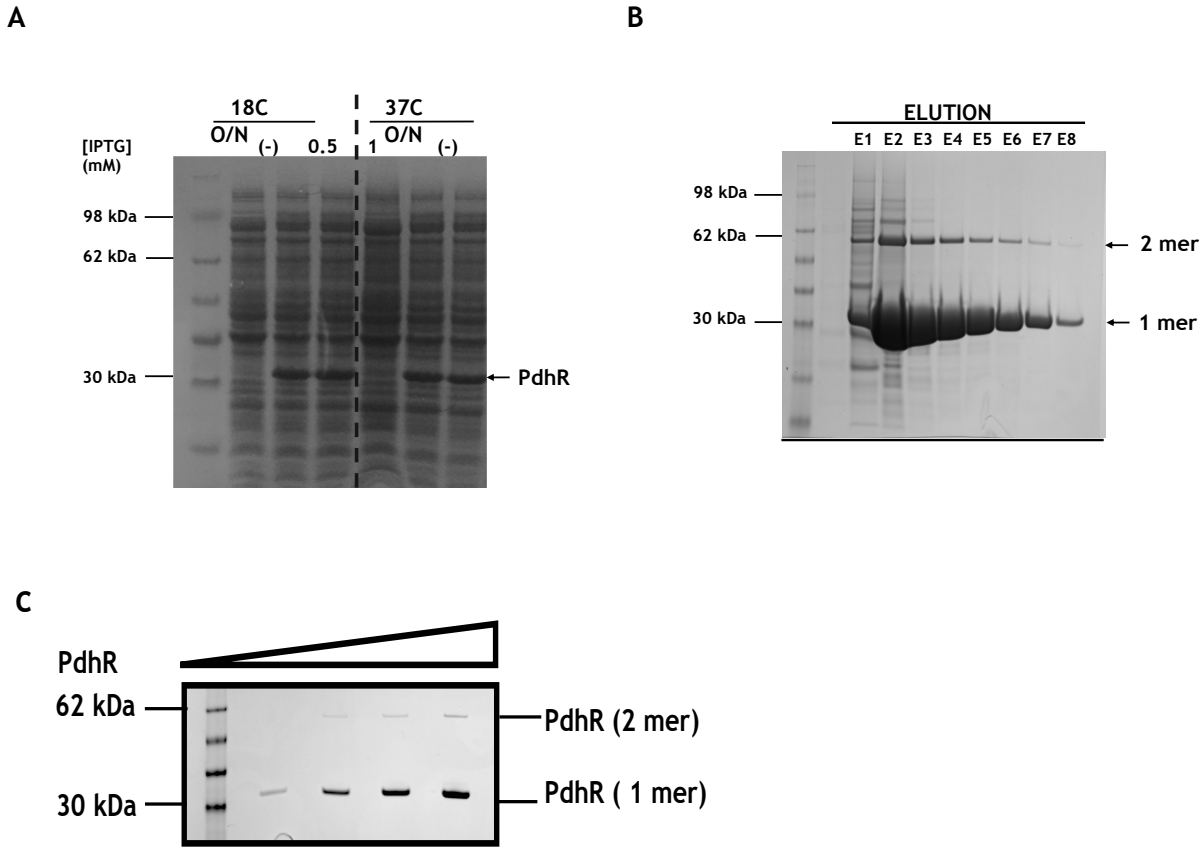

Fig. 4-4. Overexpression and purification of PdhR. (A) A small scale experimental set up of PdhR expression at 18 ºC and 37 ºC, PdhR band at ~30 kDa indicated by arrow. **(B)** Purified PdhR by Ni HisTrap columns confirmed by SDS-PAGE, revealed two oligometric states of PdhR as indicated by bands at ~30kDa and ~60kDa. **(C)** Confirmation of PdhR by western blotting using anti-His antibody, showed the 2 bands with increasing concentrations of PdhR.

4.2.5 Validating PdhR binding through electrophoretic mobility shift assays (EMSA)

FadR family of transcriptional regulators have increased affinity to bacterial promoter regions and are known to confer an auto-regulatory activity (See introduction). To evaluate significance of PdhR in EHEC, the EMSA assay was used. The assay is fundamental in a wide range of qualitative and quantitative analysis for protein-nucleic acid complex interaction. Table 4-1 contains PdhR predicted binding sites in EHEC of interest in this study. Fragments of promoter regions including predicted binding regions were used to assay for PdhR binding sites. PdhR has been reported to bind to its own promoter region thus acts in a self-regulatory manner for the PDHc operon in *E. coli* K12 strains (Kaleta et al., 2010). To attempt to find binding sites of PdhR on its own promoter region in EHEC, DNA fragment +9 to -205 with respect to *pdhR* ATG start site which included predicted PdhR binding

sequences (Table 4-1) was amplified by PCR. The resulting PCR fragments were purified, and equal concentrations of 150 nM were incubated on ice in binding buffer without and with increasing amounts of purified PdhR and 0.5 µg/ml of polydIdC in a total volume of 16µL. EMSA results confirmed that PdhR conferred an auto regulatory activity, as it was able to bind to its own promoter region, whereas no band shift was observed for the negative control *amp* gene regulatory region selected from pCP20 plasmid DNA. The data is in agreement with previous reports on the regulation of PdhR revealed that the transcriptional regulator binds in several promoter regions including the PDHc operon (Ogasawara et al., 2007).

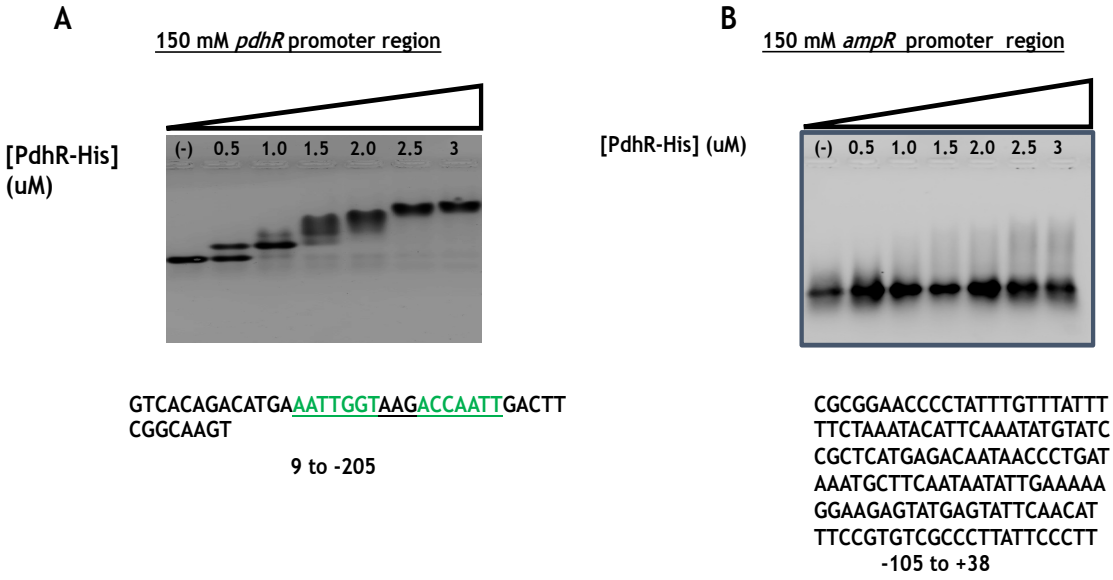

Fig. 4-5. PdhR binds to the regulatory region upstream of the *pdhR* start codon. Increasing concentrations of PdhR were used as noted by triangle on top of each gel. **(A)** DNA retardation was observed in the +9 to -205 fragment with PdhR-DNA complex being formed at the top of the gel while free DNA ran down the gel. PdhR sequence binding box is marked in green. **(B)** PdhR did not form any band shift with fragment DNA selected from *ampR* regulatory coding sequence (negative control). EMSA experiments were performed in triplicate, and similar results were obtained each time.

The T3SS is an effector protein-secreting apparatus that contributes to the overall virulence of EHEC. T3SS is employed by EHEC to deliver a plethora of effector proteins into host cells resulting in actin cytoskeletal rearrangement and disruption of host cell processes (Cameron et al., 2018). To assess the functional relevance of PdhR in EHEC virulence via its regulatory effect on *ler*, four fragments within the *ler* promoter region which included PdhR predicted binding sites (Table 4-1) were used

for EMSA assays. The first fragment used was the *LEE1* reporter (Roe et al., 2003) which is -388 to +6 (404 bp) in respect to the ATG start site of the *ler* gene. PdhR boxes were aligned to the three putative binding sites within the *LEE1* regulatory element (Fig 4-6). Box 1 lies between the -10 and -35 elements of the *LEE1* P2 promoter and overlaps the -35 element of P2, while Box 2 lies at position -76 and +40 relative to the *LEE1* P2 and P1 transcriptional start site. Finally, Box 3 lies at position -792 and -658 relative to the *LEE1* P2 and P1 transcriptional start site. EMSA results confirmed the binding of PdhR to the *LEE1* regulatory element (Fig 4-6), while no gel shift was observed for negative control selected from *amp* regulatory region which had no predicted binding sites (Fig 4-5 B). The fragment upstream of the *ler* was long (~388bp) which led to weak PdhR binding as shown by the mobility shift data (Fig.4-6). Using an unusually large DNA probe of ~500 raises a possibility of weak binding of TFs to several sites (Feng & Cronan, 2014).

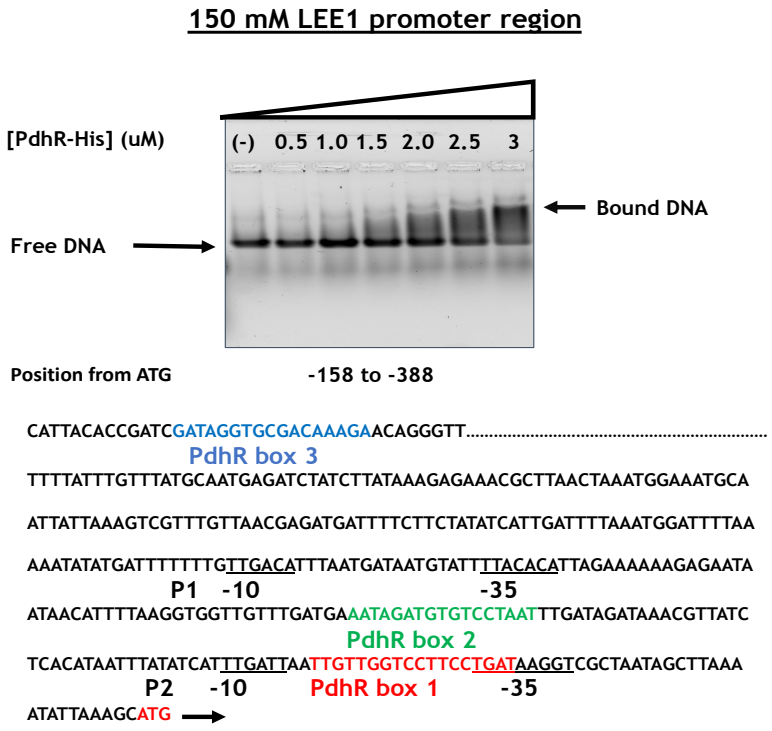

Fig. 4-6. PdhR binds to the *LEE1* regulatory region. EMSA assay of PdhR binding to -388 bp *LEE1* regulatory region. Increasing concentrations of PdhR were used as noted by triangle on top of each gel. Sequence conservation of the three predicted PdhR boxes in the *LEE1* fragment are colour coded red, green, and blue by which PdhR box correspond to. The *ler* ATG start codon is annotated. EHEC promoter 1 (P1) and promoter 2 (P2) together with the -10 and -35 elements are indicated are underlined. DNA retardation was observed with the PdhR-DNA complexes remaining at the top of the gel whilst the free DNA ran further down the gel. EMSA experiments were performed in triplicate, and similar results were obtained each time.

Next, to verify specific PdhR binding sites to the *LEE1* regulatory element and to correct for weak binding by PdhR to the *LEE1* promoter, smaller DNA fragments of ~100 bp were generated. The second and third fragments were amplified by PCR using EHEC genomic DNA containing the Promoter 1 region (-158 to -388) and Promoter 2 region (+6 to -126), respectively. Finally, the fourth fragment contained -789 to -899 bp which is further upstream from the previously reported *LEE1* promoter (Sharp & Sperandio, 2007). The putative PdhR binding sites to the three generated fragments were confirmed *in vitro* by EMSA (Fig 4-7). PdhR like other transcriptional regulators with a helix-turn-helix motifs, including Crp and Fnr, recognizes and binds to sequences with a dyad symmetry (palindromic sequence) (Quail & Guest, 1995). A 17 bp long palindromic sequence consisting of AATTGGTnnnACCAATT was previously identified as the consensus recognition sequence for PdhR (Quail et al., 1994; Quail & Guest, 1995). In recent studies PdhR was shown to have higher affinity to a DNA sequence with a palindromic trinucleotide sequence GGTnnnACC which is required for tight binding of PdhR (Anzai et al., 2020).

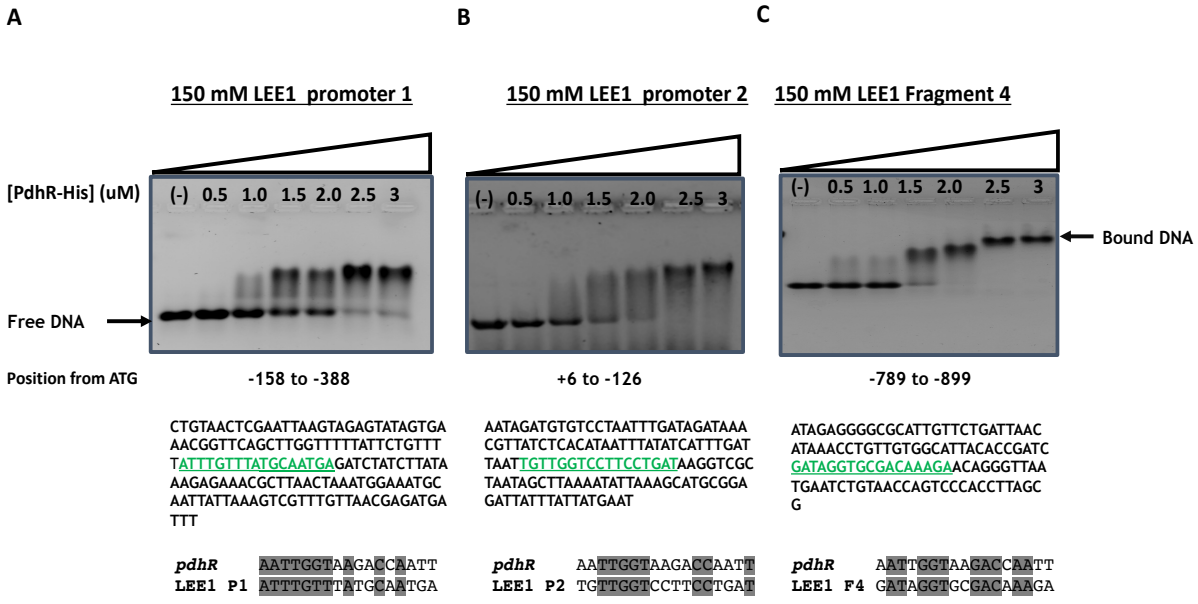

Fig. 4-7. Multiple binding sites of PdhR to *LEE1* coding sequence region. EMSA assay of PdhR binding to three fragments covering +6 to -899 *LEE1* regulatory region. Increasing concentrations of PdhR were used as noted by triangle on top of each gel. **(A)** DNA retardation was observed with the PdhR-DNA complexes in the -158 to -388 which included the P1 promoter region only **(B)** DNA retardation was observed with the PdhR-DNA complexes in the +6 to -126 which included the P2 promoter region only. **(C)** DNA retardation was observed with the PdhR-DNA complexes in the +789 to -899 which included the open reading frame between *ler* Promoter region and *espG* gene. Sequence conservation of the three

predicted PdhR boxes in the *LEE1* fragment are shown at the bottom of each gel. EMSA experiments were performed in triplicate, and similar results were obtained each time.

Identified PdhR-Boxes have a partial palindrome sequence (Fig 4-6). PdhR was found to interact with *LEE1* P1 fragment ranging from +6 to -899 upstream the *ler* transcription site. Interestingly Box 2 and 3 are located within the *LEE1* promoter region. The data suggests that Box 1 (within P2) might be a crucial binding site for PdhR on the *LEE1* regulatory region and possibly acting as an activator due to its position relative to the *LEE1* P2 promoter. However, from the *LEE1* P1 and P2 reporter assay it was shown that *LEE1* activity is largely expressed at the P1 promoter and minimal activity at the P2 promoter (Fig 4-2). Box 2 is located +41 and Box 3 is located -638 distal the relative the P1 promoter.

To further confirm the binding of PdhR between the -10 and -35 hexamer elements of the *LEE1* P2 promoter, mutations were generated by substituting the last 7 bases on the putative binding sequence of PdhR on the *LEE1* P2 promoter region (Fig 4-8B). A ~150 bp fragment covering the mutagenized putative PdhR binding sequences was used for EMSA assays. This led to a partial reduction in PdhR binding affinity to the *LEE1* P2 promoter region (Fig 4-8B) and this was also confirmed by reporter assay (Fig 4-8C). Taken together the data implies that PdhR plays a regulatory role at both the *LEE1* P2 promoter and *LEE1* P1 promoter because of the position of predicated binding sites with respect to the -10 and -35 hexamers. However, many reports have shown that *LEE1* P2 activity has a minimal role in *LEE1* activity (Connolly et al., 2016; Sharp & Sperandio, 2007).

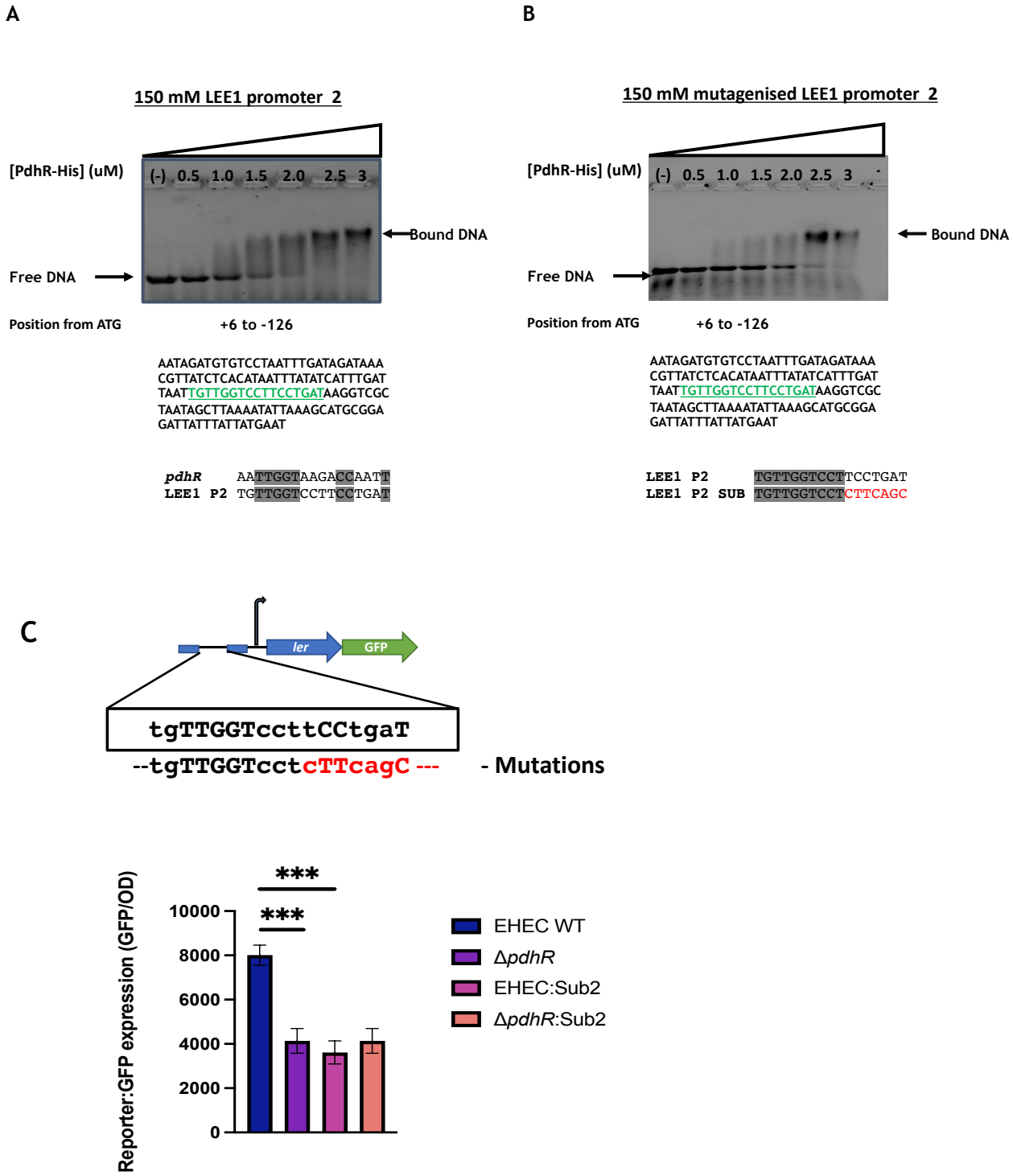

Fig. 4-8. Mutations in the PdhR box within the promoter 2 region partially reduce PdhR binding affinity. EMSA assay of PdhR binding to EHEC P2 region. Increasing concentrations of PdhR were used as noted by triangle on top of each gel. **(A)** DNA retardation was observed with the PdhR-DNA complexes in the +6 to -126 which included the P2 promoter region only. Sequence conservation of the predicted PdhR boxes in the promoter regions of the gene are shown at the bottom of each gel. **(B)** Mutations were generated by substituting the last 7 bases on the putative binding sequence of PdhR on the *LEE1* P2 promoter region. This led to partial reduction in PdhR binding affinity to the P2 *LEE1* promoter region. Substitution

mutations made on the putative binding sequence of PdhR on the *LEE1* P2 promoter region are shown at the bottom of the gel. EMSA experiments were performed in triplicate, and similar results were obtained each time. **(C)** Activity of the *LEE1* mutated promoters (EHEC:Sub2 and Δ*pdhR*:Sub2) was measured during growth in relative fluorescence units (RFU) using EHEC WT and *pdhR* in MEM-HEPES alone and MEM-HEPES supplemented with. Data was calculated from three biological replicates and was analysed by one-way ANOVA with Dunnett's test. *** indicates $p \leq 0.001$.

4.2.6 Further binding of PdhR binding sites

To further explore the regulatory function of PdhR binding to other promoters involved in *LEE1* regulation, ~150 bp fragments covering the regulatory sequences of RpoS (+10 to -142) and GrlA (+4 to -146) were amplified by PCR and used for mobility shift assays. Similarly, PdhR was predicted to bind to the promoter region of RpoS, which plays a major role in bacterial survival in response to environmental signals as well as stimulates the expression of the *LEE1* by activating the transcription of *ler* (Coldewey et al., 2007). EMSA results verified PdhR binding to the promoter region of RpoS in vitro (Fig.4-9B). Deletion of PdhR significantly reduced the transcriptional levels of RpoS (Table S3). Though PdhR was also predicted to bind to GrlA which positively regulates expression of the *LEE1* by acting on the *LEE1* P1 promoter (Islam et al., 2011), no shift was observed on the EMSA results but a smear, elucidating a non-specific binding due to high concentration of protein towards the end of the gradient (Fig.4-9A). Overall, the data suggests that PdhR does not regulate *LEE1* through GrlA however it may activate the expression of the *LEE1* in an RpoS-dependent manner.

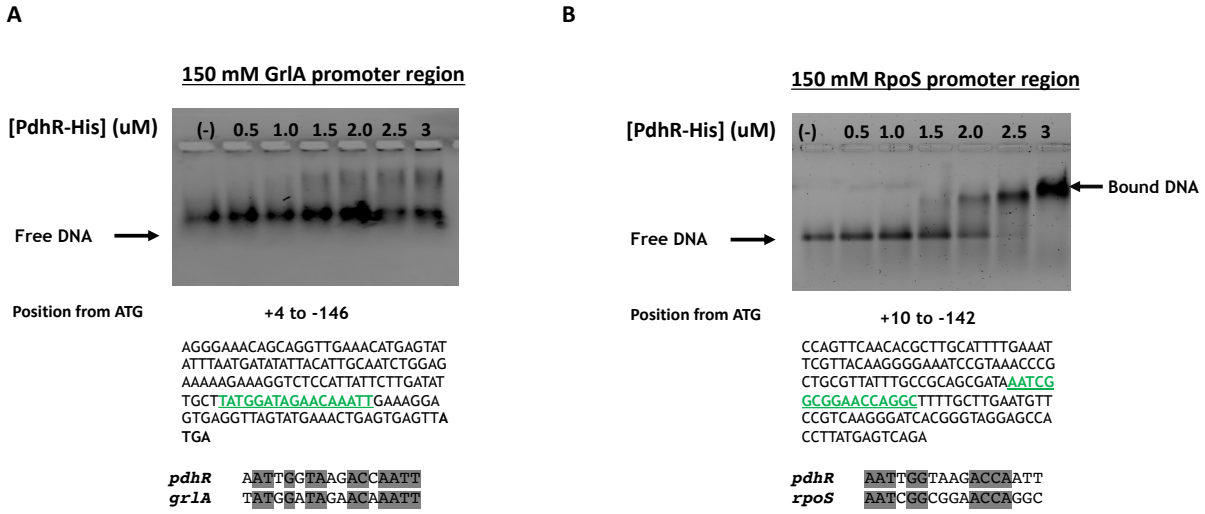

Fig. 4-9. Further binding of PdhR sites in EHEC. EMSA assay of PdhR binding to GrlA and RpoS regulatory region. Increasing concentrations of PdhR were used as noted by triangle

on top of each gel. **(A)** DNA retardation was not observed in the +4 to -146 *grlA* fragment which included the regulatory sequence. **(B)** DNA retardation was observed with the PdhR-DNA complexes in the +10 to -142 fragment of the *rpoS* promoter region. Sequence conservation of the predicted PdhR boxes in the promoter regions of the genes are shown at the bottom of each gel. EMSA experiments were performed in triplicate, and similar results were obtained each time.

4.2.7 Effect of PdhR on the transcriptomic regulon of EHEC

The role of PdhR in LEE associated virulence in EHEC has been established in the previous sections, but there is limited understanding of its function at genome level. In addition, the binding of many TFs within a promoter region is not always associated with transcription of a given gene and in this case are regarded as genomic noise (Fitzgerald et al., 2023). To gain an insight into the genes under the regulation of PdhR and to uncover any novel regulon under the control of PdhR, a transcriptomics experiment was performed. Global transcriptome profiling can enable insights into the direct and indirect regulon of a TF. Thus, RNA was extracted from three biological replicates of EHEC WT and Δ*pdhR* grown under LEE inducing conditions (MEM-HEPES,0.2% succinate, 37^{o}C, OD_{600} of 0.4). Raw reads from the RNA-Seq experiment were processed and mapped to the EDL933 genome and plasmid (NCBI accession number: NC_002655) using CLC Genomics Workbench 20. EdgeR, which is designed for the analysis of replicated count-based expression data, was used to compute differential gene expression (Robinson et al., 2009). A false-discovery rate (FDR) corrected *p*-value threshold of 0.05 and an absolute fold change of ≥ 1.5; ≤ -1.5 was considered as significant.

Quality assessment of the normalized RNA-seq data transcripts were analysed using Principal Component Analysis *(*PCA*)* plot to visualise the relationship among the samples. As observed in Figure 4-10A, EHEC WT samples are clustered together while Δ*pdhR* samples are clustered at one end. Highlighting that the cluster groups share a distinctive global transcriptome as well as genes behaving in a related manner. In total, 1335 genes (727 upregulated and 608 downregulated) were differentially expressed between EHEC WT and Δ*pdhR* strains (FDR of *p*-value ≤ 0.05, fold change of ≥ 1.5; ≤ -1.5 in RNA levels) (Fig. 4-10B). A summary of DEGs with large fold changes that are also statistically significant are shown in Table 4-2 (upregulated) and Table 4-3 (downregulated). These are visualised by a volcano plot (Fig. 4-10C) showing most upregulated genes towards the right and the most downregulated genes towards the left.

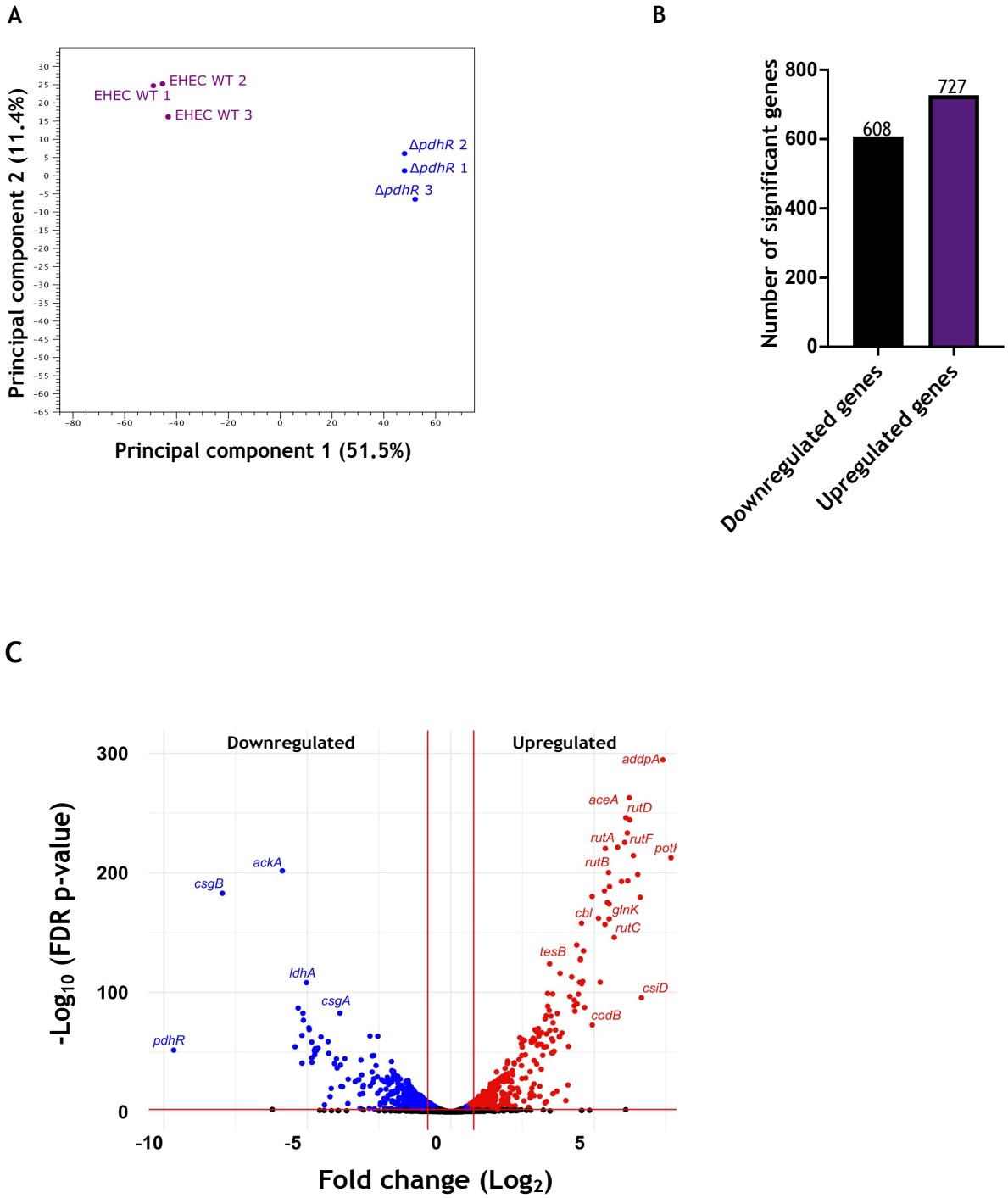

Fig. 4-10. RNA-Seq transcriptome data analysis. (A) Principal component analysis (PCA) results. The figure shows a three-dimensional scatter plot for the PCs result. Each point indicates an RNA-Seq sample. Sample groups are represented by different colors, purple (EHEC WT) and blue (Δ*pdhR*). Samples with comparable gene expression profiles are clustered together. **(B)** The bar graph represents the total number of differentially expressed genes (DEGs), together with significantly downregulates and upregulated genes between EHEC WT and Δ*pdhR*. **(C)** The figure shows a volcano plot identifying DEGs. Significant DEGs are displayed in blue for downregulated genes and red for upregulated genes. The red lines indicate the p-value cut off (p-value <0.05) and fold change cut off (≥ 1.5; ≤ -1.5) for DEGs.

Seven (7) of the top 10 significantly upregulated genes belonged to the following operons: *ddpXABCDF, aceBAK and the rutABCDEFG* (Table 4-2). In addition, positive regulation was detected for all the genes in the stated operons. *csiD*, *argT* and *astA* were among the highly upregulated genes with a 100.46 (*p*-value 1.151E-92), 91.75(*p*-value 7.34E-213) and 82.67(*p*-value 8.544E-221) fold change respectively.

Table 4-2 Top 10 upregulated genes in Δ*pdhR* as identified by RNA-seq

Upregulated genes			
Gene	**Fold change**	**FDR *p*-value**	**Function**
ddpX	205.14	4.889E-224	D-alanyl-D-alanine dipeptidase
ddpA	168.60	3.543E-298	ABC transporter substrate-binding protein
csiD	100.46	1.151E-92	carbon starvation induced protein CsiD
yhdX	97.41	1.169E-189	amino acid ABC transporter permease
argT	91.75	7.34E-213	lysine/arginine/ornithine ABC transporter substrate-binding protein ArgT
astA	82.67	8.544E-221	arginine N-succinyl transferase
aceB	75.46	2.517E-238	malate synthase A
aceA	74.92	5.133E-241	isocitrate lyase
rutE	72.09	1.54E-192	malonic semialdehyde reductase
yhdY	71.34	1.487E-217	amino acid ABC transporter permease

Table 4-3 Top 10 Downregulated genes in Δ*pdhR* as identified by RNA-seq

Downregulated genes			
Gene	**Fold change**	**FDR *p*-value**	**Function**
csgB	-249.50	3.13E-183	curlin minor subunit CsgB
csgA	-58.54	1.66E-197	curlin minor subunit CsgA
csgC	-42.97	8.64E-54	curlin minor subunit CsgC
pspD	-39.94	1.31E-87	phage shock protein PspD
sepL	-36.42	3.34E-61	type III secretion system LEE gatekeeper SepL
cesT	-36.34	3.87E-39	type III secretion system LEE chaperone CesT
pspC	-35.56	3.81E-82	envelope stress response membrane protein PspC
espZ	-35.20	7.99E-76	type III secretion system LEE cytoprotective effector EspZ
pspB	-30.822	8.62E-70	envelope stress response membrane protein PspB
pspG	-30.772	8.62E-43	envelope stress response membrane protein PspG

The most downregulated DEGs included genes belonging to the *csgBAC*, *pspABCDE*, *LEE2*, *LEE4* and *LEE5* operon and as expected. The observed operons have not been reported as PdhR targets, except for the *pdhR* gene which encodes PdhR has been shown to bind to its own promoter region thereby capable of self-regulation (Anzai et al., 2020). Although the operons have not been previously reported as being direct PdhR targets, they cannot be ruled out as being part of the PdhR regulon.

The top 10 Gene ontology (GO)-enrichment analysis was based on all available pathways in ShinyGo platform (Biological Process, cellular component, molecular function, local network cluster-(STRING)) (Fig. 4-11). Most of the upregulated genes GO terms were linked to synthesis of cellular processes e.g ribosome (Fold=4.5), translation, and ribonucleoside triphosphate biosynthetic process (Fold=3.5). In addition, other GO terms corresponding to peptide biosynthetic process (Fold=2.8), protein export (Fold=3.1) cellular nitrogen compound biosynthetic process (Fold=1.9) were enriched (Fig. 4-11A).

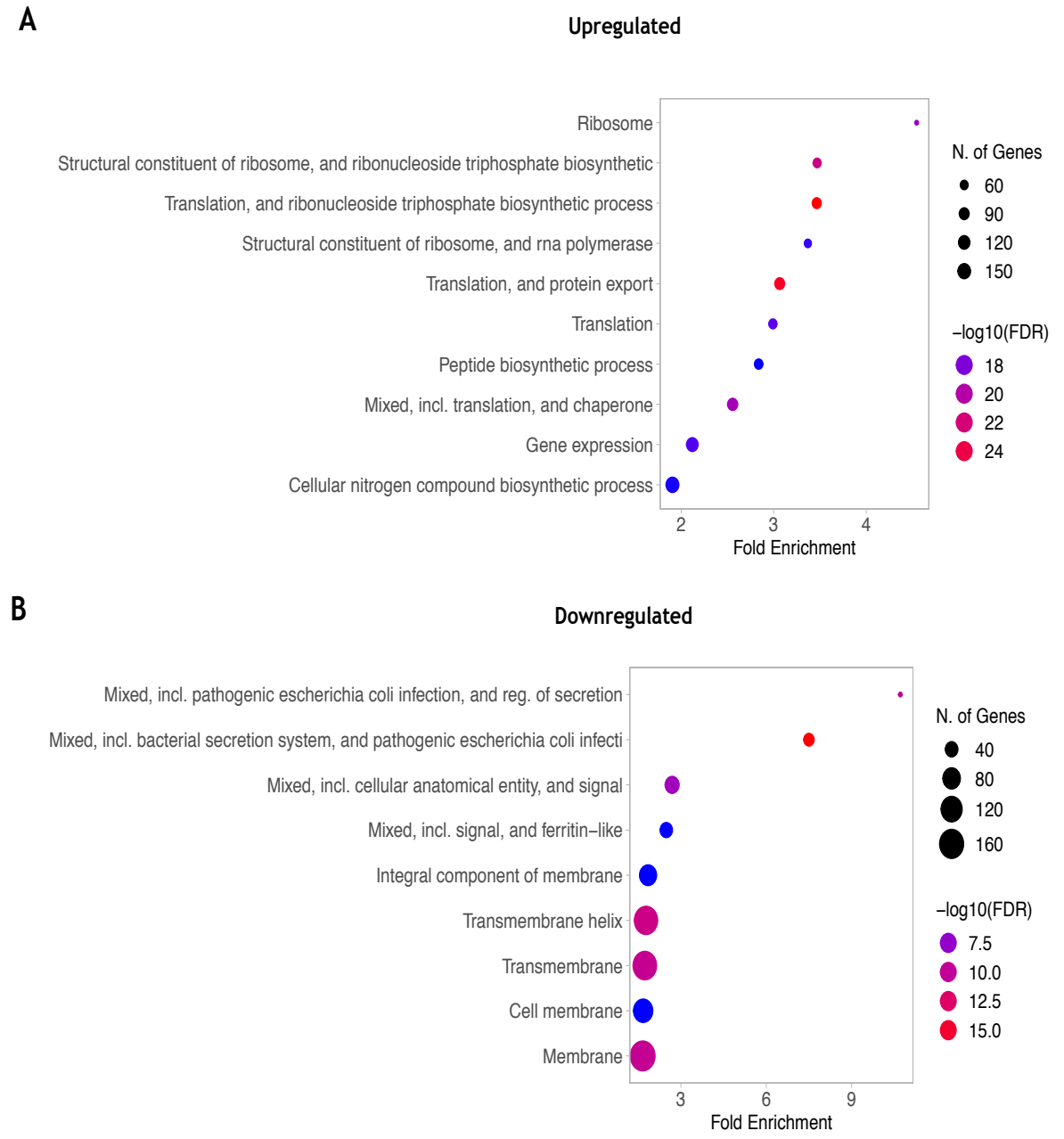

Fig. 4-11. Functional groupings of the DEGs. Figures illustrates the top 10 ranked GO terms using gene count. Log (FDR) is the log10 of the FDR value calculated based on nominal P-value. Fold Enrichment is defined as the percentage of genes in the DEGs belonging to a pathway, divided by the corresponding percentage in the background. Number of genes refers to genes enriched in a GO term. **(A)** Functional grouping based on all available pathways in ShinyGo 0.80 grouping of upregulated genes. **(B)** Functional grouping based on all available pathways in ShinyGo 0.80 grouping of downregulated.

The enrichment analysis of downregulated DEGs ranked by fold-enrichment identified pathways involved bacterial virulence, including pathogenic *Escherichia coli* infection and regulation of secretion (Fold=7.8) and bacterial secretion system (Fold=6.9). It is noteworthy to mention that several LEE PAI genes were significantly

downregulated including the master regulators *ler* and *grlA* (Table S3). Most of the downregulated DEGs functions were linked to cell membrane integrity, in particular transmembrane helix (Fold=1.8) integral component of membrane (Fold=1.8) and cell membrane pathways (Fold=1.7) (Fig. 4-11B). Overall, these results suggest that upregulated genes in the Δ*pdhR* majorly participate in an array of cellular processes, while down regulated genes highlight the specific role of *pdhR* in EHEC LEE-dependent virulence. Figure 4-12 shows the sequence read distribution across the EHEC WT and Δ*pdhR* strains, with an expanded view in the LEE PAI. The reads of Δ*pdhR* across the LEE PAI compared to EHEC WT were relatively low and this data is consistent with LEE downregulated genes reported in the previous sections (Table 4-3). There is ample read witnessed across the EHEC WT and Δ*pdhR* strains with noticeable low reads within the LEE PAI, suggesting a specific T3SS virulence regulation by PdhR.

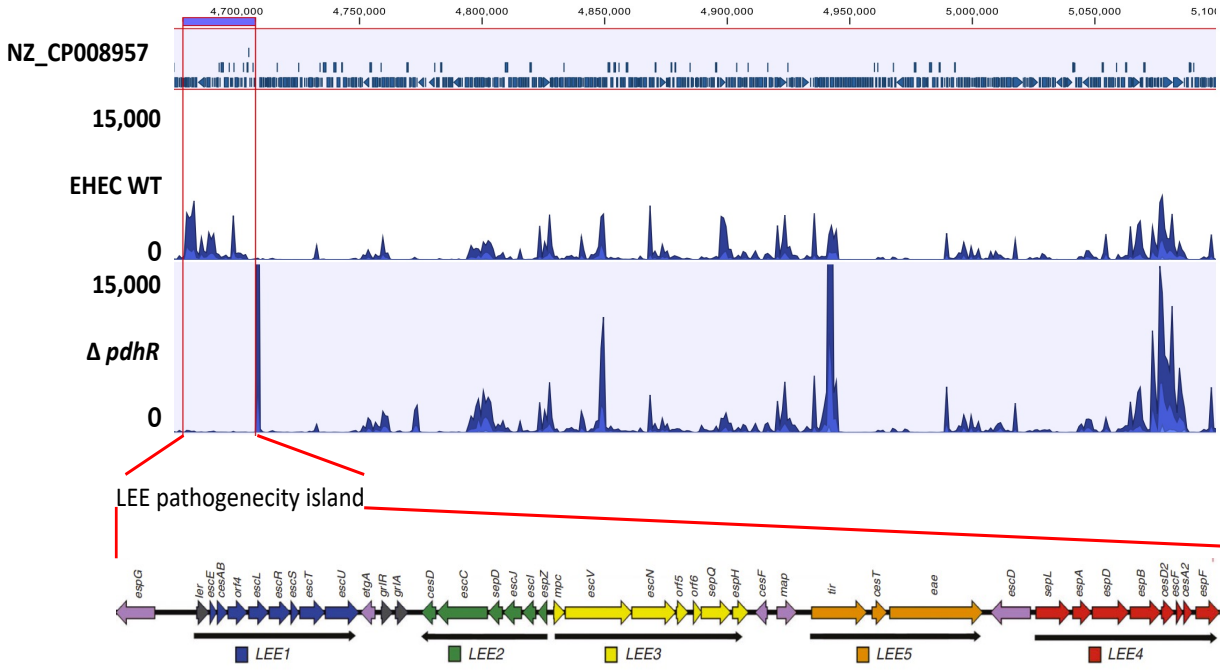

Fig. 4-12 Representative genome browser track of RNA reads coverage profile of the LEE. The LEE region is highlighted in red. The coverage represents a single biological replicate generated from CLC software. The expanded view of the LEE PAI illustration was adapted from (Connolly et al., 2016) with modification highlights *LEE1* To *LEE5* operons. The major LEE promoters (*ler* and *grlA*) are represented by a grey color. The arrows below annotated genes show the direction of transcription of the LEE operons.

A heatmap was used to illustrate the DEGs LEE genes (Fig. 4-13). Deletion of PdhR decreases expression of many LEE-encoded genes across the whole LEE operon,

including *ler*, *eae*, *espA*, *espB*, *escC* and while few non-LEE-encoded gens were downregulated (*espN*, *espL* and *espR3*) (Fig. 4-13). Overall, the data suggests that *pdhR*-dependent LEE regulation is not due to a metabolic defect caused by the deletion of *pdhR* as evidenced by only low reads within the LEE PAI.

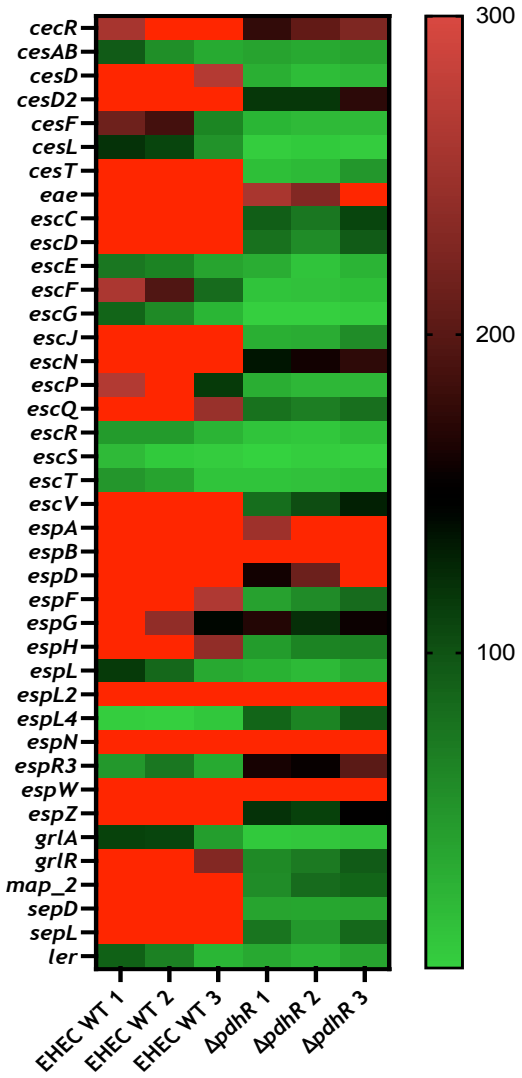

Fig. 4-13 Heat map showing down-regulated differentially expressed genes in the *pdhR* mutant. Transcriptomic Heatmap exhibiting clustering of the LEE PAI DEGs. Hierarchical clustering was presented using normalised gene expression counts from three biological replicates of EHEC WT and Δ*pdhR*. Upregulated genes are shown by red and downregulated genes in green shading as indicated in the color key.

In order to demonstrate the differentially expressed LEE genes and their interaction with human proteins involved in virulence processes, the DEGs were submitted to the KEGG pathway for pathogenic *Escherichia coli* infection (KO05130). As shown in the KEGG pathway map T3SS secreted proteins are associated with many human/host genes (Fig. 4-14). Expression of established LEE-encoded virulence effectors (EspG, EspB, EspH, EspG2, Tir, EspZ and EspF) and non-LEE-encoded (NleE, NleH) in the Δ*pdhR* were significantly downregulated. While the non-LEE-encoded (NleC, NleD, NleF, EspM1/2 and EspW) were upregulated. The data is consistent with previously shown results on the effect PdhR on *LEE1* activity (Fig. 4-1) and significantly downregulated LEE genes in the transcriptome data set (Fig. 4-13).

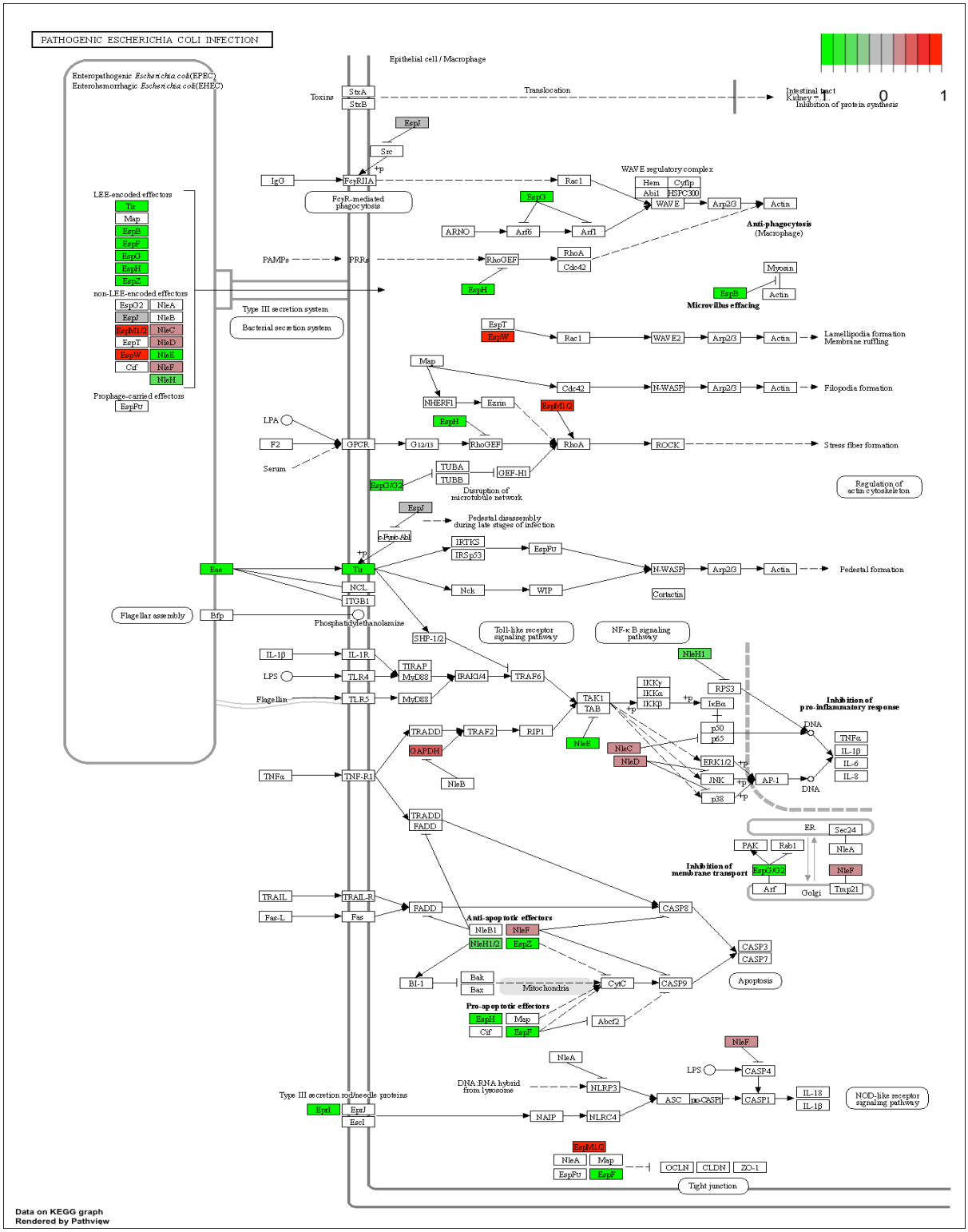

Fig. 4-14. KEGG pathway map of pathogenic *Escherichia coli* infection rendered by Pathview (Luo *et al.*, 2017). The *Escherichia coli* infection pathway is overlayed with the human proteins that associated with human-*Escherichia coli* networks. Highlighted genes are components of these pathway significantly differentially expressed genes (DEGs) in Δ*pdhR* mutant vs EHEC WT calculated as $\log_2$ fold change ratio. DEGs color codes indicates genes that are induced (red) and repressed (green).

To assess the potential role of PdhR in carbon metabolism, and further gain insight in what may be driving reduced T3SS expression in the Δ*pdhR*, the expression matrix data set was analysed using KEGG pathways (glycolysis/ gluconeogenesis, citrate cycle and Pentose phosphate pathway). Transcriptomics data from Δ*pdhR* indicated that phosphoglucomutase [EC:5.4.2.2] and glucose-6-phospahte isomerase [EC:5.3.1.9] were repressed, probably to reduce carbon flux through gluconeogenesis pathway (Fig. 4-15). These enzymes interconvert alpha-D-glucose-6-phosphate and beta-D-glucose-6-phosphate and glucose-phosphate and fructose-6-phosphate, respectively. Most of the genes encoding enzymes involved in the glycolytic and fermentative pathways were upregulated. These include, *fbaB* [EC:4.1.2.13], *gabC* [EC:1.2.1.12], *gpmM* [EC:5.4.2.12], *eno* [EC:4.2.1.11] and *pyfK* [EC:2.7.1.40], the latter encodes pyruvate kinase enzyme that catalyses the conversion of phosphoenolpyruvate and ADP to pyruvate. Genes *eutG* and *adhE* [1.1.1.1] were repressed. The steps involved in the metabolism of gluconate (glucokinase [EC:2.7.1.12] and 2-dehydro-3-deoxygluconokinase [EC:2.7.1.45]) were also repressed (Fig. 4.16) and these genes were downregulated in the RNA-seq data set. Taken together, the repression of gluconeogenic pathway, suppression of *edd* and *adhE* genes which are key in T3SS and colonisation in EHEC may explain the attenuated virulence in the Δ*pdhR*.

In parallel to increased glycolysis pathway, deleting *pdhR* enhanced the expression of PDHc, NDH-2 and Cyt bo_3. This is highlighted by induction of the following enzymes, pyruvate dehydrogenase E2 [EC:2:3.1.12] and pyruvate dehydrogenase E1 [EC:1.2.4.1] which make part of the PDHc enzymes that catalyse pyruvate to Acetyl-CoA (Fig 4-15). Likewise, the cytochrome *bo*-type oxidase encoded by genes *cyoA, cyoB, cyoC, cyoD and cyoE* belonging to the *cyoABCDE* operon were induced. Finally, the enzymes NADH dehydrogenase 2 [EC:1.65.9] and NADH-quinone oxidoreductase subunit N [EC:7.1.1.2] were also induced (Fig. 4.17B). The genes corresponding to these enzymes were significantly upregulated in the transcriptome data set (Table S3).

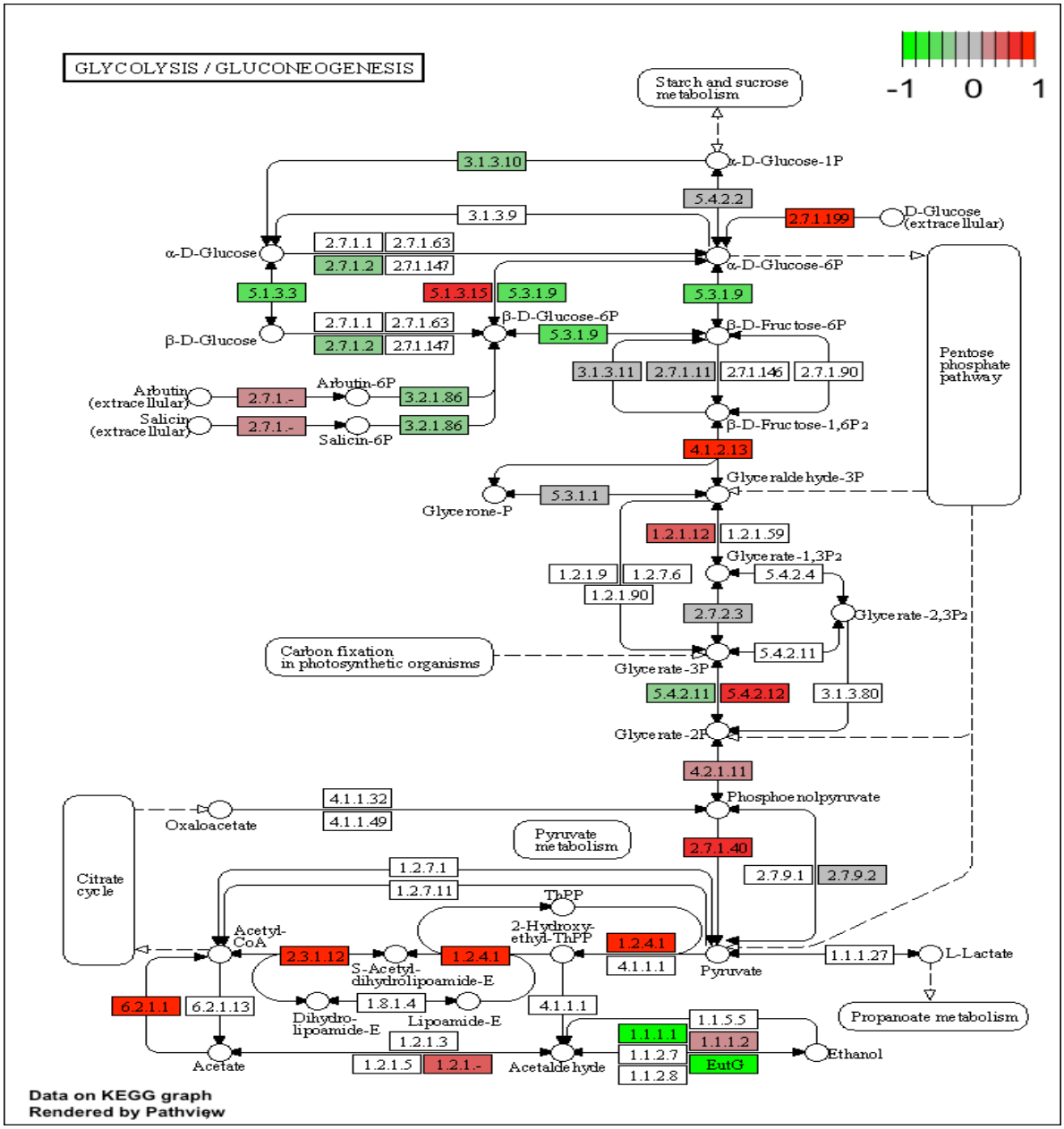

Fig. 4-15. KEGG pathway map of Glycolysis and Gluconeogenesis rendered by Pathview (Luo *et al.*, 2017). Highlighted boxes represent mapped specific enzyme steps with the relative expression of the corresponding genes in Δ*pdhR* mutant vs EHEC WT calculated as $\log_2$ fold change ratio. DEGs color codes indicates genes that are upregulated (red) and downregulated (green).

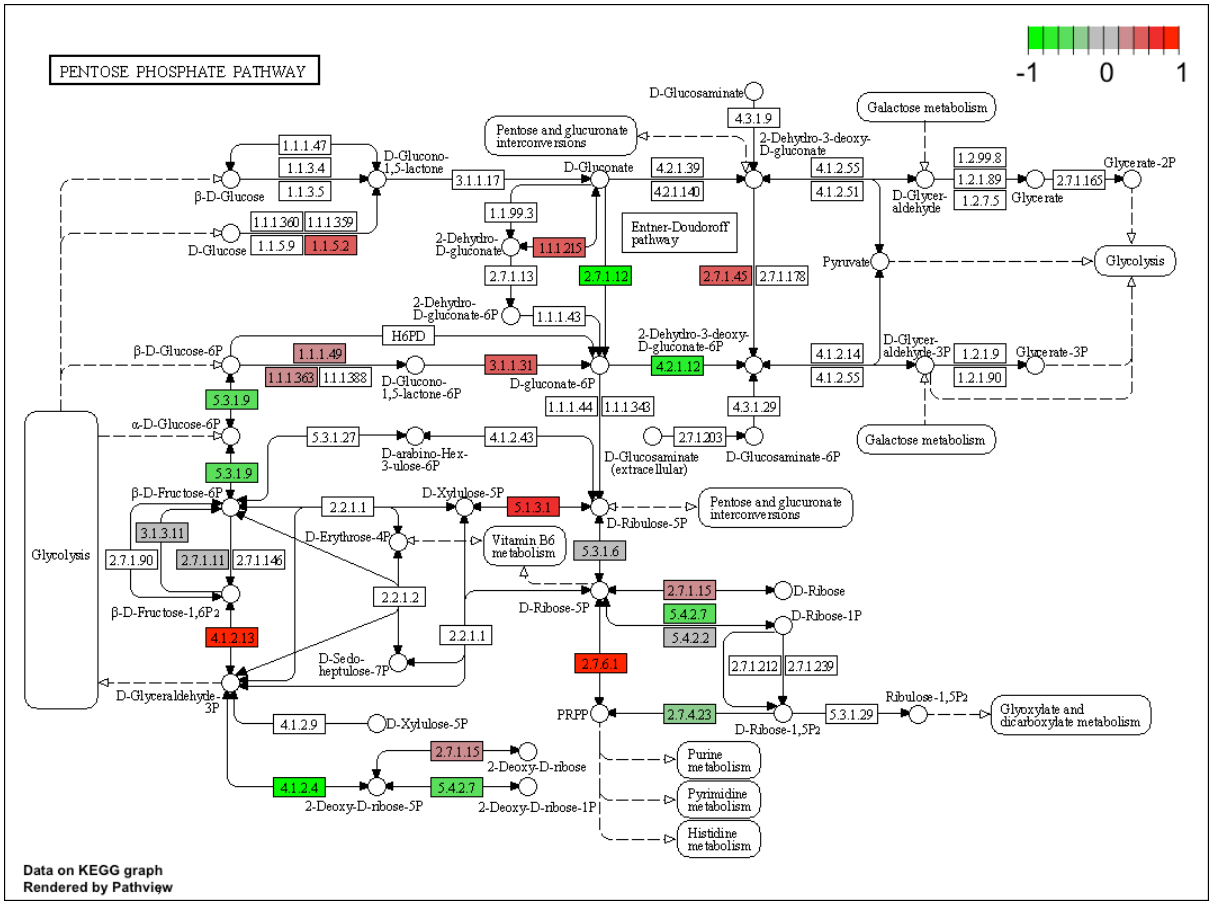

Fig. 4-16. KEGG pathway map of pentose Phosphate Pathway rendered by Pathview (Luo *et al.*, 2017). Highlighted boxes represent mapped specific enzyme steps with the relative expression of the corresponding genes in Δ*pdhR* mutant vs EHEC WT calculated as $\log_2$ fold change ratio. DEGs color codes indicates genes that are upregulated (red) and downregulated (green).

A

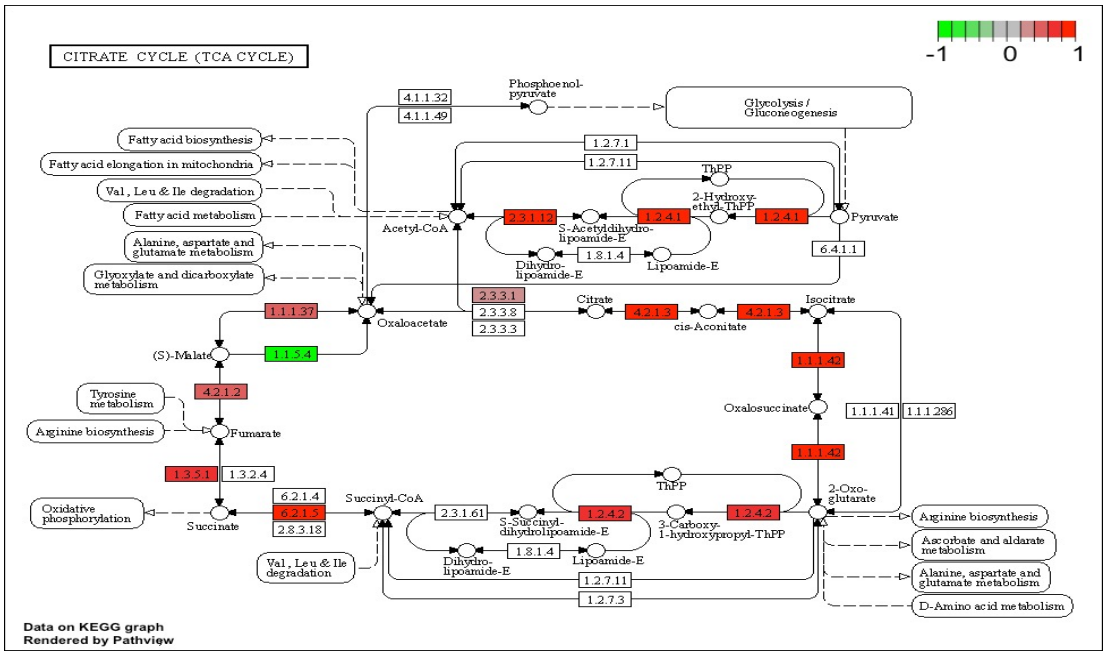

B

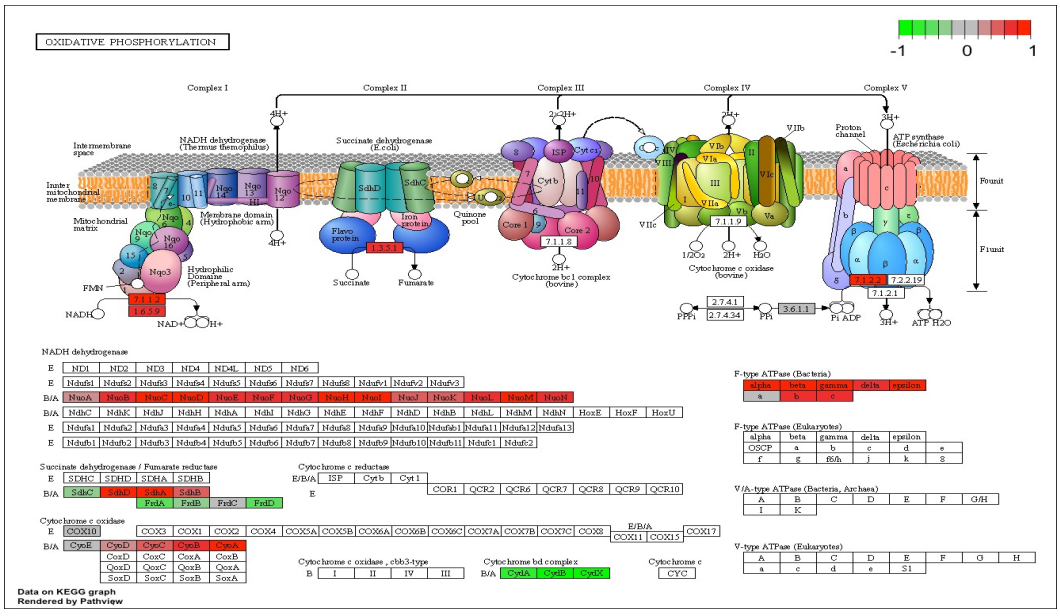

Fig. 4-17. KEGG pathway Map of the Citric Acid Cycle (A) and oxidative phosphorylation metabolism (B) in EHEC (Luo *et al.*, 2017). Highlighted boxes represent mapped specific enzyme steps with the relative expression of the corresponding genes in Δ*pdhR* mutant vs EHEC WT calculated as $\log_2$ fold change ratio. DEGs color codes indicates enzymatic activities specific for EHEC, induced enzymes (red boxes) and repressed enzymes (green boxes).

4.3 Discussion

4.3.1 Pyruvate acts as a signal for PdhR LEE dependent expression

PDHc occupies a key function in the oxidation of glucose by linking glycolysis to the TCA cycle (Schutte et al., 2015). Given its fundamental role in bacterial physiology, its expression is tightly regulated by the TF PdhR, which is derepressed in the presence of pyruvate (Anand et al., 2021). PdhR is a well-known transcription regulator that controls key genes in central metabolism in *E. coli*, including *Streptococcus pneumoniae, Legionella pneumophila* and *Chlamydia trachomatis* (Echlin et al., 2020; Oliva et al., 2018; Quail et al., 1994; Rother et al., 2018). Several TFs that control metabolic genes have also been linked to regulation of virulence genes and thus carbon metabolism and virulence expression are coordinated precisely for enhanced pathogen adaptation (Njoroge et al., 2012). Although Anzai *et* al. 2020, demonstrated the function of PdhR in flagella regulation in *E. coli* K12 strain, the current study is the first to our knowledge to link PdhR in EHEC carbon metabolism and virulence. In this chapter, we investigated the effects of PdhR on the transcription of *LEE1*, the master activator of the rest of the LEE, in the presence of pyruvate and succinate. Addition of 1mM pyruvate increased the activity of *LEE1* in EHEC WT, while there was no significant change in *LEE1* expression in the Δ*pdhR* at different time points. Moreover, deletion of PdhR leads to an increase in pyruvate pool, as the regulator controls genes encoding several enzymes within the glycolytic pathway. It should be pointed out here that, PdhR-regulated targets in carbon metabolism are also under the control of the global TFs namely [cyclic AMP (cAMP) receptor protein] CRP Cra (Anzai et al., 2020), suggesting a coordinated regulation among this TFs.

When EHEC is grown under aerobic conditions and in the presence of pyruvate, the expression of T3SS is enhanced and thought to be under the control of Cra, KdpE and FusR TFs (Carlson-Banning & Sperandio, 2016b). While the interplay between Cra, KdpE and FusR in activation of LEE genes in the presence of pyruvate is not clear, FusR LEE gene expression was found to be more repressive in the presence of pyruvate (Carlson-Banning & Sperandio, 2016b). The above conditions somewhat mimic the conditions encountered by EHEC near the intestinal epithelial barrier of the host, as it provides an aerobic environment also rich in pyruvate. The majority of bacteria including, *C. rodentium*, *Shigella* spp. and *Brucella abortus* can utilise

pyruvate as a sole carbon source though glucose and 3PG are preferred due to higher energy yields (Carson et al., 2020; J. Gao et al., 2016; Waligora et al., 2014). In *Salmonella* Typhimurium, the expression of T3SS is highly influenced by metabolism (Abernathy et al., 2013). This is translated by an increase in cell invasion when pyruvate metabolism is abolished inside neutrophils (Abernathy et al., 2013). Pyruvate has been described as a new positive regulator for *Salmonella* Typhimurium SPI-2 expression (Pardo-Esté et al., 2019) . In this study, they showed that pyruvate present in macrophages is sensed by *Salmonella* Typhimurium two-component system CreBC to positively regulate SPI-2 gene encoding T3SS (Pardo-Esté et al., 2019). During *C. rodentium* infection there is increased glycolysis in the host, thus providing pyruvate at higher concentrations (Carson et al., 2020). This might provide a highly dependable niche cue that *C. rodentium* can use for efficient LEE dependent virulence. Since *C. rodentium* share the same infection strategy we reason that pyruvate may act alternatively as a cue sensed by EHEC via PdhR, the master regulator of the PDHc to regulate its T3SS in addition to controlling pyruvate metabolism.

Gluconeogenic conditions act as a signal for LEE genes expression as confirmed by an increase in *ler* expression when EHEC and Δ*pdhR* strain are grown in 0.2% succinate. These results are consistent with the results of previous researchers, who highlighted that a switch to gluconeogenic state by adding 0.4% succinate increases *ler* mRNA levels 4-fold compared to glycolytic state (Carlson-Banning & Sperandio, 2016b). While the role of TCA cycle in *E. coli* colonization and pathogenesis is still not well understood, a *sdhAB* (encoding part of the succinate dehydrogenase enzyme) *frdA* (encoding part of the fumarate reductase enzyme) double mutant in EDL933 and MG1655 had a significant mice colonization defect (Conway & Cohen, 2015). The SUCDi (genes *sdhA, sdhB, sdhC, and sdhD* corresponding to the enzyme succinate dehydrogenase) converts succinate to fumarate in the TCA cycle. Important function of succinate metabolism linked to virulence was described in detail in *Salmonella* Typhimurium (Yimga et al., 2006). The study showed that bacterial colonization was significantly decreased by inoculating mice with a *sdhCDA* mutant strain. Though we did not find any link between PdhR and succinate metabolism to global EHEC virulence, its function on succinate metabolism cannot be disregarded. A comprehensive analysis of PdhR and succinate metabolism in EHEC

is discussed in the next section which focuses on deletion of PdhR and its effect on transcriptome.

4.3.2 PdhR regulation of EHEC virulence appears to be LEE regulon specific

In this section, we probed the effects of PdhR on the global gene expression of EHEC using RNA-seq. The transcriptome data was validated by using RT-qPCR to evaluate fold expression changes of randomly selected LEE genes in EHEC and mutant strain. PdhR mutation had a profound effect on EHEC transcriptome expression. Strikingly, deletion of PdhR led to a significant downregulation of most LEE encoded genes expressed in EHEC, while few of the non-LEE encoded genes were expressed. The data suggests that PdhR is a specific regulator for LEE encoded genes in EHEC virulence. This was also validated by EMSA results confirming that PdhR binds directly within the -10 and -35 elements of LEE P2 promoter region, and further binding was also observed within the LEE P1 promoter region. In EHEC, the *LEE1* activity has been shown to be mainly through the distal P1 promoter located 163 pairs, respective to the *ler* translation start site (Sharp & Sperandio, 2007). Indeed, YhaJ was found to activate the expression of *LEE1* by binding to a region within the P1 promoter with limited activity at P2 promoter (Connolly *et al.*, 2016). Another study on QseA also reported that under LEE-inducing conditions QseA activates *LEE1* expression at the P1 promoter not at the P2 promoter site (Sharp and Sperandio, 2007). However, even though activity of the P2 promoter is minimal it is essential for maximum *LEE1* expression (Islam et al., 2011). PdhR was found to interact with *LEE1* P1 fragment ranging from -789 to -899 upstream the *ler* transcription site. There were uncertainties with this binding site since most TFs bind close to gene promoters (Islam et al., 2011; Sharp & Sperandio, 2007; Yang et al., 2023). However, FadR was also found to bind to *LEE1* fragments ranging from -693 to -967 bp upstream of the P2 transcription start site (Pifer et al., 2018) and other TFs bind more than 1 kb upstream of the promoter through DNA looping (Bulger & Groudine, 2011). Moreover, the EHEC *LEE1* putative regulatory region is within an open reading frame between the *ler* and *espG* gene, with an approximate size of 1250 bp. Collectively, these results suggest PdhR regulates *LEE1* transcription by enabling recruitment of RNA polymerase and other transcriptional regulators to either the *LEE1* P1 and *LEE1* P2 EHEC promoters.

4.3.3 Transcriptomics reveal that several metabolic processes may control EHEC virulence

To further understand possible mechanisms of PdhR regulated processes, the RNA-seq data was used for pathway enrichment analysis which provides biological functions that are expressed in a gene data set more than would be expected by chance (Reimand et al., 2019). As already stated, the majority of the LEE genes including several T3SS effectors were downregulated. LEE effectors destabilize various host cell processes by either blocking or increasing expression of signalling pathways to enable the bacteria to colonize, proliferate and cause disease (Wanyin Deng et al., 2004). EHEC effectors, Tir and EspF interfering with inflammatory signalling (Wong et al., 2011), induce intrinsic apoptotic pathways (Dong et al., 2010) and contributing to anti-phagocytosis (Wong et al., 2011). Among the downregulated LEE effectors, the EspB effector interacts with the actin binding domains of multiple myosin family members, which are involved in phagosome closure during bacterial phagocytosis (Santos et al., 2019). While the effector EspF stimulates mitochondrial lysis by inhibiting PI_3 kinase signalling and contributes to breakdown of anti-apoptotic proteins (Wong et al., 2011). EHEC inhibits WAVE regulatory complex (WRC)-dependent phagocytosis by a subverting both Rho initiation via EspH (Dong et al., 2010) and a Arf signaling via EspG (W. Deng et al., 2001). In contrast, EspW which regulates actin filament organization (Sandu et al., 2017) was highly expressed. This is not surprising as EspW is essential in maintaining cell shape during host infection (Sandu et al., 2017), thereby likely needed regardless of the state of pathogenesis. Other non-LEE-encoded effectors (EspM1/2, NleC and NleD and NleF) were also induced in the pathway map of pathogenic *E. coli* infection. These results suggest a specific regulation of PdhR on LEE dependent virulence. Furthermore, deletion of PdhR in EHEC strains may increase bacterial phagocytosis and to a large extend attenuate its overall virulence in the host.

Complete functioning and proper regulation of gluconeogenesis and glycolysis are coupled to EHEC LEE dependent virulence (Cameron & Sperandio, 2015; Njoroge et al., 2012). We found out that genes encoding enzymes for a functional glycolytic pathway were mostly upregulated. Therefore, this implies an accumulation of pyruvate, an intermediate in several pathways throughout the cell. Interestingly, phosphoenolpyruvate synthase which converts pyruvate to phosphoenolpyruvate, a

critical step in gluconeogenesis was not induced, thus leading to suppression of the gluconeogenesis pathway. It is well documented that in glycolytic environments EHEC suppress the transcription of the LEE PAI genes (Miranda et al., 2004; Njoroge et al., 2012; Schinner et al., 2015). The glycolytic pathway provides high concentrations of fructose-1-phosphate and fructose-1,6-bisphate (Echlin et al., 2020). These substrates bind to the global carbon regulator Cra, hence this leads to a decrease in transcription of EHEC LEE genes because of reduced affinity of Cra to bind DNA (Njoroge et al., 2012). The transcriptome data also revealed that gluconate metabolism was downregulated as genes encoding its transport and/or metabolism were not induced. Gluconate metabolism is utilized via the Entner-Doudoroff (ED) pathway that relies on two enzymes phosphogluconate dehydratase (*edd*) and 2-dehydro-3-deoxyphosphpgluconate aldolase (*eda*) (Waligora et al., 2014). It has been shown that *E. coli* lacking both the *eda* and *edd* genes colonises streptomycin-treated mouse to a lesser degree compared to the WT strain (Sweeney et al., 1996). The ED pathway is also necessary for colonization and pathogenesis by *Vibrio cholerae* in a mouse model (Waligora et al., 2014), but how gluconate metabolism mediates this process is not clear. Taken together, the data suggests that reduced metabolism of gluconate and the ED pathway is one of the many factors that attenuated virulence in the Δ*pdhR* strain. Furthermore, low expression of genes encoding bifunctional alcohol/aldehyde dehydrogenase (*adhE*) may be linked to reduced EHEC LEE expression as an *adhE* mutant resulted in suppression of the T3SS and overexpression of non-functional flagella(Beckham et al., 2014). In *Salmonella* Typhimurium mutations in the *adhE* reduced its ability to survive in murine macrophages (Baumler et al., 1994) while in *Edwardsiell piscicida*, an Δ*adhE* mutant produced significantly reduced levels of T3SS and T6SS associated proteins (Q. Mao et al., 2022).

The data showed an increased expression of most genes encoding enzymes involved in the TCA cycle and respiration (Fig. 4-17), implying an elevated central carbon metabolism linked with deletion of PdhR. Within this context, the main products of the TCA cycle would be succinate which is converted by succinate dehydrogenase to fumarate. As indicated succinate dehydrogenase couples the TCA cycle to respiration by donating quinones to the latter pathway via Complex II (McCloskey et al., 2018). However, the induction of SUCDi genes was not observed, but rather the

genes *sucABCD* were upregulated in our data set (Table S3). This suggests that accumulation of succinate was primarily due to the catalyses of α-ketoglutarate (2-oxoglutarate) to generate succinyl-CoA and conversion of succinyl-CoA into succinate. The *sucABCD* operon largely participates in the anabolism of key intermediates involved in energy generation within the TCA cycle (Li et al., 2006). The expression of the LEE PAI is higher in the presence of gluconeogenic substrate succinate than in elevated glucose levels (Cameron & Sperandio, 2015). However, higher than normal cellular levels of succinate may impact Cra and KdpE function, and subsequently reduce LEE dependent Cra/KdpE virulence. This further suggest an interplay between PdhR and Cra in carbon metabolism and bacterial virulence as PdhR deletion seems to play a role decreasing the expression of the *sucABCD* operon which is key in converting succinyl-CoA into succinate.

Several other genes relating to virulence, including adhesin, phage shock genes and biofilm associated genes, such as *csgA, csgB, csgC, csgD, pspA, pspB, pspC*, *bssS, and bssR* (Additional file 2: Excel file S3) were considerably downregulated. These genes have been previously indicated to contribute to the LEE-independent attachment abilities of EHEC with abiotic surfaces and during murine intestinal colonization (Anh Le et al., 2019; Bardiau et al., 2010; Y. G. Kim et al., 2016; McWilliams & Torres, 2014). Previous studies demonstrated that curli is an adherence related factor that aids in the interaction of EHEC and host cells (McWilliams & Torres, 2014). The transcriptional regulator CsgD is the master regulator of curli and biofilm formation, through the regulation of *csgBAC* and *csgDEFG* operons (Y. G. Kim et al., 2016). Furthermore, it negatively affects cell motility by repressing flagella synthesis (Ogasawara et al., 2011). Transcription of *csgD* is under the control of Crl, H-NS, RpoS, along with the two-component system CpxA/CpxR which constantly monitor specific environmental cues for appropriate expression of curli (McWilliams & Torres, 2014). Interestingly, curli has been associated with adhesion of EHEC to spinach and lettuce leaves, making it essential for EHEC survival as justified by isolation of curli genes in numerous outbreaks globally (Fink et al., 2012). In addition, strains with *csgA* mutation were impaired in both long-term and short-term colonization of the lettuce leaf surface (Fink et al., 2012). The data implies that CsgD is activated by PdhR, since the master regulator together with operons (*csgBAC* and *csgDEFG*) under its control were downregulated subsequently attenuating EHEC

virulence. This is substantiated by a decrease in biofilm formation and motility in the *pdhR* mutant established in the previous chapter. However, further studies are required to prove that CsgD PdhR-dependent regulation occurs via an indirect or direct mechanism to control EHEC adhesion properties.

4.4 Conclusion

In this chapter we set to ask 3 questions. For the first question, we have shown that carbon sources act as signals for EHEC PdhR-LEE dependent virulence. This was confirmed by an increase in *LEE1* activity in the presence of pyruvate, thus the metabolite act as a signal for PdhR T3SS dependent regulation. For the second question we have revealed that PdhR directly binds to the *ler* regulatory region and proposed that this in turn activates expression of the *LEE1* operon and subsequently the whole LEE operon (*LEE2- LEE5*). Finally, through transcriptomics we show that LEE regulation is very complex, and several carbon metabolism pathways maybe wired into global LEE gene regulation in EHEC. Impairing the metabolism of these substrates through deletion of the TF PdhR results in various virulence defects in EHEC and underlies pathogenic outcome of an infection. Thus, this work highlights that PdhR, a transcriptional regulator that is known to regulate central metabolism underpins the intimate relationship between virulence and metabolic flux in EHEC. Potentially understanding this complex relationship could lead to better dietary interventions to reduce EHEC mediated disease.

Chapter 5: Effect of PdhR in attaching and effacing of enteropathogens in vitro and in vivo colonisation

5.1 Introduction

Members of the A/E family include the human pathogen EHEC and the mouse pathogen *C. rodentium,* as already outlined. Since *C. rodentium* shares this common infection strategy with EHEC, it is widely used to understand the molecular underpinnings of A/E lesion formation, including colonization resistance and mucosal immunity in an infection animal model (Crepin et al., 2016). Colonization and proliferation are key steps for successful EHEC infections. In the host, EHEC resides in the intestinal tract and adheres to the gut epithelium of the distal ileum and colon. Initial binding is promoted by the use of fimbriae (Ogasawara et al., 2011), followed by injection of a plethora of effector proteins under the control of a T3SS for increased attachment (Cameron et al., 2018). The region is preferred by EHEC as there is less competition with commensal *E. coli* for carbon sources (Baümler & Sperandio, 2016). This region has less simple dietary sugars available to be utilized by pathogenic bacteria, as these are largely absorbed in the small intestine (de Nisco et al., 2018). Nonetheless, it is rich in undigested plant polysaccharides and host glycans, proteins and carbohydrates which are further metabolized in this part of the gut (Carlson-Banning & Sperandio, 2016b). Thus, the colon milieu is rich in microbial communities that can utilize such metabolites, including, Bacteroidetes and Firmicutes phyla which accounts for more than 90% while Actinobacteria and Proteobacteria phyla are present but low in density (Kim et al., 2017).

The Bacteroides genus under the Bacteroidetes phyla is one of the most predominant group in the intestine known to utilize complex polysaccharide polymers as an energy source (Kim et al., 2017). Short chain fatty acids (SCFAs) are released in the degradation of these complex polysaccharides, (e.g, succinate, fucose, propionate, acetate, and butyrate) (Connolly et al., 2018; Jubelin et al., 2018; Kumar, Aman, 2019; Woodward et al., 2019). Furthermore, these SCFAs have been implicated in regulating EHEC virulence gene expression. For instance, EHEC LEE expression is increased by succinate and butyrate while indole and fucose repress the LEE (Connolly et al., 2018; Curtis et al., 2014; Kumar, Aman, 2019; Weigel & Demuth, 2016). Propionate, a product of 1,2-propanediol increases LEE expression in *C. rodentium* (Connolly et al., 2018). This was demonstrated by reduced fitness *in vivo* by a *pdu C. rodetium* mutant that is deficient in genes involved in 1,2 propanediol metabolism (Connolly et al., 2018). Apart from using microbiota and their

metabolites for virulence regulation, *C. rodentium* also circumvents microbiota resistance at the lumen interphase by inducing intestinal hyperplasia (Borenshtein et al., 2008). This in turn results in hyperproliferation of immature undifferentiated cells which have an altered metabolism and increases colonic oxygen which favours *C. rodentium* expansion (Carson et al., 2020).

C. rodentium LPS or T3SS structural components are detected by pattern recognition receptors (PRRs) in the host, and their presence triggers a strong inflammatory response. In addition, IECs initiate a protective response by activating inflammasomes thus promoting gut inflammation and host defence mechanisms (Peterson & Artis, 2014). At the onset of pathogen expansion within the host, the intestinal barrier is strengthened by expression of the cytokine interleukin 22 (IL-22), which is a member of the IL-10 family produced by type 3 innate lymphoid cells. IL-22 restricts pathogen entry by upregulation of the gut barrier proteins, including Reg3β, Reg3γ, mucins and calprotectin (Hopkins et al., 2019). Proteins belonging to the regenerating gene (REG) family are multifunctional secretory molecules that possess anti-inflammatory, anti-apoptotic, trophic, antibacterial, and perhaps immuno-regulatory properties (Hopkins et al., 2019). The role of Reg3γ in elimination of enteric pathogens was shown by enhanced clearance of the vancomycin resistant *Enterococcus* strain *in vivo* (Fomby & Cherlin, 2011). For an adaptive immune response to *C. rodentium*, CD4+ T cells are recruited, and aid in the production of IL-22 and IFN-γ (Wiles et al., 2004).

PDHc plays a fundamental role in both humans and bacterial existence. In humans it has been implicated in several diseases, including, type 2 diabetes, obesity, and degenerative diseases (Patel et al., 2014). PDHc is tightly regulated by pyruvate dehydrogenase phosphatases and pyruvate dehydrogenase kinases (PDHK) which is found in 4 tissue specific isoforms (PDHK1-4) in mammals (Golias et al., 2019). The activities of these kinases are regulated by hypoxia, available nutrients, and hormones (Golias et al., 2019). Inhibitors for the PDHc as well as enzymes involved in the complex build-up are at the core of current research to combat PHDc associated human diseases and multidrug resistant pathogens (Ginn et al., 2021; Su et al., 2018; van Doorn et al., 2021). For instance, dichloroacetate a chemical inhibitor of PDHK was found to greatly reduce intracellular survival of *Salmonella*

Typhimurium in human macrophages (van Doorn et al., 2021). For these reasons the enzyme complex has therefore gained much interest as a target to control many human diseases including certain cancers (Patel et al., 2014) and in EHEC infections could be targeted as a treatment option.

Although studies have clearly demonstrated that EHEC infection alters the gut microbiota, little is known concerning the role of PdhR in how pathogen sense and respond to different signals in the gut, as well as how it affects pathogen metabolism during host infection. Furthermore, the presence of a functional PDHc has recently been shown to be crucial in host immune response by interaction with the chemokine CXCL10 in *E. coli* (Schutte et al., 2015). The disruption of the PDHc led to a more resistant *E. coli* strain when treated with CXCL10 (Schutte et al., 2015), suggesting that while targeting PDHc is a promising treatment for S*almonella* Typhimurium infections, the same does not apply in *E. coli*. Using HeLa cells and SPF BALB/c mice infected with *C. rodentium* to model human A/E infections, this chapter provides an insight into the importance of PdhR in gut colonisation; and deletion of PdhR alters EHEC metabolism and overall microbiome metabolism *in vivo*. Additionally, the chapter demonstrates that targeting the TF PdhR rather than PDHc complex would be a better alternative to control EHEC infections. This study introduces a potential novel therapeutic target to resolve EHEC infections by directly rewiring central metabolism which feeds into virulence regulation.

5.2 Results

5.2.1 PdhR deletion has a similar effect on *C. rodentium* LEE gene expression

From the previous chapter we have shown that PdhR controls the expression of a large set of genes, including LEE genes in EHEC. To test whether this is applicable to the murine pathogen *C. rodentium*, which is extensively used as a robust model for EHEC human infections, we generated a clean deletion of the *pdhR* gene using Lambda Red recombineering in the *C. rodentium* ICC169 strain (Fig.5-1A). The ICC169 strain is a nalidixic acid resistant derivative of ICC168 with the same virulence traits (Berger et al., 2017). We compared the growth of *pdhR* mutant with the wild type *C. rodentium* grown in T3SS inducing conditions (DMEM low glucose, 1% LB, 5% CO_2) (Fig.5-1B). The growth pattern was similar between the WT and the *pdhR* mutant of *C. rodentium*. The growth rate is important in genomic expression comparison since it affects the regulation of many genes (Anand et al., 2021). Additionally, qRT-PCR assays revealed that the expression of the selected LEE genes, including *ler* (LEE1), *eae* (LEE5) and *espZ* (LEE2) were significantly downregulated (Fig.5-1 C).

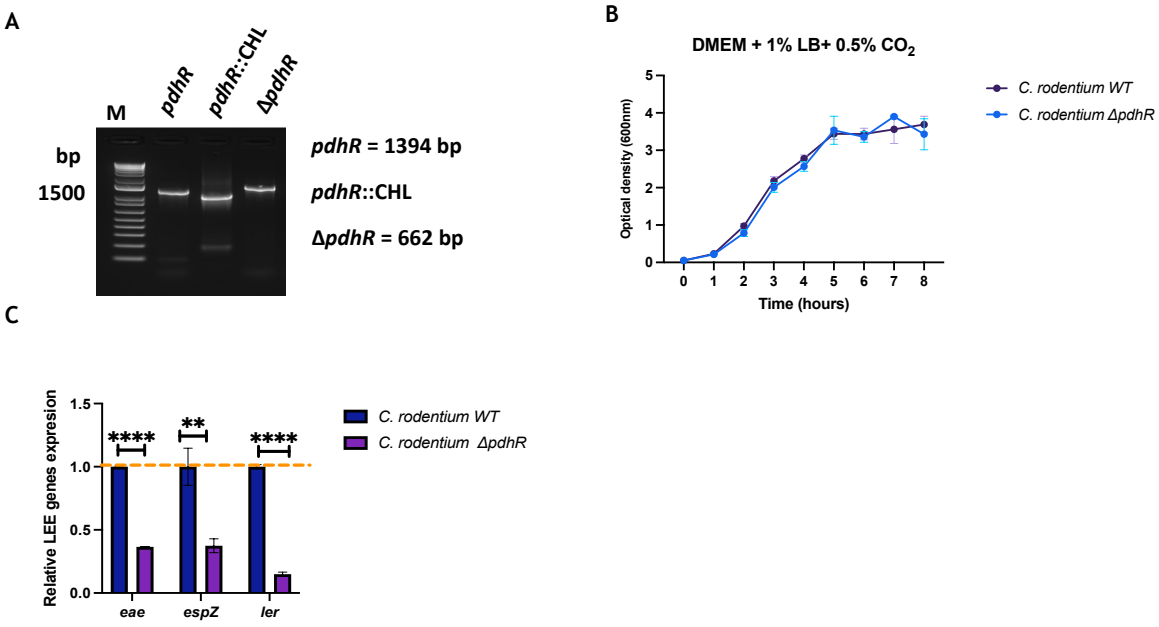

Fig. 5-1. Deletion of PdhR reduces LEE1 expression with no growth defect. (A) Confirmation of PdhR in *C. rodentium* was confirmed by colony PCR. Genomic DNA from the TUV93-0 and mutants was used to amplify the Chloramphenicol resistant cassette after Lambda Red mutagenesis using primers specific to regions of interest. Corresponding band sizes are indicated. (B) Growth curves of each mutant compared to the wild type grown in

M9 and MEM-HEPES media, measured as OD_{600} overtime. Growth curves shown represent mean values of triplicate experiments with error bars indicating standard error of the mean (SEM). (C) The expression of LEE1 activity was measured at exponential phase and plotted against OD_{600}. Each bar represents the mean of data obtained from three technical repeats of independent biological triplicates. Data was analysed by two-way ANOVA with Dunnett's test. ** denotes p≤0.01 and **** p≤0.0001.

5.2.2 Deletion of PdhR effects attachment of *C. rodentium* to HeLa cells

The LEE-encoded T3SS promotes ability to generate lesions identified as attaching and effacing (AE) during host infection. These A/E lesions are characterized by effacement of the brush border microvilli and rearrangement of the host cell actin, leading to close attachment. WT *C. rodentium* successfully attached to HeLa cells and led to actin condensation which is a distinctive phenotype for A/E pathogens (Fig.5-2A). Further, Δ*pdhR* forms fewer attaching and effacing lesions than WT *C. rodentium* and *pdhR* complemented strain (Fig. 5-2A). Bacterial attachment was significantly higher in both WT *C. rodentium* and *pdhR* complemented strains compared to the Δ*pdhR* mutant strain (Fig. 5-2B). These data implies that PdhR is required for bacterial attachment to host cells.

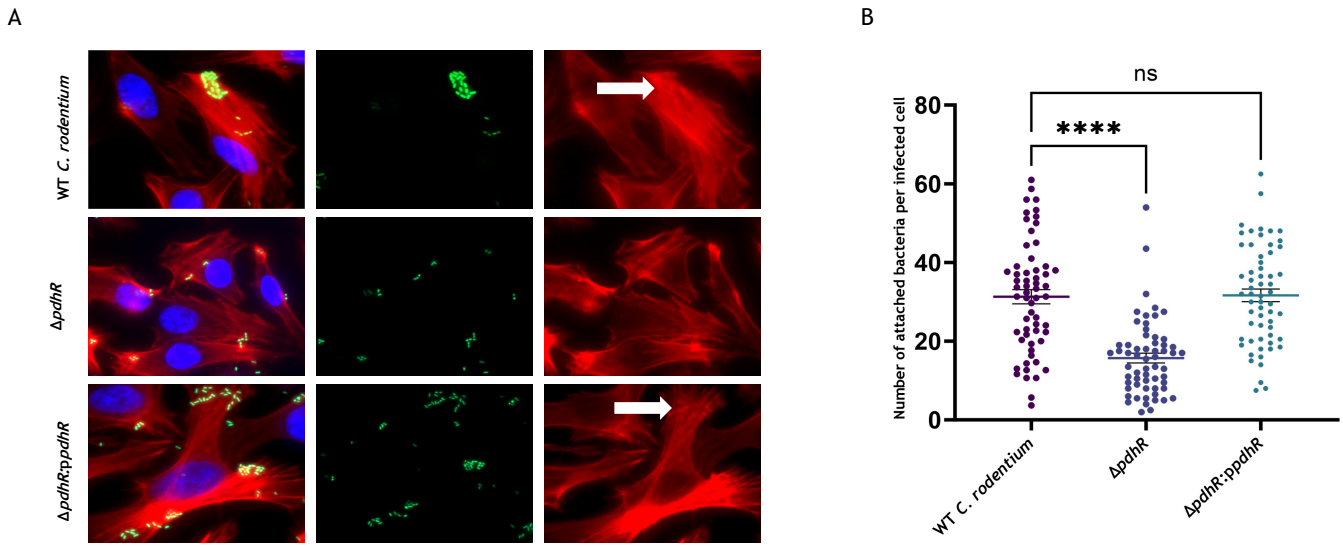

Fig. 5-2. PdhR is required for adherence to HeLa cells. (A) Fluorescence microscopy images of HeLa cells infected with WT *C. rodentium*, *ΔpdhR* or *pdhR* complement transformed with prpsM-gfp (green) at an MOI=100. Actin cytoskeleton was stained with Phalloidin-Alexa Fluor 555 (red) and DNA was counterstained with DAPI (blue). Scale bar = 20 µm. White arrows show actin condensation at the site of bacterial attachment a characteristic of A/E lesions. Images were taken at 40X magnification and processed using ZenPro software. Experiments were performed using three biological replicates. **(B)** The number of cells attached analysed from three independent experiments. **** denotes P ≤ 0.0001 and ns (no significance) p>0.05 compared to the WT.

5.2.3 PdhR is required for *C. rodentium* colonization *in vivo*

The T3SS provides an evolutionary advantage to enteric pathogens in colonizing the gut, but the mechanism in which metabolic regulators such as PdhR influence the process remains unknown. To examine whether PdhR plays a role in colonization of the murine intestinal tract, specific pathogen free (SPF) BALB/c mice were orally gavaged with either WT *C. rodentium* or isogenic mutants lacking the *pdhR* gene. Oral gavage or natural transmission are commonly used to introduce *C. rodentium* to the host (Carson et al., 2020). A high dose of 10^8-10^9 CFU is commonly used to evaluate the pathogenesis of *C. rodentium* and adaptive immune responses in infection mice models (Buschor et al., 2017). Groups of 9 SPF BALB/c mice were orally gavaged with 200 µl bacterial suspension (3 x 10^9 CFU per animal) of WT *C. rodentium* and Δ*pdhR* using the same bacterial concentration (du Sert et al., 2017). *C. rodentium* infection was then monitored by determining faecal shedding over a period of 20 days, and CFU were computed at different time points post infection. In comparison between WT *C. rodentium* and Δ*pdhR*, we observed a reduction in the survival of the *pdhR* mutant at day 1 and day 4 (DPI) (Fig.5-2A), which implies that PdhR promotes *C. rodentium* survival within the host. Shedding reached an average of 8.1 Log_{10} CFU/g for WT *C. rodentium* and 7.4 Log_{10} CFU/g for Δ*pdhR* by 8 DPI, which is observed as the peak of infection in *C. rodentium* infection (Fig 5-3A). Increased shedding of WT *C. rodentium* implied that there was better growth of the WT *C. rodentium* strain in mice gut compared to *pdhR* knockout strain. Disease progression was assessed by further examining faecal shedding through 17 DPI to 20 DPI. Additionally, most mice infected with the mutant strain had completely cleared the infection at 20 DPI, as evidenced by no bacterial colonies detected on LB plates supplemented with nalidixic acid. Taken together, the data suggests that PdhR may play a critical role in initial colonisation and during progression of disease and may be implicated in the severe form of the infection.

Infection with WT *C. rodentium* induces colonic hyperplasia which is a marker of cellular proliferation. To validate these, H&E was used to stain colonic sections (upper, lower and caecum) of mice infected with WT *C. rodentium* or *pdhR* mutant. Epithelial hyperplasia is marked by elongated crypts and loss of goblet cells due to an increase in epithelial cells (Carson et al., 2020). Colonic histological analysis showed no difference in tissue pathology between mice infected with WT or Δ*pdhR*

strain (Fig 5-3B). The observation can be explained by the fact that mice were culled after 20 DPI and hence at that period the mice generally recover from *C. rodentium* infections (Wanyin Deng et al., 2004).

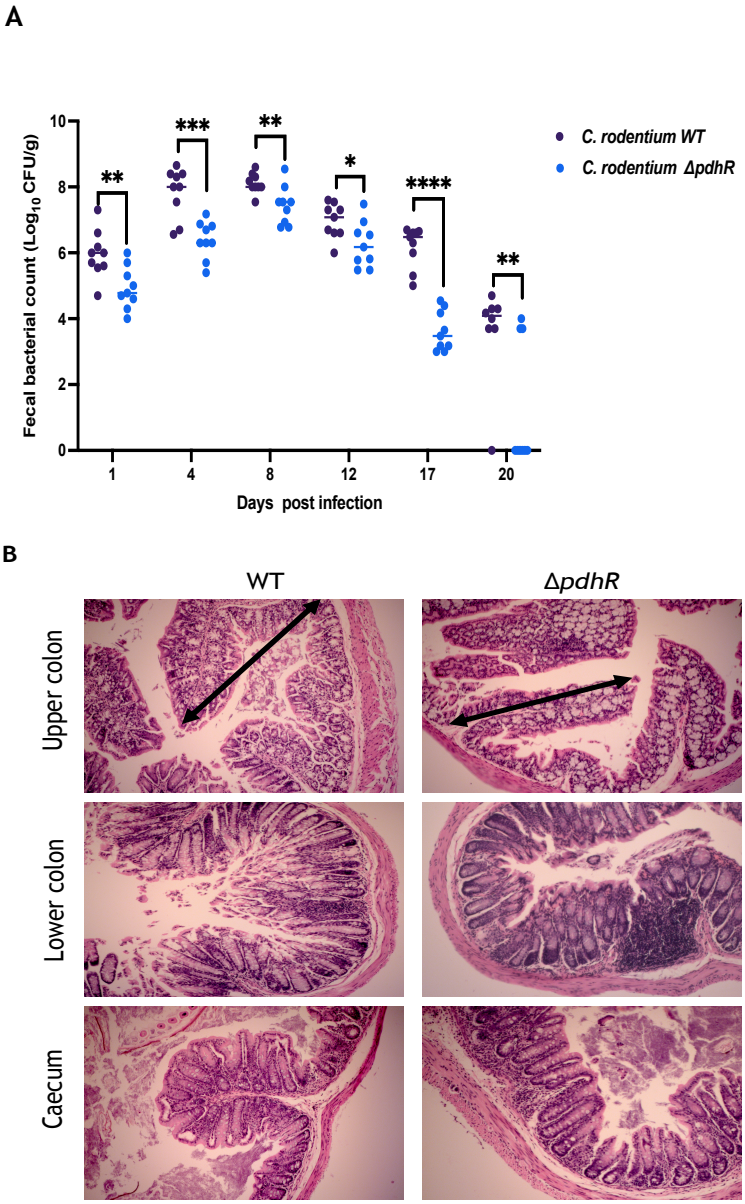

Fig. 5-3. *In vivo* colonisation of WT *C. rodentium* and Δ*pdhR*. (A) Colonization dynamics in BALB/c mice infected with WT *C. rodentium* or an isogenic Δ*pdhR* mutant (10^9 CFU). N= 9 mice per group. Error bars represent SEM; * denotes p≤0.05; ** p≤0.01; *** p≤0.001; **** p≤0.0001. **(B)** Representative of histological images of upper colon, lower colon, and caecum after culling mice (24 DPI). Slightly elongated crypts due to increase in epithelial cells shown with double headed arrows (40X magnification, scale bars: 100 µm).

5.2.4 Mice infected with *C. rodentium* Δ*pdhR* show less activation of Ler and IFN-γ

IECs initiate a protective response by promoting gut inflammation and host defence mechanisms in response to enteric pathogen infections (Mullineaux-Sanders et al., 2019b). To further explore whether PdhR contributes to host immune response and long-term persistence in the gut, we collected sections of the colon (caecum, upper and lower) after culling the mice and performed RT-qPCR for LEE genes and pro-inflammatory cytokines. In particular, only *ler* gene expression was increased in the lower colon of the WT *C. rodentium* compared to the *pdhR* mutant (Fig.5-4A). Other LEE genes were not detected, implying that at 20 DPI enteric T3SS is either no longer activated or greatly reduced. The IFN-γ pro-inflammatory cytokine had significantly increased levels in the lower colon of WT *C. rodentium* to those of the isogenic mutant lacking the *pdhR* gene (Fig.5-4D). Mice infected with the *pdhR* mutant showed decreased levels in pro-inflammatory cytokines, including CXCL-I, Idol and Mt2 across the different colon section though not statistically significant (Fig.5-4B and Fig.5-4D). The data suggests that PdhR may play a role in *C. rodentium* pathogenesis.

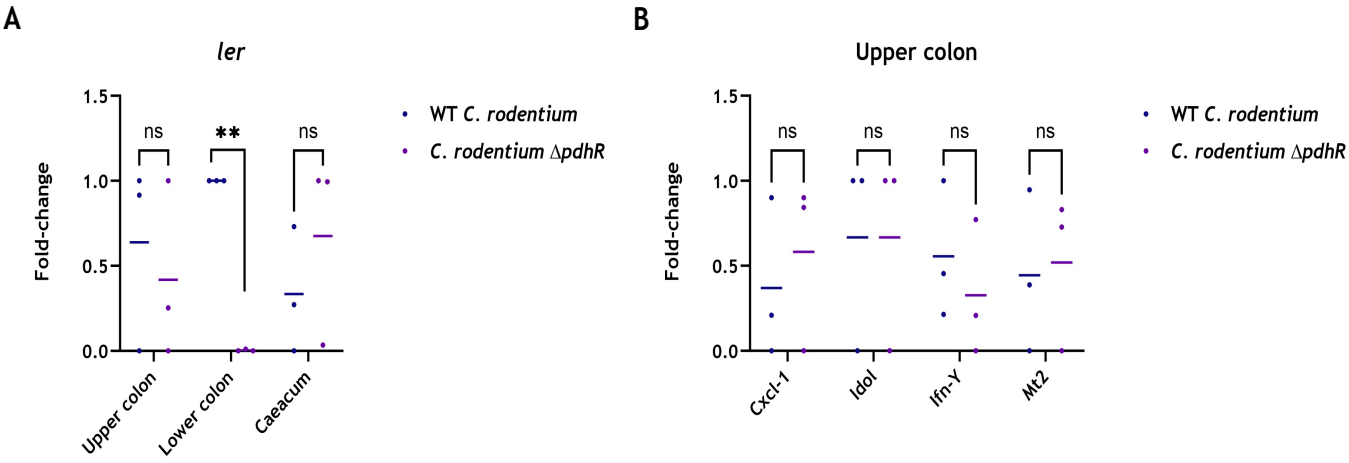

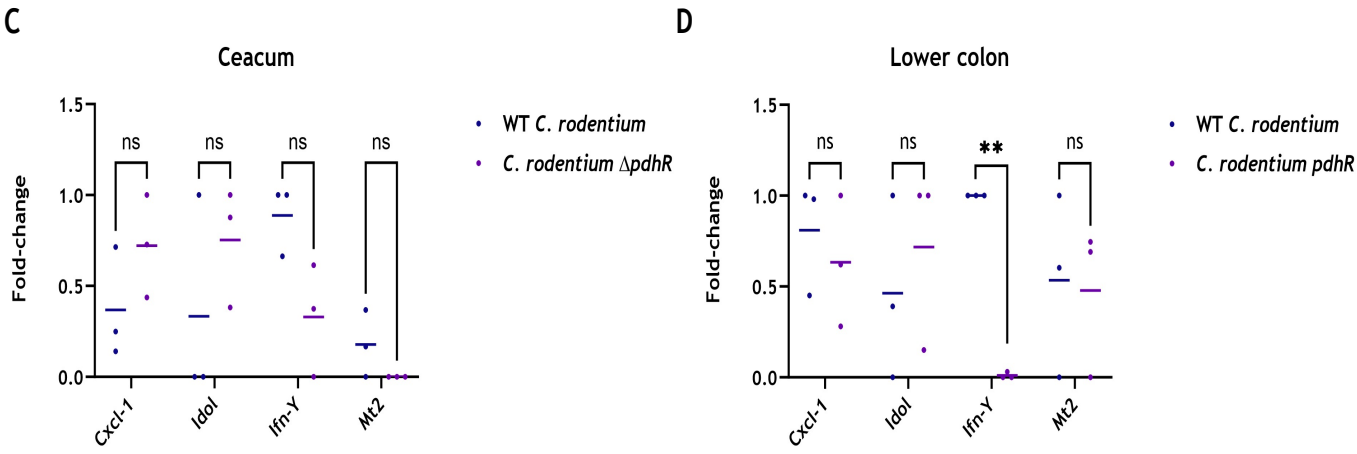

Fig. 5-4. Deletion of PdhR attenuates *Ler* and IFN-γ expression *in vivo*. (A) RT-qPCR analyses of the *ler* gene on caecal, upper colon, and lower colon tissues homogenates at day 24 post infection. **(B, C and D)** Normalised fold changes of proinflammatory cytokines CXCL-1, Idol, IFN-γ, and Mt2 on caecal, upper colon, lower colon tissues homogenates at day 24 post infection determined by RT-qPCR. Data was analysed by Two-way ANOVA with multiple comparisons. ** and ns, indicates statistically significant differences ($p \leq 0.01$) and no significance respectively.

5.2.5 *C. rodentium* induces dysbiosis in mice faecal bacterial communities

For microbiome analysis, a total of 18 faecal samples were collected from 2 different groups: group 1, mice infected with WT *C. rodentium* (WT), and group 2, mice infected with *C. rodentium* Δ*pdhR*. Samples were collected at day 0 (before infection with either WT or Δ*pdhR*), day 9 post infection and day 24 post infection. The V3-V4 region of 16s rRNA of the collected samples were sequenced and assigned operational taxonomic units (OTU). To evaluate the sequencing depth, Goods coverage scores were calculated. The scores exceeded 0.9 and were comparable amongst all the samples, this indicated that sequencing depth was satisfactory (Table S4). PCA plots were used to assess the bacterial composition similarity of faecal samples among each group (Fig.5-5A). As expected, the bacterial composition in the uninfected mice group clustered together and was spatially separated from that of the infected group (9 DPI and 24 DPI). Interestingly the WT group at 24 DPI tend to be closer to that of uninfected population at 24 DPI, while the Δ*pdhR* group at 24 DPI was spatially separated from bacterial communities at 0 DPI and 9 DPI. Fig.5-5B illustrates the similarity of bacterial communities through UTO clustering. Among the WT group 312 core taxa were shared between 0 DPI, 9

DPI and 24 DPI, while the *pdhR* mutant shared 319 core taxa among the 0 DPI, 9 DPI and 24 DPI. A high number of unique OTUs was observed across the groups at different sampling times. In summary the data corroborated a lower degree of similarity between faecal microbiota of mice infected with WT or Δ*pdhR* group indicating unambiguous difference between the groups.

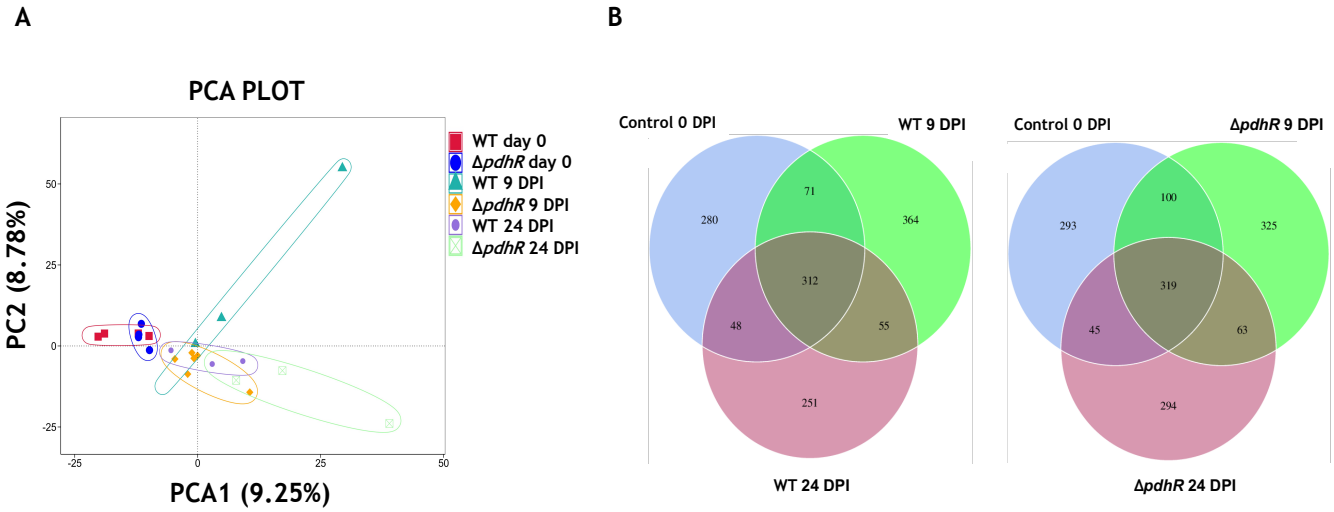

Fig. 5-5. Faecal bacterial distribution from mice infected with WT *C. rodentium* or Δ*pdhR*. (A)Principal component analysis (PCA) results of microbiota community. The figure shows a three-dimensional scatter plot for the PCs result. The circles were drawn around microbiome samples collected at the same time point, belonging to either WT *C. rodentium* or *C. rodentium* Δ*pdhR*. Sample groups, day 0 (before bacterial infection), 9 DPI and 24DPI are represented by different colours. Samples with comparable microbial community profiles are clustered together. **(B)** Venn diagram illustrating the distribution of bacterial operational taxonomic units (OTUs) between the control group and WT *C. rodentium* or Δ*pdhR* at different sampling times (before bacterial infection, 9 DPI and 24DPI).

5.2.6 Changes in faecal bacterial communities at peak of *C. rodentium* infection

After observing variability in microbial communities between mice infected with WT or the *pdhR* mutant, we further probed the data for specific microbial changes at the peak of infection (9 DPI). According to OTU clustering, common OTUs were 388 and the unique OTUs belonging to the WT and Δ*pdhR* mice, were 419 and 414 respectively (Fig.5-6A). We then used absolute abundance to take a closer look at bacterial communities in WT and Δ*pdhR* mice group at peak of infection (Fig.5-6B, Fig.5-6C and Fig.5-6D). The major phyla present in both WT and Δ*pdhR* mice were

Bacteroidota and Firmicutes, in agreement with previous reports (Wang et al., 2019). While Deferribacterota, Actinobacteria, Verrucomicobiota, Chloroflexi and Spirochaetota were present at low proportions. To compare bacterial communities that were altered, we conducted a one-way ANOVA at the phyla and genus level. There was a rise in the average absolute abundance in Firmicutes, Proteobacteria as well as Chloroflexi in both the WT and Δ*pdhR* mice at the peak of infection (Fig.5-6C). However, the WT mice had significant presence ($p< 0.05$) of the phyla Proteobacteria and Chloroflexi. A significant reduction ($p< 0.05$) in Bacteroidota was observed in the two groups. As expected, at genus level it can be pointed out that there was an upsurge in *Citrobacter*, and *Lachnospiraceae* in the WT group compared to the Δ*pdhR* group at 9 DPI (Fig.5-6B). An increase in *Intestinimonas*, *Oscilibacter* and *Acetatifactor* was observed in the Δ*pdhR* group (S Fig.5-1A). Both groups had a decline in *Bacteriodes*, *Parabacteriodes*, and *Muribaculaceae* (S Fig.5-2B and S Fig.5-2B). Undeniably, mice infected with WT or the *pdhR* mutant resulted in a divergent cluster of microbial communities, with the WT group having significant compositional changes. A rise in the phylum Proteobacteria (genus *Citrobacter*) is likely a direct reflection of an increase in *C. rodentium* population during infection. The data implies that PdhR might play significant role in enteric pathogen expansion during early phase of infection.

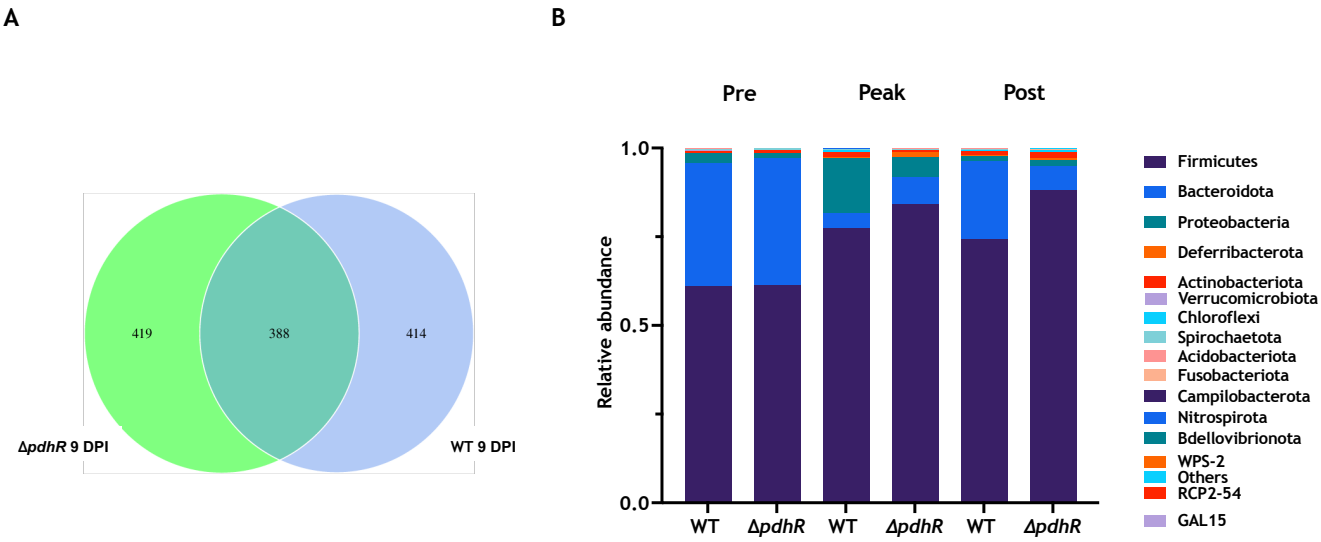

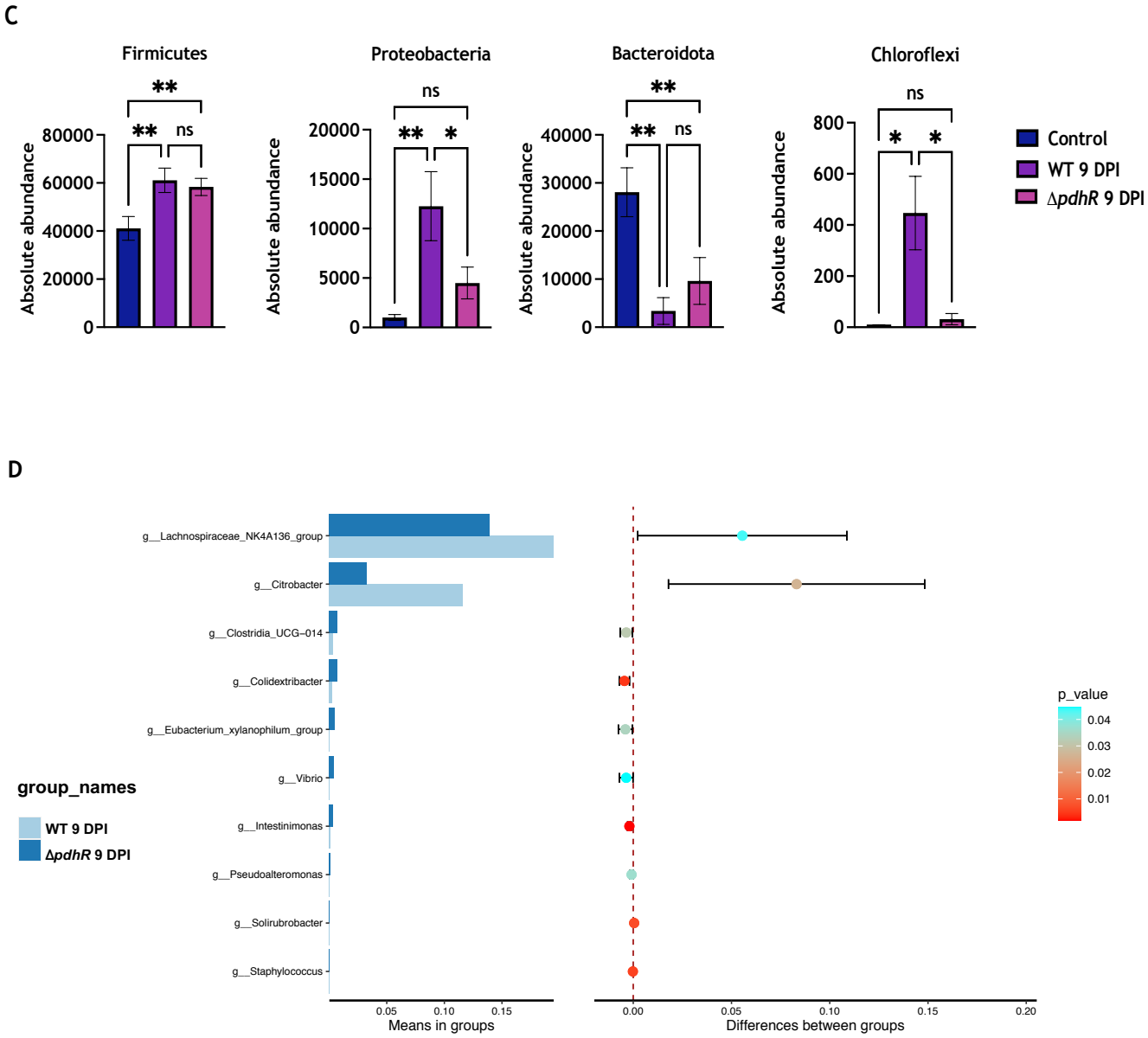

Fig. 5-6. Changes in faecal bacteral communities at peak of infection. (A) Venn diagram illustrating the distribution of OTUs between the control group and WT *C. rodentium* or Δ*pdhR* mice at different sampling times (before bacterial infection and 9 DPI). (B) A bar graph showing average relative abundance of major phyla identified. Different colors depicts relative levels of abundance in WT *C. rodentium* or Δ*pdhR* mice at pre-infection (Pre), peak-infection and post-infection (Post). Comparison of Beta devisity of main bacterial phyla (C) and at genus level (D) between mice infected with WT *C. rodentium* or Δ*pdhR* at day 9 post infection. Data are represented as the means of three independent biological replicates. * denotes p≤0.05; ** p≤0.01; ns (no significance) p>0.05.

5.2.7 Microbial communities are not completely restored after *C. rodentium* infection clearance

Host recovery phase of *C. rodentium* infection is characterized by the microbiome reverting to or close to pre-infection levels. Previously we reported a significant decline in bacterial load of *pdhR* mice at 20 DPI. In the section, we probed the role of PdhR on host microbiome at post infection. 354 core taxa were shared between the WT and *pdhR* mutant group, while 312 and 367 were unique to WT and the Δ*pdhR* group respectively (Fig.5-7A). At post infection we still observed a higher relative abundance in the phylum Firmicutes ($p<0.05$) in both WT and the Δ*pdhR* group mice compared to pre infection group (Fig.5-7B and Fig.5-7C). The Phylum Nitrospirota was significantly elevated in the *pdhR* mutant group, although the absolute abundance values were low. It is worth noting that in the WT mice Bacteroidota levels increased while in the Δ*pdhR* group remained low. As anticipated a decline in the phylum Proteobacteria with no significant difference between the groups was observed, possibly reflecting that the infection has been cleared at this point (Fig.5-7B and Fig.5-7D). A modest increase in Actinobacteriota was observed in both groups, though not significant (Fig. 5-7D). We also noticed large error bars in the phyla Actinobacteriota and Verrucomicrobiota, which likely reflects individual mouse differences in responding to enteric infections.

To further assess the changes at 20 DPI we conducted LEfSe analysis. LEfSe analysis is a tool for high-dimensional biomarker mining to find genomic characteristics in microbiome data that substantially describe two or more groups using features such as genes, pathways, and taxonomies (Segata et al., 2011). The main distinctions between the WT and the Δ*pdhR* group was the rise in abundance of the genus *Blautia* in the WT group (Phylum Firmicutes, class Clostridia, order Lachnospirales and family Lanchnospiraceae) at post infection (Fig. 5-8A and Fig. 5-8B). In addition, the control group had an abundance of the genus Muribaculaceae (Phylum Bacteroidota, class Bacteroidia, and family Muribaculaceae) compared to the peak and post infection levels (Fig. 5-8A and Fig. 5-8B). The genus *Blautia* has been previously reported to function in alleviating inflammatory diseases (Freitas et al., 2022). Several genera of the Lanchnospiraceae were elevated (*Oscillibacter*, *Lanchnospiraceae*_NK4A136_group and *Lanchnospiraceae*_UCG_001) compared to a single genus observed in the WT group (Fig. 5-8B). *Lanchnospiraceae* and

Ruminococcaceae have been reported to be the most abundant families of the phylum Firmicutes in healthy humans and vertebrates (Biddle et al., 2013). In addition, they are known to produce potent short-chain fatty acids (Vacca et al., 2020). Taken together, the data implies that elevation in the abundance of genus *Blautia* correlates with disease severity. This was further supported by the reduced diversity in the order Lachnospirales observed in the WT group, corroborating the importance of PdhR in enteric pathogen pathogenesis.

A

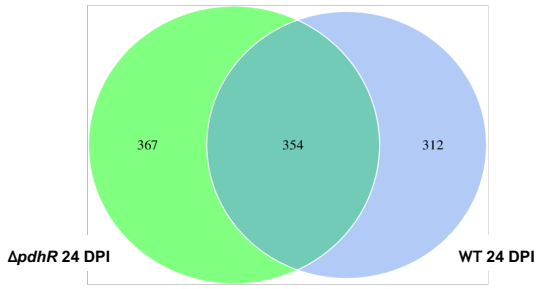

B

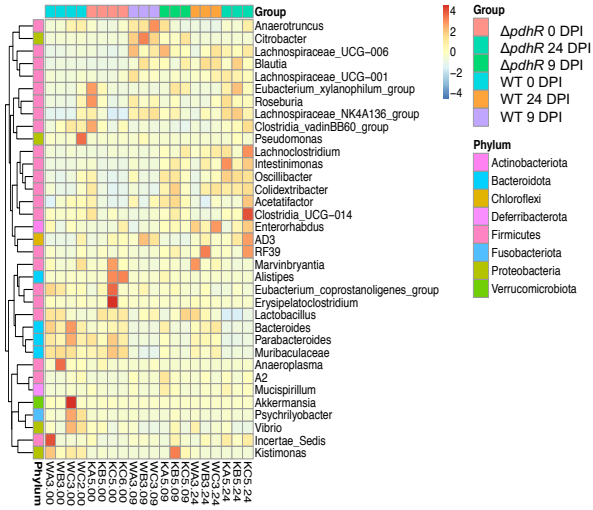

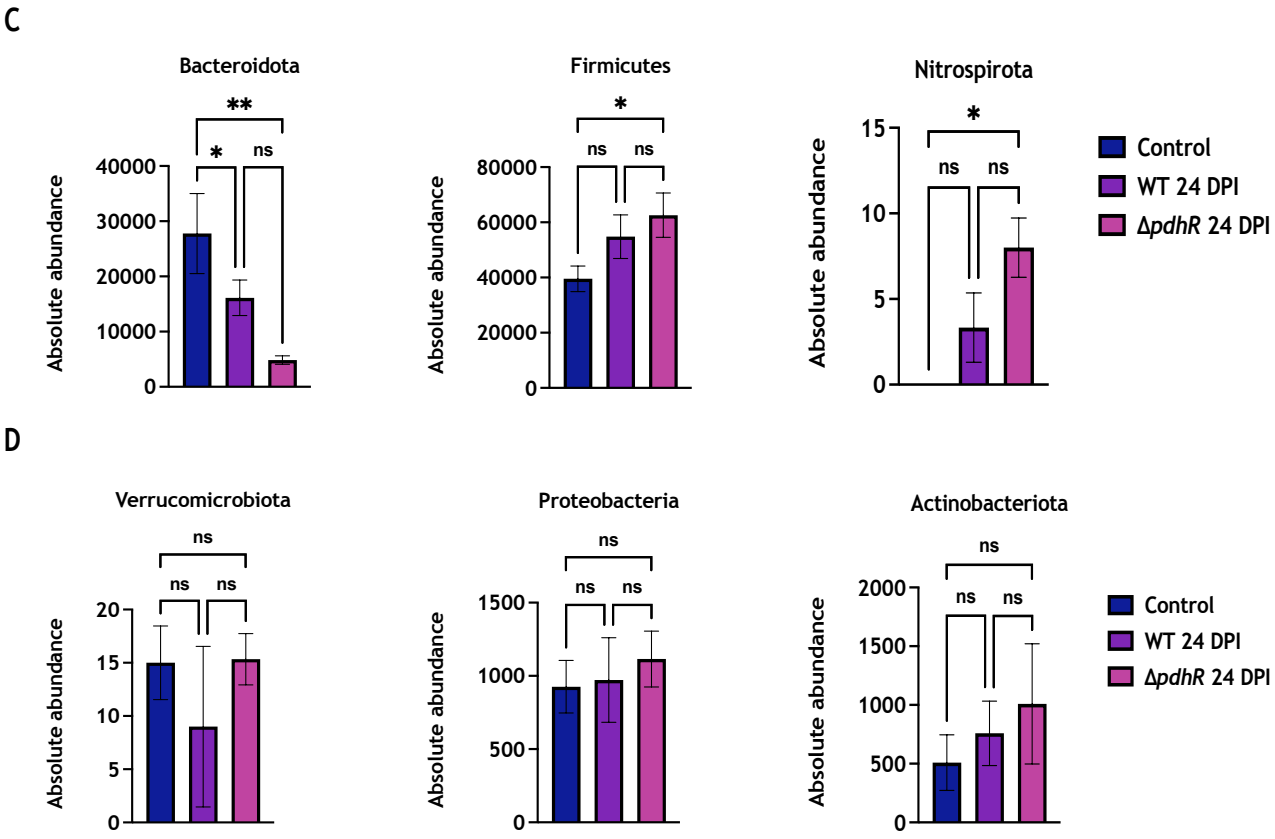

Fig. 5-7. Changes in bacterial communities after clearance of infection. (A) Venn diagram illustrating the distribution of OTUs between the control group and WT *C. rodentium* or Δ*pdhR* at different sampling times (before bacterial infection and 24 DPI). (B) Heatmap cluster showing richness of bacterial species at each time point. The color gradient from blue to red depicts relative levels of abundance: blue represents the lowest level of abundance, whereas red represents the highest level of abundance. The vertical clustering indicates similarity in the richness of all species among different samples. Shorter branch length indicates greater richness similarity between samples. Faecal samples for microbiome analyses were collected at day 0 (before bacterial infection) and 24 DPI. For presented sample names, W and K denotes; WT *C. rodentium* and *C.rodentium* Δ*pdhR* respectively. Comparison of Beta devisity of main bacterial phyla between the control group and mice infected with WT *C. rodentium* (C) or Δ*pdhR* (D) at day 24 post infection. Data are represented as the means of three independent biologicl replicates. * denotes p≤0.05; ** p≤0.01; ns (no significance) p>0.05.

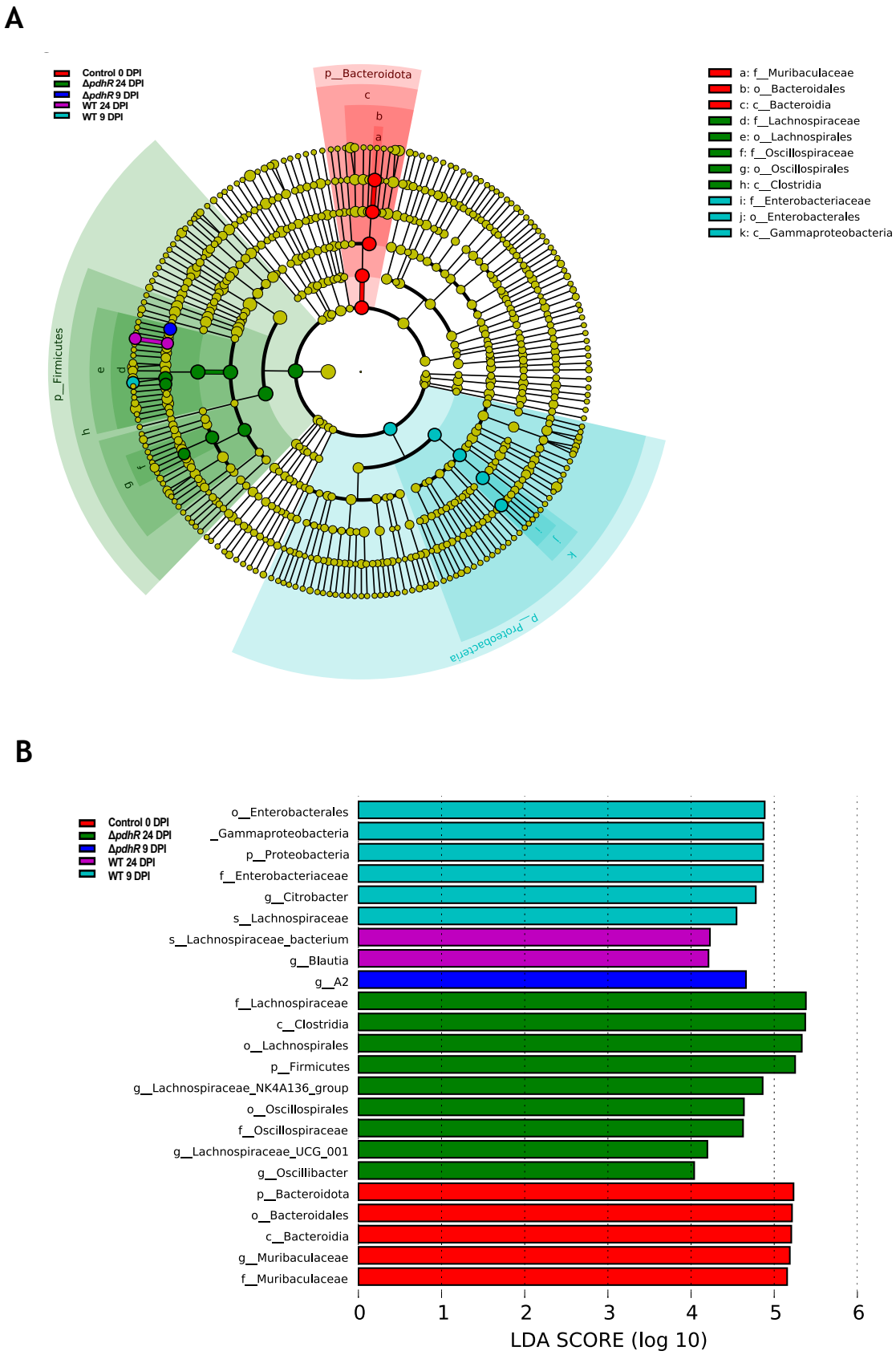

Fig. 5-8. The most differentially abundant taxa among mice infected with WT *C. rodentium* or Δ*pdhR* . (A) Comparison of Beta devisity of main bacterial phyla between mice infected with WT *C. rodentium* and Δ*pdhR* at day 24 post infection. (B) Cladogram

generated by LEfSe, represents the polygentic distribution of faecal bacterial taxa. Each circle represents a phylogenetic level. Significant taxon nodes are colored and corresponding groups are shown by in cladogram key. Yellow circles represents non-significant differences between bacterial taxa. (C) Bar graph indicates LDA scores of bacterial taxa meeting a significant threshhold with LDA scores larger than 2.0.

5.2.8 Functional predictions of faecal microbiome metabolism

To further gain insights into mechanisms responsible for deviation of gut microbiota between WT and *pdhR* mice we used PICRUSt2 (phylogenetic investigation of communities by reconstruction of unobserved states) analysis to determine whether changes in microbiota corresponded to functional pathways. PICRUSt2 is bioinformatics software used to predict metagenome functional abundances based on marker gene sequence (Wang et al., 2019), in this study 16S rRNA gene being the marker. As expected, the functional microbiomes of WT mice were divergent and significantly different from that of the *pdhR* mice (Fig.5-9 A). Microbiota pathways involved in generating or degrading amino acid (PWY-6628, PWY-6629, PWY-6630, PWY-5347, P163-PWY, HSERMETANA-PWY) carbohydrate (FUC-RHAMCAT-PWY, FUCCAT-PWY, PWY-5384), and energy metabolism (P105-PWY, PWY-5677, PWY-5913) were significantly enriched in the WT mice at 9 DPI (Fig.5-9 B). Further, pathways involved in the biosynthesis of enterobactin and enterobacterial common antigen were increased (ENTBACSYN-PWY, ECASYN-PWY). However, a few pathways were enriched in the *pdhR* mice compared to the WT, including COA_PWY, involved in energy metabolism and PWY-2942, PWY-5097 which plays a role in amino acid metabolism. Increased microbiota functional pathways in WT mice at peak of infection suggests a response by gut microbiota to WT *C. rodentium* virulence factors.

Among the enriched pathways in the WT mice at 24 DPI, three were involved in the LPS production, namely, PWY-1269, NAGLIPASYN-PWY, PWY-6467 (Fig5-9 C). Further, PWY-6471 pathway involved in peptidoglycan biosynthesis IV was significantly increased. Other significantly increased pathways include carbohydrates (GLYCOLYSIS, P124-PWY, PENTOSE-P-PWY) and amino acids (PWY-5154, PWY-5505) metabolism. In comparison to the WT mice, Δ*pdhR* mice microbiota had fewer pathways significantly increased at 24 DPI, these were mainly associated with amino acid metabolism (BRANCHED-CHAIN-AA-SYN-PWY, GLUTORN-PWY, ILEUSYN-PWY, PWY-2942, PWY-5101, SER-GLYSYN-PWY). A reasonable assumption is

that WT mice microbiota was adversely affected by *C. rodentium* infection supported by increased peptidoglycan and LPS biosynthesis and 24 DPI implying recovery of bacterial communities to the original state.

A

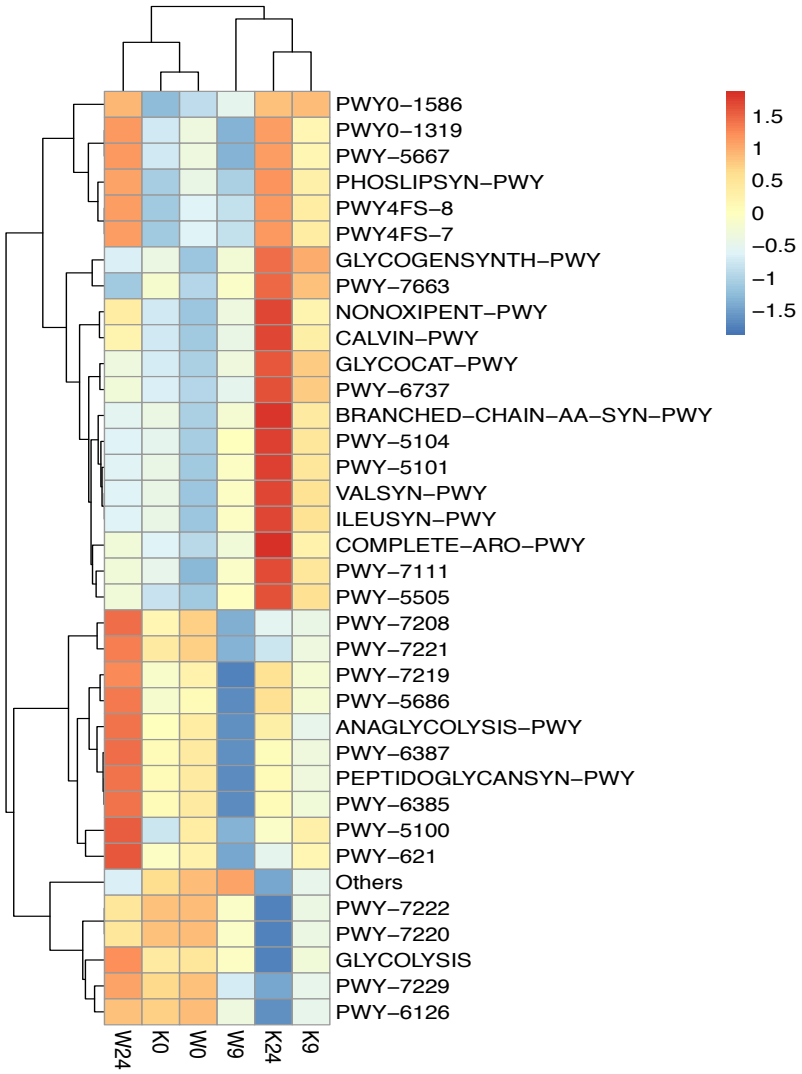

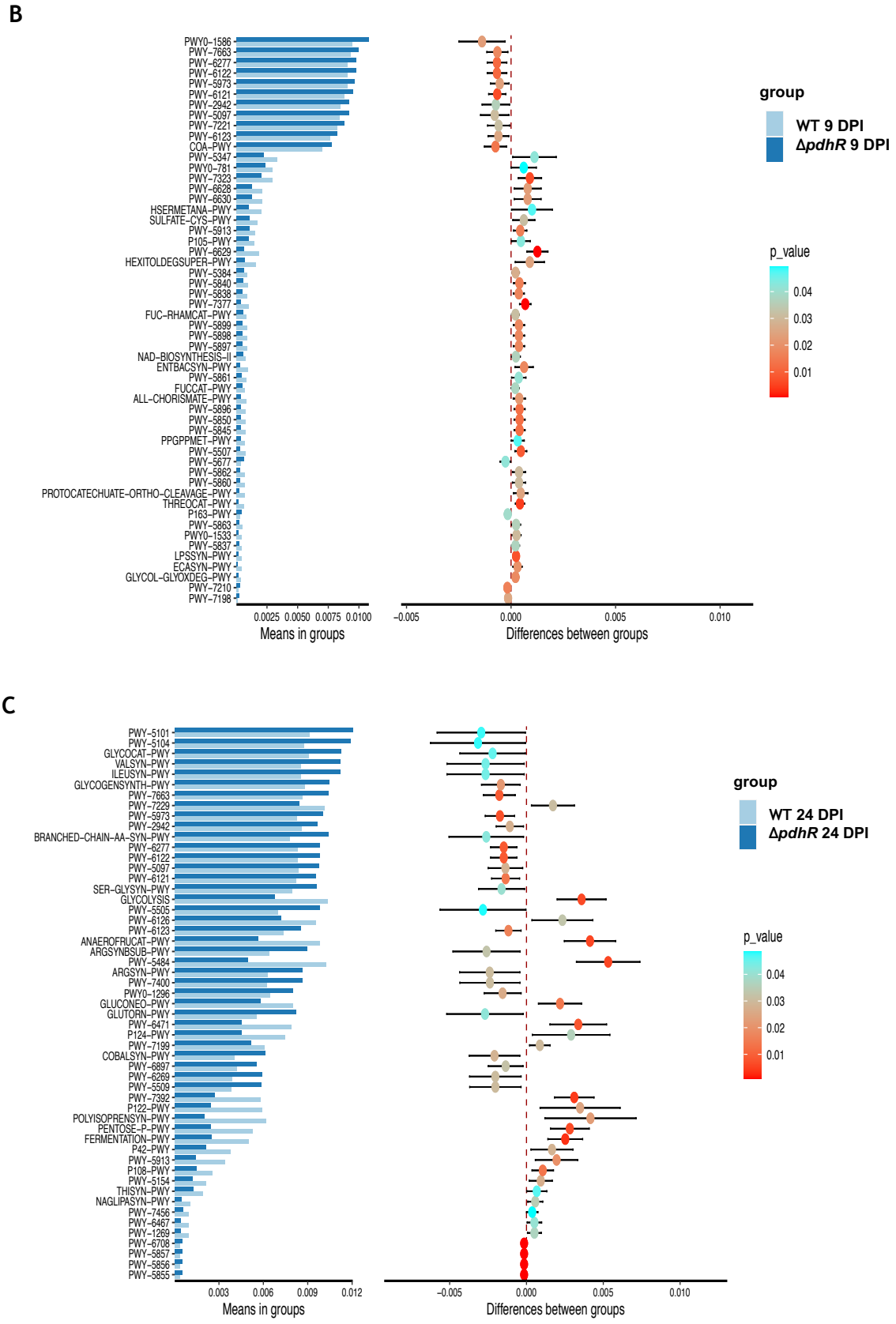

Fig. 5-9. Functional predictions for enriched pathways. (A) Heatmap shows top pathways based on average relative abundance in faecal microbiome between WT *C. rodentium* and the *pdhR* mutant group. Functional predictions for significant KEGG pathways between

faecal microbiome of WT *C. rodentium* and Δ*pdhR* group at (B) day 9 post infection and (C) day 24 post infection.

5.3 Discussion

5.3.1 PdhR is required for host colonisation and triggers host immune response

In this chapter, we show that the transcriptional regulator PdhR is essential for EHEC virulence in an *in vivo* model of infection. To establish a successful infection a pathogen should be able to adhere and colonize host cell tissues effectively. Several factors affect this process, such as adhesins, type III and type IV secretion systems (Bardiau et al., 2010; McWilliams & Torres, 2014; Santos et al., 2019). These processes are used by enteric pathogens to form a host pathogen crosstalk that leads to a subversion of host defence mechanisms and subsequently establishment of disease (Mullineaux-Sanders et al., 2019b). Interestingly, although the deletion of PdhR was nonessential for growth of *C. rodentium in vitro* (Fig.5-1B), the deletion resulted in a significant decrease in bacterial adherence to HeLa cells compared to the WT strain (Fig. 5-10). Complementation of the *pdhR* mutant by plasmid-mediated expression of *pdhR* under the control of its own promoter restored the cell adhesion phenotype of *C. rodentium* in HeLa cells to comparable levels to that of the WT strain. Further, deletion of *pdhR* significantly attenuated *C. rodentium* virulence *in vivo*, this was evidenced by reduced ability to successfully colonize and survive in BALB/c mice.

C. rodentium pdhR mutant show a significant reduction in the ability to colonize mice at early stages as well as at peak of infection compared to the WT strain. Additionally, more mice colonized with the *pdhR* mutant were observed to clear the infection faster than mice colonized with the WT. This phenotype is distinctive of colonization pattern of strains with a non-functional T3SS, or mutants attenuated in the expression of other virulence factors apart from the T3SS (Curtis et al., 2014). For instance, a *C. rodentium escN* mutant strain was incapable of forming a functional T3SS which led to a reduction in colonization capabilities (Carson et al., 2020). While a *C. rodentium cra* mutant (Curtis et al., 2014) and *E. coli* F-18 *eda* mutant (Sweeney et al., 1996) where attenuated for infection, underlining the importance of a functional genome in pathogen infection.

The data strongly support the role of PdhR in massive colonization of the host gut, which may result in increased pathogenicity. The decreased rate of colonization displayed by the *C. rodentium pdhR* mutant strain correlates with reduced expression of the LEE encoded genes, which are required for a functional T3SS as shown by RT-qPCR results (Fig.5-1 C). The difference in WT and Δ*pdhR* mutant pathogenicity is consistent with that of EHEC and its isogenic *pdhR* strain as presented in the previous chapter. The data highlights the importance of metabolic regulators in overall pathogenicity of enteric pathogens.

Several reports have demonstrated the involvement of IL-22 and IL-17 proinflammatory cytokines in early phase (1 to 5 DPI) of enteric infection (Mullineaux-Sanders et al., 2019b; Peterson & Artis, 2014), whilst IFN-γ, and IL-21, are involved at the later stages of infection (10 to 18 DPI) (Carson et al., 2020). Further, TNF-α, IL-1β, CXCL1, and CXCL2 reach peak levels just 3 hours after mice are challenged with an enteric pathogen, signifying that colonic *C. rodentium* A/E pathogenesis is dependent on early bacteria-host interactions (Buschor et al., 2017). In this study, we observed an increase in the abundance of IFN-γ by 24 DPI. The data is in agreement with previous reports (Mullineaux-Sanders et al., 2022). In their study they showed persistence of IFN-γ which is involved in antigen processing at 48 DPI, while there was no difference in the expression of other host immune response markers, in particular, Idol, Mt2 and CXCL-1 between WT mice and Δ*pdhR* group mice. This is alluded by the fact that mice were only culled by 24 DPI, hence all early induced immune response markers would have reached a normal levels at later stages of infection (Buschor et al., 2017). Studies have shown that the characteristic A/E lesions that define disease severity occurs within the first 18 hours of bacterial infection (Buschor et al., 2017). Nonetheless, we had sought to investigate what would transpire when mice are infected with a *pdhR* mutant in the late steady-state and clearance phases (15 to 20 DPI), as little is known about the molecular, cellular, and immunological changes in IECs weeks after the pathogen has cleared. Studies of *C. rodentium* infection primarily focus on the expansion and steady-state phases. However, it is critical to further determine the role of PdhR in early induction of host immune responses.

Interestingly, recent reports have confirmed the importance of PDHc in antibacterial effect of chemokines. In particular, CXCL-10 which appears to require a functioning PDHc to exert its antibacterial effect against *E. coli* (Schutte et al., 2015). Further, mutations in the PDHc complex led to an increase in resistance of CXCL-10 mediated antibacterial effect against *E. coli* (Schutte et al., 2015). In our study, deletion of *pdhR* gene increases the expression of the PDHc which is under the control of the TF PdhR. We thus reason that *pdhR* KO strains are easily recognised by the host immune system and hence provides an opportunity for increased chemokine mediated antibacterial killing.

5.3.2 Dysbiosis in mice faecal microbiome is associated with differences in *C. rodentium* strain infections

During enteric pathogen-induced gastroenteritis, commensal bacteria are one of the first lines of defence. Here, we sought to understand the impact of PdhR on host microbiome during enteric pathogen infection. To address this question, we used the natural mouse pathogen isogenic *pdhR C. rodentium* strain. As expected, we observed an overgrowth of Enterobacteriaceae (phylum Proteobacteria) in the WT mice group compared to the *pdhR* mutant mice group during peak of infection, primarily the *Citrobacter* genera, in agreement with other reports (Mullineaux-Sanders et al., 2017). Increased abundance of Enterobacteriaceae may be associated with compromised colon integrity which may lead to colitis (Zhang et al., 2021). High levels of *E. coli* is key in development of other diseases, including obesity, kidney diseases as well as diabetes (Curtis et al., 2014; Geng et al., 2022; Y. Liu et al., 2019). The bloom in mucosa-associated gamma proteobacteria was also shown to be caused by *C. rodentium* infection due to increased levels of gut cholesterol and mucosal oxygen (Berger et al., 2017).

Interestingly, we observed an increase in the species *Lachnospiraceae bacterium* in the WT mice group at the peak of infection, while a bloom in *Blautia* and *Lachnospiraceae bacterium* was also observed during recovery phase. *Lachnospiraceae* species have been reported to utilize mucin which protects underlying mucosa from interacting with pathogens (Biddle et al., 2013). Degrading this glycoprotein by *Lachnospiraceae* enhances pathogen translocation and has been linked with inflammatory bowel disease and Crohn's disease (Vacca et al., 2020). Although the genera *Blautia* produce SCFA which are beneficial for immune

stimulation and intestinal metabolic action, but some studies have implicated higher abundance of *Blautia* with disease. Enrichment of *Blautia* was reported in the faecal microbiota of irritable bowel syndrome patients compared to the control group (Nishino et al., 2018). Further, increased abundance of *Blautia* was also associated with IBS and diarrhoea (Rajilić-Stojanović et al., 2011). Consistent with the above studies, *Blautia* significantly increased in ulcerative colitis patients compared to healthy individuals, indicating a positive correlation between *Blautia* abundance and chronic inflammatory bowel disease (X. Liu et al., 2021). Other members of the microbiota, such as *B. thetaiotaomicron* have also been implicated in promoting enteric pathogen virulence by degrading monosaccharides from complex polysaccharide that cannot be utilized by nonglycophagic bacteria (Curtis et al., 2014).

On the other hand, low abundance of Proteobacteria was observed in the *pdhR* group at the peak of infection correlating to attenuated virulence of *C. rodentium pdhR* mutant. Abundance of *Oscillibacter*, *Lachnospiraceae*_UCG_001, *Lachnospiraceae* NK4A136 were significantly increased during the recovery phase in the *pdhR* group. *Oscillibacter* are poorly characterized hence its specific function in gut integrity and human health is inconclusive though they are consistently identified in human microbiota (Lam et al., 2012). However, there are some reports on the role of *Oscillibacter* in maintaining of gut barrier in mice, in addition to producing anti-inflammatory metabolites (Youssef et al., 2018). While there are numerous contradicting studies on the effect of the family *Lachnospiraceae* on gut health, some genera including *Lachnospiraceae*_UCG_001 and *Lachnospiraceae* NK4A136 groups have been described as good probiotic strains (Gryaznova et al., 2022; Menq-Rong Wu, Te-Sen Chou, Ching-Ying Huang, 2021). Further the two groups provide SCFAs, in particular butyrate which maintains the integrity of the intestinal barrier and inhibit inflammation (Vacca et al., 2020). On the contrary, lower abundance of these groups in the human gut as a result of antibiotic treatment has been linked with increase in *C. difficile* persistence (Çakır et al., 2020). Notably, the increase in the abundance of this genera in the *pdhR* mutant group could signify better recovery and growth of normal beneficial bacteria, while lower abundance in the WT group could indicate delayed recovery.

EHEC is one of the most predominant diarrheal causing pathogen worldwide, thus it is regarded as a global public health concern (Jubelin et al., 2018). Hence controlling the overgrowth *E. coli* in the gut, particularly the colon has become the centre of attention. To date antibiotics are not used for treatment of EHEC infections as they can be associated with enhanced production of these Shiga toxins, resulting in increased systemic exposure to the adverse effects of the pathogen (Law et al., 2013). Therefore, new therapies like those that target genes which are involved in host attachment and colonization should be explored and PdhR presents such avenue.

5.3.3 Shift in faecal microbiome metabolism during *C. rodentium* infection

Alterations in host metabolism during pathogen infection can negatively or positively effluence disease outcome. We used metagenomic analysis to predict microbiome metabolic changes occurring between the WT group and *pdhR* group mice. Here, functional predictions showed decreased expression of several known pathways in the *pdhR* mutant group compared to the WT group. Increased biosynthesis of gondoate biosynthesis (anaerobic) and cis-vaccenate biosynthesis was predicted in the microbiome of WT group mice. Vaccenate are unsaturated fatty acids (Seager & Slabaugh, 2015) while gondoate is involved in the synthesis of long-chain fatty acids (LCFAs) (An et al., 2022). Both function in the biosynthesis of triglycerides (the most common type of fat stored in the body) (An et al., 2022), suggesting increased triglycerides deposition and fat storage. Interestingly, Pathogen-associated patterns (PAMP) have been found to rewire lipid metabolism in macrophages resulting in increased energy storage (Rashighi & Harris, 2017). Besides the role in energy storage, triglycerides mediate other processes, including oxidative stress and secretion of inflammatory mediators such as IL-6, IL-1 and TNF-a (van Dierendonck et al., 2022). In addition, excessive storage triggers inflammatory responses in macrophages (van Dierendonck et al., 2022). Thus, the data implies that systemic metabolic inflammation was triggered due to excessive storage of triglycerides in the WT group mice in response to abundance of Enterobacteriaceae.

Increased biosynthesis of isoleucine was detected in the microbiome of WT mice at the recovery phase. Isoleucine is a branched chain amino acid with several functions in human health. Specifically, it is critical for immune functions as it stimulates

secretion of immunoreactive substances and forms part of neutrophils and lymphocytes (Burns, 1975). Administration of isoleucine to challenged animals drastically improved their health status (X. Mao et al., 2018). Indeed, l-isoleucine supplemented ORS alleviated acute diarrhoea caused by *E. coli* in children (N. H. Alam et al., 2011). Mechanisms in which isoleucine lessens disease severity are not clear, however studies have linked isoleucine to immune signalling pathways, including Toll-like receptors and MDA5 that play a role in expressing several cytokines (X. Mao et al., 2022). Further, supplementing dietary l-isoleucine to DSS-challenged rats greatly reduced colon impairment and inflammation (X. Mao et al., 2022). Thus, increased metabolism of isoleucine in the WT group implied that isoleucine was needed to prevent invading bacteria in the WT group compared to the *pdhR* group via increased immune response.

Increased biosynthesis of enterobacterial common antigen (ECA) further confirmed disease severity in the WT mice group due to the presence of Enterobacteriaceae. ECA are localised on the surfaces of the family Enterobacteriaceae, and their presence triggers the host to elicit an immune response during pathogen-host interaction (Schierova et al., 2021). In addition, we also predicted in an increase in the biosynthesis of enterobactin in the WT group. This also indicated the increased presence of the Enterobacteriaceae during peak of infection. *E. coli* produces this iron-chelating molecule that binds ferric ions which are used to provide iron for many metabolic pathways (Rajendran & Marahiel, 1999).

5.4 Conclusion

In conclusion, our study demonstrated that disturbing a pathogens metabolism landscape that permit successful colonization by deleting the TFs PdhR severely attenuates *C. rodentium* virulence *in vivo*. Based on our observations, three significant findings were revealed. (1) PdhR is essential not only for early host colonisation but also required for further persistence of enteric pathogen infection. (2) The TFs PdhR may be implicated in host chemokine antibacterial mediated killing, in addition to regulating LEE encoded bacterial virulence. (3) Infection with the *pdhR* mutant strain showed a lower degree of dysbiosis in the microbial community with no significance at the peak of infection. Interestingly it caused a bloom in some bacterial strains associated with ‘good’ gut health during the recovery

phase. This further corroborates that the TFs PdhR could be used as a potential target for the development of a safe therapeutic for control of EHEC infection

Chapter 6: Final Discussion

EHEC infections are among the leading cause of global foodborne illnesses, causing gastroenteritis in both adults and children. In severe cases EHEC cause acute HUS leading to renal failure and sometimes death (Koutsoumanis et al., 2020). Neurological symptoms such as aphasia, tremors, and coma may also occur due to brain impairment (Karpman & Ståhl, 2014). Despite significant advancements in STEC research by the scientific community, there is still no specific effective management against EHEC infections (Nguyen & Sperandio, 2012). This is due to the fact that the use of antibiotics in treatment of EHEC infections is currently not advised. Previously Chloramphenicol was frequently used for the treatment of STEC, in combination with other drugs such as, sulfonamides, quinolones, and fluoroquinolones. The use of these antibiotics resulted in overexpression of *Stx* gene leading to an increase in toxin production (Hwang et al., 2021). Additionally, STEC was frequently reported to be resistant to tetracyclines and aminoglycosides, among other antibiotics (Hwang et al., 2021). However supplementation with oral rehydration seems the best management for *E. coli* O157:H7 infections though not effective (Rahal et al., 2012).

The main virulence factor associated with EHEC pathogenicity is the production of Stx (Chong et al., 2007). Besides production of Stx, EHEC expresses intimin, encoded by the protein *eae* gene, involved in binding to IEC and leading to a A/E phenotype determined by the T3SS (Mullineaux-Sanders et al., 2019a). The T3SS is encoded by the LEE PAI containing five polycistronic operons, LEE 1 to LEE 5 (Deng et al., 2004). The first open reading frame, LEE1, encodes for the LEE master regulator (Ler), which blocks H-NS, a DNA binding protein that suppresses transcription of LEE from having its inhibitory impact (Connolly et al., 2016). Activation of *Ler* stimulates the transcription of the whole LEE operon (LEE1-5) (Arbeloa et al., 2009). Because the LEE plays a crucial role in EHEC pathogenicity it is tightly regulated by many important global regulators, including Cra, RpoS, QseA, FIS, HIS, H-NS (Sharp and Sperandio, 2007; Bustamante et al., 2011).

Independent studies have pointed out that infections caused by EHEC a subset of STEC can cause gut microbiota dysbiosis (Mullineaux-Sanders et al., 2017). Dysbiosis refers to the shift in both gut microbiota and metabolic activities.

Thus, this decrease in abundance of good bacteria may exacerbate the risk of many gut bacterial infections, including, multiple sclerosis, inflammatory bowel disease (IBD), allergies, diabetes, obesity, and inflammatory bowel disease (IBD) (Mengyu Zheng et al., 2023). In healthy individuals Bacteroidetes and Firmicutes phyla accounts for more than 90% while Actinobacteria and Proteobacteria phyla are present but low in density (Kim et al., 2017). During infection an increase in the abundance of Proteobacteria is observed at the peak of infection (Mullineaux-Sanders et al., 2017). In addition an increase in in mucosa-associated gamma proteobacteria elevates gut cholesterol and mucosal oxygen (Berger et al., 2017), causing further increase in the genera of Enterobacteriaceae which is associated with the development of other conditions stated above.

In this study, we have demonstrated that deletion of the TFs PdhR directly binds to the *Ler* regulatory region and may lead to the expression of the *LEE1* operon and subsequently the whole LEE operon (*LEE2- LEE5*). Moreover, using transcriptomics we have highlighted that LEE regulation is very complex, and several carbon metabolism pathways maybe wired into global LEE gene regulation in EHEC, by several TFs including PdhR. Potentially understanding this complex relationship could lead to better dietary interventions to reduce EHEC mediated disease. Finally, we showed that *C. rodentium* defective in the *pdhR* gene severely attenuates *C. rodentium* virulence *in vivo*. The data implies that PdhR is essential for early host colonisation and persistence in the gut, though mechanisms involved were not interrogated in this study. Most importantly the data revealed that there was a lower degree of dysbiosis in the microbial community in mice infected with the *pdhR* knockout strain. Surprisingly, an increase in the abundance of probiotic bacterial strains was observed. It's interesting to note that subsequent findings have validated the role of PDHc in chemokines' antibacterial effects. In particular, CXCL-10, which according to Schutte et al. (2015) appears to need a functional PDHc to work against *E. coli*. Additionally, changes in the PDHc complex increased *E. coli* resistance to the antibacterial activity of CXCL-10 (Schutte et al., 2015). In our work, deletion of the *pdhR* gene results in an increase in PDHc expression, which is regulated by the TF *pdhR*. Our data implies that because the *pdhR* KO strains are more readily recognized by the host immune system due to an

increase in PDHc enzymes, there is a greater potential for chemokine-mediated antibacterial death. Thus, the data suggests that TF PdhR can be a better therapeutic target to control EHEC infections compared the PDHc.

References

Abernathy, J., Corkill, C., Hinojosa, C., Li, X., & Zhou, H. (2013). Deletions in the pyruvate pathway of Salmonella Typhimurium alter SPI1-mediated gene expression and infectivity. *Journal of Animal Science and Biotechnology*, *4*(1), 1. https://doi.org/10.1186/2049-1891-4-5

Alam, M. T., Amos, G. C. A., Murphy, A. R. J., Murch, S., Wellington, E. M. H., & Arasaradnam, R. P. (2020). Microbial imbalance in inflammatory bowel disease patients at different taxonomic levels. *Gut Pathogens*, *12*(1), 1–8. https://doi.org/10.1186/s13099-019-0341-6

Alam, N. H., Raqib, R., Ashraf, H., Qadri, F., Ahmed, S., Zasloff, M., Agerberth, B., Salam, M. A., Gyr, N., & Meier, R. (2011). L-isoleucine-supplemented oral rehydration solution in the treatment of acute diarrhoea in children: A randomized controlled trial. *Journal of Health, Population and Nutrition*, *29*(3), 183–190. https://doi.org/10.3329/jhpn.v29i3.7864

An, R., Ma, S., Zhang, N., Zhang, X., Chen, L., Lin, H., Xiang, T., Chen, M., & Tan, H. (2022). *Association between maternal gut microbiome and macrosomia*. 1–18. https://doi.org/10.21203/rs.3.rs-1720994/v1

Anand, A., Olson, C. A., Sastry, A. V., Patel, A., Szubin, R., Yang, L., Feist, A. M., & Palsson, B. O. (2021). Restoration of fitness lost due to dysregulation of the pyruvate dehydrogenase complex is triggered by ribosomal binding site modifications. *Cell Reports*, *35*(1), 108961. https://doi.org/10.1016/j.celrep.2021.108961

Anh Le, T. T., Thuptimdang, P., McEvoy, J., & Khan, E. (2019). Phage shock protein and gene responses of Escherichia coli exposed to carbon nanotubes. *Chemosphere*, *224*, 461–469. https://doi.org/10.1016/j.chemosphere.2019.02.159

Anzai, T., Imamura, S., Ishihama, A., & Shimada, T. (2020). Expanded roles of pyruvate-sensing pdhr in transcription regulation of the escherichia coli K-12 genome: Fatty acid catabolism and cell motility. *Microbial Genomics*, *6*(10), 1–14. https://doi.org/10.1099/mgen.0.000442

Arbeloa, A., Blanco, M., Moreira, F. C., Bulgin, R., López, C., Dahbi, G., Blanco, J. E., Mora, A., Alonso, M. P., Mamani, R. C., Gomes, T. A. T., Blanco, J., & Frankel, G. (2009). Distribution of espM and espT among enteropathogenic and enterohaemorrhagic Escherichia coli. *Journal of Medical Microbiology*, *58*(8), 988–995. https://doi.org/10.1099/jmm.0.010231-0

Arya, G., Pal, M., Sharma, M., Singh, B., Singh, S., Agrawal, V., & Chaba, R. (2021). Molecular insights into effector binding by DgoR, a GntR/FadR family transcriptional repressor of D-galactonate metabolism in Escherichia coli. *Molecular Microbiology*, *115*(4), 591–609. https://doi.org/10.1111/mmi.14625

Bahrani-Mougeot, F. K., Scobey, M. W., & Sansonetti, P. J. (2009). Enteropathogenic Infections. *Encyclopedia of Microbiology, Third Edition*, 329–343. https://doi.org/10.1016/B978-012373944-5.00224-8

Baksh, K. A., & Zamble, D. B. (2020). Allosteric control of metal-responsive transcriptional regulators in bacteria. *Journal of Biological Chemistry*, *295*(6), 1673–1684. https://doi.org/10.1074/jbc.REV119.011444

Ballem, A., Gonçalves, S., Garcia-Meniño, I., Flament-Simon, S. C., Blanco, J. E., Fernandes, C., Saavedra, M. J., Pinto, C., Oliveira, H., Blanco, J., Almeida, G., & Almeida, C. (2020). Prevalence and serotypes of Shiga toxinproducing Escherichia coli (STEC) in dairy cattle from Northern Portugal. *PLoS ONE*, *15*(12 December), 1–12. https://doi.org/10.1371/journal.pone.0244713

Bardiau, M., Szalo, M., & Mainil, J. G. (2010). Initial adherence of EPEC, EHEC and VTEC to host cells. *Veterinary Research*, *41*(5). https://doi.org/10.1051/vetres/2010029

Barrasso, K., Watve, S., Simpson, C. A., Geyman, L. J., van Kessel, J. C., & Ng, W. L. (2020). Dual-function quorum-sensing systems in bacterial pathogens and symbionts. *PLoS Pathogens*, *16*(10), 1–7. https://doi.org/10.1371/journal.ppat.1008934

Baumler, A. J., Kusters, J. G., Stojiljkovic, I., & Heffron, F. (1994).

Salmonella typhimurium loci involved in survival within macrophages. *Infection and Immunity*, *62*(5), 1623–1630. https://doi.org/10.1128/iai.62.5.1623-1630.1994

Baümler, A. J., & Sperandio, V. (2016). Interactions between the microbiota and pathogenic bacteria in the gut. *Nature*, *535*(7610), 85–93. https://doi.org/10.1038/nature18849

Beckham, K. S. H., Connolly, J. P. R., Ritchie, J. M., Wang, D., Gawthorne, J. A., Tahoun, A., Gally, D. L., Burgess, K., Burchmore, R. J., Smith, B. O., Beatson, S. A., Byron, O., Wolfe, A. J., Douce, G. R., & Roe, A. J. (2014). The metabolic enzyme AdhE controls the virulence of Escherichia coliO157: H7. *Molecular Microbiology*, *93*(1), 199–211. https://doi.org/10.1111/mmi.12651

Berger, C. N., Crepin, V. F., Roumeliotis, T. I., Wright, J. C., Carson, D., Pevsner-Fischer, M., Furniss, R. C. D., Dougan, G., Dori-Bachash, M., Yu, L., Clements, A., Collins, J. W., Elinav, E., Larrouy-Maumus, G. J., Choudhary, J. S., & Frankel, G. (2017). Citrobacter rodentium Subverts ATP Flux and Cholesterol Homeostasis in Intestinal Epithelial Cells In Vivo. *Cell Metabolism*, *26*(5), 738-752.e6. https://doi.org/10.1016/j.cmet.2017.09.003

Bibbal, D., Loukiadis, E., Kérourédan, M., Ferré, F., Dilasser, F., de Garam, C. P., Cartier, P., Oswald, E., Gay, E., Auvray, F., & Brugère, H. (2015). Prevalence of carriage of shiga toxin-producing Escherichia coli serotypes O157:H7, O26:H11, O103:H2, O111:H8, and O145:H28 among slaughtered adult cattle in France. *Applied and Environmental Microbiology*, *81*(4), 1397–1405. https://doi.org/10.1128/AEM.03315-14

Biddle, A., Stewart, L., Blanchard, J., & Leschine, S. (2013). *Untangling the Genetic Basis of Fibrolytic Specialization by Lachnospiraceae and Ruminococcaceae in Diverse Gut Communities*. 627–640. https://doi.org/10.3390/d5030627

Borenshtein, D., McBee, M. E., & Schauer, D. B. (2008). Utility of the Citrobacter rodentium infection model in laboratory mice. *Current Opinion in Gastroenterology*, *24*(1), 32–37.

https://doi.org/10.1097/MOG.0b013e3282f2b0fb

Bulger, M., & Groudine, M. (2011). Functional and Mechanistic Diversity of Distal Transcription Enhancers. *Cell*, *144*(5), 825. https://doi.org/10.1016/j.cell.2011.02.026

Burns, C. P. (1975). Isoleucine metabolism by leukemic and normal human leukocytes in relation to cell maturity and type. *Blood*, *45*(5), 643–651. https://doi.org/10.1182/blood.v45.5.643.643

Buschor, S., Cuenca, M., Uster, S. S., Schären, O. P., Balmer, M. L., Terrazos, M. A., Schürch, C. M., & Hapfelmeier, S. (2017). Innate immunity restricts Citrobacter rodentium A/E pathogenesis initiation to an early window of opportunity. *PLoS Pathogens*, *13*(6), 1–24. https://doi.org/10.1371/journal.ppat.1006476

Bustamante, V. H., Villalba, M. I., García-Angulo, V. A., Vázquez, A., Martínez, L. C., Jiménez, R., & Puente, J. L. (2011). PerC and GrlA independently regulate Ler expression in enteropathogenic Escherichia coli. *Molecular Microbiology*, *82*(2), 398–415. https://doi.org/10.1111/j.1365-2958.2011.07819.x

Byrne, L., Dallman, T. J., Adams, N., Mikhail, A. F. W., Mccarthy, N., & Jenkins, C. (2018). Highly Pathogenic Clone of Shiga Toxin – Producing Escherichia coli. *Emerging Infectious Diseases*, *24*(12), 2303–2308.

Caballero-Flores, G., Pickard, J. M., Fukuda, S., Inohara, N., & Núñez, G. (2020). An Enteric Pathogen Subverts Colonization Resistance by Evading Competition for Amino Acids in the Gut. *Cell Host and Microbe*, *28*(4), 526-533.e5. https://doi.org/10.1016/j.chom.2020.06.018

Caballero-Flores, G., Sakamoto, K., Zeng, M. Y., Wang, Y., Hakim, J., Matus-Acuña, V., Inohara, N., & Núñez, G. (2019). Maternal Immunization Confers Protection to the Offspring against an Attaching and Effacing Pathogen through Delivery of IgG in Breast Milk. *Cell Host and Microbe*, *25*(2), 313-323.e4. https://doi.org/10.1016/j.chom.2018.12.015

Çakır, T., Panagiotou, G., Uddin, R., & Durmuş, S. (2020). Novel Approaches for Systems Biology of Metabolism-Oriented Pathogen-Human

Interactions: A Mini-Review. *Frontiers in Cellular and Infection Microbiology*, *10*(February). https://doi.org/10.3389/fcimb.2020.00052

Cameron, E. A., Curtis, M. M., Kumar, A., Dunny, G. M., & Sperandio, V. (2018). Microbiota and pathogen proteases modulate type iii secretion activity in enterohemorrhagic escherichia coli. *MBio*, *9*(6), 1–10. https://doi.org/10.1128/mBio.02204-18

Cameron, E. A., & Sperandio, V. (2015). Frenemies: Signaling and Nutritional Integration in Pathogen-Microbiota-Host Interactions. *Cell Host and Microbe*, *18*(3), 275–284. https://doi.org/10.1016/j.chom.2015.08.007

Carlson-Banning, K. M., & Sperandio, V. (2016a). Catabolite and oxygen regulation of enterohemorrhagic Escherichia coli virulence. *MBio*, *7*(6). https://doi.org/10.1128/mBio.01852-16

Carlson-Banning, K. M., & Sperandio, V. (2016b). Catabolite and oxygen regulation of enterohemorrhagic Escherichia coli virulence. *MBio*, *7*(6), 1–11. https://doi.org/10.1128/mBio.01852-16

Carson, D., Barry, R., Hopkins, E. G. D., Roumeliotis, T. I., García-Weber, D., Mullineaux-Sanders, C., Elinav, E., Arrieumerlou, C., Choudhary, J. S., & Frankel, G. (2020). Citrobacter rodentium induces rapid and unique metabolic and inflammatory responses in mice suffering from severe disease. *Cellular Microbiology*, *22*(1), 1–17. https://doi.org/10.1111/cmi.13126

Chatterjee, R., Shreenivas, M. M., Sunil, R., & Chakravortty, D. (2019). Enteropathogens: Tuning their gene expression for Hassle-Free survival. *Frontiers in Microbiology*, *10*(JAN), 1–17. https://doi.org/10.3389/fmicb.2018.03303

Chen, K., Magri, G., Grasset, E. K., & Cerutti, A. (2020). Rethinking mucosal antibody responses: IgM, IgG and IgD join IgA. *Nature Reviews Immunology*, *20*(7), 427–441. https://doi.org/10.1038/s41577-019-0261-1

Chong, Y., Fitzhenry, R., Heuschkel, R., Torrente, F., Frankel, G., & Phillips, A. D. (2007). Human intestinal tissue tropism in Escherichia coli O157:H7 - Initial colonization of terminal ileum and Peyer's patches and minimal

colonic adhesion ex vivo. *Microbiology*, *153*(3), 794–802. https://doi.org/10.1099/mic.0.2006/003178-0

Coburn, B., Sekirov, I., & Finlay, B. B. (2007). Type III secretion systems and disease. *Clinical Microbiology Reviews*, *20*(4), 535–549. https://doi.org/10.1128/CMR.00013-07

Coldewey, S. M., Hartmann, M., Schmidt, D. S., Engelking, U., Ukena, S. N., & Gunzer, F. (2007). Impact of the rpoS genotype for acid resistance patterns of pathogenic and probiotic Escherichia coli. *BMC Microbiology*, *7*, 1–13. https://doi.org/10.1186/1471-2180-7-21

Connolly, J. P. R., Gabrielsen, M., Goldstone, R. J., Grinter, R., Wang, D., Cogdell, R. J., Walker, D., Smith, D. G. E., & Roe, A. J. (2016). A Highly Conserved Bacterial D-Serine Uptake System Links Host Metabolism and Virulence. *PLoS Pathogens*, *12*(1). https://doi.org/10.1371/journal.ppat.1005359

Connolly, J. P. R., & Roe, A. J. (2016). When and where? Pathogenic escherichia coli differentially sense host d-serine using a universal transporter system to monitor their environment. *Microbial Cell*, *3*(4), 181–184. https://doi.org/10.15698/mic2016.04.494

Connolly, J. P. R., Slater, S. L., O'Boyle, N., Goldstone, R. J., Crepin, V. F., Gallego, D. R., Herzyk, P., Smith, D. G. E., Douce, G. R., Frankel, G., & Roe, A. J. (2018). Host-associated niche metabolism controls enteric infection through fine-tuning the regulation of type 3 secretion. *Nature Communications*, *9*(1). https://doi.org/10.1038/s41467-018-06701-4

Conway, T., & Cohen, P. (2015). Commensal and Pathogenic Escherichia coli Metabolism in the Gut. *Microbiology Spectrum*, *3*. https://doi.org/10.1128/microbiolspec.MBP-0006-2014

Coulthrust, S. J., Clare, S., Evans, T. J., Foulds, I. J., Roberts, K. J., Welch, M., Dougan, G., & Salmond, G. P. C. (2007). Quorum sensing has an unexpected role in virulence in the model pathogen Citrobacter rodentium. *EMBO Reports*, *8*(7), 698–703. https://doi.org/10.1038/sj.embor.7400984

Cramer, J. P. (2014). Enterohemorrhagic Escherichia coli (EHEC): Hemorrhagic Colitis and Hemolytic Uremic Syndrome (HUS). In *Emerging Infectious Diseases: Clinical Case Studies*. Elsevier Inc. https://doi.org/10.1016/B978-0-12-416975-3.00017-0

Crepin, V. F., Collins, J. W., Habibzay, M., & Frankel, G. (2016). Citrobacter rodentium mouse model of bacterial infection. *Nature Protocols*, *11*(10), 1851–1876. https://doi.org/10.1038/nprot.2016.100

Curtis, M. M., Hu, Z., Klimko, C., Narayanan, S., Deberardinis, R., & Sperandio, V. (2014). The gut commensal bacteroides thetaiotaomicron exacerbates enteric infection through modification of the metabolic landscape. *Cell Host and Microbe*, *16*(6), 759–769. https://doi.org/10.1016/j.chom.2014.11.005

Datsenko, K. A., & Wanner, B. L. (2000). One-step inactivation of chromosomal genes in Escherichia coli K-12 using PCR products. *Proceedings of the National Academy of Sciences of the United States of America*, *97*(12), 6640–6645. https://doi.org/10.1073/pnas.120163297

de Nisco, N. J., Rivera-Cancel, G., & Orth, K. (2018). The biochemistry of sensing: Enteric pathogens regulate type iii secretion in response to environmental and host cues. *MBio*, *9*(1), 1–15. https://doi.org/10.1128/mBio.02122-17

Deng, W., Li, Y., Vallance, B. A., & Finlay, B. B. (2001). Locus of enterocyte effacement from Citrobacter rodentium: Sequence analysis and evidence for horizontal transfer among attaching and effacing pathogens. *Infection and Immunity*, *69*(10), 6323–6335. https://doi.org/10.1128/IAI.69.10.6323-6335.2001

Deng, Wanyin, Puente, J. L., Gruenheid, S., Li, Y., Vallance, B. A., Vázquez, A., Barba, J., Ibarra, J. A., O'Donnell, P., Metalnikov, P., Ashman, K., Lee, S., Goode, D., Pawson, T., & Finlay, B. B. (2004). Dissecting virulence: Systematic and functional analyses of a pathogenicity island. *Proceedings of the National Academy of Sciences of the United States of America*, *101*(10), 3597–3602. https://doi.org/10.1073/pnas.0400326101

Deng, Wanyin, Yu, H. B., De Hoog, C. L., Stoynov, N., Li, Y., Foster, L. J., & Finlay, B. B. (2012). Quantitative proteomic analysis of type III secretome of enteropathogenic Escherichia coli reveals an expanded effector repertoire for attaching/effacing bacterial pathogens. *Molecular and Cellular Proteomics*, *11*(9), 692–709. https://doi.org/10.1074/mcp.M111.013672

Denzer, L., Schroten, H., & Schwerk, C. (2020). From gene to protein—how bacterial virulence factors manipulate host gene expression during infection. *International Journal of Molecular Sciences*, *21*(10), 1–37. https://doi.org/10.3390/ijms21103730

Detzner, J., Pohlentz, G., & Müthing, J. (2022). Enterohemorrhagic Escherichia coli and a Fresh View on Shiga Toxin-Binding Glycosphingolipids of Primary Human Kidney and Colon Epithelial Cells and Their Toxin Susceptibility. *International Journal of Molecular Sciences*, *23*(13). https://doi.org/10.3390/ijms23136884

Domka, J., Lee, J., & Wood, T. K. (2006). YliH (BssR) and YceP (BssS) regulate Escherichia coli K-12 biofilm formation by influencing cell signaling. *Applied and Environmental Microbiology*, *72*(4), 2449–2459. https://doi.org/10.1128/AEM.72.4.2449-2459.2006

Dong, N., Liu, L., & Shao, F. (2010). A bacterial effector targets host DH-PH domain RhoGEFs and antagonizes macrophage phagocytosis. *EMBO Journal*, *29*(8), 1363–1376. https://doi.org/10.1038/emboj.2010.33

Doyle, M. E., Archer, J., Kaspar, C. W., & Weiss, R. (2006). Human Illness Caused by E . coli O157 : H7 from Food and Non-food Sources. *FRI Briefings*, *October*, 1–37. http://fri.wisc.edu/docs/pdf/FRIBrief_EcoliO157H7humanillness.pdf

du Sert, N. P., Bamsey, I., Bate, S. T., Berdoy, M., Clark, R. A., Cuthill, I. C., Fry, D., Karp, N. A., Macleod, M., Moon, L., Stanford, S. C., & Lings, B. (2017). The Experimental Design Assistant. *Nature Methods*, *14*(11), 1024–1025. https://doi.org/10.1038/nmeth.4462

Duffy, G. (2014). Escherichia Coli: Enterohemorrhagic E. coli (EHEC), Including

Non-O157. In *Encyclopedia of Food Microbiology: Second Edition* (Second Edi, Vol. 1). Elsevier. https://doi.org/10.1016/B978-0-12-384730-0.00384-0

Echlin, H., Frank, M., Rock, C., & Rosch, J. W. (2020). Role of the pyruvate metabolic network on carbohydrate metabolism and virulence in Streptococcus pneumoniae. In *Molecular Microbiology* (Vol. 114, Issue 4, pp. 536–552). https://doi.org/10.1111/mmi.14557

Ellermann, M., Jimenez, A. G., Pifer, R., Ruiz, N., & Sperandio, V. (2021). The canonical long-chain fatty acid sensing machinery processes arachidonic acid to inhibit virulence in enterohemorrhagic escherichia coli. *MBio*, *12*(1), 1–17. https://doi.org/10.1128/mBio.03247-20

Etcheverría, A. I., & Padola, N. L. (2013). Shiga toxin-producing Escherichia coli: Factors involved in virulence and cattle colonization. *Virulence*, *4*(5), 366–372. https://doi.org/10.4161/viru.24642

Feng, Y., & Cronan, J. E. (2014). PdhR, the pyruvate dehydrogenase repressor, does not regulate lipoic acid synthesis. *Research in Microbiology*, *165*(6), 429–438. https://doi.org/10.1016/j.resmic.2014.04.005

Ferens, W. A., & Hovde, C. J. (2011). Escherichia coli O157:H7: Animal reservoir and sources of human infection. *Foodborne Pathogens and Disease*, *8*(4), 465–487. https://doi.org/10.1089/fpd.2010.0673

Fink, R. C., Black, E. P., Hou, Z., Sugawara, M., Sadowsky, M. J., & Diez-Gonzaleza, F. (2012). Transcriptional responses of Escherichia coli K-12 and O157: H7 associated with lettuce leaves. *Applied and Environmental Microbiology*, *78*(6), 1752–1764. https://doi.org/10.1128/AEM.07454-11

Fitzgerald, D. M., Stringer, A. M., Smith, C., Lapierre, P., & Wade, J. T. (2023). Genome-Wide Mapping of the Escherichia coli PhoB Regulon Reveals Many Transcriptionally Inert, Intragenic Binding Sites. *MBio*, *XX*(Xx), e0253522. https://doi.org/10.1128/mbio.02535-22

Fomby, P., & Cherlin, A. J. (2011). Role of microbiota in immunity and inflammation. *National Institute of Health*, *72*(2), 181–204.

https://doi.org/10.1016/j.cell.2014.03.011.Role

Freitas, R. G. B. de O. N., Vasques, A. C. J., Fernandes, G. da R., Ribeiro, F. B., Solar, I., Barbosa, M. G., Pititto, B. de A., Geloneze, B., & Ferreira, S. R. G. (2022). Associations of Blautia Genus With Early-Life Events and Later Phenotype in the NutriHS. *Frontiers in Cellular and Infection Microbiology*, *12*(May), 1–13. https://doi.org/10.3389/fcimb.2022.838750

Gao, J., Tian, M., Bao, Y., Li, P., Liu, J., Ding, C., Wang, S., Li, T., & Yu, S. (2016). Pyruvate kinase is necessary for Brucella abortus full virulence in BALB/c mouse. *Veterinary Research*, *47*(1), 1–11. https://doi.org/10.1186/s13567-016-0372-7

Gao, Y., Lim, H. G., Verkler, H., Szubin, R., Quach, D., Rodionova, I., Chen, K., Yurkovich, J., Cho, B.-K., & Palsson, B. O. (2021). Unraveling the functions of uncharacterized transcription factors in Escherichia coli using ChIP-exo. *BioRxiv*, 2021.06.10.447994. http://biorxiv.org/content/early/2021/06/11/2021.06.10.447994.abstract

Garimano, N., Scalise, M. L., Gómez, F., Amaral, M. M., & Ibarra, C. (2022). Intestinal mucus-derived metabolites modulate virulence of a clade 8 enterohemorrhagic Escherichia coli O157:H7. *Frontiers in Cellular and Infection Microbiology*, *12*(August), 1–11. https://doi.org/10.3389/fcimb.2022.975173

Garmendia, J., Phillips, A. D., Carlier, M. F., Chong, Y., Schüller, S., Marches, O., Dahan, S., Oswald, E., Shaw, R. K., Knutton, S., & Frankel, G. (2004). TccP is an enterohaemorrhagic Escherichia coli O157:H7 type III effector protein that couples Tir to the actin-cytoskeleton. *Cellular Microbiology*, *6*(12), 1167–1183. https://doi.org/10.1111/j.1462-5822.2004.00459.x

Gaytán, M. O., Martínez-Santos, V. I., Soto, E., & González-Pedrajo, B. (2016). Type three secretion system in attaching and effacing pathogens. *Frontiers in Cellular and Infection Microbiology*, *6*(OCT), 1–25. https://doi.org/10.3389/fcimb.2016.00129

Geng, J., Ni, Q., Sun, W., Li, L., & Feng, X. (2022). The links between gut

microbiota and obesity and obesity related diseases. *Biomedicine and Pharmacotherapy*, *147*(December 2021), 112678. https://doi.org/10.1016/j.biopha.2022.112678

Giannakopoulou, N., Mendis, N., Zhu, L., Gruenheid, S., Faucher, S. P., & Le Moual, H. (2018). The virulence effect of CpxRA in Citrobacter rodentiumIs independent of the auxiliary proteins NlpE and CpxP. *Frontiers in Cellular and Infection Microbiology*, *8*(SEP), 1–12. https://doi.org/10.3389/fcimb.2018.00320

Gigliucci, F., von Meijenfeldt, F. A. B., Knijn, A., Michelacci, V., Scavia, G., Minelli, F., Dutilh, B. E., Ahmad, H. M., Raangs, G. C., Friedrich, A. W., Rossen, J. W. A., & Morabito, S. (2018). Metagenomic characterization of the human intestinal microbiota in faecal samples from STEC-infected patients. *Frontiers in Cellular and Infection Microbiology*, *8*(FEB), 1–12. https://doi.org/10.3389/fcimb.2018.00025

Ginn, J., Jiang, X., Sun, S., Michino, M., Huggins, D. J., Mbambo, Z., Jansen, R., Rhee, K. Y., Arango, N., Lima, C. D., Liverton, N., Imaeda, T., Okamoto, R., Kuroita, T., Aso, K., Stamford, A., Foley, M., Meinke, P. T., Nathan, C., & Bryk, R. (2021). Whole Cell Active Inhibitors of Mycobacterial Lipoamide Dehydrogenase Afford Selectivity over the Human Enzyme through Tight Binding Interactions. *ACS Infectious Diseases*, *7*(2), 435–444. https://doi.org/10.1021/acsinfecdis.0c00788

Gizaw, Z., Demissie, N. G., Gebrehiwot, M., Destaw, B., & Nigusie, A. (2023). Enteric infections and management practices among communities in a rural setting of northwest Ethiopia. *Scientific Reports*, *13*(1), 1–10. https://doi.org/10.1038/s41598-023-29556-2

Göhler, A. K., Kökpinar, Ö., Schmidt-Heck, W., Geffers, R., Guthke, R., Rinas, U., Schuster, S., Jahreis, K., & Kaleta, C. (2011). More than just a metabolic regulator - elucidation and validation of new targets of PdhR in Escherichia coli. *BMC Systems Biology*, *5*. https://doi.org/10.1186/1752-0509-5-197

Golias, T., Kery, M., Radenkovic, S., & Papandreou, I. (2019). Microenvironmental control of glucose metabolism in tumors by

regulation of pyruvate dehydrogenase. *International Journal of Cancer*, *144*(4), 674–686. https://doi.org/10.1002/ijc.31812

Griesenauer, B., Tran, T. M., Fortney, K. R., Janowicz, D. M., Johnson, P., Gao, H., Barnes, S., Wilson, L. S., Liu, Y., & Spinola, S. M. (2019). Determination of an interaction network between an extracellular bacterial pathogen and the human host. *MBio*, *10*(3), 1–15. https://doi.org/10.1128/mBio.01193-19

Gryaznova, M., Dvoretskaya, Y., Burakova, I., Syromyatnikov, M., Popov, E., Kokina, A., Mikhaylov, E., & Popov, V. (2022). Dynamics of Changes in the Gut Microbiota of Healthy Mice Fed with Lactic Acid Bacteria and Bifidobacteria. *Microorganisms*, *10*(5). https://doi.org/10.3390/microorganisms10051020

Guevarra, R. B., Kim, E. S., Cho, J. H., Song, M., Cho, J. H., Lee, J. H., Kim, H., Kim, S., Keum, G. B., Lee, C. H., Cho, W. T., Watthanaphansak, S., & Kim, H. B. (2023). Gut microbial shifts by synbiotic combination of Pediococcus acidilactici and lactulose in weaned piglets challenged with Shiga toxin-producing Escherichia coli. *Frontiers in Veterinary Science*, *9*. https://doi.org/10.3389/fvets.2022.1101869

Higgins, K. (2019). Nickel metalloregulators and chaperones. *Inorganics*, *7*(8), 14–17. https://doi.org/10.3390/inorganics7080104

Ho, N. K., Henry, A. C., Johnson-Henry, K., & Sherman, P. M. (2013). Pathogenicity, host responses and implications for management of enterohemorrhagic Escherichia coli O157:H7 infection. *Canadian Journal of Gastroenterology*, *27*(5), 281–285. https://doi.org/10.1155/2013/138673

Home, J., Authors, F. O. R., & Journal, A. T. H. E. (2014). *Enterohemorrhagic Escherichia coli Pathogenesis and the Host EHEC COLONIZATION AND THE HOST RESPONSE THE ACQUIRED IMMUNE RESPONSE TO EHEC SHIGA TOXIN AND LPS INTERACTIONS WITH*. *119*.

Hopkins, E. G. D., Roumeliotis, T. I., Mullineaux-Sanders, C., Choudhary, J. S., & Frankel, G. (2019). Intestinal epithelial cells and the microbiome

undergo swift reprogramming at the inception of colonic citrobacter rodentium infection. *MBio*, *10*(2), 1–19. https://doi.org/10.1128/MBIO.00062-19

Huerta-Uribe, A., Marjenberg, Z. R., Yamaguchi, N., Fitzgerald, S., Connolly, J. P. R., Carpena, N., Uvell, H., Douce, G., Elofsson, M., Byron, O., Marquez, R., Gally, D. L., & Roe, A. J. (2016). Identification and characterization of novel compounds blocking Shiga toxin expression in Escherichia coli O157:H7. *Frontiers in Microbiology*, *7*(NOV), 1–9. https://doi.org/10.3389/fmicb.2016.01930

Hwang, S. Bin, Chelliah, R., Kang, J. E., Rubab, M., Banan-MwineDaliri, E., Elahi, F., & Oh, D. H. (2021). Role of Recent Therapeutic Applications and the Infection Strategies of Shiga Toxin-Producing Escherichia coli. In *Frontiers in Cellular and Infection Microbiology* (Vol. 11). https://doi.org/10.3389/fcimb.2021.614963

Ibáñez de Aldecoa, A. L., Zafra, O., & González-Pastor, J. E. (2017). Mechanisms and regulation of extracellular DNA release and its biological roles in microbial communities. *Frontiers in Microbiology*, *8*(JUL), 1–19. https://doi.org/10.3389/fmicb.2017.01390

Islam, M. S., Bingle, L. E. H., Pallen, M. J., & Busby, S. J. W. (2011). Organization of the LEE1 operon regulatory region of enterohaemorrhagic Escherichia coli O157:H7 and activation by GrlA. *Molecular Microbiology*, *79*(2), 468–483. https://doi.org/10.1111/j.1365-2958.2010.07460.x

Jimenez, A. G., Ellermann, M., Abbott, W., & Sperandio, V. (2020). Diet-derived galacturonic acid regulates virulence and intestinal colonization in enterohaemorrhagic Escherichia coli and Citrobacter rodentium. *Nature Microbiology*, *5*(2), 368–378. https://doi.org/10.1038/s41564-019-0641-0

Jubelin, G., Desvaux, M., Schüller, S., Etienne-Mesmin, L., Muniesa, M., & Blanquet-Diot, S. (2018). Modulation of enterohaemorrhagic escherichia coli survival and virulence in the human gastrointestinal tract. *Microorganisms*, *6*(4). https://doi.org/10.3390/microorganisms6040115

Kaleta, C., Göhler, A., Schuster, S., Jahreis, K., Guthke, R., & Nikolajewa, S. (2010). Integrative inference of gene-regulatory networks in Escherichia coli using information theoretic concepts and sequence analysis. *BMC Systems Biology*, *4*. https://doi.org/10.1186/1752-0509-4-116

Karpman, D., & Ståhl, A.-L. (2014). Enterohemorrhagic Escherichia coli Pathogenesis and the Host Response . *Microbiology Spectrum*, *2*(5). https://doi.org/10.1128/microbiolspec.ehec-0009-2013

Karygianni, L., Ren, Z., Koo, H., & Thurnheer, T. (2020). Biofilm Matrixome: Extracellular Components in Structured Microbial Communities. *Trends in Microbiology*, *28*(8), 668–681. https://doi.org/10.1016/j.tim.2020.03.016

Kim, J., & Copley, S. D. (2007). Why metabolic enzymes are essential or nonessential for growth of Escherichia coli K12 on glucose. *Biochemistry*, *46*(44), 12501–12511. https://doi.org/10.1021/bi7014629

Kim, S., Covington, A., & Pamer, E. G. (2017). The intestinal microbiota: Antibiotics, colonization resistance, and enteric pathogens. *Immunological Reviews*, *279*(1), 90–105. https://doi.org/10.1111/imr.12563

Kim, Y. G., Lee, J. H., Gwon, G., Kim, S. Il, Park, J. G., & Lee, J. (2016). Essential Oils and Eugenols Inhibit Biofilm Formation and the Virulence of Escherichia coli O157:H7. *Scientific Reports*, *6*(April), 1–11. https://doi.org/10.1038/srep36377

Kitamoto, S., Alteri, C. J., Rodrigues, M., Nagao-Kitamoto, H., Sugihara, K., Himpsl, S. D., Bazzi, M., Miyoshi, M., Nishioka, T., Hayashi, A., Morhardt, T. L., Kuffa, P., Grasberger, H., El-Zaatari, M., Bishu, S., Ishii, C., Hirayama, A., Eaton, K. A., Dogan, B., … Kamada, N. (2020). Dietary l-serine confers a competitive fitness advantage to Enterobacteriaceae in the inflamed gut. *Nature Microbiology*, *5*(1), 116–125. https://doi.org/10.1038/s41564-019-0591-6

Koutsoumanis, K., Allende, A., Alvarez-Ordóñez, A., Bover-Cid, S., Chemaly, M., Davies, R., De Cesare, A., Herman, L., Hilbert, F., Lindqvist, R., Nauta, M., Peixe, L., Ru, G., Simmons, M., Skandamis, P., Suffredini, E.,

Jenkins, C., Monteiro Pires, S., Morabito, S., … Bolton, D. (2020). Pathogenicity assessment of Shiga toxin-producing Escherichia coli (STEC) and the public health risk posed by contamination of food with STEC. *EFSA Journal*, *18*(1), 1–105. https://doi.org/10.2903/j.efsa.2020.5967

Kumar, Aman, V. S. (2019). *Indole Signaling at the Host-Microbiota-Pathogen Interface*. *10*(3).

Kumar, A., Ellermann, M., & Sperandio, V. (2019). Taming the beast: Interplay between gut small molecules and enteric pathogens. *Infection and Immunity*, *87*(9), 1–12. https://doi.org/10.1128/IAI.00131-19

Kumar, A., Russell, R. M., Pifer, R., Menezes-Garcia, Z., Cuesta, S., Narayanan, S., MacMillan, J. B., & Sperandio, V. (2020). The Serotonin Neurotransmitter Modulates Virulence of Enteric Pathogens. *Cell Host and Microbe*, *28*(1), 41-53.e8. https://doi.org/10.1016/j.chom.2020.05.004

Lam, Y. Y., Ha, C. W. Y., Campbell, C. R., Mitchell, A. J., Dinudom, A., Oscarsson, J., Cook, D. I., Hunt, N. H., Caterson, I. D., Holmes, A. J., & Storlien, L. H. (2012). Increased gut permeability and microbiota change associate with mesenteric fat inflammation and metabolic dysfunction in diet-induced obese mice. *PLoS ONE*, *7*(3), 1–10. https://doi.org/10.1371/journal.pone.0034233

Law, R. J., Gur-Arie, L., Rosenshine, I., & Brett Finlay, B. (2013). In vitro and in vivo model systems for studying enteropathogenic Escherichia coli infections. *Cold Spring Harbor Perspectives in Medicine*, *3*(3). https://doi.org/10.1101/cshperspect.a009977

Lazzarino, G., Amorini, A. M., Signoretti, S., Musumeci, G., Lazzarino, G., Caruso, G., Pastore, F. S., Di Pietro, V., Tavazzi, B., & Belli, A. (2019). Pyruvate dehydrogenase and tricarboxylic acid cycle enzymes are sensitive targets of traumatic brain injury induced metabolic derangement. *International Journal of Molecular Sciences*, *20*(22). https://doi.org/10.3390/ijms20225774

Lengeler, J. (1977). Analysis of mutations affecting the dissimilation of galactitol (dulcitol) in Escherichia coli K12. *MGG Molecular & General*

Genetics, *152*(1), 83–91. https://doi.org/10.1007/BF00264944

Lewis, S. B., Cook, V., Tighe, R., & Schüller, S. (2015). Enterohemorrhagic Escherichia coli colonization of human colonic epithelium in vitro and ex vivo. *Infection and Immunity*, *83*(3), 942–949. https://doi.org/10.1128/IAI.02928-14

Li, M., Ho, P. Y., Yao, S., & Shimizu, K. (2006). Effect of sucA or sucC gene knockout on the metabolism in Escherichia coli based on gene expressions, enzyme activities, intracellular metabolite concentrations and metabolic fluxes by 13C-labeling experiments. *Biochemical Engineering Journal*, *30*(3), 286–296. https://doi.org/10.1016/j.bej.2006.05.011

Liu, X., Mao, B., Gu, J., Wu, J., Cui, S., Wang, G., Zhao, J., Zhang, H., & Chen, W. (2021). Blautia—a new functional genus with potential probiotic properties? *Gut Microbes*, *13*(1), 1–21. https://doi.org/10.1080/19490976.2021.1875796

Liu, Y., Li, S., Li, W., Wang, P., Ding, P., Li, L., Wang, J., Yang, P., Wang, Q., Xu, T., Xiong, Y., & Yang, B. (2019). RstA, a two-component response regulator, plays important roles in multiple virulence-associated processes in enterohemorrhagic Escherichia coli O157:H7. *Gut Pathogens*, *11*(1), 1–11. https://doi.org/10.1186/s13099-019-0335-4

Loewa, A., Feng, J. J., & Hedtrich, S. (2023). Human disease models in drug development. *Nature Reviews Bioengineering*, *1*(8), 545–559. https://doi.org/10.1038/s44222-023-00063-3

Maeda, S., Shimizu, K., Kihira, C., Iwabu, Y., Kato, R., Sugimoto, M., Fukiya, S., Wada, M., & Yokota, A. (2017). Pyruvate dehydrogenase complex regulator (PdhR) gene deletion boosts glucose metabolism in Escherichia coli under oxygen-limited culture conditions. *Journal of Bioscience and Bioengineering*, *123*(4), 437–443. https://doi.org/10.1016/j.jbiosc.2016.11.004

Mao, Q., Jiang, J., Wu, X., Ma, Y., Zhang, Y., Zhao, Y., Zhang, Y., & Wang, Q. (2022). Bifunctional alcohol/aldehyde dehydrogenase AdhE controls

phospho-transferase system sugar utilization and virulence gene expression by interacting PtsH in Edwardsiella piscicida. *Microbiological Research*, *260*(December 2021), 127018. https://doi.org/10.1016/j.micres.2022.127018

Mao, X., Gu, C., Ren, M., Chen, D., Yu, B., He, J., Yu, J., Zheng, P., Luo, J., Luo, Y., Wang, J., Tian, G., & Yang, Q. (2018). L-isoleucine administration alleviates rotavirus infection and immune response in the weaned piglet model. *Frontiers in Immunology*, *9*(JUL), 1–12. https://doi.org/10.3389/fimmu.2018.01654

Mao, X., Sun, R., Wang, Q., Chen, D., Yu, B., He, J., Yu, J., Luo, J., Luo, Y., Yan, H., Wang, J., Wang, H., & Wang, Q. (2022). l-Isoleucine Administration Alleviates DSS-Induced Colitis by Regulating TLR4/MyD88/NF-κB Pathway in Rats. *Frontiers in Immunology*, *12*(January), 1–12. https://doi.org/10.3389/fimmu.2021.817583

Martin, P. C. N., & Zabet, N. R. (2020). Dissecting the binding mechanisms of transcription factors to DNA using a statistical thermodynamics framework. *Computational and Structural Biotechnology Journal*, *18*(0), 3590–3605. https://doi.org/10.1016/j.csbj.2020.11.006

McCloskey, D., Xu, S., Sandberg, T. E., Brunk, E., Hefner, Y., Szubin, R., Feist, A. M., & Palsson, B. O. (2018). Growth adaptation of gnd and sdhCB Escherichia coli deletion strains diverges from a similar initial perturbation of the transcriptome. *Frontiers in Microbiology*, *9*(AUG), 1–16. https://doi.org/10.3389/fmicb.2018.01793

McNeil, M. B., Clulow, J. S., Wilf, N. M., Salmond, G. P. C., & Fineran, P. C. (2012). SdhE is a conserved protein required for flavinylation of succinate dehydrogenase in bacteria. *Journal of Biological Chemistry*, *287*(22), 18418–18428. https://doi.org/10.1074/jbc.M111.293803

McWilliams, B. D., & Torres, A. G. (2014). Enterohemorrhagic Escherichia coli Adhesins . *Microbiology Spectrum*, *2*(3). https://doi.org/10.1128/microbiolspec.ehec-0003-2013

Mellies, J. L., Barron, A. M. S., & Carmona, A. M. (2007). Enteropathogenic

and enterohemorrhagic Escherichia coli virulence gene regulation. *Infection and Immunity*, *75*(9), 4199–4210. https://doi.org/10.1128/IAI.01927-06

Mellies, J. L., Barron, A. M. S., Haack, K. R., Korson, A. S., & Oldridge, D. A. (2006). The global regulator Ler is necessary for enteropathogenic Escherichia coli colonization of Caenorhabditis elegans. *Infection and Immunity*, *74*(1), 64–72. https://doi.org/10.1128/IAI.74.1.64-72.2006

Mellies, J. L., & Lorenzen, E. (2014). Enterohemorrhagic Escherichia coli Virulence Gene Regulation. *Microbiology Spectrum*, *2*(4), 1–15. https://doi.org/10.1128/microbiolspec.ehec-0004-2013

Menezes-Garcia, Z., Kumar, A., Zhu, W., Winter, S. E., & Sperandio, V. (2020). L-Arginine sensing regulates virulence gene expression and disease progression in enteric pathogens. *Proceedings of the National Academy of Sciences of the United States of America*, *117*(22), 12387–12393. https://doi.org/10.1073/pnas.1919683117

Menq-Rong Wu, Te-Sen Chou, Ching-Ying Huang, J.-K. H. (2021). A potential probiotic- Lachnospiraceae NK4A136 group: Evidence from the restoration of the dietary pattern from a high-fat diet. *Angewandte Chemie International Edition, 6(11), 951-952.*, 2013–2015. https://doi.org/10.21203/rs.3.rs-48913/v1

Miranda, R. L., Conway, T., Leatham, M. P., Chang, D. E., Norris, W. E., Allen, J. H., Stevenson, S. J., Laux, D. C., & Cohen, P. S. (2004). Glycolytic and Gluconeogenic Growth of Escherichia coli O157:H7 (EDL933) and E. coli K-12 (MG1655) in the Mouse Intestine. *Infection and Immunity*, *72*(3), 1666–1676. https://doi.org/10.1128/IAI.72.3.1666-1676.2004

Moreira, C. G., Russell, R., Mishra, A. A., Narayanan, S., Ritchie, J. M., Waldor, M. K., Curtis, M. M., Winter, S. E., Weinshenker, D., & Sperandio, V. (2016). Bacterial adrenergic sensors regulate virulence of enteric pathogens in the gut. *MBio*, *7*(3). https://doi.org/10.1128/mBio.00826-16

Mullineaux-Sanders, C., Collins, J. W., Ruano-Gallego, D., Levy, M., Pevsner-Fischer, M., Glegola-Madejska, I. T., Sågfors, A. M., Wong, J. L. C., Elinav, E., Crepin, V. F., & Frankel, G. (2017). Citrobacter rodentium Relies on Commensals for Colonization of the Colonic Mucosa. *Cell Reports*, *21*(12), 3381–3389. https://doi.org/10.1016/j.celrep.2017.11.086

Mullineaux-Sanders, C., Kozik, Z., Sanchez-Garrido, J., Hopkins, E. G. D., Choudhary, J. S., & Frankel, G. (2022). Citrobacter rodentium Infection Induces Persistent Molecular Changes and Interferon Gamma-Dependent Major Histocompatibility Complex Class II Expression in the Colonic Epithelium. *MBio*, *13*(1), 1–18. https://doi.org/10.1128/MBIO.03233-21

Mullineaux-Sanders, C., Sanchez-Garrido, J., Hopkins, E. G. D., Shenoy, A. R., Barry, R., & Frankel, G. (2019a). Citrobacter rodentium–host–microbiota interactions: immunity, bioenergetics and metabolism. *Nature Reviews Microbiology*, *17*(11), 701–715. https://doi.org/10.1038/s41579-019-0252-z

Mullineaux-Sanders, C., Sanchez-Garrido, J., Hopkins, E. G. D., Shenoy, A. R., Barry, R., & Frankel, G. (2019b). Citrobacter rodentium–host–microbiota interactions: immunity, bioenergetics and metabolism. *Nature Reviews Microbiology*, *17*(November), 701–715. https://doi.org/10.1038/s41579-019-0252-z

Nguyen, Y., & Sperandio, V. (2012). Enterohemorrhagic E. coli (EHEC) pathogenesis. *Frontiers in Cellular and Infection Microbiology*, *2*(July), 90. https://doi.org/10.3389/fcimb.2012.00090

Nishino, K., Nishida, A., Inoue, R., Kawada, Y., Ohno, M., Sakai, S., Inatomi, O., Bamba, S., Sugimoto, M., Kawahara, M., Naito, Y., & Andoh, A. (2018). Analysis of endoscopic brush samples identified mucosa-associated dysbiosis in inflammatory bowel disease. *Journal of Gastroenterology*, *53*(1), 95–106. https://doi.org/10.1007/s00535-017-1384-4

Njoroge, J. W., Nguyen, Y., Curtis, M. M., Moreira, C. G., & Sperandio, V. (2012). Virulence meets metabolism: Cra and KdpE gene regulation in

enterohemorrhagic Escherichia coli. *MBio*, *3*(5), 2–4. https://doi.org/10.1128/mBio.00280-12

Nobelmann, B., & Lengeler, J. W. (1996). Molecular analysis of the gat genes from Escherichia coli and of their roles in galactitol transport and metabolism. *Journal of Bacteriology*, *178*(23), 6790–6795. https://doi.org/10.1128/jb.178.23.6790-6795.1996

O'Boyle, N., Turner, N. C. A., Roe, A. J., & Connolly, J. P. R. (2020). Plastic Circuits: Regulatory Flexibility in Fine Tuning Pathogen Success. *Trends in Microbiology*, *28*(5), 360–371. https://doi.org/10.1016/j.tim.2020.01.002

Ogasawara, H., Ishida, Y., Yamada, K., Yamamoto, K., & Ishihama, A. (2007). PdhR (pyruvate dehydrogenase complex regulator) controls the respiratory electron transport system in Escherichia coli. *Journal of Bacteriology*, *189*(15), 5534–5541. https://doi.org/10.1128/JB.00229-07

Ogasawara, H., Yamamoto, K., & Ishihama, A. (2011). Role of the biofilm master regulator CsgD in cross-regulation between biofilm formation and flagellar synthesis. *Journal of Bacteriology*, *193*(10), 2587–2597. https://doi.org/10.1128/JB.01468-10

Oliva, G., Sahr, T., & Buchrieser, C. (2018). The life cycle of L. pneumophila: Cellular differentiation is linked to virulence and metabolism. *Frontiers in Cellular and Infection Microbiology*, *8*(JAN), 1–12. https://doi.org/10.3389/fcimb.2018.00003

Pardo-Esté, C., Castro-Severyn, J., Krüger, G. I., Cabezas, C. E., Briones, A. C., Aguirre, C., Morales, N., Baquedano, M. S., Sulbaran, Y. N., Hidalgo, A. A., Meneses, C., Poblete-Castro, I., Castro-Nallar, E., Valvano, M. A., & Saavedra, C. P. (2019). The Transcription Factor ArcA Modulates Salmonella's Metabolism in Response to Neutrophil Hypochlorous Acid-Mediated Stress. *Frontiers in Microbiology*, *10*(December), 1–12. https://doi.org/10.3389/fmicb.2019.02754

Patel, M. S., Nemeria, N. S., Furey, W., & Jordan, F. (2014). The pyruvate dehydrogenase complexes: Structure-based function and regulation. *Journal of Biological Chemistry*, *289*(24), 16615–16623.

https://doi.org/10.1074/jbc.R114.563148

Peterson, L. W., & Artis, D. (2014). Intestinal epithelial cells: Regulators of barrier function and immune homeostasis. *Nature Reviews Immunology*, *14*(3), 141–153. https://doi.org/10.1038/nri3608

Petri, W. A., Miller, M., Binder, H. J., Levine, M. M., Dillingham, R., & Guerrant, R. L. (2008). Enteric infections, diarrhea, and their impact on function and development. *Journal of Clinical Investigation*, *118*(4), 1277–1290. https://doi.org/10.1172/JCI34005

Pickert, G., Neufert, C., Leppkes, M., Zheng, Y., Wittkopf, N., Warntjen, M., Lehr, H. A., Hirth, S., Weigmann, B., Wirtz, S., Ouyang, W., Neurath, M. F., & Becker, C. (2009). STAT3 links IL-22 signaling in intestinal epithelial cells to mucosal wound healing. *Journal of Experimental Medicine*, *206*(7), 1465–1472. https://doi.org/10.1084/jem.20082683

Pifer, R., Russell, R. M., Kumar, A., Curtis, M. M., & Sperandio, V. (2018). Redox, amino acid, and fatty acid metabolism intersect with bacterial virulence in the gut. *Proceedings of the National Academy of Sciences of the United States of America*, *115*(45), E10712–E10719. https://doi.org/10.1073/pnas.1813451115

Quail, M. A., & Guest, J. R. (1995). *of PdhR , the transcriptional repressor of the pdhR-aceEF ~ lpd operon of Escherichia coii*. *15*, 519–529.

Quail, M. A., Haydon, D. J., & Guest, J. R. (1994). The pdhR–aceEF–lpd operon of Escherichia coli expresses the pyruvate dehydrogenase complex. *Molecular Microbiology*, *12*(1), 95–104. https://doi.org/10.1111/j.1365-2958.1994.tb00998.x

Rahal, E. A., Kazzi, N., Nassar, F. J., & Matar, G. M. (2012). Escherichia coli O157:H7-Clinical aspects and novel treatment approaches. *Frontiers in Cellular and Infection Microbiology*, *2*(November), 138. https://doi.org/10.3389/fcimb.2012.00138

Rajendran, N., & Marahiel, M. A. (1999). Multifunctional Peptide Synthetases Required for Nonribosomal Biosynthesis of Peptide Antibiotics. *Comprehensive Natural Products Chemistry*, 195–220.

https://doi.org/10.1016/b978-0-08-091283-7.00094-1

Rajilić-Stojanović, M., Biagi, E., Heilig, H. G. H. J., Kajander, K., Kekkonen, R. A., Tims, S., & De Vos, W. M. (2011). Global and deep molecular analysis of microbiota signatures in faecal samples from patients with irritable bowel syndrome. *Gastroenterology*, *141*(5), 1792–1801. https://doi.org/10.1053/j.gastro.2011.07.043

Rashighi, M., & Harris, J. E. (2017). 乳鼠心肌提取 HHS Public Access. *Physiology & Behavior*, *176*(3), 139–148. https://doi.org/10.1053/j.gastro.2016.08.014.CagY

Reimand, J., Isser, R., Voisin, V., Kucera, M., Tannus-lopes, C., Rostamianfar, A., Wadi, L., Meyer, M., Wong, J., & Xu, C. (2019). Pathway enrichment analysis and visualization of omics data using g:Profiler, GSEA, Cytoscape and EnrichmentMap-ZLO FAJN ČLANEK, TUDI RAZLAGE POSAMEZNIH TERMINOV. *Nat Protoc*, *14*(6), 1–8. https://doi.org/10.1038/s41596-018-0103-9.Pathway

Rigali, S., Derouaux, A., Giannotta, F., & Dusart, J. (2002). Subdivision of the helix-turn-helix GntR family of bacterial regulators in the FadR, HutC, MocR, and YtrA subfamilies. *Journal of Biological Chemistry*, *277*(15), 12507–12515. https://doi.org/10.1074/jbc.M110968200

Robinson, M. D., McCarthy, D. J., & Smyth, G. K. (2009). edgeR: A Bioconductor package for differential expression analysis of digital gene expression data. *Bioinformatics*, *26*(1), 139–140. https://doi.org/10.1093/bioinformatics/btp616

Roe, A. J., Yull, H., Naylor, S. W., Woodward, M. J., Smith, D. G. E., & Gally, D. L. (2003). Heterogeneous Surface Expression of EspA Translocon Filaments by. *Society*, *71*(10), 5900–5909. https://doi.org/10.1128/IAI.71.10.5900

Rojas-Lopez, M., Monterio, R., Pizza, M., Desvaux, M., & Rosini, R. (2018). Intestinal pathogenic Escherichia coli: Insights for vaccine development. *Frontiers in Microbiology*, *9*(MAR), 1–17. https://doi.org/10.3389/fmicb.2018.00440

Rother, M., Gonzalez, E., Teixeira da Costa, A. R., Wask, L., Gravenstein, I., Pardo, M., Pietzke, M., Gurumurthy, R. K., Angermann, J., Laudeley, R., Glage, S., Meyer, M., Chumduri, C., Kempa, S., Dinkel, K., Unger, A., Klebl, B., Klos, A., & Meyer, T. F. (2018). Combined Human Genome-wide RNAi and Metabolite Analyses Identify IMPDH as a Host-Directed Target against Chlamydia Infection. *Cell Host and Microbe*, *23*(5), 661-671.e8. https://doi.org/10.1016/j.chom.2018.04.002

Rowley, C. A., Sauder, A. B., & Kendall, M. M. (2020). The Ethanolamine-Sensing Transcription Factor EutR Promotes Virulence and Transmission during Citrobacter rodentiumIntestinal Infection. *Infection and Immunity*, *88*(9), e00137-20.

Sandu, P., Crepin, V. F., Drechsler, H., McAinsh, A. D., Frankel, G., & Berger, C. N. (2017). The enterohemorrhagic Escherichia coli effector EspW triggers actin remodeling in a Rac1- dependent manner. *Infection and Immunity*, *85*(9), 30–32. https://doi.org/10.1128/IAI.00244-17

Santos, F. F., Yamamoto, D., Abe, C. M., Bryant, J. A., Hernandes, R. T., Kitamura, F. C., Castro, F. S., Valiatti, T. B., Piazza, R. M. F., Elias, W. P., Henderson, I. R., & Gomes, T. A. T. (2019). The Type III Secretion System (T3SS)-Translocon of Atypical Enteropathogenic Escherichia coli (aEPEC) Can Mediate Adherence. *Frontiers in Microbiology*, *10*(July), 1–13. https://doi.org/10.3389/fmicb.2019.01527

Sarkar, D., Siddiquee, K. A. Z., Araúzo-Bravo, M. J., Oba, T., & Shimizu, K. (2008). Effect of cra gene knockout together with edd and iclR genes knockout on the metabolism in Escherichia coli. *Archives of Microbiology*, *190*(5), 559–571. https://doi.org/10.1007/s00203-008-0406-2

Schierova, D., Roubalova, R., Kolar, M., Stehlikova, Z., Rob, F., Jackova, Z., Coufal, S., Thon, T., Mihula, M., Modrak, M., Kverka, M., Bajer, L., Kostovcikova, K., Drastich, P., Hercogova, J., Novakova, M., Vasatko, M., Lukas, M., Tlaskalova-Hogenova, H., & Zakostelska, Z. J. (2021). Faecal microbiome changes and specific anti-bacterial response in patients with ibd during anti-tnf therapy. *Cells*, *10*(11). https://doi.org/10.3390/cells10113188

Schinner, S. A. C., Mokszycki, M. E., Adediran, J., Leatham-Jensen, M., Conway, T., & Cohen, P. S. (2015). Escherichia coli EDL933 requires gluconeogenic nutrients to successfully colonize the intestines of streptomycin-treated mice precolonized with E. coli Nissle 1917. *Infection and Immunity*, *83*(5), 1983–1991. https://doi.org/10.1128/IAI.02943-14

Schutte, K. M., Fisher, D. J., Burdick, M. D., Mehrad, B., Mathers, A. J., Mann, B. J., Nakamoto, R. K., & Hughes, M. A. (2015). Escherichia coli pyruvate dehydrogenase complex is an important component of CXCL10-mediated antimicrobial activity. *Infection and Immunity*, *84*(1), 320–328. https://doi.org/10.1128/IAI.00552-15

Seager, S. L., & Slabaugh, M. R. (2015). *Fatty Acids 5 6*. https://doi.org/10.1016/B978-0-12-387784-0.00005-5

Segata, N., Izard, J., Waldron, L., Gevers, D., Miropolsky, L., Garrett, W. S., & Huttenhower, C. (2011). Metagenomic biomarker discovery and explanation. *Genome Biology*, *12*(6), R60. https://doi.org/10.1186/gb-2011-12-6-r60

Segura, A., Bertin, Y., Durand, A., Benbakkar, M., & Forano, E. (2021). Transcriptional analysis reveals specific niche factors and response to environmental stresses of enterohemorrhagic Escherichia coli O157:H7 in bovine digestive contents. *BMC Microbiology*, *21*(1), 1–16. https://doi.org/10.1186/s12866-021-02343-7

Serovar, S. (2017). *crossm Genetic Characterization of the Galactitol Utilization Pathway of*. *199*(4), 1–16.

Shames, S. R., Deng, W., Guttman, J. A., de Hoog, C. L., Li, Y., Hardwidge, P. R., Sham, H. P., Vallance, B. A., Foster, L. J., & Finlay, B. B. (2010). The pathogenic E. coli type III effector EspZ interacts with host CD98 and facilitates host cell prosurvival signalling. *Cellular Microbiology*, *12*(9), 1322–1339. https://doi.org/10.1111/j.1462-5822.2010.01470.x

Sharp, F. C., & Sperandio, V. (2007). QseA directly activates transcription of LEE1 in enterohemorrhagic Escherichia coli. *Infection and Immunity*,

75(5), 2432–2440. https://doi.org/10.1128/IAI.02003-06

Singh, G., Nahirniak, S., Lamarche, Y., & Fan, E. (2020). *Since January 2020 Elsevier has created a COVID-19 resource centre with free information in English and Mandarin on the novel coronavirus COVID- company ' s public news and information website . Elsevier hereby grants permission to make all its COVID-19-r. January*.

Singh, P. K., Serrano, E., Ramachandran, G., Miguel-Arribas, A., Gago-Cordoba, C., Val-Calvo, J., López-Pérez, A., Alfonso, C., Wu, L. J., Luque-Ortega, J. R., & Meijer, W. J. J. (2020). Reversible regulation of conjugation of Bacillus subtilis plasmid pLS20 by the quorum sensing peptide responsive anti-repressor RappLS20. *Nucleic Acids Research*, *48*(19), 10785–10801. https://doi.org/10.1093/nar/gkaa797

Sistrunk, J. R., Nickerson, K. P., Chanin, R. B., Rasko, D. A., & Faherty, C. S. (2016). Survival of the fittest: How bacterial pathogens utilize bile to enhance infection. *Clinical Microbiology Reviews*, *29*(4), 819–836. https://doi.org/10.1128/CMR.00031-16

Su, Y. bin, Peng, B., Li, H., Cheng, Z. xue, Zhang, T. tuo, Zhu, J. xin, Li, D., Li, M. yi, Ye, J. zhou, Du, C. chao, Zhang, S., Zhao, X. liang, Yang, M. jun, & Peng, X. X. (2018). Pyruvate cycle increases aminoglycoside efficacy and provides respiratory energy in bacteria. *Proceedings of the National Academy of Sciences of the United States of America*, *115*(7), E1578–E1587. https://doi.org/10.1073/pnas.1714645115

Suvorova, I. A., Korostelev, Y. D., & Gelfand, M. S. (2015). GntR Family of Bacterial Transcription Factors and Their DNA Binding Motifs: Structure, Positioning and Co-Evolution. *PLoS ONE*, *10*(7 July), 1–21. https://doi.org/10.1371/journal.pone.0132618

Sweeney, N. J., Laux, D. C., & Cohen, P. S. (1996). Escherichia coli F-18 and E. coli K-12 eda mutants do not colonize the streptomycin-treated mouse large intestine. *Infection and Immunity*, *64*(9), 3504–3511. https://doi.org/10.1128/iai.64.9.3504-3511.1996

Takahashi, M., Taguchi, H., Yamaguchi, H., Osaki, T., Komatsu, A., & Kamiya,

S. (2004). The effect of probiotic treatment with Clostridium butyricum on enterohemorrhagic Escherichia coli O157:H7 infection in mice. *FEMS Immunology and Medical Microbiology*, *41*(3), 219–226. https://doi.org/10.1016/j.femsim.2004.03.010

Thorpe, C. M., Hurley, B. P., Lincicome, L. L., Jacewicz, M. S., Keusch, G. T., & Acheson, D. W. K. (1999). Shiga toxins stimulate secretion of interleukin-8 from intestinal epithelial cells. *Infection and Immunity*, *67*(11), 5985–5993. https://doi.org/10.1128/iai.67.11.5985-5993.1999

Thorpe, C. M., Smith, W. E., Hurley, B. P., & Acheson, D. W. K. (2001). Shiga toxins induce, superinduce, and stabilize a variety of C-X-C chemokine mRNAs in intestinal epithelial cells, resulting in increased chemokine expression. *Infection and Immunity*, *69*(10), 6140–6147. https://doi.org/10.1128/IAI.69.10.6140-6147.2001

Toledo, C. C., Rogers, T. J., Svensson, M., Tati, R., Fischer, H., Svanborg, C., & Karpman, D. (2008). Shiga toxin-mediated disease in MyD88-deficient mice infected with Escherichia coli O157:H7. *American Journal of Pathology*, *173*(5), 1428–1439. https://doi.org/10.2353/ajpath.2008.071218

Turner, N. C. A., Connolly, J. P. R., & Roe, A. J. (2018). Control freaks—signals and cues governing the regulation of virulence in attaching and effacing pathogens. *Biochemical Society Transactions*, *47*(1), 229–238. https://doi.org/10.1042/BST20180546

Vacca, M., Celano, G., Calabrese, F. M., Portincasa, P., Gobbetti, M., & Angelis, M. De. (2020). *The Controversial Role of Human Gut Lachnospiraceae*. 1–25.

van Dierendonck, X. A. M. H., Vrieling, F., Smeehuijzen, L., Deng, L., Boogaard, J. P., Croes, C. A., Temmerman, L., Wetzels, S., Biessen, E., Kersten, S., & Stienstra, R. (2022). Triglyceride breakdown from lipid droplets regulates the inflammatory response in macrophages. *Proceedings of the National Academy of Sciences of the United States of America*, *119*(12). https://doi.org/10.1073/pnas.2114739119

van Doorn, C. L. R., Schouten, G. K., van Veen, S., Walburg, K. V., Esselink, J. J., Heemskerk, M. T., Vrieling, F., & Ottenhoff, T. H. M. (2021). Pyruvate Dehydrogenase Kinase Inhibitor Dichloroacetate Improves Host Control of Salmonella enterica Serovar Typhimurium Infection in Human Macrophages. *Frontiers in Immunology*, *12*(September), 1–17. https://doi.org/10.3389/fimmu.2021.739938

Wale, K. R., Cottam, C., Connolly, J. P., & Roe, A. J. (2021). Transcriptional and metabolic regulation of EHEC and Citrobacter rodentium pathogenesis. *Current Opinion in Microbiology*, *63*, 70–75. https://doi.org/10.1016/j.mib.2021.06.002

Waligora, E. A., Fisher, C. R., Hanovice, N. J., Rodou, A., Wyckoff, E. E., & Payne, S. M. (2014). Role of intracellular carbon metabolism pathways in Shigella flexneri virulence. *Infection and Immunity*, *82*(7), 2746–2755. https://doi.org/10.1128/IAI.01575-13

Wang, J., Gu, X., Yang, J., Wei, Y., & Zhao, Y. (2019). Gut Microbiota Dysbiosis and Increased Plasma LPS and TMAO Levels in Patients With Preeclampsia. *Frontiers in Cellular and Infection Microbiology*, *9*(December), 1–11. https://doi.org/10.3389/fcimb.2019.00409

Weigel, W. A., & Demuth, D. R. (2016). QseBC, a two-component bacterial adrenergic receptor and global regulator of virulence in Enterobacteriaceae and Pasteurellaceae. *Molecular Oral Microbiology*, *31*(5), 379–397. https://doi.org/10.1111/omi.12138

Wiles, S., Clare, S., Harker, J., Huett, A., Young, D., Dougan, G., & Frankel, G. (2004). Organ specificity, colonization and clearance dynamics in vivo following oral challenges with the murine pathogen Citrobacter rodentium. *Cellular Microbiology*, *6*(10), 963–972. https://doi.org/10.1111/j.1462-5822.2004.00414.x

Wong, A. R. C., Pearson, J. S., Bright, M. D., Munera, D., Robinson, K. S., Lee, S. F., Frankel, G., & Hartland, E. L. (2011). Enteropathogenic and enterohaemorrhagic Escherichia coli: Even more subversive elements. *Molecular Microbiology*, *80*(6), 1420–1438. https://doi.org/10.1111/j.1365-2958.2011.07661.x

Woodward, S. E., Krekhno, Z., & Finlay, B. B. (2019). Here, there, and everywhere: How pathogenic Escherichia coli sense and respond to gastrointestinal biogeography. *Cellular Microbiology*, *21*(11), 1–15. https://doi.org/10.1111/cmi.13107

Wotzka, S. Y., Kreuzer, M., Maier, L., Zünd, M., Schlumberger, M., Nguyen, B., Fox, M., Pohl, D., Heinrich, H., Rogler, G., Biedermann, L., Scharl, M., Sunagawa, S., Hardt, W. D., & Misselwitz, B. (2018). Microbiota stability in healthy individuals after single-dose lactulose challenge—A randomized controlled study. *PLoS ONE*, *13*(10), 1–25. https://doi.org/10.1371/journal.pone.0206214

Yang, W., Sun, H., Yan, J., Kang, C., Wu, J., & Yang, B. (2023). Enterohemorrhagic Escherichia coli senses microbiota-derived nicotinamide to increase its virulence and colonization in the large intestine. *Cell Reports*, *42*(6), 112638. https://doi.org/10.1016/j.celrep.2023.112638

Yimga, M. T., Leatham, M. P., Allen, J. H., Laux, D. C., Conway, T., & Cohen, P. S. (2006). Role of gluconeogenesis and the tricarboxylic acid cycle in the virulence of Salmonella enterica serovar typhimurium in BALB/c mice. *Infection and Immunity*, *74*(2), 1130–1140. https://doi.org/10.1128/IAI.74.2.1130-1140.2006

Youssef, O., Lahti, L., Kokkola, A., Karla, T., Tikkanen, M., Ehsan, H., Carpelan-Holmström, M., Koskensalo, S., Böhling, T., Rautelin, H., Puolakkainen, P., Knuutila, S., & Sarhadi, V. (2018). Stool Microbiota Composition Differs in Patients with Stomach, Colon, and Rectal Neoplasms. *Digestive Diseases and Sciences*, *63*(11), 2950–2958. https://doi.org/10.1007/s10620-018-5190-5

Zambelloni, R., Connolly, J. P. R., Huerta Uribe, A., Burgess, K., Marquez, R., & Roe, A. J. (2017). Novel compounds targeting the enterohemorrhagic Escherichia coli type three secretion system reveal insights into mechanisms of secretion inhibition. *Molecular Microbiology*, *105*(4), 606–619. https://doi.org/10.1111/mmi.13719

Zhang, Z. J., Qu, H. L., Zhao, N., Wang, J., Wang, X. Y., Hai, R., & Li, B.

(2021). Assessment of Causal Direction Between Gut Microbiota and Inflammatory Bowel Disease: A Mendelian Randomization Analysis. *Frontiers in Genetics*, *12*(February), 1–7. https://doi.org/10.3389/fgene.2021.631061

Zheng, Meiying, Cooper, D. R., Grossoehme, N. E., Yu, M., Hung, L. W., Cieslik, M., Derewenda, U., Lesley, S. A., Wilson, I. A., Giedroc, D. P., & Derewenda, Z. S. (2009). Structure of Thermotoga maritima TM0439: Implications for the mechanism of bacterial GntR transcription regulators with Zn2+-binding FCD domains. *Acta Crystallographica Section D: Biological Crystallography*, *65*(4), 356–365. https://doi.org/10.1107/S0907444909004727

Zheng, Mengyu, Han, R., Yuan, Y., Xing, Y., Zhang, W., Sun, Z., Liu, Y., Li, J., & Mao, T. (2023). The role of Akkermansia muciniphila in inflammatory bowel disease: Current knowledge and perspectives. *Frontiers in Immunology*, *13*(January), 1–19. https://doi.org/10.3389/fimmu.2022.1089600

Zheng, Y., Valdez, P. A., Danilenko, D. M., Hu, Y., Sa, S. M., Gong, Q., Abbas, A. R., Modrusan, Z., Ghilardi, N., De Sauvage, F. J., & Ouyang, W. (2008). Interleukin-22 mediates early host defense against attaching and effacing bacterial pathogens. *Nature Medicine*, *14*(3), 282–289. https://doi.org/10.1038/nm1720

Appendix A: BIOLOG phenotype microarray

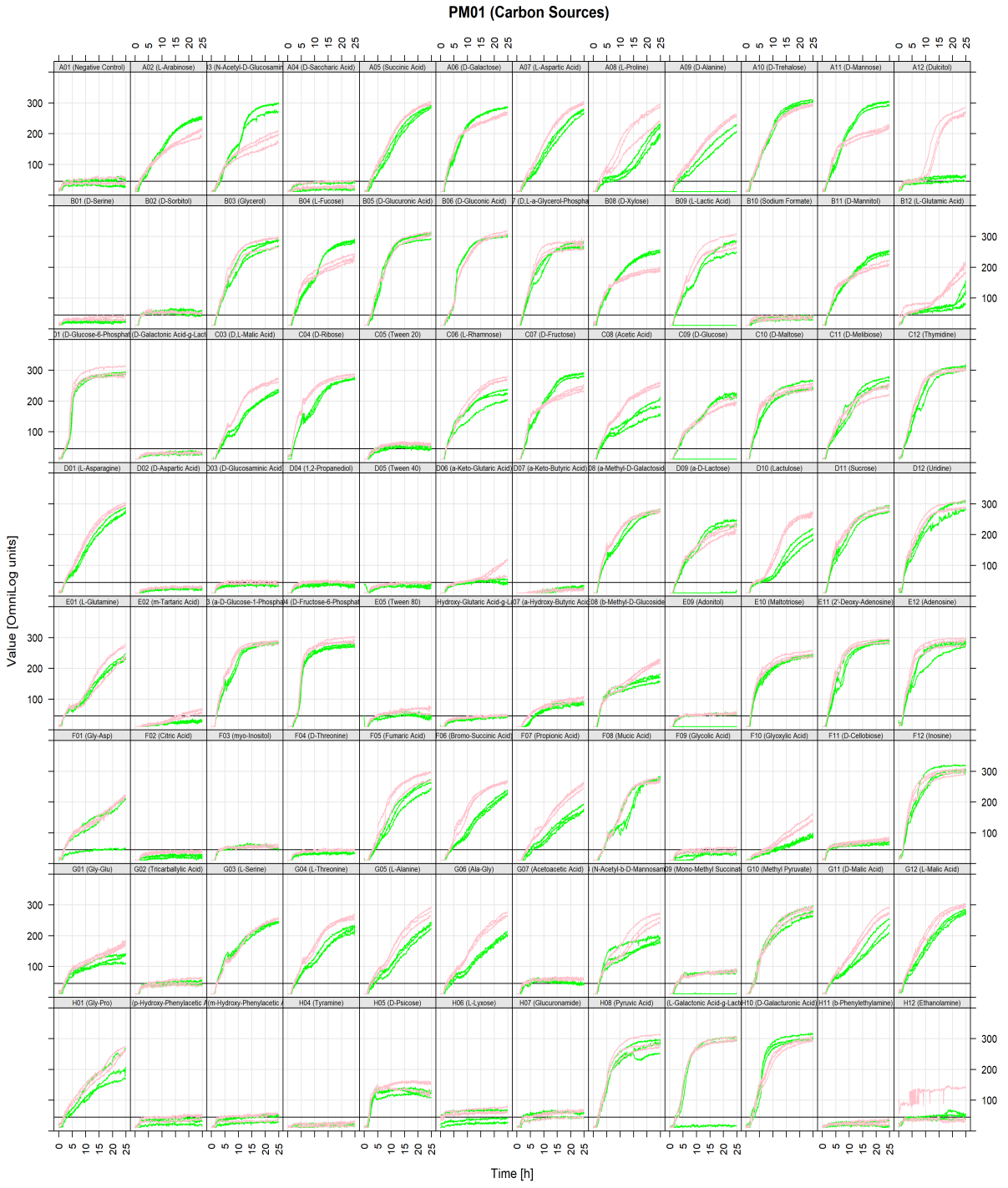

S Figure 1-1. BIOLOG phenotype microarray results of WT strain vs. Δ*pdhR* strain on plate PM1 showing less variation among carbon sources.

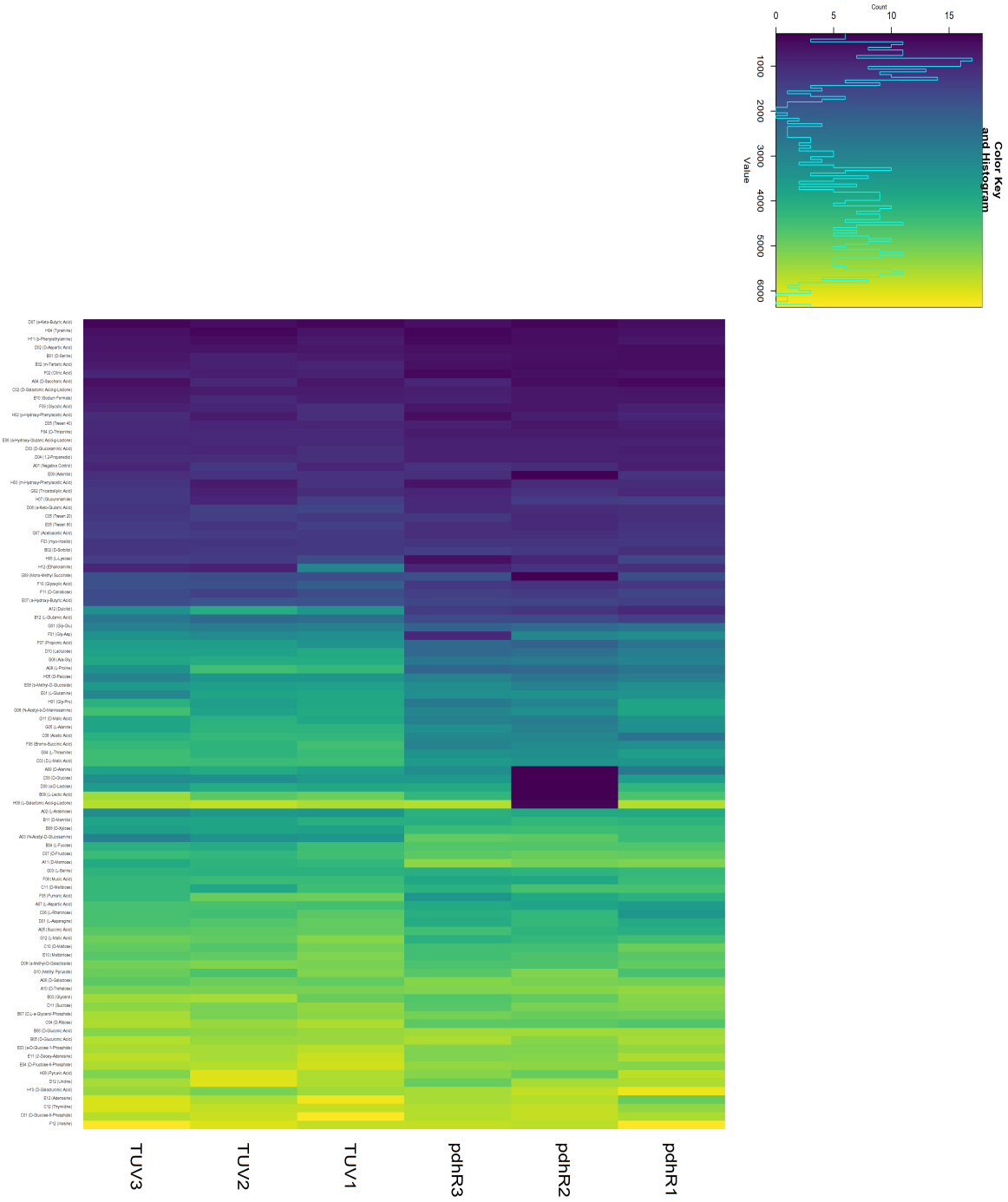

S Figure 1-2. Heatmap showing BIOLOG phenotype microarray results of WT strain vs. Δ*pdhR* strain on plate PM1 showing less variation among carbon sources.

Table S 1 Effect of pdhR deletion on growth

Strain	LB [h^{-1}]	MEM + 0.2% Succinate [h^{-1}]
EHEC	1.24 ± 0.01	1.94 ± 0.02
Δ*pdhR*	1.23 ± 0.02	1.95 ± 0.02
pdhR:pΔ*pdhR*	1.25 ± 0.07	1.96 ± 0.01

Strains were grown in rich medium (LB) and minimal medium (MM) supplied with 0.2% succinate as carbon source. The growth rate was determined in the logarithmic phase.

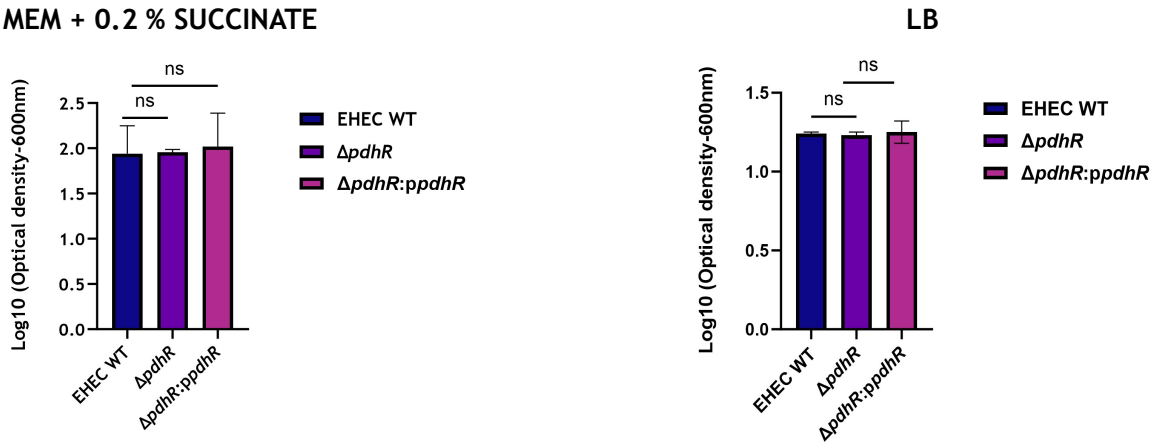

S Fig. 1-3. Effect of pdhR deletion on growth. No significant difference (P > 0.05, Student's t test) from the WT grown with the media indicated.

Appendix B: Differentially expressed genes. *pdhR* mutant vs EHEC

Table S 2_Up_sig_genes. *pdhR* mutant vs EHEC

ID	Foldchange	- Log fold change	p.value	p.adj
ddpX	205.1454982	7.680503686	5.743E-227	4.889E-224
ddpA	168.6077321	7.397526888	1.387E-301	3.543E-298
csiD	100.4672849	6.650581984	1.059E-94	1.151E-92
yhdX	97.41216112	6.606029987	3.892E-192	1.169E-189
argT	91.75572276	6.519726236	1.581E-215	7.34E-213
astA	82.67890061	6.3694473	1.171E-223	8.544E-221
aceB	75.46243041	6.237686661	1.971E-241	2.517E-238
aceA	74.92372798	6.22735078	3.015E-244	5.133E-241
rutE	72.09463014	6.171819901	4.523E-195	1.54E-192
yhdY	71.34536158	6.156747733	2.33E-220	1.487E-217
rutD	68.92171997	6.1068868	1.381E-234	1.411E-231
rutF	66.97150522	6.065475489	7.222E-219	3.689E-216
astD	61.98340186	5.953810032	7.625E-201	2.996E-198
astC	56.45583003	5.819050666	6.745E-219	3.689E-216
rutC	52.02379588	5.701099763	5.381E-156	1.057E-153
amtB	46.39403806	5.535867516	2.078E-193	6.634E-191
glnK	46.01414721	5.524005586	6.325E-171	1.346E-168
yhdZ	45.99190722	5.52330812	2.138E-179	4.964E-177
rutB	45.34107224	5.502746604	1.272E-191	3.608E-189
rutG	44.14413887	5.464149995	2.021E-180	4.917E-178
rutA	41.95787563	5.390869729	2.23E-212	9.493E-210
potF	41.64294704	5.380000266	4.233E-165	8.649E-163
astB	41.07232748	5.360094799	1.127E-183	2.878E-181
ddpB	37.06332845	5.211920543	2.22E-107	2.907E-105
astE	35.52224737	5.150650954	6.564E-155	1.242E-152
codB	30.59142086	4.935055211	1.7713E-76	1.4833E-74
nac	30.50717252	4.931076569	4.664E-177	1.036E-174

purL	25.3996704	4.666737871	5.75E-95	6.4624E-93
gabT	24.77301483	4.630697547	2.109E-129	3.591E-127
adeP	24.31998476	4.604070419	9.444E-117	1.419E-114
purM	23.68802806	4.566086199	1.136E-110	1.612E-108
cbl	23.59852823	4.560624981	3.499E-153	6.382E-151
gabD	22.97200524	4.521804891	5.74E-125	9.163E-123
purH	22.93502908	4.519480832	8.599E-126	1.417E-123
potG	22.4994223	4.491816054	6.956E-107	8.883E-105
ghxP	21.91224027	4.453665086	6.478E-100	7.8787E-98
asnB	21.21361608	4.406918659	4.177E-101	5.204E-99
aceK	21.02383231	4.393953769	2.052E-131	3.614E-129
carA	20.10090153	4.329188303	1.3676E-89	1.3697E-87
purE	19.79352202	4.30695644	9.1279E-90	9.5154E-88
xanP	19.78362285	4.306234737	5.8197E-95	6.4624E-93
lhgO	18.61524991	4.21841308	1.622E-107	2.181E-105
purK	17.81125766	4.154717484	5.1245E-97	6.0875E-95
zraP	17.25074068	4.108586402	4.7018E-56	2.555E-54
hypA_1	17.01988129	4.089149069	3.5255E-23	8.8276E-22
hycA	16.15646707	4.014039854	4.5939E-10	4.4782E-09
gabP	14.73714337	3.881384996	5.0577E-67	3.6387E-65
iclR	14.05202672	3.81270632	2.927E-108	4.041E-106
potH	13.86648645	3.793530372	8.4306E-65	5.7418E-63
purF	13.77093884	3.783555014	5.7881E-68	4.2849E-66
fdhF	13.15392956	3.717421945	4.9427E-85	4.6754E-83
espL4	13.0110285	3.701663104	4.9976E-18	1.013E-16
cvpA	12.58035024	3.653100183	1.3981E-67	1.0202E-65
yqeB	12.15738135	3.603760606	1.6431E-51	8.1483E-50
ddpD	11.85958647	3.5679818	3.1826E-72	2.622E-70
mglA	11.82865088	3.56421363	8.0954E-16	1.4612E-14
rtcB	11.81622042	3.562696738	3.6189E-50	1.7439E-48
ddpC	11.80486386	3.561309498	1.1798E-58	7.0072E-57

ygjG	11.74113955	3.553500533	3.6772E-95	4.2689E-93
pyrB	11.53517289	3.527967722	3.8435E-50	1.8348E-48
pncC	11.49340728	3.52273465	2.191E-60	1.3817E-58
hisJ	11.2940993	3.497497315	4.3414E-82	3.8905E-80
pyrD	10.93930639	3.451449362	1.8075E-69	1.3989E-67
tesB	10.91132449	3.447754331	3.01E-111	4.393E-109
pyrC	10.8083437	3.434073553	1.7959E-83	1.6381E-81
hisP	10.43567452	3.383451948	2.6844E-85	2.5872E-83
nagE	10.39130367	3.377304757	2.7089E-92	2.8827E-90
hycB	10.12466109	3.339801711	2.4133E-09	2.1513E-08
glnA	10.10832695	3.337472328	1.2568E-69	9.8768E-68
purT	10.10691831	3.337271269	8.3008E-55	4.2829E-53
aceE	10.05787778	3.330254022	2.5932E-80	2.2838E-78
aceF	9.762054833	3.287184855	7.1992E-78	6.2328E-76
carB	9.558077662	3.25672049	1.4742E-57	8.1853E-56
hypB	9.244610252	3.208612498	1.4132E-48	6.5624E-47
glnH	9.029181965	3.174595287	4.9163E-68	3.693E-66
purD	8.999603765	3.169861484	2.7965E-58	1.6232E-56
pyrI	8.923069357	3.157540054	1.2701E-36	4.7357E-35
ygeW	8.605614699	3.105278248	4.592E-22	1.1117E-20
hypC	8.596604197	3.103766884	8.4158E-14	1.2533E-12
hisQ	8.430806783	3.075670696	4.4647E-58	2.534E-56
hisM	8.422400247	3.074231436	2.2187E-63	1.4912E-61
lpdA	8.302067011	3.053470577	4.4132E-69	3.3645E-67
gcvT	8.093993104	3.01685162	3.3001E-58	1.8941E-56
purC	8.01584984	3.002855483	6.8097E-65	4.7005E-63
uraA	7.988876589	2.997992643	1.6008E-41	6.578E-40
yeaG	7.647733224	2.935032199	1.4189E-66	1.0066E-64
glnL	7.639196024	2.933420812	3.5111E-60	2.1608E-58
ygjH	7.517623	2.910276568	3.3867E-14	5.3228E-13
xdhA	7.487515505	2.904487085	6.4562E-44	2.7031E-42

hypD	7.484379682	2.903882748	3.0399E-24	7.9224E-23
glnQ	7.450023231	2.897244924	6.83E-61	4.3609E-59
gcvH	7.322489429	2.872334205	3.3912E-60	2.1125E-58
gcvP	7.220964503	2.85219155	8.8934E-59	5.3444E-57
xdhB	7.035705657	2.814695128	6.9438E-17	1.3137E-15
potI	7.027836445	2.813080617	2.2298E-56	1.2247E-54
purB	7.002803085	2.80793252	1.5013E-58	8.8143E-57
hycC	6.821866806	2.770166587	2.8448E-12	3.5988E-11
nanA	6.808783023	2.767396959	1.97E-34	7.1876E-33
livJ	6.155318785	2.621833576	8.3628E-30	2.7208E-28
tsgA	6.082830612	2.60474283	1.5769E-47	7.0655E-46
glnP	5.937283989	2.569803121	6.1632E-56	3.3139E-54
ydcV	5.869869225	2.553328362	8.5141E-10	7.9506E-09
chaC	5.639837816	2.495653676	2.8535E-55	1.4873E-53
yeaH	5.623667049	2.491511182	3.7343E-51	1.8166E-49
glnG	5.585037228	2.481566897	3.5466E-31	1.1997E-29
plaP	5.57305043	2.478467208	3.315E-46	1.435E-44
purN	5.534881825	2.468552514	6.5576E-39	2.4997E-37
upp	5.522746607	2.465385936	1.1173E-52	5.6508E-51
guaB	5.319446695	2.411276191	1.0645E-55	5.6641E-54
mglB	5.203179096	2.379393366	2.5002E-17	4.9118E-16
guaD	5.201391893	2.37889774	1.9511E-42	8.1027E-41
ydcS	5.013521969	2.325824444	1.9323E-20	4.4261E-19
ydcT	4.926339665	2.300516103	8.6565E-13	1.1545E-11
hycD	4.743819503	2.246049118	9.3523E-06	4.8647E-05
tnaA	4.728015506	2.241234767	1.6611E-14	2.6936E-13
ghoS_2	4.673574933	2.224526525	0.02040172	0.04908713
gltI	4.645084252	2.215704764	4.1524E-39	1.6191E-37
abgR	4.628926509	2.210677658	2.3284E-39	9.1902E-38
codA	4.50089967	2.170213406	5.2039E-21	1.2249E-19
gltL	4.473460563	2.161391298	2.2944E-32	8.0273E-31

ychN	4.4521895	2.154515	1.6771E-20	3.8764E-19
pqqL	4.436901269	2.14955245	1.3897E-32	4.9295E-31
putA	4.43460815	2.148806631	1.8429E-34	6.7724E-33
yqgB	4.363080409	2.125347062	2.0088E-05	9.7443E-05
ndk	4.3477021	2.120253092	2.0142E-25	5.4437E-24
yedL	4.29194479	2.101631518	3.974E-27	1.1534E-25
hyi	4.277785445	2.096864125	0.00682076	0.01899696
fiu	4.258276695	2.090269697	5.7126E-28	1.7578E-26
ompF	4.196770845	2.069279691	2.2295E-23	5.61E-22
rclR	4.052842223	2.018934012	0.0010293	0.00357421
ilvB	4.042401255	2.015212533	2.2369E-31	7.6172E-30
uacT	4.022199846	2.007984765	4.5737E-07	3.0262E-06
putP	4.015163643	2.005458788	1.5108E-27	4.5129E-26
prpC	4.013669836	2.004921946	2.1463E-06	1.2733E-05
ilvN_2	3.994249662	1.997924512	2.9873E-12	3.7584E-11
emrA	3.980648039	1.993003317	8.2295E-26	2.2971E-24
gpt	3.96292974	1.98656739	4.3825E-29	1.3991E-27
purR	3.956019772	1.984049637	2.3389E-39	9.1902E-38
acrS	3.944683967	1.979909722	0.01523617	0.03814278
prpD	3.944615274	1.979884598	4.6927E-09	4.0766E-08
yeeO	3.930120123	1.974573409	5.8258E-37	2.1881E-35
ynfM	3.883631923	1.957406474	1.3217E-27	4.0186E-26
rhaM	3.808951632	1.929393968	0.02325973	0.05477671
nupC	3.783296344	1.919643787	1.8066E-30	6.0316E-29
ydiY	3.723169561	1.896531321	2.8082E-34	1.0173E-32
ygeY	3.698948615	1.887115259	1.5877E-15	2.816E-14
ydjY	3.642500382	1.864929123	1.0157E-07	7.4545E-07
leuA	3.622256581	1.856888743	1.2965E-25	3.5796E-24
psuG	3.607629027	1.851050994	0.00420475	0.01240062
ygfK	3.53173465	1.820376953	7.1765E-12	8.605E-11
gltK	3.526096967	1.818072149	6.0349E-27	1.7416E-25

fadL	3.5103629	1.811620184	1.801E-28	5.6094E-27
gtdA	3.484567693	1.800979682	2.2893E-15	4.0047E-14
patD	3.483538709	1.800553595	6.3378E-17	1.2035E-15
ygcR	3.483141348	1.800389019	0.01237216	0.03182126
trhO	3.478977993	1.798663553	1.6256E-25	4.4405E-24
mglC	3.447247073	1.785444704	4.1232E-10	4.0425E-09
ybjO	3.436040793	1.780747164	1.6817E-10	1.7319E-09
gltJ	3.420806483	1.774336492	2.9208E-25	7.8111E-24
rdgC	3.333168064	1.736894063	1.3743E-27	4.1293E-26
maiA	3.324174045	1.73299592	2.4508E-06	1.4456E-05
ybcF	3.253275869	1.701893164	0.00027833	0.00111331
hydN	3.231798702	1.69233734	0.00023377	0.00095529
ddpF	3.197950716	1.677147705	3.4765E-21	8.2214E-20
ygiM	3.157695292	1.658871962	5.4047E-26	1.5253E-24
prpB	3.132983492	1.647537168	4.7147E-05	0.00021657
rlmD	3.131995011	1.647081915	8.1217E-25	2.1495E-23
mazG	3.115792478	1.639599148	7.3568E-24	1.8884E-22
yjfM	3.101952945	1.633176801	0.00404162	0.01196094
asnA	3.081924354	1.623831451	3.1248E-19	6.6506E-18
sdaC	3.029822036	1.599233056	1.5883E-32	5.5951E-31
gatD	3.021063645	1.595056578	0.00250183	0.00789825
ybhC	3.00722182	1.588431289	4.4909E-22	1.0924E-20
dppA	2.987157683	1.578773395	2.8913E-14	4.5997E-13
thiB	2.981600463	1.576086948	2.5419E-11	2.8474E-10
yieH	2.980251204	1.57543394	6.0331E-20	1.3576E-18
xdhC	2.980225908	1.575421694	6.6072E-05	0.00029735
ghxQ	2.976578976	1.573655173	4.6774E-14	7.1749E-13
espR3	2.974039444	1.572423782	1.3517E-10	1.4005E-09
relA	2.935188468	1.553453141	1.0032E-19	2.2088E-18
dadA	2.93330597	1.552527565	1.2478E-21	2.9645E-20
xthA	2.929820209	1.550812135	7.4351E-25	1.9781E-23

hycE	2.884920838	1.528531732	9.8847E-07	6.2181E-06
speC	2.876928053	1.524529142	9.999E-24	2.5285E-22
mipA	2.872713475	1.522414105	7.7782E-21	1.806E-19
dadX	2.852113589	1.51203144	5.0674E-19	1.0696E-17
mepS	2.836523787	1.504123962	2.6039E-18	5.3417E-17
rph	2.830722513	1.501170333	8.0969E-20	1.8061E-18
bdm	2.822934912	1.497195865	0.01756748	0.04307954
folD	2.811744701	1.491465607	8.8747E-20	1.971E-18
ssnA	2.798873798	1.484846437	0.00011988	0.00051848
aroA	2.782297019	1.47627644	1.5274E-17	3.024E-16
cycA	2.774669215	1.472315789	1.4209E-18	2.9266E-17
rnk	2.773790538	1.471858847	1.1326E-16	2.1349E-15
rimO	2.757029933	1.463114931	2.0416E-19	4.4003E-18
rlhA	2.740872067	1.45463499	9.5469E-18	1.9049E-16
yfhL	2.732172502	1.450048574	0.01244553	0.03197774
yjjU	2.724796291	1.446148376	5.7735E-22	1.3911E-20
nanT	2.673187444	1.418561003	9.7727E-07	6.1552E-06
ygfT	2.664059776	1.413626454	2.5261E-09	2.2479E-08
hypE	2.660512101	1.411703965	5.5553E-12	6.7725E-11
nusA	2.650419786	1.406220878	5.8066E-17	1.1067E-15
nanS	2.64473079	1.403120876	1.334E-05	6.7333E-05
ydjI	2.636742829	1.398756867	8.6379E-06	4.53E-05
tuf_2	2.632711528	1.396549451	6.3032E-15	1.0488E-13
nuoM	2.616134826	1.387436894	4.7432E-23	1.1819E-21
suhB	2.602575721	1.379940139	2.165E-14	3.4996E-13
rimP	2.590852927	1.373427122	2.366E-19	5.0566E-18
dppB	2.590215854	1.373072329	1.3613E-08	1.1107E-07
cysS	2.581447542	1.368180281	1.078E-17	2.1426E-16
leuB	2.575911575	1.36508307	4.3901E-15	7.4896E-14
hycF	2.560610892	1.356488039	0.00068814	0.00248588
ybcI	2.560120484	1.356211707	0.00036723	0.00141893

sucC	2.553056161	1.352225274	3.1328E-15	5.37E-14
rpoC	2.552786363	1.352072807	4.3988E-15	7.4896E-14
acs	2.539552223	1.344574142	1.3076E-06	8.0474E-06
leuC	2.533246725	1.340987595	2.2755E-15	3.9943E-14
espW	2.524517588	1.336007729	4.4037E-13	6.1292E-12
cirA	2.521260395	1.334145127	3.1166E-11	3.4607E-10
intS	2.494990897	1.319034552	1.0097E-05	5.2252E-05
nudG	2.482031462	1.311521403	2.9741E-06	1.7244E-05
yobF	2.453404317	1.294785007	2.1675E-13	3.1099E-12
pinE	2.450045691	1.292808654	0.01428506	0.03599808
yebQ	2.449290874	1.292364116	6.6392E-12	8.0173E-11
leuD	2.442116208	1.288131852	4.422E-13	6.1379E-12
yedE	2.43957535	1.286630044	1.6402E-12	2.1211E-11
yceI	2.429836783	1.280859408	5.9812E-14	9.039E-13
ycjW	2.429643621	1.280744716	7.2972E-08	5.4335E-07
yajG	2.427414177	1.279420289	6.4969E-13	8.8027E-12
yddB	2.419411321	1.274656061	1.3414E-15	2.4041E-14
espN	2.412698265	1.270647502	1.3008E-12	1.7037E-11
rapA	2.405065984	1.266076476	1.3648E-15	2.4375E-14
ydiJ	2.396228734	1.260765629	5.5374E-14	8.4182E-13
rplW	2.387370493	1.255422474	9.4595E-13	1.2583E-11
rpsS	2.387063835	1.255237148	1.4769E-12	1.9244E-11
yfiF	2.379259178	1.250512436	2.048E-13	2.9551E-12
ychF	2.363703268	1.241048935	3.546E-14	5.5561E-13
yeeN	2.361838975	1.239910608	2.3365E-13	3.3244E-12
dppC	2.357167706	1.237054406	5.3335E-10	5.1306E-09
tsx	2.356138153	1.236424134	5.7159E-15	9.6042E-14
ydjH	2.355571262	1.236076978	1.1087E-05	5.6915E-05
mdfA	2.355335495	1.235932573	7.2078E-11	7.6504E-10
pheA	2.349878659	1.232586262	5.9915E-15	1.003E-13
glyA	2.343646996	1.228755285	1.3999E-13	2.0489E-12

dppF	2.335950019	1.224009406	7.0051E-11	7.4702E-10
dbpA	2.330533826	1.220660453	3.1723E-13	4.4886E-12
rplP	2.330094483	1.220388456	5.8437E-14	8.8575E-13
cspE_2	2.32995989	1.220305119	1.7022E-11	1.9365E-10
rplV	2.329060829	1.219748319	2.3982E-12	3.0779E-11
tdk	2.327608442	1.218848384	2.8464E-12	3.5988E-11
rplA	2.326354223	1.218070786	1.9404E-12	2.5029E-11
prs	2.326282598	1.218026367	4.1599E-13	5.8057E-12
ttcA	2.321222983	1.214885119	3.0514E-14	4.8256E-13
rplD	2.320700103	1.214560099	4.5029E-12	5.5291E-11
mdoG	2.312911611	1.209710134	4.1713E-14	6.4372E-13
sctN	2.311672266	1.208936877	0.00555517	0.01586126
sucD	2.310399672	1.208142442	7.0635E-14	1.0612E-12
ydiB	2.310229519	1.208036189	0.00115486	0.00397777
dppD	2.304321786	1.204342196	1.7327E-09	1.5598E-08
galU	2.303412962	1.203773085	2.2163E-14	3.56E-13
spy	2.296474765	1.19942093	2.2273E-12	2.8657E-11
yciE	2.294920675	1.198444287	3.7935E-05	0.00017648
argS	2.288056281	1.194122539	1.5197E-15	2.7047E-14
yeiP	2.285192624	1.192315778	1.3627E-14	2.2168E-13
rsuA	2.283732528	1.191393691	4.7077E-11	5.1273E-10
rplK	2.2831922	1.191052312	8.2618E-12	9.8602E-11
ompT	2.263986859	1.178865584	1.1997E-12	1.5754E-11
ydeM	2.263652726	1.178652647	0.00318736	0.00976083
speA	2.26316038	1.178338826	1.7199E-13	2.51E-12
pyrF	2.260681963	1.176758045	1.0392E-12	1.3788E-11
ycaO	2.257963873	1.175022403	8.836E-14	1.3082E-12
yehL	2.257238139	1.174558631	0.00842913	0.02289429
fusA	2.254299788	1.172679385	1.8492E-11	2.0898E-10
guaA	2.252945705	1.171812546	4.0258E-12	4.9791E-11
ybiX	2.25286234	1.171759161	3.8107E-09	3.3388E-08

prmB	2.250900082	1.170502017	2.1939E-13	3.1391E-12
rplB	2.240135999	1.163586321	2.2462E-11	2.5272E-10
rpnB	2.237876525	1.162130438	1.7081E-10	1.7555E-09
coaD	2.235629668	1.160681226	1.5602E-12	2.0228E-11
rpsF	2.228538472	1.156097867	2.9863E-12	3.7584E-11
ompG	2.226824848	1.154988087	0.00182206	0.00595595
dpaL	2.225604559	1.15419728	1.45E-06	8.8066E-06
rpoB	2.223583451	1.15288655	2.3821E-11	2.6742E-10
yqeF	2.2211817	1.151327415	9.7014E-10	8.9773E-09
atpG	2.22076337	1.151055677	4.1332E-10	4.0445E-09
waaA	2.219953189	1.150529256	3.1756E-12	3.966E-11
ugpB	2.214533433	1.147002778	0.00010653	0.00046549
rpsJ	2.212961017	1.145978037	1.0524E-11	1.2301E-10
hdeB	2.212350048	1.145579674	1.3184E-11	1.5201E-10
rpsG	2.212214908	1.145491545	5.7926E-11	6.2161E-10
rbsB	2.209562567	1.143760783	4.2614E-12	5.2451E-11
pabB	2.206953926	1.142056511	7.8435E-14	1.1749E-12
greA	2.205359732	1.141014003	3.1717E-13	4.4886E-12
rpsL	2.202665156	1.139250197	6.1393E-11	6.5605E-10
ihfB	2.202262333	1.138986333	5.6269E-16	1.0339E-14
dacA	2.201836484	1.138707333	3.781E-12	4.6992E-11
murC	2.201448294	1.13845296	7.484E-15	1.2372E-13
adk	2.20128417	1.138345399	3.367E-14	5.3083E-13
yeiQ	2.201107365	1.138229519	7.2207E-19	1.5054E-17
elfD	2.197855911	1.136096808	0.01806085	0.04416219
atpD	2.197241165	1.135693226	8.0041E-11	8.4299E-10
yjeJ	2.196618313	1.135284207	8.0686E-06	4.2533E-05
pphB	2.195942253	1.134840116	0.00332947	0.0101163
rplC	2.193869307	1.133477584	5.455E-11	5.8737E-10
rnb	2.19114963	1.131688007	9.0978E-12	1.0708E-10
puuA	2.189877844	1.130850396	1.8352E-05	8.9793E-05

rlmF	2.18517115	1.127746281	1.3378E-09	1.2246E-08
livK	2.184643089	1.127397602	3.3392E-13	4.7117E-12
yddA	2.180133277	1.124416333	4.8034E-11	5.2204E-10
ydiO	2.176065113	1.121721726	0.00205361	0.00660571
uhpA	2.17157817	1.118743886	5.205E-07	3.413E-06
epmA	2.170363838	1.117936915	7.9698E-16	1.4436E-14
glyQ	2.169720164	1.117508986	6.3654E-13	8.6475E-12
rlmN	2.169103378	1.117098812	3.7464E-13	5.2574E-12
apt	2.162499614	1.112699875	2.0091E-10	2.0443E-09
speB	2.162404747	1.112636584	1.1066E-10	1.1559E-09
mazE	2.15326373	1.106525031	4.0958E-11	4.48E-10
yqeC	2.150505845	1.104676052	0.00214823	0.00687973
rpmC	2.14945529	1.103971102	1.0059E-13	1.4851E-12
udk	2.148093862	1.103057034	8.5218E-12	1.0123E-10
yahB	2.144234058	1.100462394	2.622E-06	1.5307E-05
emrR	2.143976426	1.100289043	7.9896E-10	7.5158E-09
ansA	2.140087373	1.097669699	2.4417E-10	2.4698E-09
gndA	2.137463719	1.095899932	7.2191E-11	7.6504E-10
allE	2.13619033	1.095040194	8.8964E-12	1.0544E-10
wecB	2.131193315	1.091661462	7.9702E-13	1.0686E-11
prfA	2.128479377	1.089823112	1.0577E-10	1.1071E-09
ppiA	2.124505661	1.087127188	7.9045E-13	1.0625E-11
era	2.120640306	1.084499938	3.1741E-12	3.966E-11
rpsA	2.120283366	1.084257087	5.6829E-10	5.4462E-09
fadD	2.116122112	1.081422881	9.0077E-12	1.0626E-10
nemA	2.114289488	1.080172924	7.9947E-12	9.5637E-11
rnc	2.113118	1.079373332	2.0466E-11	2.3078E-10
serB	2.111544241	1.078298475	1.0424E-10	1.0933E-09
rpsC	2.108986831	1.076550087	8.0522E-10	7.5469E-09
ydcI	2.10623603	1.074667117	9.6871E-07	6.1088E-06
yihQ	2.104199956	1.073271807	0.00218433	0.00698658

ybiT	2.102996801	1.072446656	9.2035E-12	1.0807E-10
solA	2.101702604	1.071558539	3.6939E-11	4.0665E-10
gmd_2	2.100082148	1.070445762	2.076E-06	1.2374E-05
ydiF	2.091456506	1.064507996	8.7364E-05	0.00038704
yggP	2.084036697	1.059380682	0.00038717	0.00149369
ydgI	2.0780793	1.055250709	6.7291E-10	6.3771E-09
ygiQ	2.068797516	1.048792448	2.8272E-10	2.8261E-09
icmH	2.059481111	1.042280894	0.0004503	0.00170758
nanE	2.051853033	1.036927399	0.00080503	0.00285148
cbtA_2	2.050528358	1.035995696	0.00639638	0.01797178
yqcC	2.050292191	1.035829525	7.0959E-07	4.5707E-06
yeiR	2.050185763	1.035754635	5.9606E-11	6.383E-10
purU	2.049765259	1.035458701	4.1193E-10	4.0425E-09
nfeF	2.0458516	1.0327015	2.8031E-12	3.5618E-11
zapC	2.044837121	1.031985932	7.1738E-12	8.605E-11
rpoD	2.038092905	1.027219817	8.324E-10	7.7874E-09
rlmG	2.037000039	1.026446008	8.5862E-09	7.1547E-08
gyrA	2.031732487	1.022710458	1.0801E-09	9.9592E-09
serC	2.030329613	1.02171396	1.5396E-09	1.3993E-08
yeaW	2.027981453	1.020044458	3.1735E-08	2.4824E-07
rsmF	2.02733447	1.019584125	3.1271E-11	3.4649E-10
ftrA	2.026284444	1.01883671	1.7433E-10	1.7881E-09
guaC	2.02436303	1.017468033	4.8793E-10	4.7383E-09
rlmI	2.022934638	1.016449707	5.7655E-10	5.515E-09
aspC	2.022316746	1.016008978	2.6846E-10	2.6941E-09
mltB	2.022101799	1.015855629	9.0171E-09	7.4893E-08
otsA	2.018849898	1.01353365	6.1823E-09	5.2632E-08
pth	2.016144818	1.01159927	1.2212E-09	1.1219E-08
opgD	2.014704273	1.010568089	1.0791E-11	1.2585E-10
chbA	2.014383423	1.010338316	0.0064145	0.01801279
katE	2.01403758	1.010090603	2.189E-09	1.9616E-08

pyrG	2.013709938	1.009855887	1.7249E-09	1.5567E-08
yoaB	2.00996815	1.00717264	2.9415E-08	2.3116E-07
ylbG	2.008226476	1.005921977	0.00034811	0.00135222
mazF	2.005953406	1.004288096	1.5854E-10	1.636E-09
bfd	1.999052011	0.999316008	0.00028732	0.00113859
mnmG	1.998966686	0.999254429	7.4955E-09	6.2869E-08
glpE	1.997963027	0.998529886	8.8262E-10	8.227E-09
infB	1.996045015	0.997144257	5.1724E-09	4.4479E-08
yncD	1.993733597	0.995472649	2.7485E-10	2.7528E-09
yihN	1.991128616	0.993586415	0.01197483	0.03097086
yqeI	1.988354077	0.991574689	0.00065451	0.00237445
flk	1.980745776	0.986043725	3.657E-10	3.6131E-09
ppiD	1.976914752	0.983250661	3.4269E-10	3.3924E-09
rffA	1.974470202	0.981465595	8.3169E-14	1.2422E-12
rplR	1.972424518	0.979970092	6.075E-09	5.1831E-08
otsB	1.971301238	0.979148254	1.9104E-07	1.3591E-06
ydgT	1.970716213	0.978720041	0.02289976	0.0540536
tdcE	1.969455369	0.977796723	2.0153E-05	9.7666E-05
rluE	1.967546684	0.976397867	4.0853E-06	2.2831E-05
galF	1.966394665	0.975552907	1.9868E-10	2.0256E-09
uxuA	1.960622551	0.971311822	1.319E-09	1.2096E-08
speE	1.959260741	0.970309406	7.7202E-09	6.4648E-08
hflD	1.956787392	0.968487014	3.6637E-09	3.2155E-08
groL	1.944413773	0.959335259	2.5484E-07	1.7735E-06
rfbE	1.944389029	0.959316899	3.274E-08	2.5532E-07
alaC	1.943639922	0.958760971	9.6657E-09	7.9891E-08
cmk	1.941016869	0.956812656	9.6363E-10	8.9333E-09
avtA	1.940301639	0.956280951	2.1249E-07	1.4971E-06
rbsC	1.939461416	0.955656075	0.00220309	0.00703599
mreB	1.938714116	0.955100079	3.148E-09	2.7724E-08
rplF	1.935013804	0.952343858	1.494E-08	1.2094E-07

sdhA	1.934987503	0.952324249	4.1767E-06	2.3291E-05
ompA	1.931421993	0.949663411	6.9563E-08	5.2177E-07
gmd_1	1.930229448	0.948772352	9.3075E-09	7.7179E-08
cybB	1.929392649	0.948146775	3.1197E-07	2.1247E-06
priB	1.927332116	0.946605197	6.3836E-08	4.8164E-07
secG	1.927200441	0.946506629	1.691E-09	1.5288E-08
glgP	1.925192509	0.945002715	1.6571E-08	1.3372E-07
gadA	1.92385728	0.944001778	1.1222E-06	7.0076E-06
dnaC	1.92379897	0.94395805	5.0671E-11	5.4721E-10
chuS	1.919110096	0.940437479	2.8221E-07	1.9378E-06
trmL	1.918691266	0.940122588	1.1054E-05	5.6803E-05
rlmB	1.918467374	0.93995423	1.4889E-09	1.3581E-08
hha	1.917244807	0.939034562	6.3323E-09	5.3598E-08
yebV	1.916275123	0.938304706	1.7532E-07	1.256E-06
ynjE	1.914415403	0.936903909	9.4297E-10	8.7577E-09
yibF	1.91117953	0.934463306	1.4027E-06	8.5501E-06
rlmKL	1.909735534	0.933372863	4.8246E-09	4.1699E-08
rnt	1.909381575	0.933105443	2.8225E-07	1.9378E-06
oppA	1.901938866	0.927470874	1.3219E-07	9.591E-07
nuoI	1.897973206	0.924459625	1.5011E-10	1.5521E-09
rpsQ	1.896741283	0.923522907	6.2136E-08	4.6951E-07
uxuB	1.896389315	0.923255169	1.7894E-08	1.4372E-07
osmF	1.894241691	0.92162042	3.3673E-05	0.00015823
rpsP	1.893815146	0.921295517	1.5347E-07	1.101E-06
rpmD	1.890558556	0.918812535	2.2912E-07	1.6032E-06
hdeA	1.890331106	0.918638956	6.4907E-08	4.8829E-07
ftsZ	1.889473748	0.917984474	5.413E-08	4.1145E-07
wcaL	1.886413766	0.915646152	0.00405317	0.01198819
yidC	1.886386367	0.915625197	6.5202E-08	4.8978E-07
nleG	1.882399532	0.912572867	9.922E-09	8.1877E-08
yqjD	1.881926506	0.912210289	0.00023556	0.00096105

yigI	1.877113945	0.908516227	0.00313696	0.009618
rpsE	1.877112581	0.90851518	1.1676E-07	8.5194E-07
yhcH	1.875996336	0.90765701	0.00076125	0.00271729
envC	1.871808021	0.904432475	5.9511E-09	5.0918E-08
rplE	1.868641816	0.901990057	9.7878E-08	7.1937E-07
atpC	1.866856925	0.900611365	7.2941E-08	5.4335E-07
ydcU	1.865762824	0.899765602	0.01843159	0.04498258
ygaH	1.863844295	0.898281343	3.9507E-05	0.00018312
yciH	1.859359394	0.894805654	1.7395E-06	1.0478E-05
murE	1.858719243	0.89430887	2.5851E-09	2.2964E-08
proC	1.858700446	0.89429428	2.1177E-07	1.4959E-06
yjjV	1.858409424	0.894068375	1.9115E-10	1.9567E-09
nanM	1.855488053	0.891798712	8.9805E-07	5.7056E-06
prfC	1.855278229	0.891635558	1.3947E-08	1.1362E-07
odhB	1.850440916	0.887869071	1.1177E-08	9.1938E-08
tpx	1.847062109	0.885232379	3.9874E-07	2.6694E-06
livH	1.846931909	0.885130679	2.3954E-06	1.4162E-05
rplI	1.846055067	0.884445589	2.6889E-07	1.8611E-06
tsf	1.842926902	0.881998849	1.1897E-07	8.6567E-07
ykgE	1.842318485	0.881522485	0.00735019	0.02022887
ygaC	1.842272591	0.881486545	0.00199895	0.00646651
tig	1.836386148	0.876869455	1.5554E-06	9.4024E-06
mdtA	1.836355449	0.876845337	0.00015027	0.00063804
murD	1.835812868	0.876419007	4.7447E-09	4.1147E-08
gadC	1.83533597	0.876044182	3.4586E-06	1.963E-05
uvrY	1.833593451	0.874673796	4.3368E-09	3.7933E-08
rpsH	1.829211453	0.871221857	1.386E-07	1.0014E-06
potA	1.828924229	0.870995306	1.8895E-08	1.5128E-07
eptC	1.826988674	0.86946769	2.3714E-07	1.657E-06
rpsR	1.820926179	0.864672436	1.9289E-07	1.3703E-06
rcsF	1.820314481	0.864187714	2.8352E-08	2.2314E-07

truC	1.817500981	0.861956143	8.1033E-07	5.2E-06
nudE	1.817178585	0.861700208	5.0784E-08	3.8717E-07
rplS	1.816552421	0.861202999	2.4546E-08	1.9409E-07
atpA	1.816535019	0.861189178	2.6115E-06	1.5262E-05
mnmA	1.816340691	0.861034835	4.2664E-08	3.2771E-07
lpxT	1.814989728	0.859961383	0.00010402	0.00045489
tkt_2	1.814043757	0.859209256	1.757E-07	1.257E-06
degP	1.812193996	0.857737404	2.4178E-08	1.9147E-07
ubiX	1.811951741	0.857544532	1.9237E-08	1.5378E-07
fepA	1.811406311	0.857110189	7.2517E-06	3.8425E-05
rimM	1.806835115	0.853464857	3.3537E-07	2.275E-06
nuoH	1.806687976	0.853347367	1.4809E-11	1.7037E-10
yedF	1.806138743	0.852908721	0.00011138	0.00048543
tdcD	1.805261605	0.852207917	0.0212539	0.05089775
rho	1.80136303	0.849088958	2.7322E-07	1.8885E-06
lysO	1.799958107	0.847963329	3.8809E-07	2.6084E-06
cdgI	1.799550235	0.847636376	0.02026021	0.04883868
aldA	1.796345662	0.845064987	4.5561E-09	3.9782E-08
mppA	1.795600334	0.84446627	8.1002E-08	5.9965E-07
yhjV	1.795299598	0.84422462	8.2529E-08	6.1007E-07
icd	1.790853085	0.840646988	3.3162E-06	1.8969E-05
nuoC	1.789280825	0.839379834	1.1692E-07	8.5194E-07
tolC	1.787544303	0.837978998	4.1679E-07	2.7757E-06
sdaB	1.78463747	0.835631036	5.4434E-07	3.5511E-06
yneE	1.783821751	0.834971461	6.8429E-06	3.6296E-05
wzzE	1.783260177	0.834517207	7.2612E-08	5.4225E-07
tyrS	1.778507437	0.830667007	2.1202E-07	1.4959E-06
rplO	1.778449256	0.830619811	1.3396E-06	8.2142E-06
rlmA	1.777429717	0.829792514	1.1888E-06	7.3783E-06
yidL	1.776471299	0.82901438	0.00128539	0.00437425
msrC	1.77299869	0.82619147	3.6534E-07	2.4652E-06

livM	1.771656198	0.825098666	3.4561E-06	1.963E-05
tsaB	1.771000346	0.824564494	2.6735E-07	1.8529E-06
rluA	1.770362431	0.824044741	8.5246E-05	0.00037798
lepA	1.768784763	0.822758502	1.4251E-07	1.0282E-06
proQ	1.768676936	0.822670552	2.6286E-07	1.8268E-06
fcl	1.767009314	0.821309645	0.02027062	0.04884072
cyoA	1.766697923	0.821055384	5.623E-05	0.00025601
sppA	1.762727086	0.817809127	2.1718E-08	1.728E-07
menI	1.762381863	0.817526553	8.6889E-07	5.5409E-06
cstA	1.760416961	0.815917177	3.7943E-07	2.5535E-06
dctR	1.758067076	0.813990115	4.3432E-07	2.8849E-06
ygjV	1.757203158	0.813280998	1.7722E-05	8.6959E-05
rsmG	1.756270474	0.812515044	2.8609E-07	1.9616E-06
mioC	1.753877596	0.810548065	1.0258E-05	5.3036E-05
rpsI	1.753660049	0.810369105	4.1598E-08	3.2097E-07
mepH	1.752881425	0.809728407	2.327E-06	1.3773E-05
dnaT	1.752366741	0.809304739	5.5637E-06	3.0073E-05
speD	1.749716387	0.807121094	6.5016E-07	4.2038E-06
rhlE	1.748160979	0.805838041	5.3485E-07	3.4981E-06
sdhD	1.74799842	0.805703881	0.00052012	0.00194349
yecF	1.745141732	0.80334421	4.8004E-06	2.6338E-05
rpsN	1.744807575	0.803067938	3.1685E-06	1.8247E-05
cra	1.742824046	0.801426923	4.0494E-08	3.134E-07
rcnB	1.74102639	0.799938071	6.1005E-05	0.00027601
plsB	1.740347926	0.799375755	2.2502E-08	1.7876E-07
prmC	1.738916474	0.798188637	6.122E-06	3.2814E-05
yahD	1.738547932	0.797882843	0.00220391	0.00703599
ychO	1.736851529	0.796474433	6.2005E-05	0.00028029
opgB	1.733881156	0.794005016	9.4779E-08	6.986E-07
yaiL	1.731998649	0.792437805	3.9781E-05	0.00018423
napA	1.731022443	0.791624429	0.00182246	0.00595595

efeO	1.731014343	0.791617679	3.6882E-06	2.0771E-05
yieE	1.730051619	0.790815083	7.2965E-06	3.8622E-05
trmD	1.729866284	0.790660524	2.0925E-06	1.2443E-05
rpmG	1.729261724	0.790156238	0.00233123	0.00739624
proS	1.728178955	0.789252618	9.4091E-07	5.9556E-06
crl	1.726247875	0.787639638	1.3352E-06	8.1971E-06
sucA	1.725811223	0.787274665	3.572E-06	2.0183E-05
bdcR	1.724821667	0.786447206	0.00117909	0.00405303
ndh	1.72364869	0.785465758	2.6419E-06	1.5405E-05
yjfZ	1.722129123	0.784193318	0.00033477	0.00130634
sbcD	1.721970112	0.784060102	9.0538E-07	5.7449E-06
ydcR	1.72159321	0.783744293	1.7089E-05	8.4095E-05
ggt	1.720857777	0.783127868	0.00441754	0.01296082
znuC	1.720588657	0.782902232	5.3377E-06	2.8974E-05
pldA	1.719754972	0.782203027	1.1058E-07	8.0923E-07
ygdI	1.715917361	0.778980074	0.00022471	0.0009212
glsB	1.713990486	0.777359101	5.8785E-07	3.8202E-06
yjjA	1.713170456	0.776668703	2.9615E-06	1.719E-05
tsaD	1.712584529	0.776175198	5.1051E-06	2.786E-05
setB	1.711395802	0.775173457	0.00044505	0.00168896
yehY	1.711260815	0.775059659	0.00834751	0.02271084
srmB	1.708702421	0.772901166	3.2344E-06	1.8542E-05
sthA	1.707832481	0.77216647	5.5441E-06	2.9999E-05
rpe	1.705402459	0.770112242	2.1761E-07	1.5247E-06
pabA	1.70498149	0.769756077	0.00030564	0.00120371
potB	1.702043533	0.767267937	6.4035E-06	3.4143E-05
coaBC	1.701364175	0.766691982	1.4408E-06	8.7616E-06
radA	1.698066582	0.763893029	4.3379E-06	2.4111E-05
poxB	1.697743147	0.763618209	9.119E-06	4.7628E-05
tolB	1.696583251	0.762632225	5.8931E-06	3.1686E-05
pcnB	1.695966692	0.762107836	1.3653E-06	8.3422E-06

wecC	1.695347333	0.761580874	3.4271E-06	1.9494E-05
tuf_1	1.694669686	0.7610041	6.2267E-06	3.327E-05
nuoB	1.694311842	0.760699431	1.5614E-05	7.7886E-05
osmY	1.693428346	0.759946944	0.0003169	0.00124485
zraS	1.689456733	0.756559403	0.00066223	0.00239734
wrbA	1.689294566	0.756420916	3.8298E-05	0.00017784
ybiV	1.688692039	0.755906253	2.1831E-05	0.00010491
allC	1.688222796	0.75550531	0.00398455	0.01182631
nuoL	1.686675409	0.754182362	5.3509E-06	2.9015E-05
gltX	1.683534268	0.751493087	1.0709E-06	6.7039E-06
uup	1.68270212	0.750779807	2.3117E-06	1.3699E-05
ydhP	1.681431219	0.749689765	1.5704E-05	7.826E-05
rsmI	1.680759265	0.749113102	1.523E-05	7.6123E-05
murG	1.679840589	0.748324333	9.9335E-07	6.2411E-06
yegD	1.678795576	0.747426567	2.333E-05	0.00011127
iraP	1.676039709	0.74505633	0.01398106	0.0353366
rplJ	1.67541872	0.744521698	9.2041E-06	4.7925E-05
rplL	1.67535327	0.744465338	3.9032E-06	2.1885E-05
modF	1.674578466	0.743797978	3.4005E-06	1.9364E-05
menA	1.674329402	0.743583387	2.1005E-05	0.00010141
purA	1.672628689	0.742117213	5.7483E-06	3.094E-05
yeaD	1.670971345	0.740686993	4.0986E-06	2.2881E-05
acrA	1.670853928	0.740585613	6.378E-06	3.4043E-05
nudJ	1.670078489	0.739915907	2.7676E-07	1.9104E-06
pykF	1.668544713	0.738590348	1.5991E-05	7.9457E-05
hxpB	1.666612166	0.736918417	1.1871E-05	6.0697E-05
gpmM	1.665537297	0.735987661	2.0861E-06	1.242E-05
mraY	1.664855512	0.735396975	3.609E-06	2.0347E-05
fhuF	1.661031186	0.73207916	1.048E-05	5.4128E-05
yjeM	1.657260088	0.728800035	0.00150901	0.00502479
ytfL	1.65685633	0.728448508	2.2072E-05	0.00010576

rplX	1.655345194	0.727132098	2.0352E-05	9.8539E-05
nuoG	1.654292362	0.726214224	4.3076E-06	2.3969E-05
pdxY	1.653629823	0.725636313	6.1064E-06	3.2764E-05
queA	1.65346288	0.725490657	1.2511E-05	6.346E-05
rdgB	1.653392357	0.725429123	1.5695E-06	9.4763E-06
rpoZ	1.652930664	0.725026209	0.00514323	0.01484272
rplU	1.652553267	0.724696775	1.3615E-05	6.8654E-05
hypF	1.65233559	0.724506729	0.00024028	0.00097876
hemA	1.651259281	0.72356667	1.4271E-06	8.6885E-06
pnp	1.65049023	0.722894599	1.224E-05	6.2397E-05
yojI	1.64957816	0.722097137	8.9029E-06	4.6547E-05
trmA	1.648746167	0.721369305	8.7543E-06	4.5864E-05
dut	1.64857455	0.721219128	1.4591E-05	7.3283E-05
rtcA	1.646948436	0.719795387	0.00452435	0.01323617
rluB	1.646711281	0.719587629	2.1977E-05	0.00010549
rpsK	1.646351997	0.719272823	9.9531E-06	5.1562E-05
ddlA	1.644989426	0.718078311	3.1606E-06	1.8222E-05
alaS	1.64463837	0.717770393	1.2032E-05	6.1462E-05
yejK	1.644206095	0.717391147	1.4885E-05	7.469E-05
pagP	1.642194639	0.715625131	0.00916646	0.02457861
rpoA	1.640744833	0.71435089	2.3766E-05	0.00011324
yiiG	1.640726885	0.714335108	0.00987697	0.02623585
rplM	1.639821182	0.713538502	2.7131E-05	0.0001288
atpH	1.638968239	0.712787897	7.1599E-05	0.00032053
yraQ	1.638807601	0.71264649	5.1547E-05	0.00023594
coaA	1.637488958	0.711485179	9.4382E-06	4.8994E-05
yihM	1.636015995	0.710186853	0.00301946	0.00930441
gluQRS	1.635308515	0.709562838	9.2475E-05	0.00040862
prfB	1.634736722	0.709058306	5.2146E-06	2.8367E-05
rplN	1.633466028	0.707936451	3.1508E-05	0.00014874
ureG_2	1.630956835	0.7057186	2.1017E-06	1.2483E-05

rplQ	1.630483945	0.705300235	1.6954E-05	8.3593E-05
yccJ	1.628890708	0.703889808	0.02169149	0.05171741
xni	1.627931036	0.703039584	0.00176439	0.00579211
terC_2	1.626469824	0.701744056	1.0851E-05	5.5986E-05
mrcA	1.624142494	0.699678213	5.7087E-06	3.0805E-05
murF	1.620991963	0.696876937	1.9678E-05	9.5639E-05
mdtF	1.618812382	0.694935789	1.6462E-05	8.1637E-05
yegS	1.618507084	0.69466368	0.00566039	0.01613465
potD	1.618386987	0.694556624	3.7755E-05	0.0001758
pheS	1.616933598	0.693260433	1.2507E-05	6.346E-05
gadB	1.616091178	0.692508595	0.00016146	0.00068104
truB	1.615923026	0.692358478	6.6213E-06	3.5231E-05
mdtE	1.615830906	0.692276231	5.8986E-07	3.8285E-06
dmsD	1.615117807	0.691639399	0.00023473	0.00095845
ptsG	1.614704608	0.691270264	9.8687E-05	0.0004327
ydeP	1.61229065	0.689111844	0.00021353	0.00087962
rpsD	1.60982787	0.686906437	6.3025E-05	0.0002845
rcnA	1.607456355	0.684779567	0.01608523	0.03992388
yhdJ	1.60699587	0.684366221	0.00833835	0.02270379
mcbR	1.606864304	0.684248102	0.01409253	0.03556553
cyoB	1.604868553	0.682455138	0.0007829	0.00278485
lacA	1.601311379	0.679253871	0.00347267	0.0104837
yjiA	1.601159637	0.679117153	9.5842E-07	6.0589E-06
sodA	1.60051622	0.678537297	0.00031852	0.00124866
yceJ	1.600039224	0.678107272	0.00019419	0.00080709
yffB	1.599730313	0.677828712	2.5619E-05	0.00012184
rpmA	1.598776814	0.676968556	5.408E-05	0.00024686
ytfJ	1.598279518	0.676519738	0.0012205	0.00418129
proB	1.594655938	0.673245183	1.5305E-05	7.642E-05
yphH	1.593069933	0.6718096	0.00044138	0.00167628
ybaY	1.593042185	0.671784471	2.5915E-05	0.00012314

ilvI	1.591734146	0.670599395	3.7035E-06	2.0834E-05
gstB	1.590433296	0.669419865	9.4244E-06	4.8973E-05
mutS	1.589469853	0.668545653	1.6488E-05	8.169E-05
priA	1.589393267	0.668476138	4.4008E-05	0.0002027
oppF	1.589364386	0.668449923	9.109E-05	0.00040285
fbaB	1.588887445	0.66801693	6.6421E-05	0.00029866
ydgH	1.588799577	0.667937144	1.8436E-05	9.0114E-05
rlmC	1.588323919	0.667505162	0.00011215	0.00048837
fdnG_2	1.588171622	0.667366822	6.824E-06	3.6234E-05
lpxM	1.587380247	0.666647759	4.6726E-06	2.5775E-05
parE	1.584397476	0.663934308	1.7274E-05	8.4925E-05
pheT	1.584259222	0.663808414	3.5671E-05	0.00016701
trpE	1.584112138	0.663674466	0.01255983	0.032239
nuoF	1.583057526	0.662713682	5.4965E-05	0.00025068
ydfG	1.57904521	0.659052478	2.1654E-05	0.00010415
atpF	1.578590049	0.65863656	0.00016508	0.00069514
menB	1.577675004	0.657800046	4.6871E-05	0.0002155
yodB	1.577591066	0.657723287	0.0034481	0.01043418
oppB	1.576225356	0.656473814	0.00020955	0.0008653
chaA	1.574989636	0.655342335	0.00010171	0.00044518
rbfA	1.572598874	0.653150726	9.6853E-06	5.0226E-05
pal	1.571045832	0.651725269	0.00021294	0.0008779
ampC	1.567962667	0.648891209	0.01551782	0.03868473
yciF	1.566309471	0.647369288	0.01529776	0.03822944
cadC	1.566106437	0.647182266	0.00027026	0.00108451
yaaA	1.564867726	0.646040715	1.2599E-05	6.3846E-05
betB	1.563028216	0.644343823	0.00376153	0.01122381
folA	1.562153093	0.643535846	4.1182E-05	0.00019037
typA	1.56056482	0.642068283	0.00015695	0.00066422
ampG	1.560412924	0.641927853	0.00014702	0.00062581
epmB	1.553885186	0.635879909	3.66E-05	0.0001712

yncE	1.552326474	0.634432007	0.00016716	0.00070161
murJ	1.552187548	0.634302887	3.2901E-06	1.8841E-05
glyS	1.548260788	0.630648499	0.00021707	0.00089275
aroM	1.547534882	0.629971928	0.0221212	0.05250028
aspS	1.547401607	0.629847677	3.7468E-05	0.00017475
gfcC	1.546609388	0.629108875	0.00018686	0.00077916
pdeC	1.545054311	0.627657552	0.01680691	0.04147328
ascB	1.544281487	0.626935747	0.00470429	0.01372331
recF	1.543713774	0.626405282	0.00049984	0.00187407
bglX	1.542803304	0.625554141	0.00012925	0.00055432
ugd	1.541888005	0.624697979	0.0001362	0.00058171
entC	1.541676852	0.624500397	0.00015155	0.00064297
der	1.539784549	0.622728499	6.5309E-05	0.00029418
ptsI	1.538087109	0.621137212	0.0002185	0.0008972
ivy	1.53690625	0.620029165	0.001223	0.00418704
nuoE	1.536458	0.61960833	8.416E-05	0.00037382
fghA	1.533593783	0.616916394	0.00869506	0.02351405
ycgN	1.532351139	0.61574693	0.00070365	0.00253116
ydeI	1.531435483	0.61488459	0.0043102	0.01266044
rihC	1.53067997	0.61417268	0.00011445	0.00049669
yijO	1.529533218	0.613091439	0.00377254	0.01124936
dinF	1.527387634	0.611066249	8.4517E-05	0.00037508
ybhJ	1.526290231	0.610029323	0.00368684	0.01103891
murA	1.525981248	0.609737233	0.00024883	0.00100874
rnd	1.524923633	0.608736995	0.00021531	0.00088621
opgE	1.523111924	0.60702196	0.00017697	0.00073912
ureG_1	1.522124046	0.606085936	3.7177E-05	0.00017359
adeD	1.520453245	0.604501454	0.01924877	0.04677579
atpE	1.518837174	0.602967215	0.00027289	0.00109412
terC_1	1.518213959	0.602375121	0.00019809	0.00082197
dcm	1.516781653	0.601013419	8.2306E-05	0.00036622

nuoN	1.515918395	0.600192092	4.0843E-05	0.00018897
iha_2	1.515070469	0.599384898	9.2701E-05	0.00040926
cmoB	1.514506387	0.598847662	0.00057717	0.00212866
terD_1	1.512452728	0.596890051	0.00010106	0.00044271
ispC	1.510712695	0.595229317	0.00012991	0.00055624
fsr	1.509478241	0.594049961	0.00231959	0.00736388
yebC	1.508524555	0.59313818	0.00016003	0.00067612
btuE	1.508340188	0.592961848	0.00063646	0.00231887
ydjG	1.507964195	0.592602174	0.0219718	0.0522252
entE	1.507815126	0.59245955	0.00052766	0.0019645
wcaM	1.507766444	0.59241297	0.00904217	0.02433479
tssH	1.507514872	0.592172235	0.00354183	0.01066724
gfcD	1.506226826	0.590939045	0.00019894	0.00082483
yaeQ	1.50612563	0.590842114	0.00613996	0.01736596
cysM	1.505554526	0.590294959	1.3177E-05	6.6642E-05
msrB	1.503828324	0.588639879	0.00024661	0.00100134
yqjE	1.501698149	0.586594851	0.00010823	0.00047252
miaB	1.501696769	0.586593525	0.0001539	0.00065238

Table S 2_Down_sig_genes. *pdhR* mutant vs EHEC

ID	foldchange	log2fold	p	p.adj
pdhR	-808.772838	-9.659590736	4.14E-52	2.0733E-50
csgB	-249.502492	-7.962910413	1.167E-185	3.136E-183
csgA	-58.544021	-5.871449933	4.559E-200	1.663E-197
csgC	-42.9792225	-5.42556748	1.6425E-55	8.6493E-54

pspD	-39.9486518	-5.320074911	1.2898E-89	1.3177E-87
sepL	-36.427562	-5.186958539	5.0432E-63	3.3455E-61
cesT	-36.3460922	-5.183728352	9.5627E-41	3.8767E-39
pspC	-35.5625615	-5.152287338	4.1071E-84	3.8143E-82
espZ	-35.205801	-5.137741264	9.3917E-78	7.9955E-76
pspB	-30.8225074	-4.945912323	1.0634E-71	8.6221E-70
pspG	-30.5524684	-4.933217038	1.4487E-70	1.1562E-68
cesD	-28.8145148	-4.848723823	2.3614E-45	1.0052E-43
sepD	-28.8078625	-4.848390715	3.019E-59	1.8359E-57
sctI_2	-28.6615533	-4.841044892	1.6097E-41	6.578E-40
eae	-26.9994514	-4.754858186	1.868E-49	8.7538E-48
escJ	-26.7882606	-4.743529005	1.8696E-47	8.3041E-46
pspA	-26.5889388	-4.732754293	1.254E-47	5.719E-46
espD	-26.5091866	-4.728420498	3.2477E-51	1.5951E-49
espA	-25.5136345	-4.673196527	6.5624E-50	3.1038E-48

escC	-24.6569527	-4.623922607	9.0739E-53	4.6349E-51
pspE	-23.0094893	-4.524157058	1.55E-65	1.0846E-63
etgA	-21.1293192	-4.401174378	1.8528E-06	1.1108E-05
cesD2	-19.3439474	-4.273810321	2.103E-61	1.3772E-59
espB	-19.0832667	-4.254236247	4.3087E-48	1.9828E-46
escG	-18.4577236	-4.206152729	1.8794E-13	2.7273E-12
cesL	-17.9631048	-4.166964829	2.8917E-20	6.5941E-19
tir	-16.58874	-4.052132407	4.4691E-39	1.7164E-37
escV	-15.8439543	-3.985860536	6.7872E-45	2.8652E-43
map_2	-15.5784272	-3.961477677	1.4808E-36	5.4811E-35
ytfE	-14.5807931	-3.86599729	1.267E-87	1.2446E-85
escD	-14.3374345	-3.841714989	1.2303E-39	4.9483E-38
escF	-14.1575224	-3.823496904	6.4759E-22	1.553E-20
escN	-12.9207048	-3.691612864	1.3887E-46	6.0628E-45

espF	-11.9106372	-3.57417869	1.3642E-27	4.1234E-26
escP	-10.0789289	-3.333270428	5.9374E-26	1.6664E-24
espH	-9.31857177	-3.220108855	1.247E-27	3.8143E-26
ymdA	-9.22499033	-3.205547399	1.8156E-27	5.3608E-26
grlA	-8.98604453	-3.167686211	2.2035E-15	3.8812E-14
alaE	-8.74155878	-3.127890562	8.8981E-46	3.8194E-44
hmpA	-8.5995943	-3.104268599	3.6222E-32	1.2502E-30
cesF	-8.3682108	-3.064919195	5.7149E-16	1.0463E-14
grlR	-8.3175409	-3.056157055	5.7093E-21	1.3378E-19
escQ	-8.24232423	-3.043051217	9.3251E-23	2.3123E-21
ldhA	-7.03123574	-2.813778266	2.7251E-61	1.762E-59
ygbA	-6.99355856	-2.806026735	2.4027E-22	5.8723E-21
focA	-6.68045903	-2.739947237	1.6068E-37	6.0795E-36
melR	-6.66239241	-2.736040331	4.7732E-47	2.1019E-45
lgoR	-6.43440864	-2.685807561	1.462E-47	6.6087E-46

ynfD	-6.42198708	-2.683019762	2.417E-30	8.017E-29
fliQ	-6.32377801	-2.660786725	0.00385466	0.01146745
tehA	-6.08247237	-2.604657862	2.1464E-39	8.5653E-38
nrdD	-5.88641256	-2.55738866	3.2223E-32	1.1197E-30
ackA	-5.82486429	-2.542224437	1.4522E-57	8.1512E-56
nirD	-5.4643787	-2.450057471	4.2606E-08	3.2771E-07
ychH	-5.29249644	-2.403948393	2.7776E-29	8.9231E-28
glpA	-5.02341971	-2.328669818	9.9628E-12	1.1672E-10
ssrS	-4.94265164	-2.305285227	1.5193E-28	4.7611E-27
yohC	-4.76490018	-2.25244599	3.132E-20	7.1104E-19
ydcH	-4.63158749	-2.211506765	6.3711E-30	2.0996E-28
grcA	-4.61340782	-2.20583283	7.8964E-11	8.3336E-10
tehB	-4.60239128	-2.202383643	1.7854E-27	5.3021E-26
soxR	-4.56433314	-2.190404094	2.2122E-14	3.56E-13

nrdI	-4.56286588	-2.189940248	7.1512E-30	2.3416E-28
nrdF	-4.54367053	-2.183858227	1.2257E-28	3.8646E-27
yodD	-4.48334815	-2.164576534	5.6489E-24	1.4573E-22
yhhA	-4.45742633	-2.156210955	2.6548E-25	7.1372E-24
escS	-4.42412818	-2.145393185	0.00474751	0.01384147
nleA	-4.33299781	-2.115365508	1.0533E-24	2.7734E-23
dmlA	-4.29914306	-2.104049119	2.4512E-15	4.2444E-14
uspB	-4.20781237	-2.073070374	1.5459E-17	3.0488E-16
yjcB	-4.1815807	-2.064048404	4.2226E-39	1.634E-37
murR	-4.17197995	-2.060732224	0.00154671	0.00514027
nrdE	-4.17032811	-2.060160895	3.8753E-27	1.1312E-25
pta_1	-4.13958247	-2.049485262	1.1301E-33	4.065E-32
gntU	-4.13221348	-2.046914788	6.2734E-09	5.323E-08
ybiJ	-4.02856963	-2.010267691	1.0221E-31	3.5041E-30

metF	-4.01592804	-2.00573342	2.1655E-29	7.0008E-28
adhE	-4.00358874	-2.001293784	3.6932E-17	7.2004E-16
gntK	-3.99185289	-1.997058556	1.4069E-09	1.2856E-08
ybdK	-3.9906921	-1.996638972	1.8932E-27	5.5577E-26
ybdL	-3.97319911	-1.990301093	1.2183E-32	4.3519E-31
ybhS	-3.9090648	-1.966823501	1.1862E-18	2.4631E-17
pgaB	-3.89850229	-1.962919983	3.6408E-28	1.1271E-26
erpA	-3.67510544	-1.877785644	7.0867E-27	2.0336E-25
nirB	-3.61182168	-1.852726668	6.0515E-07	3.9227E-06
cydA	-3.60134705	-1.848536634	9.5221E-29	3.021E-27
yahN	-3.59535405	-1.846133847	8.9091E-09	7.4117E-08
ftnB	-3.58005759	-1.839982794	2.3997E-24	6.286E-23
nrdH	-3.57643317	-1.838521482	9.2556E-20	2.0467E-18
hcp	-3.51963896	-1.815427445	1.5555E-11	1.7776E-10
cydX	-3.51151616	-1.812094073	1.7525E-19	3.8093E-18

bssR	-3.50929222	-1.811180087	4.9996E-13	6.8835E-12
yjfY	-3.50730298	-1.810362062	1.7587E-06	1.0581E-05
yidH	-3.47866749	-1.798534784	0.00906362	0.02436683
frwB	-3.3952273	-1.76350816	0.00026279	0.00105861
cydB	-3.38945769	-1.761054463	2.1173E-26	6.0419E-25
espL	-3.32552458	-1.733581935	1.9604E-06	1.1712E-05
escR	-3.31735896	-1.730035128	1.2129E-05	6.1895E-05
tar	-3.28612274	-1.716386369	1.4997E-11	1.7214E-10
umuD	-3.28473873	-1.715778622	3.8216E-12	4.738E-11
raiA	-3.25988739	-1.70482213	1.143E-22	2.8204E-21
ybhQ	-3.19726458	-1.676838136	7.8472E-13	1.0576E-11
ybjM	-3.16959078	-1.66429659	8.5283E-11	8.9635E-10
aspA	-3.16953136	-1.66426954	5.6021E-20	1.2662E-18
metA	-3.102508	-1.633434933	1.852E-16	3.4779E-15
hcr	-3.09121821	-1.6281755	3.7748E-07	2.5438E-06

yrbG	-3.08580231	-1.625645641	4.2378E-18	8.6242E-17
ybhF	-3.07340562	-1.619838182	6.6637E-20	1.4929E-18
ybhR	-3.07320856	-1.619745675	2.3652E-19	5.0566E-18
bssS	-3.0625394	-1.614728403	2.8996E-14	4.5997E-13
sgrT	-3.0492147	-1.608437736	0.00762801	0.02092582
tnpA_2	-3.04332678	-1.605649253	1.1182E-10	1.1657E-09
ytfP	-2.95401097	-1.562675182	7.4186E-24	1.8947E-22
yncG	-2.95238456	-1.56188065	0.01360232	0.0344817
yfdY	-2.94949207	-1.560466529	8.6047E-24	2.1867E-22
cysP	-2.94176735	-1.556683157	4.5386E-13	6.2827E-12
acrZ	-2.94054267	-1.556082425	3.3897E-10	3.3621E-09
cspD	-2.88979837	-1.530968835	5.8896E-19	1.238E-17
ygeV	-2.86649314	-1.519286826	3.5811E-13	5.0392E-12
uhpT	-2.85704608	-1.514524305	0.00415828	0.01227065
ybaE	-2.85429172	-1.513132794	3.1161E-12	3.9108E-11

escE	-2.85428519	-1.513129488	3.7112E-05	0.00017344
symE	-2.85214176	-1.512045689	0.02277903	0.05384326
yohD	-2.83111306	-1.501369365	8.7098E-14	1.2933E-12
ydeN	-2.81538422	-1.493331821	3.3873E-24	8.783E-23
adiY	-2.80213182	-1.486524823	3.0375E-07	2.0771E-06
yohK	-2.79714555	-1.483955326	1.8345E-25	4.9843E-24
escT	-2.78701678	-1.47872169	0.00146736	0.00489567
yqgA	-2.77739232	-1.47373098	1.2219E-06	7.556E-06
glpD	-2.77027273	-1.470028015	1.1661E-13	1.7116E-12
appB	-2.76575093	-1.467671239	3.2152E-05	0.00015137
yqfA	-2.74801218	-1.458388397	8.2288E-18	1.6614E-16
yihV	-2.74158826	-1.455011918	0.00012408	0.00053463
copD	-2.73074302	-1.449293556	1.2333E-18	2.5505E-17
zapA	-2.72888594	-1.448312095	1.9012E-19	4.1149E-18

uspG	-2.72832714	-1.448016642	4.8533E-14	7.4224E-13
yhaK	-2.7258017	-1.446680612	3.8492E-10	3.7884E-09
mqo	-2.72254839	-1.444957693	1.7319E-15	3.0611E-14
sufB	-2.71992415	-1.443566417	1.5128E-12	1.9663E-11
yccT	-2.70983194	-1.438203382	1.7915E-07	1.2799E-06
leuO	-2.70537292	-1.435827472	7.139E-08	5.3432E-07
aslA	-2.70490939	-1.435580269	6.3376E-12	7.6894E-11
norW	-2.70109587	-1.433544849	3.1967E-06	1.8368E-05
allS	-2.6859154	-1.425413866	0.00403157	0.01193812
yjdI	-2.68189675	-1.423253698	0.00056429	0.00208923
soxS	-2.67796994	-1.421139767	4.9829E-13	6.8791E-12
rmf	-2.67740728	-1.420836614	4.2841E-14	6.5913E-13
glpF	-2.67209616	-1.417971927	9.2084E-08	6.7972E-07
cysD	-2.65299629	-1.407622658	6.8297E-05	0.00030683
pgaA	-2.64917555	-1.405543446	5.7262E-17	1.0955E-15

pdeB	-2.62787397	-1.393896088	5.4241E-17	1.0455E-15
tatD	-2.61112376	-1.38467084	9.117E-18	1.8263E-16
bsmA	-2.61009024	-1.384099687	2.9976E-10	2.9848E-09
dcuA	-2.6062218	-1.381959871	4.3056E-19	9.1258E-18
chpS	-2.59695275	-1.376819766	8.9425E-12	1.0574E-10
umuC	-2.59636235	-1.376491742	2.6863E-11	2.9895E-10
yidF	-2.59377841	-1.375055234	3.3493E-06	1.9115E-05
hspQ	-2.59347758	-1.3748879	1.1032E-12	1.4599E-11
emrE	-2.57778914	-1.366134256	5.1185E-09	4.409E-08
asnC	-2.57545702	-1.364828467	2.4072E-10	2.4396E-09
ada	-2.57192733	-1.362849878	2.3328E-15	4.0531E-14
ygiD	-2.54014184	-1.344909058	7.0342E-09	5.9194E-08
sufC	-2.53238276	-1.340495477	1.8147E-11	2.0553E-10
cecR	-2.53114521	-1.339790274	6.2274E-10	5.9236E-09

allR	-2.53020945	-1.339256815	4.3023E-16	7.9336E-15
hlyD	-2.52113989	-1.334076169	2.5017E-14	4.0058E-13
ubiV	-2.51266531	-1.329218515	9.7078E-05	0.00042674
yhhN	-2.50634241	-1.325583528	2.467E-15	4.2573E-14
rof	-2.50502715	-1.324826237	4.0486E-14	6.2667E-13
ucpA	-2.50197666	-1.323068329	6.0084E-15	1.003E-13
malQ	-2.49864818	-1.321147779	5.5658E-08	4.2244E-07
tdcA	-2.49082501	-1.316623671	5.8283E-05	0.00026463
yijE	-2.48474636	-1.313098592	6.1208E-16	1.1166E-14
ldtE	-2.48278698	-1.311960484	4.8582E-15	8.2444E-14
ycjM	-2.47738644	-1.308818928	1.3726E-06	8.3767E-06
yeeE	-2.47715327	-1.308683134	0.00064026	0.00232938
uidR	-2.46697261	-1.302741697	8.8256E-18	1.7749E-16
exuT	-2.45757328	-1.297234438	6.5894E-12	7.9759E-11

yibH	-2.45318085	-1.294653594	0.00034912	0.00135508
qorA	-2.44715942	-1.291108089	5.292E-17	1.0239E-15
dkgB	-2.44438794	-1.289473267	2.541E-14	4.0561E-13
fryC	-2.42241775	-1.276447679	0.00428664	0.01259848
yhcO	-2.41281892	-1.270719646	0.00035274	0.00136809
chpB	-2.4098121	-1.268920657	3.9001E-06	2.1885E-05
hybE	-2.40274141	-1.264681387	2.3167E-09	2.0724E-08
fucP	-2.38565234	-1.254383817	0.00225327	0.00717562
yqjA	-2.38258899	-1.252530102	5.5995E-15	9.4709E-14
cysN	-2.3770671	-1.249182627	1.8672E-07	1.3317E-06
ypeC	-2.37227105	-1.246268859	9.339E-15	1.529E-13
yfbV	-2.36981492	-1.244774391	8.3129E-15	1.3654E-13
sufA	-2.36174783	-1.239854932	2.1941E-10	2.2282E-09
zapB	-2.36023395	-1.238929866	1.1707E-12	1.5412E-11
tnpA_1	-2.35867147	-1.237974486	3.8636E-14	6.0169E-13

sufD	-2.35850806	-1.237874533	1.5078E-09	1.3729E-08
narI_1	-2.35666942	-1.236749399	5.4114E-07	3.5347E-06
fdnH	-2.3541555	-1.235209621	0.00035724	0.00138346
ubiU	-2.35001455	-1.232669692	0.00083506	0.0029478
yohJ	-2.34025247	-1.22666418	3.5574E-14	5.5569E-13
ycgB	-2.33646698	-1.22432865	1.1763E-11	1.3594E-10
yhdN	-2.32681866	-1.218358779	1.8692E-07	1.3317E-06
fucO	-2.32605897	-1.217887671	7.9598E-08	5.9011E-07
sulA	-2.31606294	-1.211674458	2.757E-12	3.512E-11
yqaE	-2.30753024	-1.206349555	4.7798E-07	3.1544E-06
hcxA	-2.29193014	-1.196563072	7.0885E-15	1.1756E-13
rhaR	-2.28419504	-1.191685843	4.8964E-07	3.2272E-06
malP	-2.27936448	-1.188631635	3.1761E-06	1.827E-05
yobA	-2.27714285	-1.187224795	6.1876E-14	9.3234E-13

nrdA	-2.27171166	-1.183779733	3.4197E-11	3.7728E-10
yjbH	-2.26043989	-1.176603551	1.8242E-06	1.0949E-05
dtpA	-2.25778268	-1.174906628	6.6741E-10	6.3366E-09
yniB	-2.25514874	-1.17322259	2.6345E-12	3.3642E-11
clpB	-2.25334867	-1.172070563	5.1037E-05	0.00023381
ydiH	-2.25036209	-1.170157155	2.3172E-13	3.3063E-12
amiD	-2.24737524	-1.168241029	4.0862E-12	5.0416E-11
ygiW	-2.2388558	-1.16276161	1.1134E-08	9.173E-08
adiC	-2.23482455	-1.160161571	0.00042658	0.00162852
ydgD	-2.23349208	-1.159301137	3.9177E-11	4.2944E-10
yghB	-2.23107472	-1.157738829	4.9831E-14	7.5981E-13
clsC	-2.23055493	-1.15740268	5.2596E-13	7.222E-12
lipA	-2.22653795	-1.154802201	8.154E-13	1.0903E-11
treF	-2.2263264	-1.15466512	2.9097E-10	2.9029E-09
cdd	-2.22603673	-1.154477399	2.0006E-13	2.8949E-12

malK	-2.2229373	-1.152467258	4.9294E-06	2.7016E-05
chiP	-2.22000035	-1.150559906	1.5018E-05	7.528E-05
yihO	-2.21644499	-1.148247557	0.00028081	0.00111971
yadI	-2.21496301	-1.147282609	2.7951E-06	1.6261E-05
yeeY	-2.2085382	-1.143091788	1.0804E-13	1.5904E-12
nleE	-2.20316618	-1.139578316	1.2859E-14	2.0985E-13
yfeC	-2.20054828	-1.137863027	3.1784E-11	3.5141E-10
cpxP	-2.19959771	-1.137239687	1.1548E-10	1.2014E-09
sufS	-2.19916354	-1.136954892	6.078E-09	5.1831E-08
yfcZ	-2.19113128	-1.131675928	3.9255E-07	2.6314E-06
fdnI	-2.18980432	-1.13080196	0.00176155	0.00578648
ssrA	-2.18508693	-1.127690673	7.6856E-10	7.2432E-09
yiiR	-2.1843674	-1.127215531	1.4273E-08	1.1609E-07
yniA	-2.17745148	-1.122640574	5.2929E-12	6.4679E-11
mntH	-2.17712606	-1.122424943	1.0878E-11	1.2657E-10

ybhL	-2.1761628	-1.121786489	7.1872E-11	7.6484E-10
napC	-2.17611178	-1.121752666	3.3767E-05	0.00015853
epd	-2.17570869	-1.121485404	5.2812E-10	5.0995E-09
rraA	-2.17471192	-1.120824301	1.1587E-12	1.5293E-11
ygjR	-2.1729365	-1.119646016	5.64E-13	7.7236E-12
espL2	-2.1680992	-1.11643077	3.5129E-12	4.3765E-11
deoC	-2.15581491	-1.108233317	2.1384E-13	3.0768E-12
uidC	-2.15567233	-1.108137899	0.01793304	0.04389824
yidG	-2.14670704	-1.102125322	0.00041788	0.00159891
pdxI	-2.14243911	-1.099254204	6.9824E-09	5.8855E-08
uspA	-2.13896187	-1.096910762	2.6151E-11	2.9229E-10
cynS	-2.13583976	-1.094803416	4.694E-06	2.5865E-05
ler	-2.13097305	-1.09151235	0.00475293	0.0138415
ydhL	-2.12991634	-1.090796765	0.00047498	0.00179054
yaaU	-2.12873103	-1.089993674	0.00127245	0.00433601

yidE	-2.12703614	-1.088844543	4.2269E-07	2.8113E-06
yjbQ	-2.12416879	-1.086898408	1.4245E-12	1.861E-11
tusA	-2.12272451	-1.08591715	1.9896E-09	1.7861E-08
hokE_2	-2.12154291	-1.085113856	0.00139476	0.00470572
eamB	-2.11784976	-1.082600245	5.1628E-06	2.8145E-05
xylE	-2.11719398	-1.082153457	7.2822E-11	7.7013E-10
sra	-2.11389777	-1.079905609	2.8783E-05	0.00013626
metN	-2.11223346	-1.078769302	4.6049E-12	5.6408E-11
lsrR	-2.11092922	-1.077878202	1.1376E-06	7.0952E-06
mntS	-2.10477592	-1.073666649	5.1689E-10	5.01E-09
yoaG	-2.10401948	-1.073148065	0.0004034	0.00155164
yhhT	-2.09871797	-1.069508308	4.0623E-06	2.2728E-05
pgaC	-2.09865275	-1.069463476	1.7812E-06	1.0704E-05
lsrD	-2.09522277	-1.067103646	0.02292561	0.05408962

alkB	-2.093014	-1.065581962	1.9325E-06	1.1559E-05
feoC	-2.08921358	-1.062959984	0.00049495	0.00186171
ygaP	-2.08692611	-1.061379518	7.2403E-09	6.0828E-08
rimL	-2.08358061	-1.059064919	3.7862E-13	5.2986E-12
ybiI	-2.08207952	-1.058025168	0.00024096	0.00098067
fic	-2.07730825	-1.054715311	0.00036692	0.0014188
yfcC	-2.07399522	-1.05241257	0.00010908	0.00047583
ybgE	-2.06792677	-1.048185094	6.3338E-13	8.6275E-12
yhjX	-2.06636284	-1.047093605	0.00099914	0.0034813
gpr	-2.06121107	-1.043492245	5.7896E-09	4.962E-08
uspF	-2.04818632	-1.03434696	3.0504E-08	2.3934E-07
flgL	-2.0475488	-1.033897835	1.8455E-08	1.4798E-07
tap	-2.04610719	-1.032881727	0.00022574	0.0009247
yacL	-2.0422462	-1.030156799	1.2774E-06	7.8802E-06
kdpD	-2.04210665	-1.030058213	2.1637E-08	1.7269E-07

grxA	-2.03976542	-1.028403247	0.00482613	0.01401471
ybjC	-2.03452445	-1.024691616	5.8965E-05	0.00026749
srlA	-2.02958092	-1.021181862	0.00458786	0.01339895
nrdB	-2.0229649	-1.016471289	3.8204E-10	3.7673E-09
recN	-2.02221766	-1.015938292	1.336E-08	1.0919E-07
yegH	-2.02194543	-1.015744058	1.111E-11	1.2898E-10
uspC	-2.02069846	-1.014854054	2.6394E-11	2.9437E-10
agaD	-2.01704242	-1.012241427	0.01544954	0.03858285
zitB	-2.01366679	-1.009824976	4.2155E-08	3.2478E-07
hcaD	-2.01240069	-1.008917586	0.00077402	0.0027571
phnP	-2.00801352	-1.005768986	0.00892191	0.02406183
hofQ	-2.00231132	-1.001666305	0.01524068	0.03814278
torT	-2.00104603	-1.000754355	0.00259284	0.0081503
lysA	-2.00075752	-1.000546333	5.3155E-10	5.1229E-09

pbpC	-1.99623993	-0.997285129	7.9754E-05	0.00035579
ychE	-1.99448742	-0.996018021	2.5977E-10	2.6172E-09
narJ	-1.99442511	-0.995972952	2.0417E-05	9.876E-05
yegP	-1.99171473	-0.994011028	3.4585E-07	2.343E-06
yijD	-1.98844141	-0.99163805	8.861E-10	8.2445E-09
yicJ	-1.98756426	-0.991001507	0.00030302	0.00119524
sufE	-1.98586695	-0.989768968	2.7901E-07	1.9233E-06
cobU	-1.98493429	-0.989091247	5.6855E-15	9.5847E-14
bioP	-1.98218546	-0.987091952	6.122E-10	5.845E-09
narH_1	-1.97718238	-0.983445958	3.5836E-08	2.7862E-07
slyA	-1.97651712	-0.982960455	2.6149E-10	2.6293E-09
dtpB	-1.97332623	-0.980629482	1.6897E-05	8.339E-05
emrD	-1.972098	-0.979731244	5.652E-05	0.00025708
fumD	-1.97025989	-0.978385941	0.00100537	0.00350062

malS	-1.96835326	-0.976989162	2.252E-05	0.00010781
csrA	-1.96577283	-0.975096611	1.3283E-10	1.3791E-09
yhaH	-1.96365628	-0.973542422	1.4628E-07	1.0539E-06
yhhL	-1.95984122	-0.970736779	3.0654E-06	1.7733E-05
ypfH	-1.95355061	-0.966098631	7.6524E-10	7.2252E-09
yjjI	-1.95190857	-0.96488548	0.00147371	0.00491045
lhr	-1.95167403	-0.96471211	4.3804E-11	4.781E-10
bioC	-1.94808719	-0.962058249	6.4918E-09	5.481E-08
ybfA	-1.94712058	-0.961342226	1.2187E-08	9.9921E-08
yjbJ	-1.9461972	-0.9606579	3.9037E-07	2.6203E-06
yecE	-1.94592465	-0.960455844	2.9612E-09	2.626E-08
yhhS	-1.9419364	-0.957495954	2.5229E-08	1.9918E-07
gntT	-1.93635241	-0.95334154	1.5312E-07	1.1001E-06
torA	-1.9351295	-0.952430116	0.00026002	0.00104993
ydhR	-1.93343569	-0.951166782	6.1353E-10	5.8468E-09

pnuC	-1.92852862	-0.947500558	1.661E-08	1.3382E-07
appA	-1.92323506	-0.9435351	1.6648E-05	8.2401E-05
yciN	-1.91917127	-0.940483462	3.2024E-07	2.1781E-06
nimT	-1.91795512	-0.939568961	0.00029952	0.00118324
nrfE	-1.91770537	-0.939381089	0.02155939	0.05148452
ytfK	-1.91377477	-0.936421048	0.00046269	0.00174938
nleB	-1.90532756	-0.930039043	2.9779E-09	2.6363E-08
copA	-1.90277717	-0.928106621	1.1776E-06	7.3174E-06
hybD	-1.90008293	-0.926062389	0.00016191	0.00068238
nupG	-1.89861051	-0.924943978	3.0974E-07	2.1124E-06
yejE	-1.89424402	-0.921622196	1.7456E-11	1.9814E-10
fliK	-1.8919539	-0.919876935	0.00579516	0.01646368
btsS	-1.89060588	-0.918848647	7.898E-09	6.6028E-08
ybjQ	-1.8881095	-0.916942436	8.1462E-05	0.00036278
yjbR	-1.88644181	-0.915667602	3.4782E-08	2.7083E-07

cesAB	-1.88363243	-0.913517468	0.01045673	0.02761788
hokD_5	-1.88137495	-0.911787401	6.209E-07	4.0197E-06
ynfF	-1.87930227	-0.910197132	6.0826E-05	0.00027544
yhdP	-1.87924075	-0.9101499	1.4407E-08	1.1681E-07
psiE	-1.87771459	-0.908977795	2.1692E-08	1.728E-07
fldB	-1.87690196	-0.908353289	1.1374E-09	1.0468E-08
ydhU	-1.86877997	-0.902096717	0.0031063	0.00953843
viaA	-1.86528206	-0.899393806	1.5207E-08	1.2291E-07
ydcJ	-1.86420635	-0.898561564	0.0018891	0.0061462
cynX	-1.86418491	-0.898544972	0.00653828	0.01833014
malZ	-1.85560359	-0.891888544	1.6871E-05	8.3344E-05
yhjE	-1.85522507	-0.891594218	1.6586E-09	1.5022E-08
espG	-1.85218168	-0.889225622	0.00080376	0.00284912
malE	-1.85197148	-0.889061882	0.00142567	0.00478784

hofC	-1.85132064	-0.888554785	5.5054E-07	3.5869E-06
mdtD_2	-1.84856958	-0.886409347	5.1993E-10	5.0299E-09
yeaO	-1.84853257	-0.886380462	0.00016602	0.00069798
yjcO	-1.84775791	-0.885775751	4.6876E-09	4.0766E-08
zntA	-1.84184943	-0.881155125	4.0825E-07	2.7295E-06
ypfN	-1.84079149	-0.880326222	1.1029E-05	5.6734E-05
hofM	-1.83826741	-0.878346646	0.00302011	0.00930441
ypeB	-1.83683463	-0.877221748	5.4665E-06	2.961E-05
smg	-1.830097	-0.87192012	4.3476E-08	3.3294E-07
fxsA	-1.83004655	-0.871880344	0.00507683	0.01467598
aer	-1.82552537	-0.868311718	0.00201126	0.00650222
yfeR	-1.82398129	-0.867090935	1.1916E-06	7.3868E-06
osmB	-1.82385757	-0.866993073	0.00975852	0.02600235
fau	-1.82212152	-0.86561918	1.7345E-09	1.5598E-08

priC	-1.82019781	-0.864095246	3.4847E-07	2.3576E-06
adrA	-1.81885293	-0.863028894	0.00024241	0.00098505
prlF	-1.81485193	-0.859851846	2.5766E-06	1.5111E-05
frvX	-1.81275972	-0.85818771	0.00540065	0.01549804
rpoE	-1.81231943	-0.857837262	5.6279E-07	3.6621E-06
yrdD	-1.81071598	-0.856560273	3.212E-08	2.5087E-07
csiE	-1.81066419	-0.856519009	2.5468E-06	1.4953E-05
zur	-1.80553655	-0.852427626	1.3633E-06	8.3399E-06
yiaC	-1.802863	-0.850289773	0.00230366	0.0073224
nfeR	-1.80185682	-0.849484376	4.8557E-05	0.00022285
nleL	-1.79708701	-0.845660261	4.4528E-08	3.4049E-07
metE	-1.7954425	-0.844339448	5.732E-06	3.0885E-05
hexR	-1.79359219	-0.842851898	7.731E-06	4.0838E-05
hxpA	-1.78890542	-0.839077115	4.0688E-08	3.1442E-07
yhcB	-1.78545454	-0.836291402	7.8039E-08	5.7939E-07

sbmC	-1.78523311	-0.836112471	0.00033623	0.00131106
modA	-1.78386023	-0.835002577	0.01119116	0.02927007
moaA	-1.77832137	-0.830516068	2.8898E-06	1.6793E-05
yjfF	-1.77753438	-0.829877466	0.00139144	0.00469762
ibpB	-1.77562441	-0.828326444	0.00065062	0.00236233
mobA	-1.77546342	-0.828195633	5.7153E-09	4.9065E-08
ppnN	-1.7751432	-0.827935408	5.0826E-07	3.3413E-06
dgcN	-1.77299913	-0.826191828	3.0605E-08	2.3977E-07
aes	-1.76703186	-0.821328056	0.01055182	0.02784024
yphA	-1.76700518	-0.821306272	0.00982609	0.02611428
mzrA	-1.76365013	-0.818564393	4.3831E-07	2.9077E-06
yphG	-1.76161348	-0.816897417	0.00135061	0.00457186
yaiA	-1.76144752	-0.816761493	2.0967E-05	0.00010133
ldtA	-1.76110739	-0.816482883	4.1577E-07	2.7725E-06

add	-1.76088918	-0.816304113	2.7015E-06	1.5735E-05
chbG	-1.75554364	-0.811917856	1.3133E-06	8.0726E-06
ycdZ	-1.75496132	-0.811439237	7.3829E-06	3.9039E-05
oxyR	-1.75453093	-0.811085383	4.6697E-06	2.5775E-05
araC	-1.75432501	-0.810916047	0.00275499	0.00858079
phoR	-1.75339584	-0.810151733	0.00012679	0.00054469
queE	-1.75278843	-0.809651864	9.6699E-07	6.1056E-06
ynbD	-1.75238794	-0.809322193	0.00278302	0.00864699
ycbJ	-1.75008695	-0.807426601	4.7354E-06	2.6065E-05
ihfA	-1.74362432	-0.80208923	2.4179E-06	1.4278E-05
lysS_2	-1.74161727	-0.800427621	1.3936E-05	7.0132E-05
yhaV	-1.74130052	-0.800165211	0.00081718	0.00288868
macB	-1.74116395	-0.800052058	2.1506E-07	1.511E-06
yraR	-1.73890222	-0.798176813	0.00534411	0.01535305

yajO	-1.73810183	-0.79751261	6.3717E-05	0.00028726
osmC	-1.73758883	-0.797086732	1.1686E-05	5.9934E-05
malG	-1.73710291	-0.796683223	0.00335101	0.01016448
yfeH	-1.73683075	-0.796457175	2.1665E-07	1.5201E-06
yoaE	-1.73440986	-0.794444862	2.094E-07	1.4814E-06
yhhM	-1.73216545	-0.792576736	5.2211E-05	0.00023876
dinD	-1.72836327	-0.789406474	8.801E-07	5.6054E-06
rutR	-1.72611396	-0.787527716	0.00262157	0.00821397
lpfE	-1.72577936	-0.787248025	0.01082022	0.02847486
yifB	-1.7244192	-0.786110532	0.00030414	0.00119872
kdpA	-1.7228768	-0.784819539	0.01583871	0.03938859
dsbB	-1.72132448	-0.783519083	3.3658E-06	1.9188E-05
nleH1-2	-1.72101967	-0.78326359	7.1445E-08	5.3432E-07
ravA	-1.71663092	-0.779579891	3.5794E-06	2.0203E-05
yfhM	-1.71589029	-0.778957313	1.0212E-06	6.4003E-06

cutC	-1.71539795	-0.778543303	2.518E-05	0.00011987
ygaM	-1.71515933	-0.778342604	0.00187928	0.00611814
fepD	-1.70933218	-0.773432786	8.4924E-07	5.4292E-06
yccA	-1.70858863	-0.772805088	4.3654E-06	2.4185E-05
metJ	-1.70850538	-0.772734787	1.6021E-09	1.4536E-08
mokC	-1.70658562	-0.771112797	6.132E-06	3.2833E-05
yeaR	-1.70482445	-0.769623192	0.00391027	0.01161936
hycI	-1.70461352	-0.769444678	0.00024114	0.00098067
ompX	-1.70453607	-0.769379133	3.5394E-06	2.0043E-05
mgsA	-1.70414109	-0.769044784	7.4281E-08	5.523E-07
zntR	-1.70354308	-0.768538431	0.00019743	0.00081991
yhfK	-1.70344307	-0.768453735	3.3256E-06	1.9002E-05
rpoS	-1.70218376	-0.76738679	3.5616E-06	2.0147E-05
folB	-1.7014298	-0.766747631	0.01704619	0.04194216

cysC	-1.70026871	-0.765762769	0.00642311	0.01802706
ulaE	-1.69676917	-0.762790317	0.0199782	0.04836429
yidB	-1.69656812	-0.762619356	0.00448649	0.01314048
ubiF	-1.69453123	-0.760886226	3.5288E-06	2.0006E-05
glgX	-1.69427936	-0.760671773	4.4682E-07	2.9603E-06
shiA	-1.69402597	-0.760455993	5.256E-06	2.8561E-05
yfbS	-1.69226847	-0.758958464	5.3336E-08	4.0602E-07
ccmA	-1.68986969	-0.756911999	0.02315976	0.05459161
yhbQ	-1.68981362	-0.756864132	0.00525027	0.01511746
sapF	-1.6897469	-0.756807167	8.3314E-06	4.3828E-05
yafD	-1.68952285	-0.756615859	1.2339E-06	7.6214E-06
cpxA	-1.6887924	-0.755991995	4.1896E-06	2.3337E-05
malY	-1.68636731	-0.753918803	2.4761E-07	1.7255E-06
nagA_2	-1.68447439	-0.752298496	0.00262008	0.00821397
csgE	-1.68387414	-0.751784305	0.00027673	0.00110866

ampD	-1.6817274	-0.749943874	4.9341E-09	4.2573E-08
ygbE	-1.67878987	-0.747421662	0.00536971	0.01541792
clpS	-1.67793833	-0.746689692	0.00074946	0.00268083
yfbM	-1.6773018	-0.746142298	0.00868849	0.02351405
frlB	-1.67677207	-0.745686593	0.02013167	0.0486206
arcC	-1.67376253	-0.743094852	0.00041669	0.00159554
dcuB	-1.67135834	-0.741021084	0.00352434	0.01062711
csgD	-1.67048263	-0.740264978	1.9802E-05	9.615E-05
yabI	-1.66962738	-0.739526163	1.9005E-05	9.2631E-05
glgB	-1.66873821	-0.738757642	3.1057E-06	1.7945E-05
yejB	-1.66829913	-0.738377988	5.3118E-05	0.00024269
fdrA_1	-1.66706706	-0.737312137	0.0205564	0.0493663
sixA	-1.6659114	-0.736311671	2.2837E-05	0.00010912
glpB	-1.66499506	-0.735517901	0.01793571	0.04389824
ampE	-1.66323128	-0.733988795	2.6426E-07	1.834E-06

yjiM	-1.66256653	-0.733412075	0.01352065	0.03435994
rstB	-1.66104544	-0.732091537	3.8681E-06	2.1736E-05
yrbL	-1.65872771	-0.730077076	1.8846E-05	9.1943E-05
yhhJ	-1.65759858	-0.729094675	0.00120982	0.00415587
grxB	-1.65632318	-0.727984195	6.184E-06	3.3076E-05
satP	-1.6553553	-0.727140906	3.0761E-05	0.00014549
comR	-1.6546086	-0.726489988	8.448E-06	4.435E-05
panE	-1.65319134	-0.72525371	1.6221E-05	8.0522E-05
hokD_3	-1.65218697	-0.724376955	9.1522E-06	4.7703E-05
fdhD	-1.65126591	-0.723572459	4.3342E-05	0.00020017
ydgK	-1.65071223	-0.723088637	7.7411E-07	4.9738E-06
nlpD	-1.64957982	-0.722098587	8.8363E-06	4.6246E-05
lapB	-1.64919047	-0.721758026	6.8253E-07	4.402E-06
fepG	-1.64637755	-0.719295211	1.9068E-05	9.2848E-05
tusE	-1.64591204	-0.71888724	5.002E-06	2.7356E-05

rbsD	-1.64571757	-0.718716768	0.00065785	0.00238319
garD	-1.64521804	-0.718278797	0.00456339	0.01333514
ybiW	-1.6447399	-0.717859453	0.0093164	0.02495447
ydhX	-1.64392364	-0.717143288	0.01224664	0.03156197
ybaP	-1.64363353	-0.716888671	1.6688E-06	1.0064E-05
ssuB	-1.64268114	-0.716052462	0.01197368	0.03097086
yhgE	-1.63975302	-0.71347853	6.3048E-05	0.0002845
yibL	-1.63894411	-0.712766657	1.2261E-05	6.2442E-05
yciY	-1.63696149	-0.711020378	0.00012945	0.00055474
cobS	-1.63621215	-0.710359815	3.8093E-05	0.00017705
araJ	-1.63411213	-0.708506983	3.0222E-06	1.7503E-05
miaA	-1.63260487	-0.707175662	2.1994E-05	0.00010549
glgS	-1.63222669	-0.706841441	0.00494546	0.01432053
metI	-1.62982252	-0.704714871	4.3469E-06	2.4135E-05

ycjF	-1.62568097	-0.701044165	0.0002772	0.00110967
appC	-1.62535479	-0.700754668	0.01459063	0.03667762
yejM	-1.62363478	-0.699227147	4.363E-06	2.4185E-05
fliD	-1.62348826	-0.69909695	0.00740631	0.02037235
ydcY	-1.62296862	-0.698635105	1.8082E-05	8.8553E-05
hrpB	-1.62277328	-0.698461455	1.0749E-07	7.8774E-07
thpR	-1.61989075	-0.695896516	0.01511903	0.03787543
araG	-1.61944279	-0.695497502	0.0049122	0.01424037
yqcA	-1.61844174	-0.694605434	2.4558E-06	1.4469E-05
ugpQ	-1.61748855	-0.693755497	7.0922E-05	0.00031778
ybeL	-1.61517332	-0.691688986	0.000171	0.00071656
pflB	-1.61492567	-0.691467765	0.00036404	0.00140872
yihY	-1.61449758	-0.69108528	2.8139E-07	1.9371E-06
cls	-1.61204942	-0.688895968	2.1301E-05	0.00010274

bioD_2	-1.61092484	-0.687889186	0.00134936	0.00457064
xylB	-1.6108757	-0.687845176	5.7291E-08	4.3416E-07
yhhW	-1.60962722	-0.686726608	4.9478E-06	2.7088E-05
yfhH	-1.60729722	-0.684636739	0.00913098	0.02450922
lptG	-1.60581415	-0.683304934	2.4872E-06	1.4636E-05
ypdC	-1.60366973	-0.681377058	1.1965E-07	8.6935E-07
lapA	-1.60160544	-0.679518783	0.00011622	0.00050352
tssF	-1.60123208	-0.679182421	0.01050224	0.02772375
hybC	-1.60009742	-0.678159747	0.00011238	0.00048897
ynfH	-1.59938418	-0.67751652	0.00020585	0.0008514
dmsC	-1.5992936	-0.677434815	0.00224252	0.00714584
ybbJ	-1.5987153	-0.676913047	0.01175179	0.03047113
acrF	-1.59524992	-0.67378246	4.746E-06	2.6096E-05
gss	-1.59327231	-0.671992861	1.7049E-05	8.398E-05
ybaQ	-1.59300222	-0.67174828	2.7241E-05	0.0001292

fhuA	-1.59209777	-0.670928934	4.3398E-05	0.00020025
pxpA	-1.59085025	-0.669798034	2.2907E-05	0.00010935
robA	-1.58816357	-0.667359505	1.3329E-05	6.7333E-05
rpsU	-1.58696138	-0.666267018	1.2654E-05	6.4058E-05
focB	-1.58533406	-0.664786873	0.00202132	0.00652837
yfgO	-1.58351691	-0.663132277	3.2999E-05	0.00015521
ybbP	-1.58301933	-0.66267887	0.00012128	0.00052412
mdaB	-1.58229409	-0.662017772	0.00015874	0.00067123
ccmH	-1.58038604	-0.660277004	0.00193499	0.00628348
garK	-1.57941859	-0.659393572	0.00158429	0.00525149
hdfR	-1.5790656	-0.659071103	1.1698E-05	5.9934E-05
edd	-1.57793649	-0.658039142	0.00086094	0.00303289
ydiU	-1.57635041	-0.656588266	8.7776E-05	0.00038853
yicI	-1.57134463	-0.651999633	0.00012429	0.00053484

ybeQ	-1.57060384	-0.651319333	0.00234235	0.00742688
evgS	-1.57010592	-0.650861887	0.00019247	0.00080061
yicN	-1.57005945	-0.65081919	0.00327816	0.00999751
ybaT	-1.56790068	-0.648834178	0.00069526	0.00250804
malF	-1.56686593	-0.647881738	0.00402666	0.01193051
yfaL	-1.56484064	-0.64601574	3.1624E-05	0.00014915
htpX	-1.56401119	-0.645250834	5.0685E-05	0.00023241
djlC	-1.56340247	-0.644689225	0.02018902	0.04871304
ydhC	-1.56048757	-0.641996868	0.00062927	0.00229595
moaD	-1.55947301	-0.641058585	0.01042715	0.02755401
hemD	-1.55933322	-0.640929253	7.8858E-06	4.1612E-05
mobB	-1.55746719	-0.639201771	0.00421087	0.0124115
slyB	-1.55507954	-0.636988371	1.0888E-05	5.6122E-05
helD	-1.55091671	-0.633121207	3.8412E-05	0.00017821

srlE	-1.55049644	-0.632730212	0.01415208	0.0356982
pspF	-1.54991489	-0.632188999	0.00026201	0.00105633
yebG	-1.54957006	-0.631867982	5.7627E-05	0.00026189
thiK	-1.54909805	-0.631428462	0.00040705	0.00156213
fumE	-1.54762153	-0.630052705	0.00127418	0.004339
psiF	-1.54718302	-0.629643864	0.00106652	0.00369091
secM	-1.54659092	-0.629091652	1.8455E-05	9.0124E-05
yqhD	-1.54535012	-0.62793374	2.8623E-05	0.00013563
ehaG	-1.54111424	-0.62397381	6.9904E-05	0.00031349
mdlA	-1.54024394	-0.623158858	8.4024E-05	0.00037354
qmcA	-1.54017254	-0.623091977	7.743E-05	0.00034603
ydcK	-1.54001277	-0.622942318	0.01588729	0.03947094
ribB	-1.53862258	-0.621639389	0.00029658	0.00117255
yddM	-1.53793405	-0.620993638	0.00285416	0.00882509

abrB	-1.53403855	-0.617334736	0.00410313	0.01212191
mdlB	-1.53287103	-0.61623632	0.00022888	0.00093681
ribD	-1.5317579	-0.61518829	1.5053E-05	7.5381E-05
mdtH	-1.52988917	-0.61342714	0.00042555	0.00162581
aaeB	-1.5293445	-0.612913429	0.00092955	0.00325661
dcuR	-1.52924353	-0.61281817	0.00040429	0.00155389
eutK	-1.5265636	-0.610287697	0.01102446	0.02892294
yebY	-1.5265304	-0.610256318	0.00022057	0.00090495
pfkB	-1.52651724	-0.610243883	9.8492E-05	0.00043221
dinB	-1.52497187	-0.608782629	9.3109E-05	0.00041071
yjfP	-1.52422553	-0.608076382	0.00027023	0.00108451
ybjD	-1.52398012	-0.607844081	0.00032198	0.00126127
ptsP_2	-1.52242513	-0.606371281	0.000258	0.00104262
moaB	-1.52157101	-0.605561661	0.001578	0.00523406
uspE	-1.52103492	-0.605053275	0.00031755	0.00124581

yafV	-1.52073223	-0.604766148	0.00033811	0.00131738
ldtD	-1.51783424	-0.602014241	7.3502E-05	0.00032876
ymdB	-1.51744094	-0.601640366	5.6234E-05	0.00025601
uxuR	-1.5174179	-0.601618459	0.00077034	0.0027459
pflA	-1.51584234	-0.600119707	0.00017646	0.00073761
yfiR	-1.51516888	-0.599478607	0.0008976	0.00315333
hprS	-1.51457267	-0.598910801	0.00019154	0.00079737
kefB	-1.51454458	-0.598884044	0.00074174	0.00265507
metK	-1.5136928	-0.598072448	0.00057032	0.00210948
feoA	-1.51359785	-0.597981942	0.00097553	0.00340603
tccP	-1.51290501	-0.597321413	0.00059988	0.00219653
tamB	-1.51259227	-0.59702315	0.0001724	0.00072181
yedQ	-1.51125568	-0.595747765	2.1417E-05	0.00010311
ilvY	-1.51019741	-0.594737149	0.00174802	0.00574943
cysQ	-1.50729138	-0.591958337	0.00083148	0.0029372

rlmE	-1.50694835	-0.591629972	0.00026809	0.00107913
narG	-1.50683331	-0.591519834	0.01167329	0.03032919
yfcD	-1.50528647	-0.590038071	0.00054052	0.002008
yfbU	-1.50491524	-0.589682238	9.5836E-05	0.00042237
deoB	-1.50405955	-0.588861687	0.00046258	0.00174938
prpE	-1.50285339	-0.587704272	0.02282522	0.05390255
mdtD_1	-1.50282497	-0.587676993	0.00373767	0.01117145
glsA	-1.50153423	-0.58643736	0.00043252	0.00164749
fpr	-1.50041424	-0.585360856	0.00049693	0.00186639

Appendix C: Microbiome data

Table S4. Indicating the depth of sequencing (Goods coverage)

Sample ID	Goods coverage
WA3.00	1.0
WB3.00	0.999965040465661
WC3.00	0.999965040465661
WC2.00	0.999930080931322
KA5.00	0.9998426820954744
KB5.00	0.999965040465661
KC5.00	0.999965040465661
KC6.00	0.9999825202328305
WA3.09	0.999965040465661
WB3.09	0.9999825202328305
WC3.09	0.999965040465661
KA5.09	1.0
KB5.09	0.9999825202328305
KC5.09	1.0
KA5.10	0.999895121396983
KB5.10	0.9999825202328305
KC5.10	1.0
WA3.24	0.9999475606984914
WB3.24	0.999930080931322
WC3.24	0.9999825202328305
KA5.24	1.0
KB5.24	0.999965040465661
KC5.24	0.9999825202328305

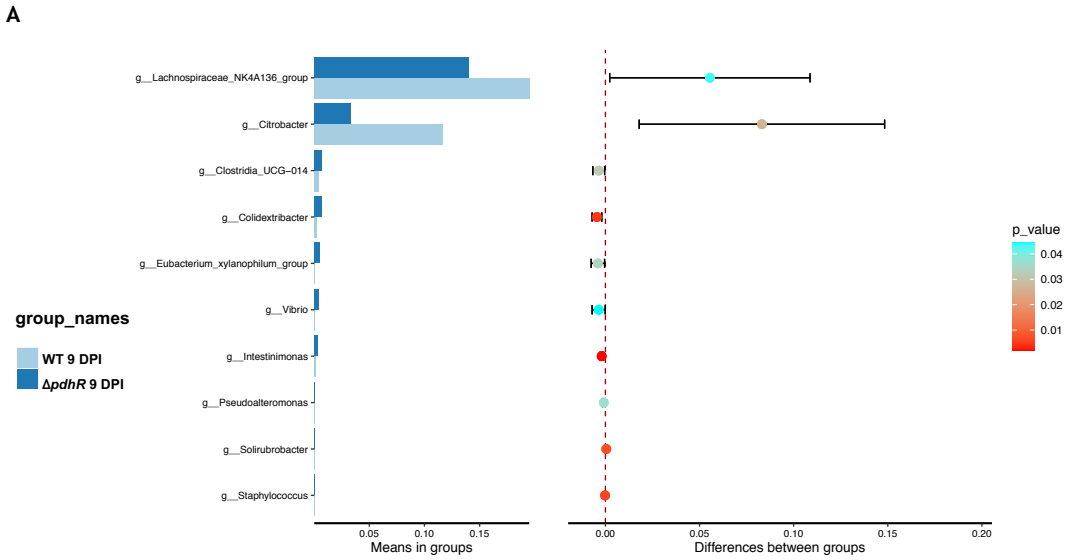

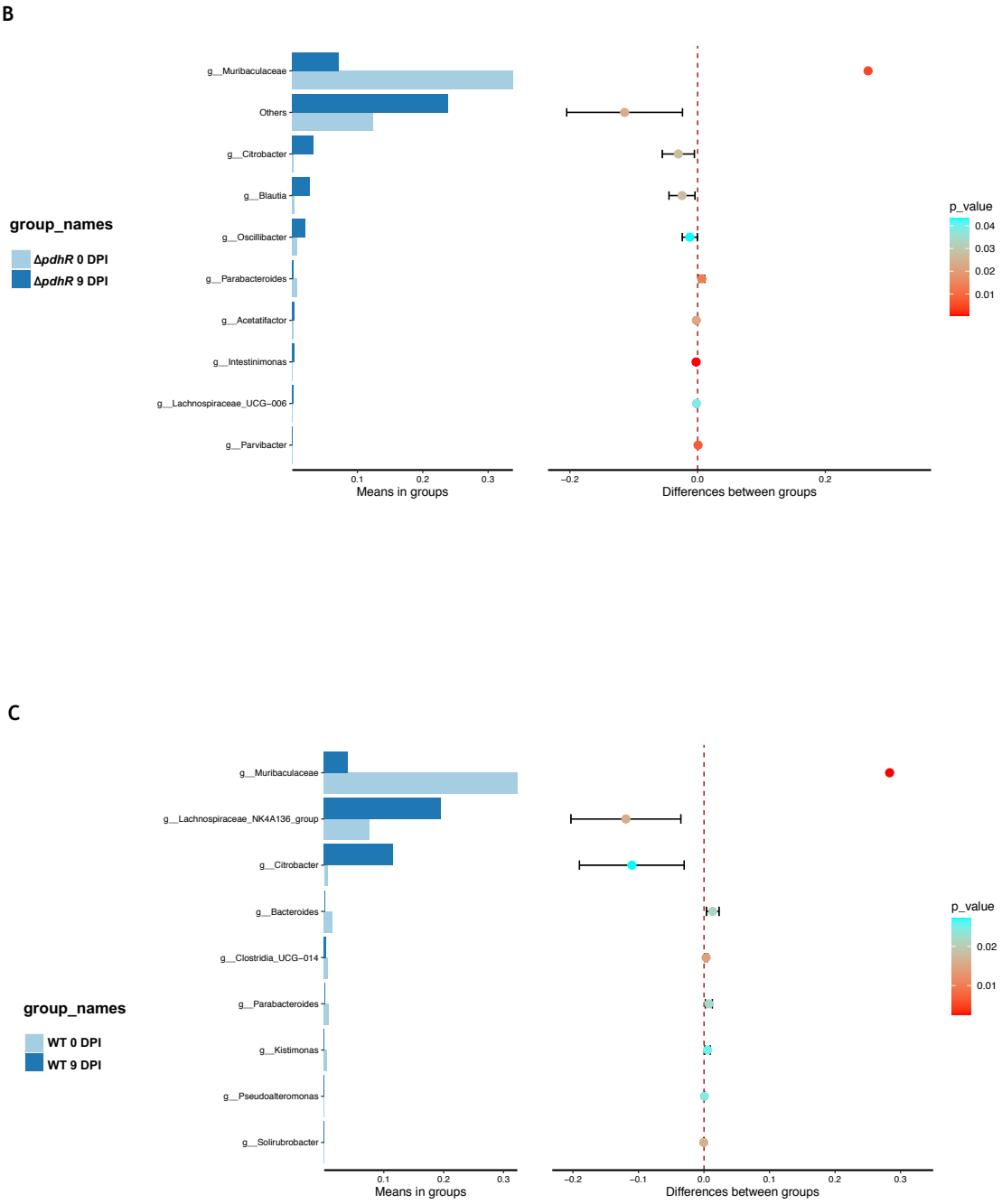

Fig. S 5-1. Significant changes at genus level at peak of infection *pdhR* vs EHEC group mice.